NISTIR 8208

Applied and Computational Mathematics Division

Summary of Activities for Fiscal Year 2017

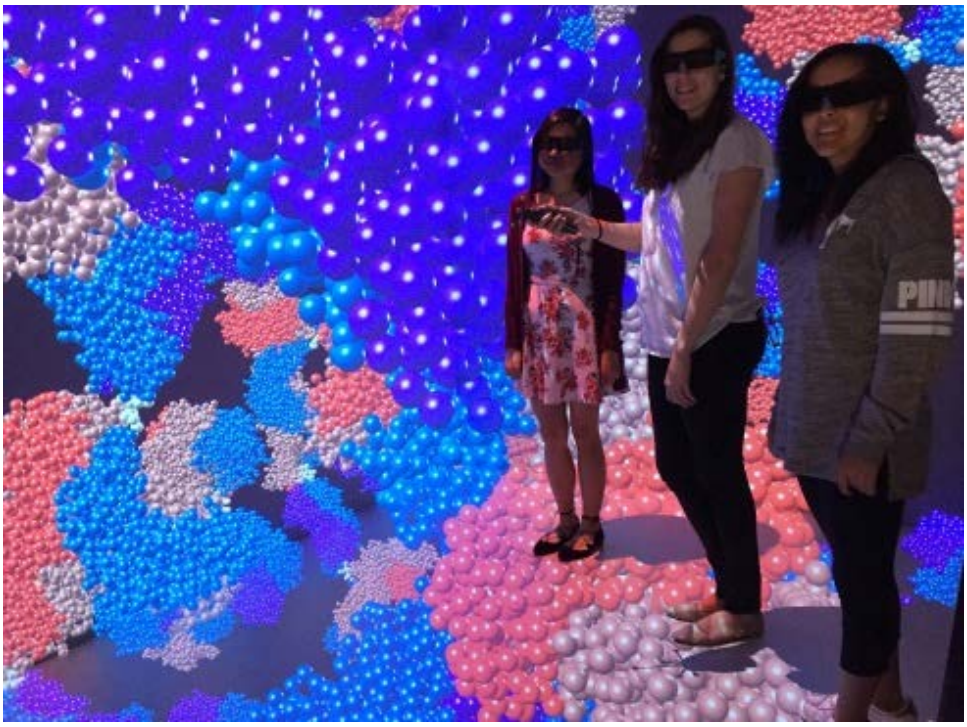

This publication is available free of charge from:
https://doi.org/10.6028/NIST.IR.8208

National Institute of Standards and Technology
U.S. Department of Commerce

NISTIR 8208

Applied and Computational Mathematics Division

Summary of Activities for Fiscal Year 2017

Ronald F. Boisvert, Editor
Applied and Computational Mathematics Division
Information Technology Laboratory

This publication is available free of charge from:
https://doi.org/10.6028/NIST.IR.8208

April 2018

U.S. Department of Commerce
Wilbur L. Ross, Jr., Secretary

National Institute of Standards and Technology
Walter Copan, NIST Director and Under Secretary of Commerce for Standards and Technology

Abstract

This report summarizes recent technical work of the Applied and Computational Sciences Division of the Information Technology Laboratory at the National Institute of Standards and Technology (NIST). Part I (Overview) provides a high-level overview of the Division's activities, including highlights of technical accomplishments during the previous year. Part II (Features) provides further details on three projects of particular note this year. This is followed in Part III (Project Summaries) by brief synopses of all technical projects active during the past year. Part IV (Activity Data) provides listings of publications, technical talks, and other professional activities in which Division staff members have participated. The reporting period covered by this document is October 2016 through December 2017.

For further information, contact Ronald F. Boisvert, Mail Stop 8910, NIST, Gaithersburg, MD 20899-8910, phone 301-975-3812, email boisvert@nist.gov, or see the Division's Web site at https://www.nist.gov/itl/math/.

Keywords: applied mathematics; computational science and engineering; high-performance computing; materials modeling and simulation; mathematical knowledge management; mathematical modeling; mathematics of metrology; network science; scientific visualization; quantum information science.

Cover Visualization: Student interns view molecular data in ACMD's immersive visualization facility. They are (left to right): Diana Chou and Margaret Sanger, University of Maryland, College Park, and Aida Nurit Shumburo of Thomas Sprigg Wootton High School.

Section Visualizations: The "word cloud," which is found at the start of each Part of this document was created using Wordle, http://www.wordle.net/, and the text of this document as input.

Acknowledgements: Thanks to Lochi Orr for assisting in the compilation of Parts III and IV of this document. Thanks also to Brian Cloteaux and Patrice Pages who each carefully read the manuscript and offered many corrections and suggestions for improvement.

Disclaimer: Certain commercial entities, equipment, and materials are identified in this document in order to describe an experimental procedure or concept adequately. Such identification is not intended to imply recommendation or endorsement by the National Institute of Standards and Technology, nor is it intended to imply that the entities, materials, and equipment are necessarily the best available for the purpose.

Contents

Part I

Overview

Introduction

Founded in 1901, the National Institute of Standards and Technology (NIST) is a non-regulatory federal agency within the U.S. Department of Commerce. NIST's mission is to promote U.S. innovation and industrial competitiveness by advancing measurement science, standards, and technology in ways that enhance economic security and improve our quality of life. The NIST Laboratory program is broad ranging, with research efforts encompassing physics, electrical engineering, nanotechnology, materials science, chemistry, bioscience, engineering, fire research, and information technology.

The Information Technology Laboratory (ITL) is one of seven major laboratories and user facilities at NIST. ITL's overarching purpose is to cultivate trust in information technology and metrology. This purpose is accomplished primarily through the development of measurements, tests and guidance to support innovation in and deployment of information technology by industry and government, as well as through the application of advanced mathematics, statistics and computer science to help ensure the quality of measurement science.

The Applied and Computational Mathematics Division (ACMD) is one of seven technical Divisions in ITL. At its core, ACMD aims to nurture trust in NIST metrology and scientific computing. To do so, ACMD provides leadership within NIST in the use of applied and computational mathematics to solve science and engineering problems arising in measurement science and related applications. In that role ACMD staff members

- perform research and development in applied mathematics and computational science and engineering, including analytical and numerical methods, high-performance computing and visualization;
- engage in peer-to-peer collaborations to apply such techniques and tools to NIST problems;
- develop and disseminate mathematical reference data, software, and related tools; and
- work with internal and external groups to develop standards, tests, reference implementations, and other measurement technologies for scientific computation on current and future architectures.

Division staff is organized into four groups:

Mathematical Analysis and Modeling Group (*Timothy Burns, Leader*)

Performs research and maintains expertise in applied mathematics, mathematical modeling, and numerical analysis for application to measurement science.

Mathematical Software Group (*Michael Donahue, Leader*)

Performs research and maintains expertise in the methodology and application of mathematical algorithms and software in support of computational science within NIST as well as in industry and academia.

High Performance Computing and Visualization Group (*Judith Terrill, Leader*)

Performs research and maintains expertise in the methodologies and tools of high-performance scientific computing and visualization for use in measurement science.

Computing and Communications Theory Group (*Ronald Boisvert, Acting Leader; Isabel Beichl and Xiao Tang, Project Leaders*)

Performs research and maintains expertise in the fundamental mathematics, physics, and measurement science necessary to enable the development and analysis of current and future computing and communications systems.

The technical work of the Division is organized into six thematic areas; these are described in the sidebar. Project descriptions in Part III of this document are organized according to these broad themes.

Division Thematic Areas

Broad Areas

Mathematics of Metrology. Mathematics plays an important role in measurement science. Mathematical models are needed to understand how to design effective measurement systems and to analyze the results they produce. Mathematical techniques are used to develop and analyze idealized models of physical phenomena to be measured, and mathematical algorithms are necessary to find optimal system parameters. Mathematical and statistical techniques are needed to transform measured data into useful information. The goal of this work is to develop fundamental mathematical methods and tools necessary for NIST to remain a world-class metrology institute, and to apply these methods and tools to problems in measurement science.

High Performance Computing and Visualization. Computational capability has been advancing rapidly for some time. Modeling and simulation now can be done with greatly increased fidelity (e.g., higher resolution and more complex physics). However, developing the necessary large-scale parallel applications remains highly challenging, requiring expertise that application scientists rarely have. In addition, the hardware landscape is changing rapidly, so new algorithmic techniques must constantly be developed. We are developing such expertise for application to NIST problems. Such computations, as well as modern laboratory experiments, often produce large volumes of scientific data, which cannot be readily comprehended without some form of analysis. We are developing the infrastructure necessary for advanced interactive, quantificative visualization and analysis of scientific data, including the use of 3D immersive environments and applying this infrastructure to NIST problems. One of our goals is to develop the 3D immersive environment into an interactive measurement laboratory.

Current Focus Areas

Advanced Materials. Delivering technical support to the nation's manufacturing industries as they strive to out-innovate and out-perform the international competition has always been a top priority at NIST. Mathematical modeling, computational simulation, and data analytics are key enablers of emerging manufacturing technologies. A clear case in point is the Materials Genome Initiative, an interagency program with the goal of significantly reducing the time from discovery to commercial deployment of new materials using modeling, simulation, and informatics. ACMD's role in advanced manufacturing centers on the development and assessment of modeling and simulation tools, with emphasis on uncertainty quantification, as well as support of efforts by other NIST Laboratories in materials modeling and smart manufacturing.

Quantum Information. An emerging discipline at the intersection of physics and computer science, quantum information science is likely to revolutionize 21st century science and technology in the same way that lasers, electronics, and computers did in the 20th century. By encoding information into quantum states of matter, one can, in theory, exploit the unique properties of quantum systems to enable phenomenal increases in information storage and processing capability, as well as communication channels with high levels of security. Although many of the necessary physical manipulations of quantum states have been demonstrated experimentally, scaling these up to enable fully capable quantum computers remains a grand challenge. We engage in (a) theoretical studies to understand the power of quantum computing, (b) collaborative efforts with the multi-laboratory experimental quantum science program at NIST to characterize and benchmark specific physical implementations of quantum information processing, and (c) demonstration and assessment of technologies for quantum communication.

Foundations of Measurement Science for Information Systems. Modern information systems are astounding in their complexity. Software applications are built from thousands of interacting components. Computer networks interconnect millions of independently operating nodes. Large-scale networked applications provide the basis for services of national scope, such as financial transactions and power distribution. Despite our increasing reliance on such systems, our ability to build far outpaces our ability to ensure security and reliability. Protocols controlling individual nodes can lead to unexpected macroscopic system behavior. Local power anomalies propagate in unexpected ways leading to large-scale outages. Computer system vulnerabilities are exploited in viral attacks resulting in widespread loss of data and system availability. The actual resilience of our critical infrastructure is largely unknown. Measurement science has long provided a basis for the understanding and control of physical systems. Such deep understanding and insight is lacking for complex information systems. We seek to develop the mathematical foundations needed for a measurement science for complex networked information systems.

Mathematical Knowledge Management. We work with researchers in academia and industry to develop technologies, tools, and standards for representation, exchange, and use of mathematical data. Of particular concern are semantic-based representations which can provide the basis for interoperability of mathematical information processing systems. We apply these representations to the development and dissemination of reference data for applied mathematics. The centerpiece of this effort is the Digital Library of Mathematical Functions, a freely available interactive and richly linked online resource, providing essential information on the properties of the special functions of applied mathematics, the foundation of mathematical modeling in all of science and engineering.

Highlights

In this section we identify some of the major accomplishments of the Division during the past year. We also provide news related to ACMD staff.

Recent Technical Accomplishments

ACMD has made significant technical progress on many fronts during the past year. Here we highlight a few notable technical accomplishments. Further details are provided in Part II (Features) and Part III (Project Summaries).

Mathematics of Metrology. We work closely with NIST scientists to apply our expertise in applied mathematics to improve measurement science. This collaboration effort is nicely illustrated by recent work with the NIST Fluid Metrology Group, which is working to overcome barriers to the adoption of microfluidic devices. Such devices offer the promise of cheaper, faster, and data-driven diagnostic tools that can simultaneously test for hundreds of medical conditions via labs-on-a-chip. However, such assays require precise control over operating conditions such as flow-rate, which is difficult to measure in situ and at the required scales. ACMD scientists have had remarkable success in using mathematical modeling to guide the development of highly accurate flow-rate sensors that can be embedded in microfluidic channels and operate down to nanoliters per minute. See page 13.

Advanced Materials. At NIST, published experimental measurement results must come with an assessment of their uncertainty. As computer models become more capable, and are more heavily relied upon for identifying new materials with desired properties, the question arises: what is the uncertainty in the computational results? An invited 75-page manuscript by two ACMD researchers entitled "Uncertainty Quantification for Molecular Dynamics," which will soon appear in *Reviews in Computational Chemistry*, introduces this subject to materials scientists. The paper introduces fundamental concepts of uncertainty quantification to the molecular dynamics community, illustrating the processes in the analysis of several topical problems. Analyses described in the paper are demonstrated in accompanying tutorial scripts which will be made available with publication of the manuscript.

High Performance Computing and Visualization. NIST has released its first standard reference material (SRM) designed with the use of a supercomputer. SRM 2493: Standard Reference Mortar for Rheological Measurements can be used to calibrate rheometers (which measure viscosity) when the material measured contains suspended particles, such as mortar. ACMD staff enabled the characterization of this material via large-scale simulations performed on Argonne National Laboratory Blue Gene systems. This accomplishment is part of a long-term effort to study the rheological properties of suspensions, such as concrete. Over the course of this project we have used more than 160 million CPU-hours of compute time, running individual simulations on up to 128 000 processors. This work was enabled through awards from the competitive DOE INCITE program. See page 16.

Quantum Information. The first ever end-to-end generation of randomness from quantum-based sources in the device-independent paradigm was completed by ACMD in 2017, providing the first protocol for randomness generation that can adapt to changing experimental conditions on the fly. Using data generated by colleagues in PML from a loop-hole-free Bell test, 1 024 uniform random bits with error bounded by 10^{-12} were generated. This work required the development of new randomness extraction theory, which is more resilient to fluctuating and uncertain experimental conditions, and which can extract more randomness than previous methods. A paper describing the accomplishment has been accepted for publication in *Nature*. See page 20.

In future quantum communication systems, single photons, which serve as information carriers, must possess very narrow linewidths and accurate wavelengths for an efficient interaction with atomic systems which serve as quantum memories. Spectral characterization of such single-photon sources is necessary and must be performed with very high spectral resolution, wavelength accuracy, and detection sensitivity.

ACMD researchers have proposed a method to precisely characterize spectral properties of narrow-linewidth single-photon sources using an atomic vapor cell based on electromagnetically-induced transparency (EIT). By using an atomic cesium vapor cell, the researchers have experimentally demonstrated a spectral resolution of better than 150 kHz, an absolute wavelength accuracy of within 50 kHz and an exceptional detection sensitivity suitable for optical signals as weak as −117 dBm. Such performance is 10 000 times better than conventional spectrometers. See page 82.

Foundations of Measurement Science for Information Systems. Ingestible wireless capsule endoscopy (WCE) is a novel, painless and effective, diagnostic technology for inspecting the entire gastrointestinal (GI) tract. Next generation capsules (medical micro-robots) are expected to deliver higher quality images and videos than current systems. These capsules will require wireless communication links with higher bandwidth. Ultra-Wideband (UWB) technology is an attractive candidate for such wireless communication links. Unfortunately, comprehensive data on radio wave propagation for ingestible electronics is not available. To respond to this need we are developing a computational platform for the study of radio wave propagation inside the human body. The platform includes a detailed human body model, transmitter and receiver antenna models, a simulation engine, and a 3D immersive visualization capability. See page 97.

Mathematical Knowledge Management. The NIST Digital Library of Mathematical Functions (DLMF), a free, online source of reference data on the special functions of applied mathematics, continues to be a popular community resource. Released in 2010, along with a print companion published by Cambridge University Press, the DLMF has since seen more than 3 700 citations (as identified by Google Scholar). Online usage remains very high, with 3.4 million pages downloaded during more than 415 000 sessions initiated by more than 261 000 unique visitors during calendar year 2017. The DLMF continues to be enhanced. In 2017 three new releases with various corrections and clarifications, improved notation for integral transforms, a new section on *Fourier Transforms of Special Distributions*, and improvements to icons, decorations and mouse-cursors (including the introduction of scalar vector graphics (SVG)) were issued. Work is underway with four external authors to develop a new chapter on *Orthogonal Polynomials of Several Variables*, as well as to make significant additions to existing chapters on *Algebraic Methods*, *Orthogonal Polynomials*, and *Painlevé Transcendents*. See page 23.

Technology Transfer and Community Engagement

The volume of technical output of ACMD remains high. During the last 15 months, Division staff members were (co-)authors of 46 articles appearing in peer-reviewed journals, 34 papers in conference proceedings, and 11 published in other venues. Nineteen additional papers were accepted for publication, while 37 others are undergoing review. Division staff gave 74 invited technical talks and presented 47 others in conferences and workshops.

ACMD continues to maintain an active website with a variety of information and services, most notably the Digital Library of Mathematical Functions, though legacy services that are no longer actively developed, like the Guide to Available Mathematical Software, the Matrix Market, and the SciMark Java benchmark still see significant use. During calendar year (CY) 2017, the division Web server satisfied more than 5.2 million requests for pages during more than 1 million user visits. Another indication of the successful transfer of our technology is references to our software in refereed journal articles. For example, our software system for nano-magnetic modeling (OOMMF) was cited in 157 such papers published in CY 2017 alone; see page 55.

Members of the Division are also active in professional circles. Staff members hold a total of 14 editorial positions in peer-reviewed journals. For example, Barry Schneider is an Associate Editor-in-Chief and Isabel Beichl is an Editorial Board Member for IEEE's *Computing in Science and Engineering*. Staff members are also active in conference organization, serving on 37 organizing/steering/program committees. Of note, ACMD played an important role as sponsor or (co-)organizer of several significant events this year, including the following:

- *Numerical Reproducibility at Exascale*, at SC16[1], Salt Lake City, UT, November 18, 2016 and at SC17, Denver, CO, November 12, 2017. (M. Mascagni and Walid Keyrouz, Co-Organizers)

  A cornerstone of the scientific method is experimental reproducibility. As computation has grown into a powerful tool for scientific inquiry, the assumption of computational reproducibility has been at the heart of numerical analysis in support of scientific computing. With ordinary CPUs, supporting a single, serial, computation, the ability to document a numerical result has been a straightforward process. However, as computer hardware continues to develop, it is becoming harder to ensure computational reproducibility, or to even completely document a given computation. These two workshops explored the current state of computational reproducibility in high-performance computing, and sought to organize solutions at different levels.

- *Circumventing Turing's Achilles Heel*, Santa Fe Institute, NM, November 14-15, 2016.

  A NIST grant provided partial funding for this event. Subject to the limitations of finite memory, time, and processor speed, today's general-purpose computers are (near) Turing complete; that is, capable of computing anything that is computable. But it's exactly that strength that makes our computer and network systems so vulnerable to attack: If outsiders can gain control of your system, then, in principle, they can use it for whatever tasks they are clever enough to trick your system into executing. This SFI Working Group explored strategies for retaining the hardware and software advantages of general purpose computers, while denying those same general-purpose capabilities to outside attackers.

- *Workshop on Computational Complexity and High Energy Physics*, College Park, MD, July 31 - August 2, 2017. (Stephen Jordan, Lead Organizer)

  The workshop, which was sponsored by the Joint UMD/NIST Center for Quantum Information and Computer Science (QuICS) explored emerging connections between computational complexity theory and high energy physics. In particular, what difficult problems in high energy physics can be attacked by insights and tools from the theory of computation and future quantum computing technologies? Some 70 researchers from academia, government and industry participated.

Service within professional societies is also prevalent among our staff. For example, Geoffrey McFadden served as Member-at-Large of the Council of the Society for Industrial and Applied Mathematics (SIAM). Faculty appointee Michael Mascagni is a Member of the Board of Directors of the International Association for Mathematics and Computers in Simulation (IMACS). Ronald Boisvert completed an unprecedented 20 years of service as a member of the Publications Board of the Association for Computing Machinery (ACM). Staff members are also active in a variety of working groups. For example, Ronald Boisvert and Andrew Dienstfrey serve as members of the International Federation for Information Processing (IFIP) Working Group 2.5 on Numerical Software, Donald Porter is a member of the Tcl Core Team, Bruce Miller is a member of W3C's Math Working Group, and Sandy Ressler is a member of the Web3D Consortium. Barry Schneider represents NIST on the High-End Computing (HEC) Interagency Working Group of the Federal Networking and Information Technology Research and Development (NITRD) Program. Further details can be found in Part IV of this report.

[1] http://www.cs.fsu.edu/~nre/

Staff News

The past year saw a few staffing changes. Among these are the following.

Arrivals

Charles Baldwin joined ACMD's quantum information research team in Boulder in early October 2016 as an NIST/NRC Postdoctoral Associate. Charles recently completed a PhD in Physics at the University of New Mexico. He worked with ACMD's Scott Glancy on the development of new, practical methods for quantum state tomography. Unfortunately, Dr. Baldwin departed NIST after just one year following a job offer from Honeywell.

Heman Gharibnejad, a postdoctoral researcher at the University of North Texas with a Ph.D. in physics from the University of Nevada at Reno in 2014, began a tenure as an NIST/NRC Postdoctoral Associate in January 2017. With a background in computational physics, Heman is working with Barry Schneider on the development and application of numerical methods for the time-dependent Schrödinger equation.

Lucas Kocia began an appointment as a NIST/NRC Postdoctoral Associate in September 2017. Lucas received a Ph.D. in Chemistry from Harvard 2016 and held a postdoctoral position at Tufts University in 2016-17. His research is in mathematical physics, with an emphasis on quantum information, quantum dynamics and semiclassical methods. At NIST he is working with Stephen Jordan on the application of semiclassical techniques to problems in quantum information science.

Departures

John Hagedorn, a computer scientist in the ACMD High Performance Computing and Visualization Group, retired in January 2017 after nearly 22 years at NIST. Hagedorn made important contributions to Division research on RF propagation for wireless body area networks, as well as in techniques and tools for 3D immersive scientific visualization.

Barry Hershman, an IT Specialist who provided technical support to the Division's Quantum Communications Project, retired in April 2017 after 20 years of Federal service.

ACMD mathematician **Bert Rust**, an expert in data modeling, time series analysis and inverse problems, retired in July 2017 after 37 years with NIST. At NIST Rust's most important contributions included novel methods for selecting regularization parameters for ill-posed problems, including a remarkably effective method for truncating the singular-value decomposition for such problems, and numerical methods for nonlinear least squares problems. Over the years he contributed to applications such as dosimeter calibration, processing of radar doppler spectra and the analysis of cryopreservation solutions on proteins.

Yolanda Parker, secretary for the High-Performance Computing and Visualization Group, retired in May 2017 after 31 years of Federal service, 19 of which were with NIST.

Students

During FY 2017 ACMD supported the work of 41 student interns, including 9 graduate students, 12 undergraduates, and 20 high school students. See Table 1 and Table 2 in the Appendix for a complete listing. ACMD staff members are also active in the education of graduate students, serving both as Ph.D. advisers and as members of thesis committees. For a complete list, see page 130.

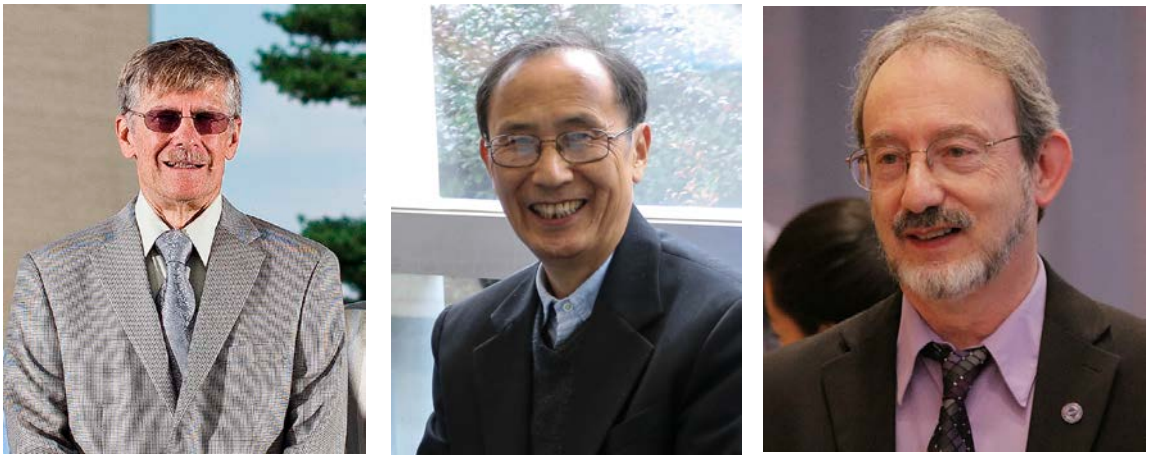

Figure 1. *Three ACMD staff members were elevated to Fellow status this year in separate organizations. (l ot r): Daniel Lozier (Washington Academy of Sciences Fellow), Xiao Tang (APS Fellow) and Ronald Boisvert (AAAS Fellow).*

Recognition

The landmark loophole-free Bell test performed at the NIST Boulder Laboratories in November 2015 was the subject of a 2016 Department of Commerce Gold Medal awarded to the NIST Physical Measurement Laboratory and Information Technology Laboratory. ACMD staff members **Manny Knill** and **Scott Glancy**, as well as ACMD postdoc **Peter Bierhorst** were part of the team whose work was honored by the Department.

Bradley Alpert was part of a NIST team recognized with a 2017 Department of Commerce Gold Medal for revolutionizing x-ray spectroscopy. The group is recognized for developing first-in-the-world research tools able to make stop-action X-ray measurements of light interacting with molecules on near-instantaneous time scales. Using their innovative tabletop system, they obtained results with 10 times better time resolution than is available at large X-ray synchrotron facilities costing hundreds of millions of dollars, and collected X-rays with 10 to 100 times better efficiency. The group's work enables fast turnaround measurements of materials for photonics, energy storage, and industrial catalysis. by developing experimental capabilities on a tabletop that rival massive national user facilities**.**

Three Division staff members were elevated to Fellow status in external professional organizations:

- **Ronald Boisvert** was named a Fellow of the American Association for the Advancement of Science (AAAS) "for distinguished contributions to the fields of mathematical software and computational science, excellence in public administration of science, and service to the computing profession." The honor was conferred at the AAAS Annual Meeting in Boston in February 2017.
- **Xiao Tang** was named a Fellow of the American Physical Society (APS). He was cited "for outstanding contributions in optical technologies and systems, with application to quantum communications, spectrometry, and digital preservation." He

Figure 2. *ITL Director Charles Romine presents the 2017 Outstanding Contribution to ITL Award to Bonita Saunders for her technical leadership in the development of visualizations of mathematical functions.*

was nominated by the APS Topical Group on Quantum Information, and was inducted at the APS Meeting in March 2017. Tang joins three current ACMD staff members with this honor: Manny Knill, Geoffrey McFadden, and Barry Schneider.

- **Daniel Lozier** was named a Fellow of the Washington Academy of Sciences in conjunction with the WAS's Annual Award in Mathematics and Computer Science, in recognition of outstanding contributions to the field of applied mathematics, notably for his leadership in the development of the NIST Digital Library of Mathematical Functions. The honor was conferred at an event at the AAAS Headquarters in Washington, DC on May 11, 2017.

Bonita Saunders received the 2017 ITL Outstanding Contribution Award for excellence in technical leadership resulting in outstanding scientific visualizations in the NIST Digital Library of Mathematical Functions. See Figure 2.

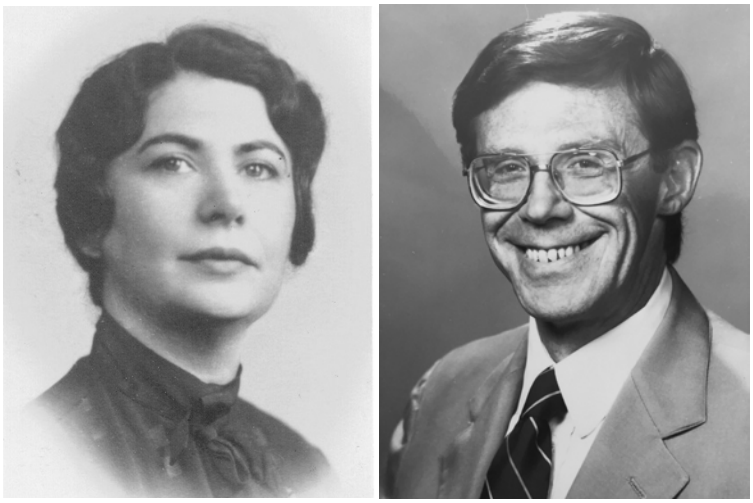

Figure 3. *Gertrude Blanch (NIST 1938-54) and Francis Sullivan (NIST 1982-93) were inducted into the NIST Portrait Gallery of Distinguished Scientists, Engineers and Administrators*

Two former NIST mathematicians were inducted into the NIST Portrait Gallery of Distinguished Scientists, Engineers and Administrators in October 2017. **Gertrude Blanch**, who was at NIST during the period 1938-54, was cited for excellence as Technical Director of the Mathematical Tables Project, and for pioneering contributions to the field of numerical analysis for early computers. **Francis Sullivan**, a NIST staff member from 1982-93, and a NIST guest researcher 1979-82 and 1993-present, was cited for establishing and leading the NIST Computing and Applied Mathematics Laboratory, which pioneered modern computing technologies and techniques for NIST.

Part II

Features

Metrology for Microfluidics

Microfluidic devices offer the promise of cheaper, faster, and data-driven diagnostic tools that can simultaneously test for hundreds of medical conditions via labs-on-a-chip. However, scientists must overcome fundamental measurement problems if such devices are to become reliable and commercially viable. In particular, microfluidic assays require precise control over operating conditions such as flow-rate, which is difficult to measure in situ and at the required scales. To address this problem, ACMD staff members are working with the PML Fluid Metrology group to develop flow-rate sensors that can be embedded in microfluidic channels and operate down to nanoliters per minute. Given the scales involved, accurate models are needed to infer the flow-rates based on indirect measurements, i.e., the total fluorescence of tracer molecules (which cannot be seen individually). Remarkably, we demonstrated how certain classes of models yield similarity solutions that can be used for accurate measurements without the need to know the device dimensions, except within an order of magnitude. Moreover, such similarity solutions can be used as the basis for uncertainty quantification. Preliminary experiments confirmed the validity of this approach.

Paul Patrone

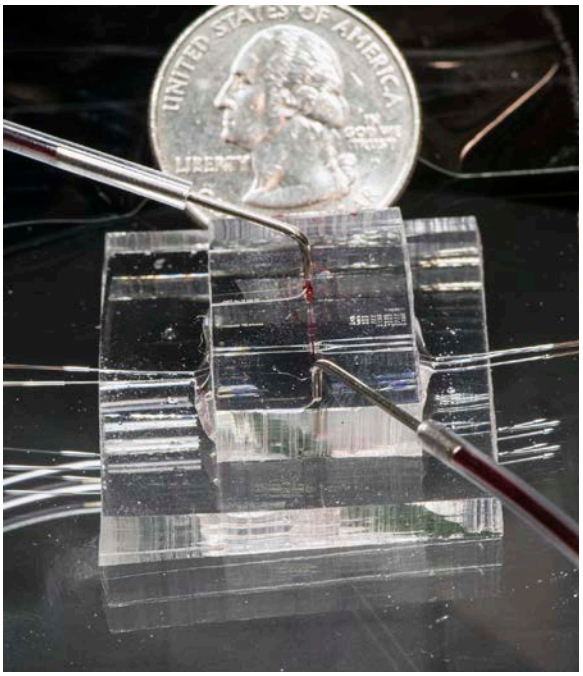

Figure 4. *An example of a microfluidic lab-on-a-chip. The metal prongs are entry and exit points for the fluid, whereas the transparent fibers on the left and right are fiber optic cables used for fluorescence intensity measurements. Note the scale of the chip relative to a quarter. Photo courtesy of G. Cooksey*

In the past few years, the medical community has begun turning towards *precision medicine* as a promising model for patient care. As defined by the U. S. National Research Council Committee on A Framework for Developing a New Taxonomy of Disease [1], precision medicine refers to "the tailoring of medical treatment to the individual characteristics of each patient," and "the ability to classify individuals into sub-populations that differ in their susceptibility to a particular disease, in the biology and/or prognosis of those diseases they may develop, or in their response to a specific treatment." More colloquially, this approach amounts to the practice of developing and using testing protocols that remove ambiguity from medical diagnostics. To this end, a key goal of precision medicine is to quickly and inexpensively differentiate molecular disease markers, so that, for example, doctors can distinguish H5N1 avian flu from anthrax without relying on a patient's subjective description of "flu-like" symptoms. Ultimately, the desire is to be able to collect sufficient and reliable information about a patient's status to optimize treatments and outcomes.

Fundamental to the success of this model is providing physicians with precise, targeted, and robust measurement of the many cellular markers that differentiate patients into various sub-populations. While relatively precise tests exist for many conditions, typical costs can rise to thousands of dollars or more with wait-times on the order of weeks [2]. Moreover, advanced tests must often be performed at locations far from patients, further contributing to cost and time. To make precision medicine affordable and widely marketable, scientists must therefore address the problems associated with reducing the size and time of testing, in effect, by bringing the lab to patients.

In the past few decades, the development and realization of advanced and nanoscale manufacturing techniques has suggested a path forward through microfluidic blood-testing assays. Conceptually, such devices direct small quantities of fluid down microscopic channels that contain receptor-molecules attuned to markers of a given disease. Given the length scales involved, bioengineers can fabricate "labs-on-a-chip" containing hundreds of such channels, each able to detect a unique medical condition; see Figure 4. This technology therefore offers the promise of realizing precision medicine through rapid and inexpensive diagnosis of hundreds of diseases, using only a single drop of blood [3]. Moreover, it heralds an age of big data in medicine wherein physicians can assess patient health and epidemiological trends based on a more holistic picture than currently is possible.

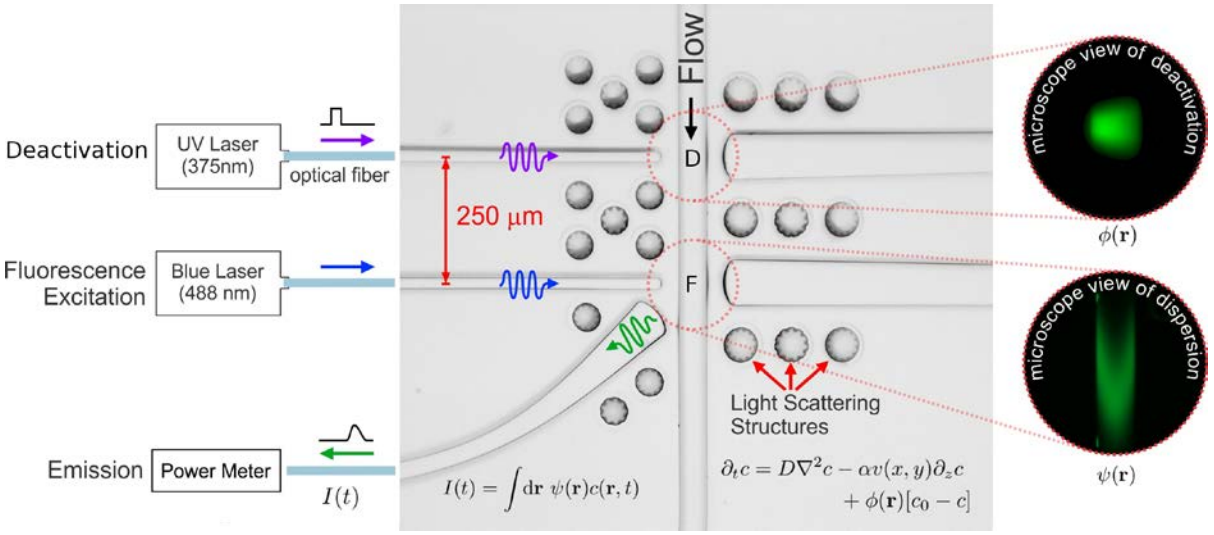

Figure 5. *Schematic of the experimental device. Fluid carrying fluorescent particles travels down the channel in the direction indicated by the arrow. At the location labeled D, a deactivation beam destroys some fraction of the fluorescent particles. At the location F, a second laser causes the remaining particles to fluoresce. This fluorescence is captured by a waveguide that measures the intensity I(t).*

Despite these potential benefits, commercial deployment of microfluidic assays has remained an elusive and challenging goal [3]. This is illustrated most clearly by the recent and high-profile failure of a microfluidics-based blood-testing company that was once valued at nearly $9 billion. While precise details were not made public, FDA reports and information from academic researchers suggest that lack of reliability and reproducibility of methods were the key problems that doomed the technology. Thus, these hurdles must be overcome if microfluidic assays are to become a successful diagnostic tool. Nonetheless, with the blood-testing market estimated at $51 billion, the drivers for such innovation are present [4].

Fundamentally, the challenges associated with microfluidic assays are a result of two competing interests. On the one hand, such tools must satisfy stringent regulatory constraints ensuring that test results are accurate. On the other hand, the associated testing protocols are designed to use the smallest sample possible (e.g., 1 % of a drop of blood). However, this latter goal is confounded by the fact that reliable and widely accessible metrology tools do not yet exist for measuring and controlling many properties of fluid flows at the relevant scales. For example, typical concentrations of biological disease markers are on the order of parts-per-billion, which is difficult for most instruments to detect at the nanoliter scales of interest. Moreover, state-of-the art measurements of microfluidic flow-rates are relatively crude, lack rigorous uncertainty quantification methods, and therefore can have uncertainties on the order of 50 %. Under such circumstances, it is difficult to control drug delivery rates, continuous manufacturing processes, and chemical reaction rates.

Flow-rate metrology for microfluidic assays. The ability to inexpensively and accurately measure flow-rates is a prerequisite to controlling microfluidic assays. The scales of interest in cutting-edge devices, however, may be as small as nanoliters per minute (which corresponds to teaspoons per month). As such, conventional methods of measuring flow rates (e.g., based on mass-balance or pressure gradients) are unsuitable if only because the relevant devices are too noisy at these scales. Optical methods are sometimes used as a substitute, but they frequently rely on expensive microscopes that would be cost-prohibitive in commercial applications.

To overcome these problems, ACMD staff are working with the PML Fluid Metrology Group to build a novel nanoscale flowmeter based on time-lapse measurements of fluorescent particles. Given the scales involved, these efforts require substantial development of both advanced manufacturing techniques and theoretical models to create and use these devices. Moreover, because the measurements must be precise to within a few percent or better, uncertainty quantification is a fundamental component of the analysis and modeling.

A schematic of how the flowmeter works is shown in Figure 5. The fluid flows down a long channel (with a characteristic cross-sectional dimension of 100 microns) carrying fluorescent particles. At the position labeled (D), the flow encounters a laser beam that deactivates a fraction of the particles, depending on their residence time in the beam. Further down the channel, a second beam, labeled (F), causes the remaining activated particles to fluoresce. This fluorescence is then picked up by an optical sensor that returns an intensity signal I proportional to the amount of light collected. Conceptually, the residence time of particles in the deactivation beam (and therefore also the fluorescence

intensity I) depend on the flow-rate α, which allows us to measure the latter. From a theoretical standpoint, however, this measurement approach is challenging because: (i) particle diffusion is significant at these scales, which can introduce noise into the fluorescence signal; and (ii) device features such as the channel width and laser beam spatial intensity profiles are difficult to non-destructively determine. Ultimately, this means that there are significant sources of uncertainty that cannot be adequately quantified.

To address these issues, we have adopted a modeling approach that leverages similarity solutions to certain classes of partial differential equations. In more detail, one can show that under certain experimentally attainable conditions, the fluorescent particle motion becomes convection dominated with a flow-profile whose shape is independent of the volumetric fluid flow rate α. Under these assumptions, it is possible to show that the steady-state fluorescent intensity is given by an expression of the form

$$I_s(p/\alpha) = c_0 \int d\mathbf{r}\ \psi(\mathbf{r}) \exp[-\frac{p}{\alpha}\Phi(x,y)]$$

where the flow is in the z-direction, c_0 is the total fluorescent particle concentration, $\psi(\mathbf{r})$ is the intensity profile of the second laser beam, $\Phi(x,y)$ is the dosage of the deactivation laser given to a fluorescent particle in the x, y stream for a laser at full power, and $0 \leq p \leq 1$ is the laser power (where $p = 0$ means the laser is off and $p = 1$ means the laser is at 100 % power). Notably, the functions ψ and Φ are non-negative and have finite-domains in which they are strictly positive, although we otherwise know very little about their shape.

To make use of these observations, we note that I_s is a strictly monotone function of p/α. As such, if we know the volumetric flow-rate associated with a particular α (say $\alpha = 1$), then we may vary the laser power to experimentally map out $I_s(x)$ for $0 \leq x \leq 1$. To measure an unknown flow rate, we then fix p and measure $I_s(p/\alpha) = I_s(x)$. Given that $I_s(x)$ is strictly monotone, it is also a bijection, and we can therefore infer $I_S \Rightarrow x = p/\alpha$, or $\alpha = p/x$. Importantly, this procedure does not actually require knowledge of ψ or Φ, which we cannot measure. Moreover, it shifts all the uncertainty quantification to the data-analysis of the raw signal output by the optical sensor I_s and estimation of the errors associated with the convection assumption, tasks that are easier to handle analytically.

Preliminary experiments by PML staff indicate that typical microfluidic devices indeed exhibit the scaling behavior predicted by our models. Thus, these results are being written up for a manuscript that we anticipate submitting for publication in FY 2018. Provisional patent applications for this technology have been submitted. Future work aims to use these methods in support of cancer cell metabolism measurements.

References

[1] *Toward Precision Medicine: Building a Knowledge Network for Biomedical Research and a New Taxonomy of Disease.* The National Academies Press, Washington D. C., 2011. DOI: 10.17226/13284

[2] R. Y. Hsia, Y. A. Antwi and J. P. Nath. Variation in Charges for 10 Common Blood Tests in California Hospitals: A Cross-Sectional Analysis. *BMJ Open* **4** (2014), e005482. DOI: 10.1136/bmjopen-2014-005482

[3] Nick Stockton. Theranos Isn't the Only One Chasing Needle-Free Blood Tests. *Wired*, October 16, 2015.

[4] *Blood Testing Market Analysis by Test Type, (Glucose, Lipid panel, Direct LDL, Prostate Specific Antigen, BUN, A1C, High Sensitivity CRP, Vitamin D, ALT, AST, Thyroid Stimulating Hormone, Creatinine, Serum Nicotine/Cotinine, Cortisol, Testosterone) and Segment Forecasts to 2024*. Grand View Research. URL: https://www.grandviewresearch.com/industry-analysis/blood-testing-market

Participants

Anthony Kearsley and Paul Patrone (ACMD); Gregory Cooksey (NIST PML)

Development of a Standard Reference Mortar

Rotational rheometers, devices that measure fluid properties such as viscosity, are routinely used for homogeneous materials such as oils, but their use on dense suspensions, such as concrete, is a relatively new phenomenon. As measurements with rheometers can involve flow in a complex geometry, it is important that they are calibrated with a standard reference material (SRM). NIST has produced an SRM for cement paste, SRM 2492, as the first step for the development of a reference material for concrete rheometers. The second step, described here, is the development of an SRM for mortar, composed of the SRM 2492 with added spherical beads. Here, material properties, such as viscosity, cannot be measured in fundamental units with certainty. Thus simulation, which requires the use of a high-performance computing facility to obtain the necessary fidelity is required to determine the viscosity of the SRM mortar, which has been in turn compared with the results of physical experiments.

William George

Accurately measuring the rheology of complex suspensions, such as concrete, is a crucial and widespread problem in the construction and other industries. The current practice in the concrete industry is to use the *slump flow test* (see Figure 6), which gives only a general idea of the workability of the fresh mixture, not a specific value of viscosity or other rheological property. To quantitatively measure rheological properties, a rotational rheometer is typically used. In these devices, one surface remains stationary while the other rotates. Various geometries for these rheometers are possible, examples of which are shown in Figure 7. However, the necessary rheometer geometry for suspensions does not permit an analytic solution of internal fluid flow, which limits their ability to accurately convert empirical measurements like torque and rotational speed to fundamental quantities like stress and strain rate.

For a more accurate measurement, a calibrated rheometer, specifically designed for these materials is needed. To date, this has not been possible. Current rheometers in use for concrete and mortar can give relative measurements, however measurements from two different rheometers cannot be compared as their output is not in the form of fundamental units. For this reason, NIST has been conducting research on the flow of these dense suspensions with the goal of enabling accurate and repeatable measurement of the rheology of these materials. A crucial part of this project is the development of a set of standard reference materials (SRMs) for calibrating concrete and mortar rheometers.

Figure 6. *The slump flow test to assess flowability and flow rate, state-of-the-art since 1918. Left: lifting the cement-filled cone. Right: diameter of the resulting flow is measured.* [Images: Wikimedia Commons author Knipptang, CC BY-SA 4.0]

Figure 7. *Rheometer spindles. The rotational speed of the spindle with a given applied torque can be used to infer viscosity. Left: traditional blade designs. Right: a novel helical design.*

In collaboration with the Materials and Structural Systems Division of the Engineering Laboratory, we are studying of the rheology of dense suspensions. The work includes physical experiments, mathematical model development, and extensive computer simulations. The overall objectives are to design rheometers and standard reference materials to develop new measurement science across the multiple length scales found in concrete rheology to benefit the concrete industry. In the process, we will add a novel computational design of materials and rheometers capability to the concrete industry. ACMD's focus in this project is computational simulation of these materials. A detailed discussion of the development of the mortar SRM, including the experimental work, was published in 2014 [1].

The materials under study are disordered systems consisting of a variety of components with disparate properties and complex interactions. Modeling and predicting the flow of such systems is a significant challenge requiring large-scale simulations. To accomplish this, we have had to unite the major length scales of concrete rheology: cement paste, mortar, and concrete. While cement paste is not a separate commercial product (except in the limited industry of grout flow), mortar is such a product; concrete is, of course, the main product. Each length scale (hundreds of micrometers for cement paste, millimeters for mortar, and hundreds of millimeters for concrete) has its own separate rheological behavior and complexities, and its own measurement

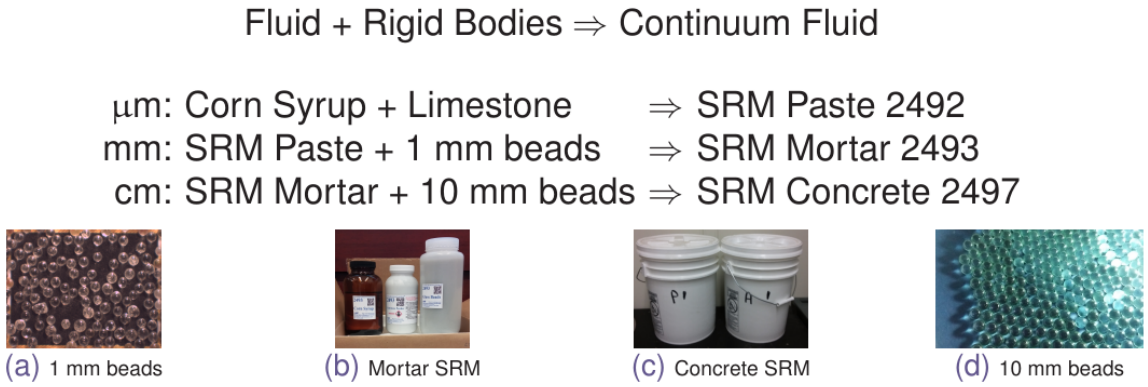

Figure 8. *Multi-scale nature of cement and concrete standard reference materials.*

devices, i.e. rheometers. Our simulations have taken a multi-scale approach, using the cement paste as the matrix fluid for mortar simulations, and then using the mortar as the matrix fluid for the simulation of concrete (see Figure 8). Finally, we bring the length scales back together, using computations to enable the design of standard reference materials for cement paste, mortar, and concrete as well as rheometers for each scale.

Our computational model for the flow of dense suspensions is based on a *smoothed particle hydrodynamics* approach [2, 3]. This model is mesh-free, using mesoscopic particles and a Lagrangian formulation of the generalized Navier-Stokes equations, which gives us great flexibility in handling moving boundaries. Because these suspensions have a non-Newtonian matrix fluid, specifically a shear thinning fluid, we also needed to implement spatially varying viscosity, which the model enables. Most importantly, this model allows for a highly parallel implementation. Because of the size of these simulations, we have utilized the computational facilities at DOE's Argonne National Laboratory, running simulations on Intrepid, an IBM Blue Gene/P, and Mira, an IBM Blue Gene/Q. Over the course of this project we have used more than 160 million CPU-hours of compute time, running individual simulations on up to 128 000 processors. Most of this compute time was awarded to our project through the competitive DOE INCITE program.

Our computations include the simulation of various rheometer geometries, including rheometers with 6-blade spindles and double-helix spindles, with various types of suspensions. The parameters varied for each simulation are the matrix fluid (cement paste or mortar), the volume fractions of suspended particles, the rheometer spindle geometry, and the magnitude of the torque applied to the spindle. The desired output is the rotational speed with a given constant applied torque. An important contribution of the simulations, however, is that they also provide very detailed information about the system at regularly spaced time intervals. This information includes the position and velocity of each mesoscopic matrix fluid particle, and the position, velocity, and angular velocity of each suspended inclusion (sand, gravel, millimeter sized hard glass sphere, etc.), the stress on each suspended inclusion, and other system state data. This information is used to study the interactions between the inclusions, the fluid particles, and the rheometer spindle and walls, as well as the distribution of the stresses and forces in the system over time. Our results are also compared against corresponding physical experiments and the expected results based on our theoretical models of these suspensions. We produce animations of these systems to visually inspect the behavior of the suspensions. These visualizations have access to all the data output by the simulator and can be customized to probe this data interactively, as needed, to augment the visualization with numeric, graphical, and other analytic information.

Over the last year we have resolved an observed discrepancy between the model-predicted rheological properties of the proposed mortar SRM and experimentally measured properties. In Figure 9 we see that at a

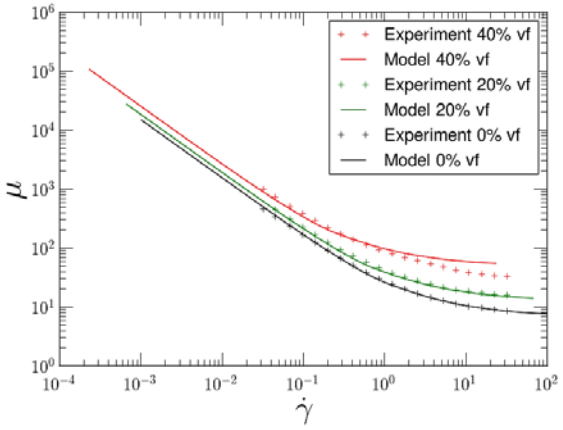

Figure 9. *Plots of viscosity μ versus shear rate $\dot{\gamma}$ for several different percent volume fractions (vf) of suspended particles in a mortar as it is measured in a double-helix rheometer. For each volume fraction, results are shown for both a physical experiment and the expected resultsas computed by our theoretical model. Note the discrepancy at 40% volume fraction.*

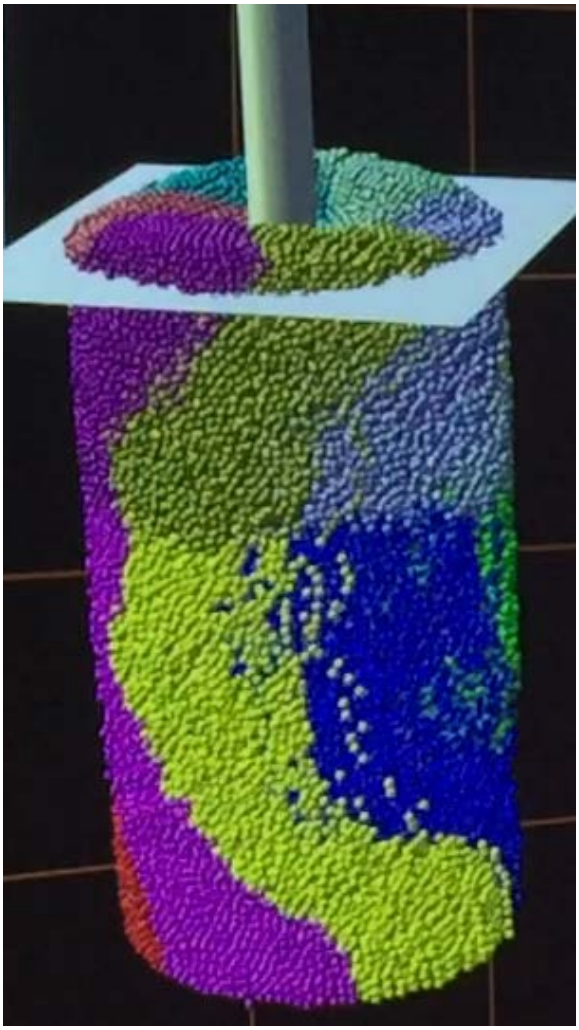

Figure 10. *Snapshot of the mortar SRM in a double-helix rheometer. The white plane shows the initial location of the top of the suspension before starting the rheometer. Colors correspond to the starting quandrant of the suspended beads.*

20% volume fraction of suspended particles, our model closely matches the experimental results when using a rheometer with a double-helix spindle. However, when a suspension with a 40% volume fraction of suspended particles is measured, there is a significant discrepancy with respect to the model. The measured values are much too low, especially as the shear rate is increased. This discrepancy can be explained, as shown in Figure 10, by observing that a portion of the suspension expanded above its initially placement, something the model does not account for. Taking this into account corrects the discrepancy. A similar issue was identified when using a 6-blade spindle, except that in this case the suspension was migrating away from the volume between the blades, resulting in an even greater measurement discrepancy (see Figure 11). In general, our simulations have shown that a rheometer with a double-helix spindle is more effective than a 6-blade, or 4-blade spindle when measuring a dense suspension.

This year we have completed the work on the mortar SRM, including a suite of simulations on the proposed SRM. The mortar SRM has now been released as NIST SRM 2493. A detailed report on this SRM is available as NIST Special Publication 260-187 [4].

Our focus in the coming year is the development of an SRM for concrete. Our efforts will include a suite of simulations of the proposed SRM, using the properties of the mortar SRM as the matrix fluid and 10 mm beads in suspension. As an additional verification, we will also run simulations of the concrete using the paste SRM as the matrix fluid and containing both the 1 mm beads and 10 mm beads as suspended inclusions.

Acknowledgements

This research used resources of the Argonne Leadership Computing Facility at Argonne National Laboratory, which is supported by the Office of Science of the U.S. Department of Energy under contract DE-AC02-06CH11357.

References

[1] C. F. Ferraris, N. S. Martys and W. L. George. Development of Standard Reference Materials for Rheological Measurements of Cement-based Materials. *Cement and Concrete Composites* **54** (2014), 29-33.

[2] N. S. Martys, W. L. George, B-W. Chun and D. Lootens. A Smoothed Particle Hydrodynamics-Based Fluid Model with A Spatially Dependent Viscosity: Application to Flow of a Suspension with a Non-Newtonian Fluid Matrix. *Rheologica ACTA* **49**:10 (2010), 1059–69.

[3] R. A. Gingold and J. J. Monaghan. Smoothed Particle Hydrodynamics: Theory and Application to Non-Spherical Stars. *Monthly Notices of the Royal Astronomical Society* **181** (1977), 375–89.

[4] A. Olivas, C.F. Ferraris, N. S. Martys, W. L. George, E. J. Garboczi and B. Toman. Certification of SRM 2493: Standard Reference Mortar for Rheological Measurements, NIST Special Publication 260-187 (2017).

Participants

William George, Steven Satterfield, Judith Terrill (ACMD); Chiara Ferraris and Nicos Martys (NIST EL); Didier Lootens (Sika AG, Switzerland); Blaza Toman (NIST ITL).

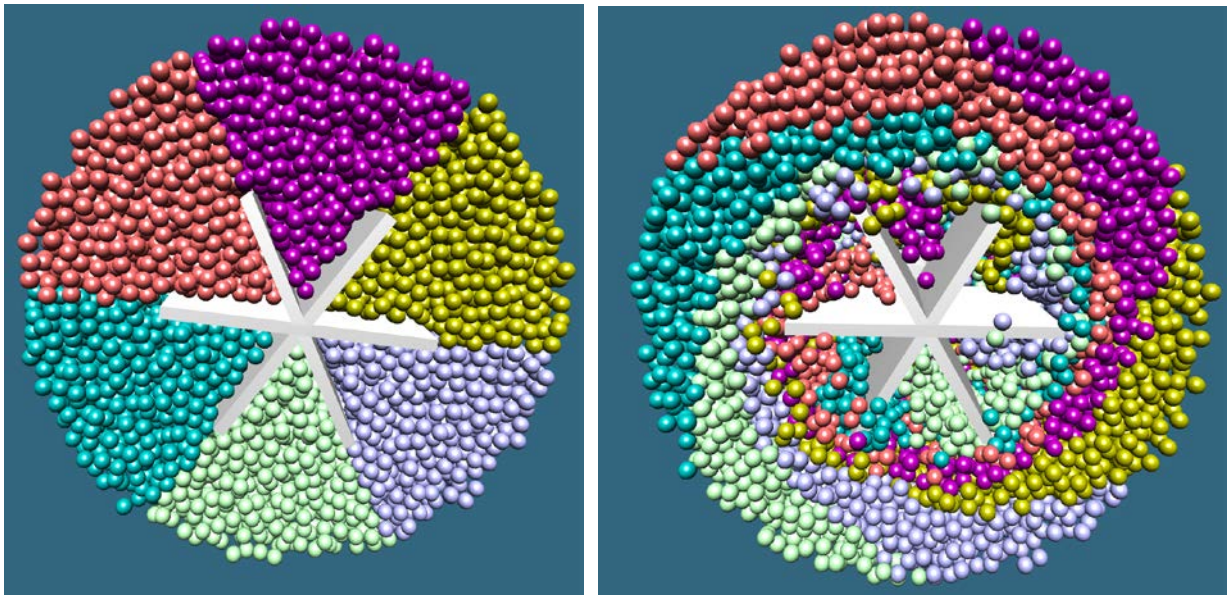

Figure 11. *Mortar in a six-blade spindle as shown from below. Left: initial packing of suspended particles. Right: state of the system after the spindle has rotated 180 degrees. Note the absence of suspended particles between the blades.*

Device-Independent Secure Randomness from Loophole-Free Bell Tests

Two years ago, ACMD researchers participated in a NIST-led team that achieved a landmark loophole-free Bell test of local realism, confirming quantum theory and demonstrating that local realism is violated with strong statistical significance. That work was part of a NIST Innovations in Measurement Science project entitled Quantum Randomness as a Secure Resource, whose goal was to demonstrate the use of such a Bell test to produce verifiably random bits. The motivation for this project was to demonstrate a new class of entropy source for the NIST Randomness Beacon, a Web service that periodically publishes time-stamped random strings that can be checked by anyone and are unpredictable prior to publication. A source based on a Bell test can provide a quantitative statement about the unpredictability of its output without detailed knowledge of its devices; i.e., it is "device independent." This makes it a particularly compelling source for a randomness beacon and a paradigm shift in random number generation. This year, ACMD researchers achieved the world's first production of near-uniform device-independent random bits from a loophole-free Bell test.

Peter Bierhorst and Scott Glancy

Quantum theory has properties that seem surprising and strange from the perspective of classical physics and everyday intuition. These include unavoidable randomness, systems existing in superpositions of states, and entanglement between systems. The most profound divide between classical physics and quantum physics is that classical physics obeys the principle of local realism, but quantum physics does not. This divide was discovered by John S. Bell in 1964 [1]. Since then, physicists have performed a series of experiments suggesting violation of local realism, all of which have suffered from loopholes, and thereby have not definitively ruled out local realism. In the fall of 2015 ACMD researchers participated in a loophole-free test of local realism, a so-called "Bell test," rejecting the hypothesis that the universe obeys local realism with a very high level of statistical significance and ending a decades long quest of foundational physics [2]. See Figure 12.

In 2006 researchers discovered that Bell tests could be used to generate random bits for cryptographic applications in a device-independently secure manner [3]. This discovery means that, given a secure random seed, trust in the unpredictability of the secure string of bits can be derived solely from the outcomes of the Bell test experiment, without needing to trust the internal workings of the hardware, even under the most pessimistic assumption that an untrustworthy adversary provided the hardware.

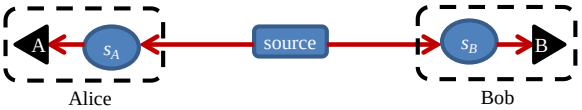

Figure 12. *Basic diagram of an experiment to test local realism. A source sends a pair of particles to measurement stations "Alice" and "Bob." They randomly choose measurement settings s_A and s_B, which determine what property of the particles Alice and Bob measure. They obtain measurement results A and B. If the particles obey the principle of local realism, the probability distribution of (s_A, s_B, A, B) is constrained by Bell inequalities. The experiment is designed to observe violation of one of the inequalities. In the 2015 NIST experiment, the source made entangled photon pairs, which traveled to Alice and Bob along optical fibers. Alice and Bob chose an angle along which to measure the photons' polarization, and detected the photons.*

NIST's development of a loophole-free Bell test was performed with this application in mind. It was part of a five-year NIST-Director-funded project entitled "Quantum Randomness as a Secure Resource." A long-term goal for this project is integration of the test of local realism with the NIST Randomness Beacon [4], a service of the Computer Security Division. The Beacon is designed to ensure that users cannot predict bits before they are made available, that outside parties cannot alter the distribution of the random bits, and that a set of users can access the source in a way that makes them confident they all receive the same random string. The Beacon broadcasts full-entropy bit-strings in blocks of 512 bits every 60 seconds. Each such value is time-stamped, is signed, and includes the hash of the previous value to chain the sequence of values together. This process prevents all, even the source, from retroactively changing an output packet without being detected. The beacon keeps all output packets and provides them online.

Generating Random Bits. Data collected from the NIST Bell test (shown in Figure 13) was used to generate random bits with applications like the Beacon in mind. This process is not as straightforward as it might seem, however. After certifying the violation of local realism, it was necessary to quantify the amount of device-independent randomness in such a data set. Although many theoretical papers describe methods to quantify such randomness, ACMD researchers found none of them to be suitable, because they made unjustified (or false) assumptions or were not sensitive enough to detect the randomness in the data. Thus, ACMD researchers adapted their own prediction-based-ratio (PBR) method (originally used for calculating p-values

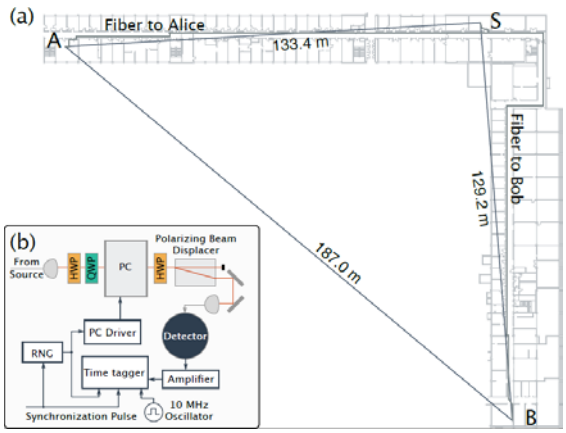

Figure 13. *Diagram of the randomness generation experiment. (a) Alice's lab is located at the end of the spine of NIST Building 1 in Boulder, Bob's lab is at the end of wing 5, and the entanglement source is at the junction. (b) The measurement system used by Alice and Bob. Both Alice and Bob use a fast Pockels cell (PC), two half-waveplates (HWP), a quarter-waveplates (QWP), and a polarizing beam displacer to switch between their respective polarization measurements. A pseudorandom number generator (RNG) governs the choice of each measurement setting for every trial. After passing through the polarization optics, the photons are sent to a high-efficiency, superconducting nanowire detector. The signals from the detector are amplified and sent to a time tagger, where their arrival times are recorded.*

in a hypothesis test of local realism) so that it can quantify randomness. This approach resulted in a new quantification method that is more powerful than prior techniques, can accommodate experimental drifts, and is much more sensitive to the randomness in real-world photonic experiments.

The final step is randomness extraction, in which one converts the data from the test of local realism, which is highly biased and whose distribution may drift in time, into a string of uniformly distributed random bits. The Trevisan extractor was used for this purpose [5]. ACMD researchers adopted existing Trevisan software to run with the NIST Bell test data and made enhancements that reduced the number of seed bits required during the extraction.

Applying these techniques to data obtained from the 2015 NIST Bell test, ACMD researchers extracted 256 random bits that are uniform to within 0.001 and cannot be predicted within any physical theory that allows one to make independent measurement choices and limits all signals to travel no faster than the speed of light [6]. This year, after several improvements were made to the Bell test experiment, which increased the fidelity of quantum states and measurements and the randomness generation rate, ACMD researchers extracted 1 024 bits, uniform to within 10^{-12}. A paper describing this achievement has been accepted by *Nature* [7]. This achievement is the first end-to-end production of secure randomness from a Bell test. It was achieved using the world's most powerful loophole-free Bell-test experiment and the most sensitive and robust theoretical analysis.

Related Efforts. ACMD released their version of the Trevisan extractor on GitHub [8]. ACMD researchers also preformed tests to determine the computation time that would be needed to extract 10 Mbits from an input data set of 1 Gbit. These tests reveal that more than 100 years would be required for a single computer to complete the extraction. However, the Trevisan extraction algorithm is highly parallelizable, so if the work is distributed across 10 000 processors (the number typically found in today's supercomputers) the execution time for such a 1 Gbit dataset could be reduced to a few days.

ACMD researchers also developed a streaming version of the Trevisan code for the NIST Randomness Beacon. This version waits for data sets of varying sizes to arrive (along with metadata) and extracts the randomness present. This version can also be parallelized to meet the current Beacon rate of 512 bits every minute.

In work with Yanbao Zhang, ACMD researchers established a probability estimation framework for randomness generation with classical side information [9]. Implementations of this framework achieve asymptotically optimal randomness generation rates from quantum devices by taking advantage of test supermartingales, a generalization of the PBR method. Further, they demonstrated significantly better results for extracting randomness from historical data, including that analyzed in ACMD's earlier work [6, 7] and data from the first device-independent quantum randomness experiment [10]. Notably, data collection for the latter experiment took about one month, but it would have been less than 4 days with ACMD's new methods.

In 2017 ACMD researchers also participated in The Big Bell Test [11], a collaboration of 13 laboratories around the world, each performing some kind of Bell test. In the Big Bell Test instead of using a typical random number generator, the measurement choices were made by humans through an online game-like system, which collected the human random choices and distributed them to each of the 13 laboratories. Despite significant bias in the human-generated randomness, ACMD was able to demonstrate statistically significant violation of local realism [12].

Future work at NIST includes engineering to develop the technology used in the test of local realism into a reliable device that can operate continuously for long periods without human intervention. Such a device could serve as an entropy source for the NIST Randomness Beacon. Integrating the test of local realism with the Beacon will provide greater assurance both to NIST and the public that the Beacon output is truly unpredictable, which will increase its utility for applications such as unpredictable sampling, new authentication mechanisms, and secure multi-party computation.

References

[1] J. S. Bell. On the Einstein-Podolsky-Rosen Paradox. *Physics* **1** (1964), 195-200.

[2] L. K. Shalm, E. Meyer-Scott, B. G. Christensen, P. Bierhorst, M. A. Wayne, M. J. Stevens, T. Gerrits, S. Glancy, D. R. Hamel, M. S. Allman, K. J. Coakley, S. D. Dyer, C. Hodge, A. E. Lita, V. B. Verma, C. Lambrocco, E. Tortorici, A. L. Migdall, Y. Zhang, D. R. Kumor, W. H. Farr, F. Marsili, M. D. Shaw, J. A. Stern, C. Abellán, W. Amaya, V. Pruneri, T. Jennewein, M. W. Mitchell, P. G. Kwiat, J. C. Bienfang, R. P. Mirin, E. Knill and S. W. Nam. A Strong Loophole-Free Test of Local Realism. *Physical Review Letters* **115** (2015), 250402.

[3] R. Colbeck. Quantum and Relativistic Protocols for Secure Multiparty Computation. PhD Thesis, University of Cambridge, 2006. URL: http://arxiv.org/abs/0911.3814

[4] NIST Randomness Beacon. URL: https://www.nist.gov/programs-projects/nist-randomness-beacon

[5] L. Trevisan. Extractors and Pseudorandom Generators. *Journal of the ACM* **48** (2001), 860.

[6] P. Bierhorst, E. Knill, S. Glancy, Y. Zhang, A. Mink, S. Jordan, A. Rommal, Y.-K. Liu, B. Christensen, S. W. Nam, M. J. Stevens and L. K. Shalm. Experimentally Generated Randomness Certified by the Impossibility of Superluminal Signals, arXiv:1702.05178, 2017.

[7] P. Bierhorst, E. Knill, S. Glancy, Y. Zhang, A. Mink, S. Jordan, A. Rommal, Y.-K. Liu, B. Christensen, S. W. Nam, M. J. Stevens and L. K. Shalm. Experimentally Generated Randomness Certified by the Impossibility of Superluminal Signals. *Nature*, to appear.

[8] Libtrevisan. URL: https://github.com/usnistgov/libtrevisan

[9] E. Knill, Y. Zhang and P. Bierhorst. Quantum Randomness Generation by Probability Estimation with Classical Side Information. arXiv:1709.06159, 2017.

[10] S. Pironio, A. Acin, S. Massar, A. Boyer de la Giroday, D. N. Matsukevich, P. Maunz, S. Olmschenk, D. Hayes, L. Luo, T. A. Manning and C. Monroe. Random Numbers Certified by Bell's Theorem. *Nature* **464** (2010), 1021.

[11] The Big Bell Test, 2017. URL: https://thebigbelltest.org/

[12] The BIG Bell Test Collaboration: C. Abellán, A. Acín, A. Alarcón, O. Alibart, C. K. Andersen, F. Andreoli, A. Beckert, F. A. Beduini, A. Bendersky, M. Bentivegna, P. Bierhorst, D. Burchardt, A. Cabello, J. Cariñe, S. Carrasco, G. Carvacho, D. Cavalcanti, R. Chaves, J. Cortés-Vega, A. Cuevas, A. Delgado, H. de Riedmatten, C. Eichler, P. Farrera, J. Fuenzalida, M. García-Matos, R. Garthoff, S. Gasparinetti, T. Gerrits, F. Ghafari Jouneghani, S. Glancy, E. S. Gómez, P. González, J.-Y. Guan, J. Handsteiner, J. Heinsoo, G. Heinze, A. Hirschmann, O. Jiménez, F. Kaiser, E. Knill, L. T. Knoll, S. Krinner, P. Kurpiers, M. A. Larotonda, J.-Å. Larsson, A. Lenhard, H. Li, M.-H. Li, G. Lima, B. Liu, Y. Liu, I. H. López Grande, T. Lunghi, X. Ma, O. S. Magaña-Loaiza, P. Magnard, A. Magnoni, M. Martí-Prieto, D. Martínez, P. Mataloni, A. Mattar, M. Mazzera, R. P. Mirin, M. W. Mitchell, S. Nam, M. Oppliger, J.-W. Pan, R. B. Patel, G. J. Pryde, D. Rauch, K. Redeker, D. Rieländer, M. Ringbauer, T. Roberson, W. Rosenfeld, Y. Salathé, L. Santodonato, G. Sauder, T. Scheidl, C. T. Schmiegelow, F. Sciarrino, A. Seri, L. K. Shalm, S.-C. Shi, S. Slussarenko, M. J. Stevens, S. Tanzilli, F. Toledo, J. Tura, R. Ursin, P. Vergyris, V. B. Verma, T. Walter, A. Wallraff, Z. Wang, H. Weinfurter, M. M. Weston, A. G. White, C. Wu, G. B. Xavier, L. You, X. Yuan, A. Zeilinger, Q. Zhang, W. Zhang and J. Zhong. Challenging Local Realism with Human Randomness. *Nature*, to appear.

Participants

Peter Bierhorst, Scott Glancy, Stephen Jordan, Emanuel Knill, Yi-Kai Liu and Alan Mink (ACMD); Thomas Gerrits, Richard P. Mirin, Sae Woo Nam, Lynden K. Shalm, Martin J. Stevens and Varun B. Verma (NIST PML); Bradley G. Christensen (University of Illinois at Urbana-Champaign); Morgan Mitchell (The Institute of Photonic Sciences, Spain); Andrea Rommal (SURF student, Muhlenberg College); Yanbao Zhang (University of Waterloo, Canada)

Digital Library of Mathematical Functions

Progress in science has often been catalyzed by advances in mathematics, while cutting-edge science has been a major driver of mathematical research. This symbiotic relationship has been extremely beneficial to both fields. Often the mathematical objects at the intersection of mathematics and physical science are mathematical functions. Effective use of these tools requires ready access to their many properties, a need that was capably satisfied for more than 50 years by the 1964 National Bureau of Standards Handbook of Mathematical Functions with Formulas, Graphs, and Mathematical Tables. *The 21st century successor to the NBS Handbook, the* Digital Library of Mathematical Functions *(DLMF), continues as the gold standard reference for the properties of what are termed the special functions of mathematical physics. A free online resource, the DLMF is a living reference work, undergoing continual updating and improvement. The project has also spawned several related efforts in underlying mathematical knowledge management technology and tools.*

Barry Schneider and Ronald Boisvert

Figure 14. *The online NIST Digital Library of Mathematical Functions (DLMF) is the 21st successor to the 1964 NBS Handbook of Mathematical Functions (top left). A printed companion to the DLMF, published by Cambridge University Press is also available.* Image credit: Bruce Miller

Published by the National Bureau of Standards (NBS) in 1964, the *Handbook of Mathematical Functions with Formulas, Graphs, and Mathematical Tables* [1] remains the most cited and most widely distributed reference work ever produced by NIST. With more than 1 million copies in print, this handbook, which is often referred to as "Abramowitz and Stegun" (A&S) in homage to its two editors, continues to receive more than 2000 citations each year. Thishigh number of citations attests to the fact that the so-called special functions of applied mathematics that this handbook documents are among the most useful tools for mathematical modeling in science, engineering and beyond. Despite its age, A&S continues to be highly referenced, due to its presentation of the essential mathematical properties of both elementary and special functions in an easy-to-digest form. Yet, A&S is a product of the pre-computer era, with more than half of its 1 046 pages devoted to tables of function values for use in hand computation. Since its publication there have been many advances in applied mathematics, leading to a better understanding of these functions, as well as the introduction and use of many additional functions. In addition, there has been a shift from the use of printed publications to online information resources, which can provide many advantages over traditional books.

In 1998 NIST undertook an effort to perform an extensive survey of the research literature, with the goal of producing an up-to-date online reference on the properties of special functions. Some 12 years later, in 2010, the NIST-led project, which represented the collective efforts of some 50 researchers from around the world, released the Digital Library of Mathematical Functions [2]. At the same time, Cambridge University Press published a printed companion, the *NIST Handbook of Mathematical Functions* [3]. We collectively refer to these works as the DLMF.

The DLMF has considerably extended the scope of the original handbook, as well as providing improved accessibility to the worldwide community of scientists and mathematicians [4]. For example, the new handbook contains more than twice as many formulas as the old one, coverage of more functions, in more detail, and an up-to-date list of references. The website covers everything in the printed handbook and much more: additional formulas and graphics, interactive search, zooming and rotation of 3D graphs, internal links to symbol definitions and cross-references for each equation, and external links to online references and sources of software.

Many of the online features of the DLMF are the result of NIST research in the emerging field of mathematical knowledge management. For example, a highly capable tool for the conversion of LaTeX, a popular typesetting system used for mathematically rich documents, to MathML, the W3C standard for the display of

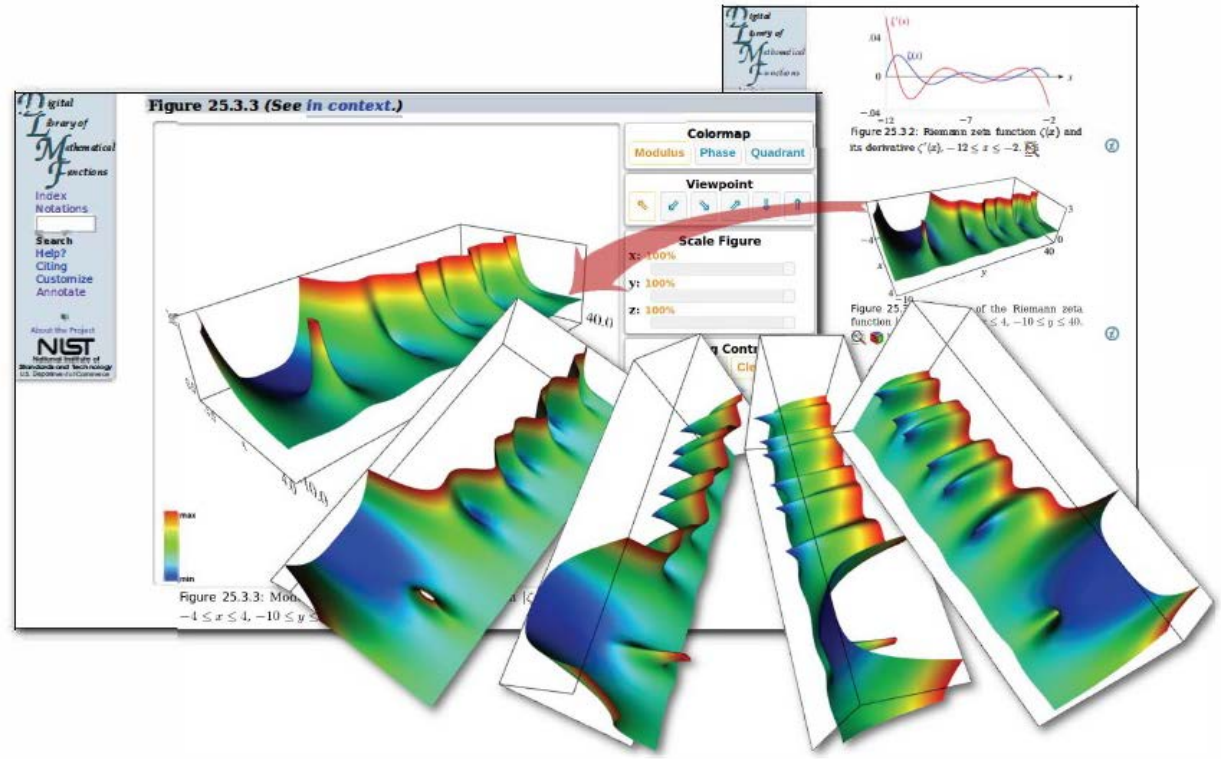

Figure 15. *DLMF's interactive 3D graphics allow the user to change viewpoints, rotate and zoom, rescale, change colormaps and to explore the intersection of the surface with cutting planes.* Image credit: Bruce Miller and Bonita Saunders.

mathematics on the Web, was developed as part of the DLMF project [5]. In addition, a novel system for search in mathematically rich textual databases was developed [6]. At the onset of the DLMF project, techniques for the interactive display of mathematical functions on the Web, which the DLMF project innovated, were hampered by primitive Web technology, requiring specialized plug-ins which were not available in all browsers. Today, DLMF 3D graphics are based on Web3D technology which is universally available [7]. Work on such technologies and tools continues today, see page 100 of this report for details.

To help assess the impact of the DLMF, the NIST library has undertaken a project to track citations to the DLMF, as well as to the original NBS Handbook. While the original Handbook still receives an enormous number of citations, principally due to its large "installed base," citations to the DLMF are steadily growing. As of this writing, more than 3 700 citations are identified by Google Scholar. Online usage remains very high, with 3.4 million pages downloaded during more than 415 000 sessions initiated by more than 261 000 unique visitors during calendar year 2017.

The appearance of the DLMF in 2010 was not the end of the project. To assure the continued vitality of the DLMF deep into the 21st century, corrections to errors, clarifications, bibliographic updates, and addition of new material must continually be made, and new chapters covering emerging subject areas need to be added. In 2017, for example, new releases with various corrections and clarifications, improved notation for integral transforms, a new section on *Fourier Transforms of Special Distributions*, and improvements to icons, decorations and mouse-cursors, including the introduction of scalar vector graphics (SVG) were issued in June, September and December.

One of the design goals for the DLMF was that each formula would be connected to a proof in the literature. This data, visible as metadata annotations on the website, provides either a short proof for the formula, a reference to a proof, or, for definitions, a reference which gives that definition. Unfortunately, this information was not provided by DLMF authors in all cases. We have undertaken an effort to systematically verify the completeness and traceability to published proofs for DLMF formulae. This audit has been completed for Chapter 25 (Zeta and Related Functions) and is actively continuing for Chapters 1-5 and 22-30. In addition, work has progressed to make proof-related information visible in metadata at the equation level. Improvements in markup to more accurately identify the nature of the added material have been developed and deployed (see Chapter 9, Airy and Related Functions, for example).

Larger-scale additions and modifications to the technical content of the DLMF are also in the works. Four external authors have been engaged to develop a new chapter on *Orthogonal Polynomials of Several Variables*, and to make significant additions to existing chapters on *Algebraic Methods*, *Orthogonal Polynomials*, and *Painlevé Transcendents*. Outlines for the new content have been accepted and full drafts are currently under development. We expect to receive these in early 2018. W. P. Reinhardt of the University of Washington, T. Koornwinder of the University of Amsterdam, Y. Yu of the University of Oregon, P. Clarkson of the University of Kent and N. Temme of CWI Amsterdam are contributing to this effort.

Several additional research efforts related to the DLMF are ongoing. These include the DLMF Tables [8], an on-demand Web-based table generation service for special functions, and the Digital Repository of Mathematical Formulae (DRMF) [9], a broad community-based context-free compendium of mathematical formulas and associated mathematical data. In addition, research in mathematical language processing, semantic-preserving translation/interchange of mathematical data, and the visualization of mathematical functions are ongoing. See pages 101-105 of this document for further details. Each of these efforts are contributing to the overall NIST goal to present important and useful mathematical information to the community in a trustworthy manner.

Finally, visibility of the project will be enhanced within the physics community with the publication of an invited article on the DLMF in *Physics Today*, the flagship publication of the American Physical Society, in February of 2018 [10].

References

[1] M. Abramowitz and I. Stegun, eds. *Handbook of Mathematical Functions with Formulas, Graphs and Mathematical Tables*. Applied Mathematics Series 55, National Bureau of Standards, Washington, DC, 1964.

[2] F. W. J. Olver, A. B. Olde Daalhuis, D. W. Lozier, B. I. Schneider, R. F. Boisvert, C. W. Clark, B. R. Miller and B. V. Saunders, eds. NIST Digital Library of Mathematical Functions. URL: http://dlmf.nist.gov/.

[3] F. Olver, D. Lozier, R. Boisvert and C. Clark, eds. *NIST Handbook of Mathematical Functions*. Cambridge University Press, 2010.

[4] R. Boisvert, C. Clark, D. Lozier and F. Olver. A Special Functions Handbook for the Digital Age. *Notices of the American Mathematical Society* **58**:7 (August 2011), 905-911.

[5] B. R. Miller. LaTeXML: A LaTeX to XML Converter. URL: http://dlmf.nist.gov/LaTeXML/

[6] B. Miller and A. Youssef. Technical Aspects of the Digital Library of Mathematical Functions. *Annals of Mathematics and Artificial Intelligence* **38**:1-3, 121136, Springer Netherlands, 2003.

[7] B. Saunders, B. Antonishek, Q. Wang and B. R. Miller. Dynamic 3D Visualizations of Complex Function Surfaces using X3DOM and WebGL. In *Proceedings of the 20th International Conference on 3D Web Technology*, Heraklion, Greece, June 18-21, 2015, 219-225. DOI: 10.1145/2775292.2777140

[8] F. Backeljauw, S. Becuwe, A. Cuyt, J. Van Deun and D. Lozier. Validated Evaluation of Special Mathematical Functions. *Science of Computer Programming* **90**:A (May 2013), 2-20. DOI: 10.1016/j.scico.2013.05.006. See also http://dlmftables.uantwerpen.be/.

[9] H. S. Cohl, M. A. McClain, B. V. Saunders, M. Schubotz and J. C. Williams. Digital Repository of Mathematical Formulae. *Lecture Notes in Artificial Intelligence* **8543**, Proceedings of the Conferences on Intelligent Computer Mathematics 2014, Coimbra, Portugal, July 7-11, 2014, (S. M. Watt, J. H. Davenport, A. P. Sexton, P. Sojka and J. Urban, eds.), Springer, 419-422.

[10] B. I. Schneider, B. R. Miller and B. V. Saunders. NIST's Digital Library of Mathematical Functions. *Physics Today* **71**:2 (February 2018), to appear.

Participants

Ronald F. Boisvert, Howard S. Cohl, Daniel W. Lozier Marjorie A. McClain, Bruce R. Miller, Bonita V. Saunders, and Barry I. Schneider (ACMD); Brian Antonishek (NIST EL); Charles W. Clark (NIST PML); Adri B. Olde Daalhuis (University of Edinburgh); William P. Reinhardt (University of Washington); Tom Koornwinder (University of Amsterdam); Yuan Yu (University of Oregon); Peter Clarkson (University of Kent, UK); Nico Temme (CWI Amsterdam); Amanda Hu and Nina Tang (Poolesville High School); Ananya Krishnan, Jonathan Lin, Jeff Tran and Derek Yao (Richard Montgomery High School)

Combinatorial Testing for Software-based Systems

Checking that software produces correct results for all possible inputs, so-call exhaustive testing, is far beyond the reach of even modest size systems, since the number of tests grows exponentially with the number of parameters and their possible settings. So, the question arises: how does one select tests that will provide the most confidence that a system is operating correctly? One useful observation is that while the behavior of a software system may be affected by many factors, only a few are involved in any given failure. Failures of this type are known as interaction faults. Combinatorial testing (CT) is a versatile methodology for detecting interaction faults. CT began as pairwise testing to detect interaction faults involving two factors. However, NIST investigations of failures in actual systems showed that while most faults involved single factors or interactions between two factors, some faults involved three or more factors. Thus, while pairwise (2-way) testing is useful, it may not be sufficient. About a decade ago, NIST took the initiative to extend 2-way CT to higher strength t-way CT for t > 2. NIST has helped make CT practical by developing research tools and techniques for generating combinatorial test suites. CT has now gained significant interest from international software testing community. Many successful results from the use of CT in aerospace, automotive, and financial service industries, as well as defense, security, and electronic medical systems have since been reported.

Raghu Kacker

In 1997 the Mars Pathfinder began experiencing system resets at seemingly unpredictable times soon after it landed and began collecting data. Fortunately, engineers were able to deduce and correct the problem, which occurred only when (1) a particular type of data was being collected, and (2) intermediate priority tasks exceeded a certain load, allowing a blocking condition that eventually triggered a reset. Many critical system failures have been traced to situations of this type, which are known as *interaction faults*. Interaction faults are often insidious in that they may remain hidden until the unfortunate combination is encountered during system operation.

Combinatorial testing (CT) is based on an empirical observation, referred to as the *interaction rule*, that while the behavior of a software system may be affected by a large number of factors, only a few are involved in any given failure. NIST investigations of actual faults show that most involved just one or two factors, though some may involve three, four or more [1]. (A fault involving more than six factors has not yet been reported.) CT began as pairwise (2-way) testing to detect faults involving two factors. More than a decade ago, NIST took the lead to advance CT from 2-way to higher strength *t*-way testing for $t > 2$ [2].

	Parameters									
Rows	**1**	**2**	**3**	**4**	**5**	**6**	**7**	**8**	**9**	**10**
1	0	0	0	0	0	0	0	0	0	0
2	1	1	1	1	1	1	1	1	1	1
3	1	1	1	0	1	0	0	0	0	1
4	1	0	1	1	0	1	0	1	0	0
5	1	0	0	0	1	1	1	0	0	0
6	0	1	1	0	0	1	0	0	1	0
7	0	0	1	0	1	0	1	1	1	0
8	1	1	0	1	0	0	1	0	1	0
9	0	0	0	1	1	1	0	0	1	1
10	0	0	1	1	0	0	1	0	0	1
11	0	1	0	1	1	0	0	1	0	0
12	1	0	0	0	0	0	0	1	1	1
13	0	1	0	0	0	1	1	1	0	1

Figure 16. *A covering array of 13 rows includes all eight triplets (000, 001, 010, 011, 100, 101, 110, and 111) between two possible values (0 and 1) for every three of the 10 parameters represented by columns (for example, see colored entries).*

A combinatorial suite of test cases for *t*-way testing covers (includes) all *t*-way combinations of factor values among the complete set of *k*-factors that are tested ($k > t$). Mathematical objects called covering arrays make it possible to test all *t*-way combinations with a small number of test cases. Figure 16 shows a covering array of only 13 rows which covers all 960 3-way combinations of ten 2-valued factors. In practice, many factors have dependencies and constraints, with the consequence that not all *t*-way combinations may be logically valid. A combinatorial test suite must avoid such forbidden combinations.

In practice, one wants a minimal covering array, that is, one containing all *t*-way combinations in the smallest number of rows possible, since this leads to the least number of tests. However, generating minimal covering arrays is notoriously difficult; it is NP hard in general. As a result, a great deal of research has been done to develop heuristics that can generate covering arrays with relatively small numbers of rows. NIST has developed several such algorithms.

NIST-Developed Tools. NIST and its collaborators have developed several research tools to serve as a testbed for its new algorithms and to study the practicality of CT. ACTS (for Automated Combinatorial Testing for Software), which was developed in cooperation with the University of Texas at Arlington, generates high strength test suites for CT. The ACTS tool is optimized

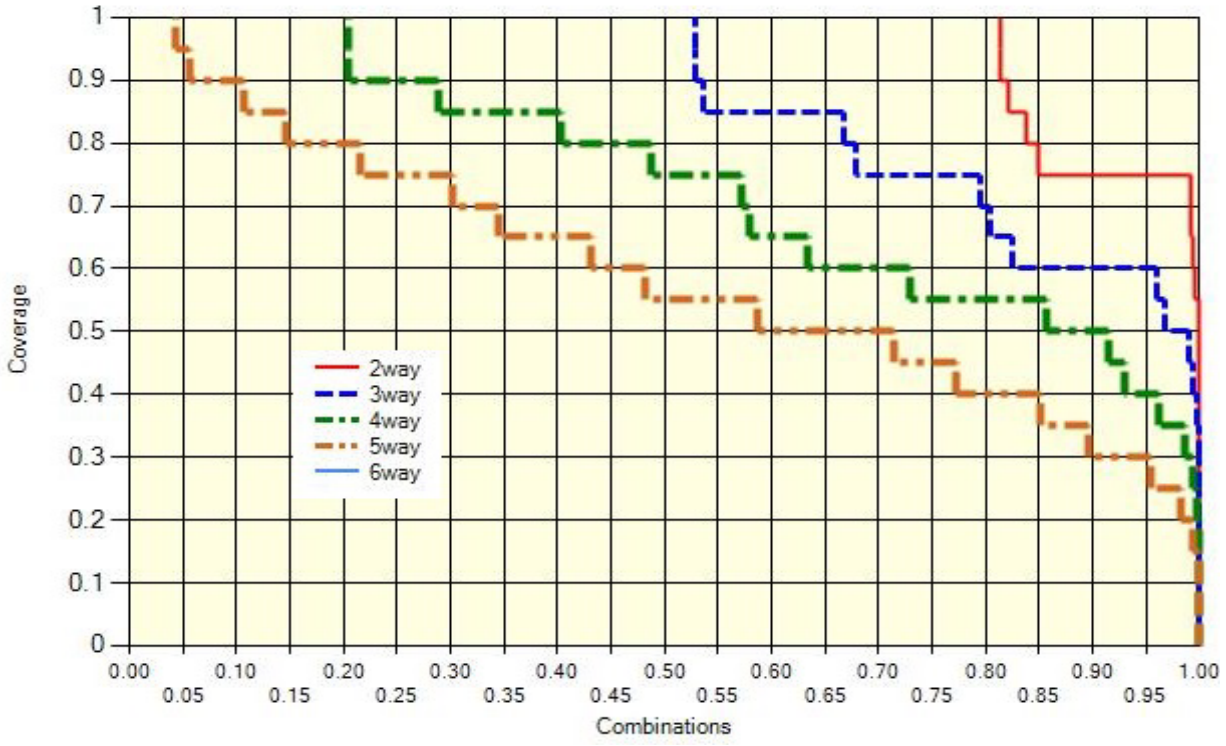

Figure 17. *Combinatorial t-way coverage of a test suite of 7489 tests of 82 variables for t=2, 3, 4, and 5. The graph show the percentage (ordinate) of the fraction (abscissa) of all t-way combinations that are covered by a given test suite*

to efficiently avoid forbidden combinations of test settings. About 3000 users have downloaded an executable version of the ACTS tool from NIST [2]. (Others are now redistributing it.) We are now at version 3.0.

A second research tool, CCM (for Combinatorial Coverage Measurement), developed jointly by NIST and a guest researcher from CENAM, the national metrology institute of Mexico, determines the combinatorial coverage of a test suite that may not have been developed from a CT viewpoint. The extent of combinatorial coverage may be illustrated by graphing the percentage (ordinate) of the fraction (abscissa) of all *t*-way combinations that are covered by a given test suite. Figure 17 shows combinatorial *t*-way coverage of a test suite of 7 489 tests of 82 factors for $t = 2, 3, 4,$ and 5. The area under a curve represents the proportion of combinations that are covered by the test suite. Conversely, the area above the curve represents input parameter combinations for which correct operation has not been verified. The combinatorial deficiency of a test suite can be remedied by additional tests. Thus, CCM can help guide the expansion of a test suite to satisfy stated combinatorial requirements [11]. The latest version of CCM supports constraints. A parallel processing version is also available [2].

Impact of NIST Research. NIST efforts have sparked a surge of research and application of CT technology. A NIST Special Publication on CT has been downloaded more than 30 000 times [3]. In 2013, we published a book with CRC Press on this topic [4].

One of the first large-scale users with whom we worked was a group at the U.S. Air Force Base in Eglin, Florida. The behavior of one of their systems depended on the sequential order of certain events. This observation led to the problem of testing sequences of events, which required development of new mathematical objects called sequence covering arrays [7, 8, 9]. Lockheed-Martin, a large U.S. defense contractor, reported (based on eight projects) that use of CT reduced cost of testing by about 20 % with 20 % to 50 % improvement in test coverage [10]. CT methods are now being used in diverse areas such as financial services, automotive, automation, avionics, video coding standards, and for security testing. CT is now included in software engineering courses taught in more than 18 U.S. universities. NIST efforts on technology transfer of CT tools and techniques received the 2009 Excellence in Technology Transfer Award from the Federal Laboratory Consortium-Mid Atlantic Region.

CT has also gained significant interest from the software testing research community. In 2012, NIST took lead in organizing an International Workshop on CT (IWCT) in conjunction with the IEEE International Conference on Software Testing, Verification, and Validation (ICST), a premier conference in this field [5]. Since then, IWCT has become an annual event for sharing advancements in CT tools and techniques, as well as

results from practical industrial use of CT [6]. The 6th such IWCT was held at Waseda University, Tokyo, Japan on March 13-17, 2017. Four of us (Kacker, Kuhn, Lei and Simos) were among co-organizers. The workshop received 37 submissions of which 14 papers were selected by the Program Committee [6].

Recent Research Efforts. We are jointly investigating the use of CT methods for cyber-security applications with a consortium of universities and industry led by SBA-Research, a leading Austrian research center for information security. The NIST CCM tool was used to analyze the combinatorial coverage of test inputs of some open-source cryptographic suites. In most cases combinatorial coverage was low, suggesting that standard test sets for these widely used cryptographic packages may provide insufficient testing [12, 13].

Complete Modified Condition Decision Coverage (MC/DC) is a "gold standard" criterion for the thoroughness in testing software. Complete MC/DC requires each condition of every decision in the program to be tested by showing its independent effect on the whole decision. The U.S. Federal Aviation Administration (FAA) requires complete MC/DC for systems that are most safety critical (Level A). The cost of assuring complete MC/DC may exceed 75 % of the total development cost. Even achieving high (but not complete) MC/DC can be difficult and expensive. This year, we conducted an empirical study to determine whether CT can generate test cases to achieve high MC/DC. We also investigated the use of CT to efficiently improve statement coverage and branch coverage in testing software. We determined that CT can improve MC/DC, statement coverage, and branch coverage in an efficient way. The gain in increased MC/DC, statement coverage, and branch coverage from the use of 5-way combinatorial testing is limited, but the number of test cases required for 5-way testing is very large. So, we recommend only 3-way or 4-way test sets when CT is used to improve MC/DC, statement coverage, and branch coverage [14].

We also investigated effectiveness of CT for testing data mining algorithms (DMA). Testing DMA is challenging because they involve complex computations and decision logic, and the datasets typically have complex structure. Also, DMA are designed to process large datasets (which is impractical for testing in development stages). Major findings from our investigations are as follows. Large datasets do not necessarily achieve higher branch coverage. After 4-way testing, further higher strength (5-way to 6-way) test sets no longer provide significant increase in branch coverage. Branch coverage correlates well with mutation coverage (which is more expensive to measure) This suggests that branch coverage could be used as a good indicator of fault detection effectiveness for DMA [15].

We investigated the number of factors involved in software failures from faults that are difficult to reproduce. We determined that, not surprisingly, faults that are generally difficult to reproduce (which involve indirect factors) tend to be triggered by larger number of factors. So, they require higher strength CT [16].

We developed a mathematical model for the observed real-life distributions of faults detected by combinatorial testing. The model predicts that more complex faults are exponentially more difficult to detect because *t*-way combinations for higher values of *t* have lower density. One-way and 2-way faults tend to decline rapidly as software is tested [17].

References

[1] D. R. Kuhn, D. R. Wallace and A. M. Gallo, Jr. Software Fault Interactions and Implications for Software Testing. *IEEE Transactions on Software Engineering* **30**:6 (June 2004), 418-421. DOI: 10.1109/TSE.2004.24

[2] https://csrc.nist.gov/projects/automated-combinatorial-testing-for-software

[3] D. R. Kuhn, R. N. Kacker and Y. Lei. Practical Combinatorial Testing, Special Publication 800-142, NIST, Gaithersburg, Maryland, October 2010. URL: http://nvlpubs.nist.gov/nistpubs/Legacy/SP/nistspecialpublication800-142.pdf

[4] D. R. Kuhn, R. N. Kacker and Y. Lei. *Introduction to Combinatorial Testing*. CRC Press, 2013.

[5] http://aster.or.jp/conference/icst2017/

[6] http://iwct2017.sba-research.org/

[7] D. R. Kuhn, J. M. Higdon, J. F. Lawrence, R. N. Kacker and Y. Lei. Combinatorial Methods for Event Sequence Testing. In *Proceedings of the 5-th IEEE International Conference on Software Testing, Verification and Validation Workshops (ICSTW)*, Montreal, Quebec, Canada, April 17-21, 2012, 601-609. DOI: 10.1109/ICST.2012.147

[8] D. R. Kuhn, J. M. Higdon, J. F. Lawrence, R. N. Kacker and Y. Lei. Efficient Methods for Interoperability Testing using Event Sequences. *CrossTalk: The Journal of Defense Software Engineering*, July/August 2012, 15-18.

[9] Y. M. Chee, C. J. Colbourn, D. Horsley and J. Zhou. Sequence Covering Arrays. *SIAM Journal of Discrete Mathematics* **27** (2013) 1844-1861.

[10] J. Hagar, D. R. Kuhn, R. N. Kacker and T. Wissink. Introducing Combinatorial Testing in a Large Organization. *IEEE Computer* **48** (April 2015) 64-72.

[11] D. R. Kuhn, R. N. Kacker and Y. Lei. Combinatorial Coverage as an Aspect of Test Quality. *CrossTalk (Hill AFB): The Journal of Defense Software Engineering*, (March/April 2015), 19-21.

[12] D. E. Simos, K. Kleine, A. G. Voyiatzis, D. R. Kuhn and R. N. Kacker. TLS Cipher Suites Recommendations: A Combinatorial Coverage Measurement Approach. In *Proceedings of the IEEE International Conference on Software Quality, Reliability and Security (QRS 2016)*, Vienna, Austria, August 1-3, 2016. DOI: 0.1109/QRS.2016.18

[13] D. E. Simos, D. R. Kuhn, A. G. Voyiatzis and R. N. Kacker. Combinatorial Methods in Security Testing. *IEEE Computer* **49** (October 2016), 80-83. DOI: 10.1109/MC.2016.314

[14] D. Li, L. Hu, R. Gao, W. E. Wong, D. R. Kuhn and R. N. Kacker. Improving MC/DC and Fault Detection Strength Using Combinatorial Testing. In *Proceedings of the IEEE International Conference on Software Quality, Reliability, and Security (QRS 2017)*, Prague, Czech Republic, July 25-29, 2017. DOI: 10.1109/QRS-C.2017.131

[15] J. Chandrasekaran, H. Feng, Y. Lei, D. R. Kuhn and R. N. Kacker. Applying Combinatorial Testing to Data Mining Algorithms. In *Proceedings of the 10th IEEE International Conference on Software Testing, Verification and Validation Workshops(ICSTW)*, Tokyo, Japan, March 13-17, 2017, 253-261. DOI: 10.1109/ICSTW.2017.46

[16] Z. B. Ratliff, D. R. Kuhn, R. N. Kacker, Y. Lei and K. S. Trivedi. The Relationship Between Software Bug Type and Number of Factors Involved in Failures. In *Proceedings of the 27th IEEE International Symposium on Software Reliability Engineering (ISSRE) Workshops*, Ottawa, Canada, October 23-27, 2016, 119-124. DOI: 10.1109/ISSREW.2016.26

[17] D. R. Kuhn, R. N. Kacker and Y. Lei. A Model for *t*-way Fault Profile Evolution During Testing. In *Proceedings of the 10th IEEE International Conference on Software Testing, Verification and Validation Workshops(ICSTW)*, Tokyo, Japan, March 13-17, 2017, 162-170. DOI: 10.1109/ICSTW.2017.35

Participants

Raghu N. Kacker and James F. Lawrence (ACMD); D. Richard Kuhn (NIST ITL); Yu Lei (University of Texas at Arlington); Mohammad S. Raunak (Loyola University Maryland); Eric Wong (University of Texas at Dallas); Dimitris E. Simos (SBA-Research, Austria); Itzel Dominguez-Mendoza (CENAM, Mexico)

Part III

Project Summaries

Mathematics of Metrology

Mathematics plays an important role in measurement science. Mathematical models are needed to understand how to design effective measurement systems and to analyze the results they produce. Mathematical techniques are used to develop and analyze idealized models of physical phenomena to be measured, and mathematical algorithms are necessary to find optimal system parameters. Mathematical and statistical techniques are needed to transform measured data into useful information. The goal of this work is to develop fundamental mathematical methods and tools necessary for NIST to remain a world-class metrology institute, and to apply these methods and tools to problems in measurement science.

A Thousand-Fold Performance Leap in Ultrasensitive Cryogenic Detectors

Joel Ullom, et al. (NIST PML)
Lawrence Hudson et al. (NIST PML)
Terrence Jach (NIST MML)
Bradley Alpert

Small arrays of ultrasensitive cryogenic detectors developed at NIST have driven breakthroughs in x-ray materials analysis, nuclear forensics, and astrophysics. They have played a large role in prominent international science collaborations in recent years. Despite these successes, NIST's existing cryogenic sensor technology is inadequate for new applications such as in-line industrial materials analysis, energy resolved x-ray imaging, and next-generation astrophysics experiments, which all require faster sensors, much larger arrays, or both.

Three years ago, NIST initiated an Innovations in Measurement Science (IMS) project whose goal was a 1000-fold increase in sensor throughput, to be accomplished via a completely new sensor readout (microwave multiplexer) enabling much larger detector arrays and through major new, higher throughput, processing capabilities. The program underwent its three-year review this year to evaluate progress. The result was an award of unanticipated additional funding for evaluating the feasibility of new quantum-noise-limited amplifiers during the final two years of the project.

New collaborations this year include one with BAE, funded by IARPA, for x-ray tomographic imaging of the internal structure of microcircuits at 20 nm resolution, and with SLAC, funded by DOE, for development of a spectrometer for an upgrade of the LINAC Coherent Light Source (LCLS-II), an ultra-fast, ultra-bright free electron laser. Both require new transition-edge-sensor (TES) microcalorimeter detector arrays operated at higher photon rates than previously achieved, with the LCLS-II collaboration also stipulating better energy resolution than ever achieved with TES detectors.

This year, Alpert demonstrated a method for processing a sample data collection at rates anticipated for the new collaborations. In addition to detector nonlinearity at these rates, an important hurdle is the lack of visibility of the detector baseline response and the associated difficulty of characterizing system drift. The ACMD component of the project team's multidisciplinary expertise has led to key interaction between signal analysis and the design of next-generation detector arrays with improved instrumentation.

Related project work on calibration curves and spectrum analysis methods have led to improved energy resolution and decreased uncertainty of positions and shapes of fluorescence lines of certain lanthanide metals and initial demonstration of potential for standard reference data based on microcalorimeter measurements.

[1] L. Miaja-Avila, G. C. O'Neil, Y. I. Joe, B. K. Alpert, N. H. Damrauer, W. B. Doriese, S. M. Fatur, J. W. Fowler, G. C. Hilton, R. Jimenez, C. D. Reintsema, D. R. Schmidt, K. L. Silverman, D. S. Swetz, H. Tatsuno and J. N. Ullom. Ultrafast Time-Resolved Hard X-Ray Emission Spectroscopy on a Tabletop. *Physical Review X* **6** (2016), 031047. DOI: 10.1103/PhysRevX.6.031047

[2] G. C. O'Neil, L. Miaja-Avila, Y. Il Joe, B. K. Alpert, M. Balasubramanian, S. Dodd, W. B. Doriese, J. W. Fowler, W. K. Fullagar, G. C. Hilton, R. Jimenez, B. Ravel, C. D. Reintsema, D. R. Schmidt, K. L. Silverman, D. S. Swetz, J. Uhlig and J. N. Ullom. Ultrafast Time-Resolved X-Ray Absorption Spectroscopy of Ferrioxalate Photolysis with a Laser Plasma X-Ray Source and Microcalorimeter Array. *The Journal of Physical Chemistry Letters* **8** (2017), 1099-1104. DOI:10.1021/acs.jpclett.7b00078

[3] W. B. Doriese, P. Abbamonte, B. K. Alpert, D. A. Bennett, E. V. Denison, Y. Fang, D. A. Fischer, C. P. Fitzgerald, J. W. Fowler, J. D. Gard, J. P. Hays-Wehle, G. C. Hilton, C. Jaye, J. L. McChesney, L. Miaja-Avila, K. M. Morgan, Y. I. Joe, G. C. O'Neil, C. D. Reintsema, F. Rodolakis, D. R. Schmidt, H. Tatsuno, J. Uhlig, L. R. Vale, J. N. Ullom and D. S. Swetz. A Practical Superconducting-Microcalorimeter X-Ray Spectrometer for Beamline and Laboratory Science. *Review of Scientific Instruments* **88** (2017), 053108. DOI:10.1063/1.4983316

[4] J. W. Fowler, B. K. Alpert, W. B. Doriese, J. Hays-Wehle, Y.-I. Joe, K. M. Morgan, G. C. O'Neil, C. D. Reintsema, D. R. Schmidt, J. N. Ullom and D. S. Swetz. When Optimal Filtering Isn't. *IEEE Transactions on Applied Superconductivity* **27**:4 (2017), 2500404. DOI:10.1109/TASC.2016.2637359

[5] J. W. Fowler, B. K. Alpert, W. B. Doriese, G. C. Hilton, L. T. Hudson, T. Jach, Y.-I. Joe, K. M. Morgan, G. C.

O'Neil, C. D. Reintsema, D. R. Schmidt, D. S. Swetz, C. Szabo-Foster and J. N. Ullom. A Reassessment of Absolute X-ray Line Energies for Lanthanide Metals. *Metrologia* **54**:4 (2017), 494-511. DOI: 10.1088/1681-7575/aa722f

[6] J. W. Fowler, C. G. Pappas, B. K. Alpert, W. B. Doriese, G. C. O'Neil, J. N. Ullom and D. S. Swetz. Approaches to the Optimal Nonlinear Analysis of Microcalorimeter Pulses, in review.

Scanning Microwave Impedance Microscopy

Zydrunas Gimbutas
Andrew Dienstfrey
Samuel Berweger (NIST PML)
Pavel Kabos (NIST PML)

Scanning microwave impedance microscopy (sMIM) is a near-field measurement technique for mapping electromagnetic material properties over broad bandwidths with nanometer resolution. The measurement device consists of a microwave source driving a custom designed, shielded atomic force microscopy (AFM) probe. The reflected microwave signal is coupled to a vector network analyzer for subsequent analysis [1-3]. Applications include chip structure imaging and defect detection, material characterization (e.g., conductors, semiconductors, dielectrics), and subsurface imaging.

In FY 2017 we considered an electromagnetic model for this measurement technique and developed associated numerical software for computing solutions assuming axisymmetric geometries. Initial comparisons with measured data obtained by our PML collaborators show qualitative agreement with our computations. In the FY 2018 we plan to investigate the possibility of making quantitative comparisons between our electromagnetic model and NIST measurements, and will extend the computational tools to solve the problem in general three-dimensional configurations assuming no symmetry conditions.

As the characteristic length scales for AFM are tens of nanometers and freespace microwave wavelengths are measured in tens of centimeters, sMIM is deeply sub-wavelength and near-field. Thus, Maxwell's equations may be replaced by an electrostatic problem with piecewise constant material properties

$$\nabla \cdot \varepsilon \, \mathbf{E} = 0, \quad \mathbf{E} = -\nabla\varphi$$

with boundary conditions

$$\begin{cases} \varphi = C, & \text{conductor} \\ [\varphi] = 0, \quad \left[\varepsilon \dfrac{\partial \varphi}{\partial n}\right] = 0, & \text{dielectric} \end{cases}$$

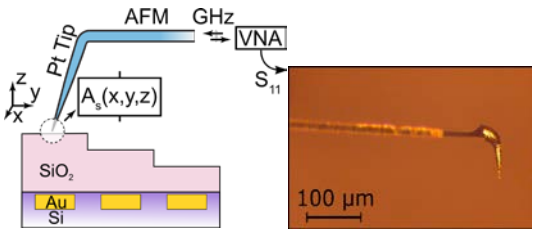

Figure 18. *Atomic Force Microscopy schematic and electrochemically etched platinum tip. This non-standard, conductive AFM tip is used to act as a microwave waveguide.*

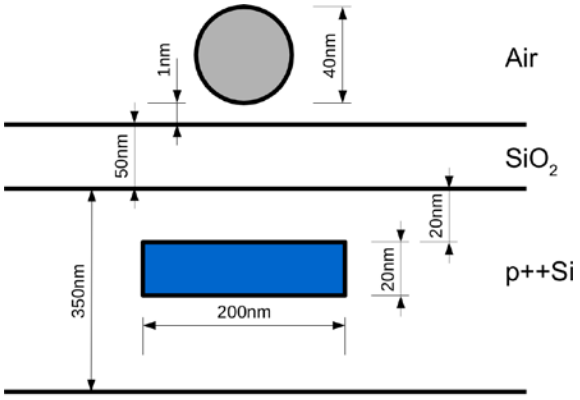

Figure 19. *Sample experiment setup where the material properties are: ε_r = **1** (air), ε_r = **3.0** (silicon oxide, SiO_2), and ε_r = **11.9**, $\sigma \approx$ **1 S/m** (doped silicon, p++Si).*

on conductors and dielectric interfaces, respectively. The effective electromagnetic material properties may be modeled using constant permittivity and conductivity (ε_r and σ). The result is a complex, frequency-dependent dielectric function ε given by $\varepsilon = \varepsilon_r\varepsilon_0 + \frac{\sigma}{i\omega}$ where $\varepsilon_0 \approx 8.8542 \times 10^{-12}$ F/m. We choose a potential representation for the solution to the partial differential equation

$$\varphi(x) = \int_\Gamma G(x,x')\,\sigma(x')\,d\Gamma$$

where $G(x,x') = 1/(4\pi|x-x'|)$ is the free-space Green's function for the Laplace equation in 3D.

As first step toward investigating the model, we assume an axisymmetric configuration between probe tip and a metallic inclusion embedded in doped silicon under a silicon dioxide layer. The geometry is shown in Figure 19. This axisymmetric configuration allows for further reduction in the complexity of the solver, as we may decompose the Green's function into its Fourier modes in cylindrical coordinates

$$\mathrm{G}(x,x') = \frac{1}{4\pi^2\sqrt{rr'}} \times$$

$$\sum_{m=-\infty}^{\infty} Q_{m-1/2}\left(\frac{r^2+r'^2+(z-z')^2}{2rr'}\right) e^{im(\theta-\theta')}$$

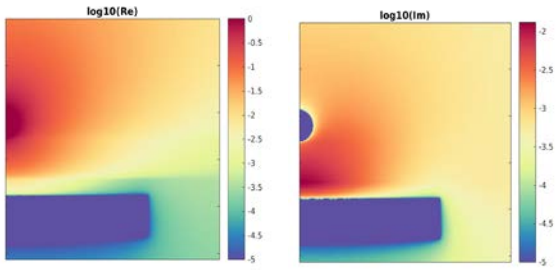

Figure 20. *Probe tip radius* 20 nm, *gap* 1 nm; SiO_2 50 nm *over* p++Si. *Target PEC disk radius* 200 nm, *thickness* 50 nm, *located at depth* 2 0nm *inside* p++Si *layer. Real and imaginary parts of solution* φ *are shown (in logarithmic scale).*

where $\mathbf{x} = (r\cos\theta, r\sin\theta, z)$, likewise for the primed variables, and $Q_{m-1/2}$ are the toroidal functions (half degree Legendre functions of the second kind). We refer to the relatively recent papers by Cohl for a derivation [4, 5].

Using this decomposition, the surface integrals over AFM probe tip and material discontinuities may be replaced with one-dimensional integrals over their defining contours. In principal, this geometric simplification comes at the cost of coupling the equations across Fourier modes *m*. As only zero-th mode $m = 0$ is needed for our problem, we solve a 1-D integral equation using adaptive quadratures to resolve singularities at corners. Note that while the AFM tip is shown as a sphere in the figure, our solver is designed for a general axisymmetric tip shape. As the true AFM tip geometry can be hard to determine experimentally, one of the issues to be investigated using the model is the sensitivity of sMIM measurement capabilities to this shape.

We verified our solver by comparison of solutions to test problems with those obtained using a commercial finite element package. The solutions agree to several digits in evaluation of the complex capacitance. As the finite element solver discretizes all of space (2-D in the axisymmetric case), whereas we solve for a potential on a contour, our solver is orders of magnitude faster. An example of the complex *E*-field computed by us is shown in Figure 20.

In future investigations, we would like to recover cantilever stiffness parameters and electrostatic force contributions to match the measured forces, connect instrument microwave measurements (admittance and impedance) to the solver, build layered media Green's functions for full 3D scan modeling, and perform sensitivity studies for material parameters and resolution.

[1] J. Smolin, H. P. Huber, M. Hochleitner, M. Moertelmaier and F. Kienberger. Scanning Microwave Microscopy/Spectroscopy on Metal-Oxide Semiconductor Systems. *Journal of Applied Physics* **108** (2010), 064315.

[2] D. Wu, *et al.* Uncovering Edge States and Electrical Inhomogeneity in MoS_2 Field-effect Transistors. *Proceedings of the National Academy of Sciences* 113:31 (2016), 8583-8588.

[3] S. Berweger, *et al.* Near-field Microwave Microscopy of One-dimensional Nanostructures. International Microwave Symposium, San Francisco, CA, 2016

[4] H. S. Cohl and J. E. Tohline. A Compact Cylindrical Green's Function Expansion for the Solution of Potential Problems. *The Astrophysical Journal* 527 (1999), 86-101.

[5] H. S. Cohl, *et al.* Useful Alternative to the Multipole Expansion of $1/r$ Potentials. *Physical Review A* **64** (2001), 052509.

Quantitative MRI

Andrew Dienstfrey
Zydrunas Gimbutas
Stephen Russek (NIST PML)
Katy Keenan (NIST PML)
Karl Stupic (NIST PML)
Michael Boss (NIST PML)

Magnetic resonance imaging (MRI) is maturing as a quantitative biomedical imaging technology. For example, imaging facilities routinely report tumor volumes in units of mm^3, blood perfusion in units of ml g^{-1} min^{-1}, apparent diffusion coefficient in mm^2 s^{-1}, and temperature in K. In addition to these biophysical quantities, new parameters specific to MRI physics such as T_1 and T_2 proton relaxation times, reported in s, are being considered as biomarkers for a variety of pathologies including traumatic brain injury, multiple sclerosis, and liver disease. Despite such use, as of a few years ago the attachment of SI units to MRI-based measurements of these quantities was potentially unwarranted as SI traceability chains for these MRI measurement modalities were unclear if not non-existent. In recent years, NIST and partner institutions have made substantial investments to develop such traceability chains.

In FY 2017, we collaborated with several researchers from the NIST Applied Physics Division to complete specifications of a new NIST measurement service reporting proton relaxation times. Thus, for the first time, in vivo measurements of these MRI parameters can exhibit traceability to a national metrology institute. Initial customers have requested the measurement service and we anticipate providing the first such calibrations in the second quarter of FY 2018.

MRI is a technique for imaging the distribution of magnetic resonance features within a substance. Whereas the spatial variation of these features is critically relevant for medical applications, a quantitative calibration service is better served by restricting to smaller volumes for purposes of controlling uniformity of magnetic fields, temperature, and material homogeneity. In practice, such "single-voxel" MRI is referred to as nuclear magnetic resonance, or NMR.

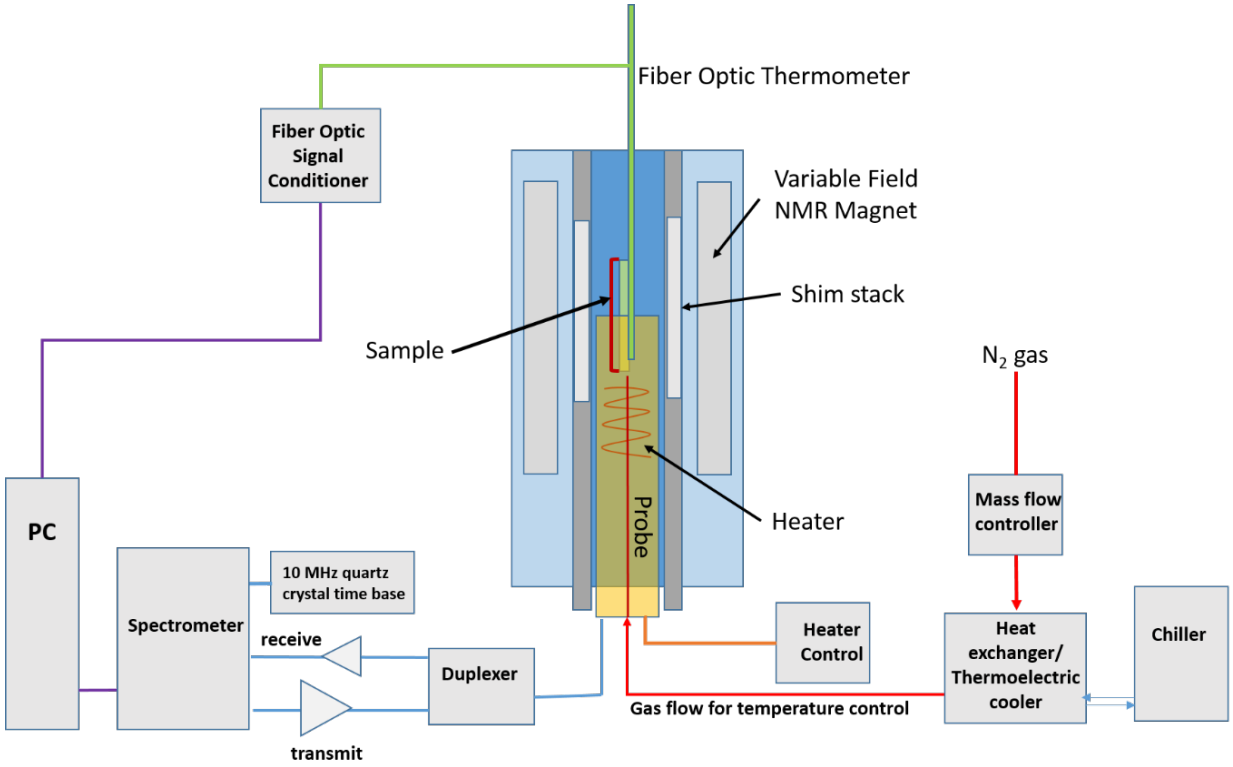

Figure 21. *Schematic of the NIST NMR measurement system.*

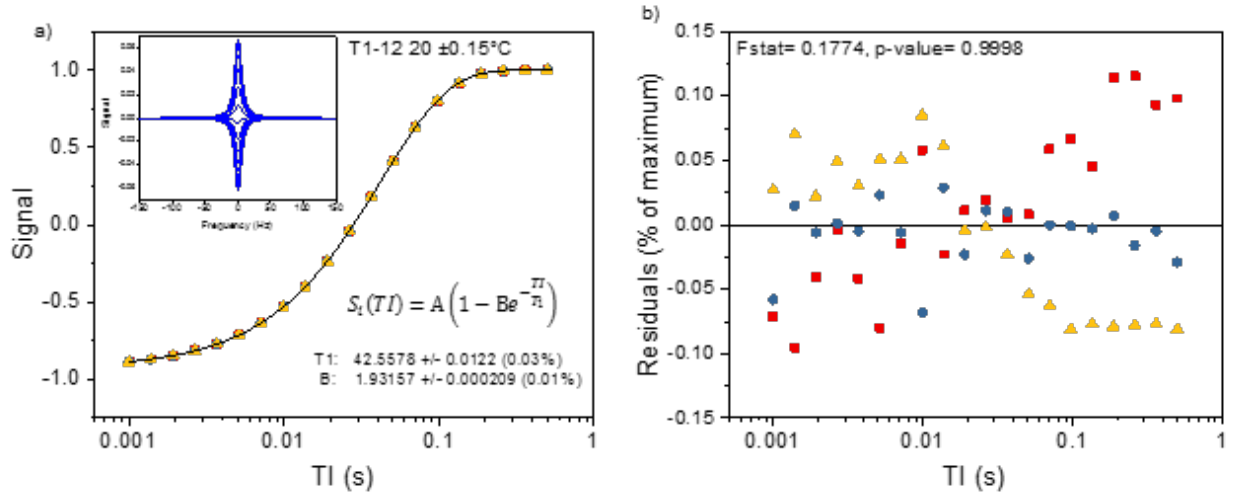

Figure 22. *Inversion recovery data: a) Area of the real part of spectra plotted as a function of the inversion time TI. The data shows results from three identical runs. The solid line is the fit to the governing e quation used to obtain T_1. The inset shows the real part of spectral data used to generate the intergrated signal vs TI plot. B) residuals from the three inversion recovery sequences.*

A schematic of the NIST-built NMR system is shown in Figure 21. The system time base is calibrated against a NIST-traceable rubidium frequency reference. Magnetic field strengths are calibrated against this same time base using the CODATA value for the proton gyromagnetic ratio which serves to convert field field-strength to Hertz. The fiber optic temperature probe is calibrated against a water triple point cell and a gallium melting point cell as per NIST Special Publication 260-157. This calibration ensures that all physical parameters are traceable within the SI system.

NMR proton dynamics are governed by the Bloch-Torrey equations

$$\frac{d\mathbf{M}}{dt} = \gamma\mathbf{M} \times \mathbf{B} - \frac{M_x\hat{\mathbf{x}} + M_y\hat{\mathbf{y}}}{T_2} + \frac{(M_0 - M_z)\hat{\mathbf{z}}}{T_1} + D\nabla^2\mathbf{M}$$

Here, the NMR quantities of medical interest are the tissue-dependent relaxation times T_1, T_2 and the effective diffusion coefficient D which reflects a combination of tissue porosity and anatomical structure. **B** is the forcing magnetization which is further resolved as a sum of gradient and radio-frequency (RF) terms. Finally, the gyromagnetic ratio, γ, is a physical constant and **M** is the magnetic moment arising from collections of nuclear spins.

An NMR measurement consists of a preparation stage in which **M** is preferentially aligned along a fixed axis. This preparation stage is followed by a sequence of RF pulses, represented by **B**, which rotate **M** by nominal amounts following the dynamics of the Bloch-Torrey equations. Ultimately, the component of $d\mathbf{M}/dt$ lying transverse to a receiver coil is detected as the primary measurement signal. Sequences of RF pulses, distinguished with respect to timing, duration, and orientation, have the effect of emphasizing distinct terms in the Bloch-Torrey equations. The goal at NIST is to transform this qualitative understanding into a quantitative analysis returning *in vivo* volumetric parameter maps traceable to the SI units.

An example of a T_1 calibration and associated uncertainty analysis is shown in Figure 22. This uncertainty analysis is accompanied by extensive Monte Carlo simulations of the Bloch equations, taking into account approximately 30 different sources of uncertainty in the measurement system.

In FY 2018 we plan to extend this new calibration service to include measurements of apparent diffusion coefficient. Prior to this a thorough re-examination of the uncertainty analysis will be required as the expense of Monte Carlo may be too great in this context.

[1] M. Boss, A. Dienstfrey, Z. Gimbutas, K. E. Keenan, J. D. Splett, K. F. Stupic and S. E. Russek. MRI Biomarker Calibration Service: Proton Relaxation Times. NIST Special Publication, to appear.

[2] H. L. Cheng, *et al.* "Practical Medical Applications of Quantitative MR Relaxometry," *Journal of Magnetic Resonance Imaging* (2012) 36, 805-824.

Biomolecular Metrology

Ryan M. Evans
Anthony Kearsley
Arvind Balijepali (NIST PML)

The ability to tailor therapies to individuals or specific subsets of a population to deliver personalized care has the potential to fundamentally remake healthcare delivery. The most promising therapeutic candidates for such targeted care are new classes of biologic drugs based on naturally occurring molecules, made possible due to rapid advances in genomics and proteomics [7]. Importantly, such therapies can be safer and yield better outcomes at lower doses when treating debilitating conditions such as diabetes, Alzheimer's disease, or certain cancers [2]. Unfortunately, widespread use of personalized care is currently limited by our ability to routinely measure pathology in individuals, including biomarkers, metabolites, tissue histology, and gene expression. Moreover, existing clinical diagnostics are cumbersome, require specialized facilities, can take days to weeks to perform, and are in many cases prohibitively expensive.

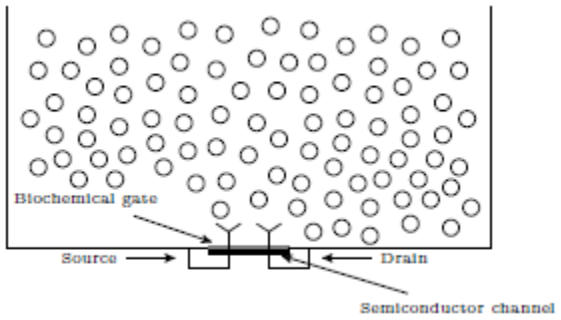

Figure 23. *Nanoscale electronics instrument. This schematic shows ligand molecules diffusing through a buffer fluid in the biological region, to bind with receptors immobilized on a biochemical gate on the floor of the instrument.*

This has led to the development of new portable detection tools, including antibody-based lateral ow assays [5], microelectromechanical sensor (MEMS) based resonators that can detect binding of biomarkers to the sensor surface [8], surface plasmon resonance [9], ring cavity resonators [1] and electronic measurements with field effect transistors (FET) [4, 10, 11]. The latter are particularly well-suited for biomarker measurements due their high charge sensitivity and direct signal transduction, allowing label-free measurements at physiological concentrations. Furthermore, by leveraging semi-conductor processing techniques, measurements with FETs can be made massively parallel, cost-effective, and portable.

A FET is a three-terminal device represented in Figure 23. A semiconductor channel between the source and drain terminals conducts a current that is strongly modulated by an electrostatic potential applied to the gate. Biomarkers in aqueous solution exhibit a well-defined electrostatic surface potential [3] arising from charged hydrophilic residues that interact with water. When these molecules adsorb to the FET biochemical gate, they strongly modulate the channel current proportional to the magnitude of their surface potential. This phenomenon allows FETs to be used to detect and quantify adsorbed biomarkers in solution. Furthermore, functionalizing the FET, by attaching molecules to the gate surface that have a high inherent affinity for biomarkers of interest, allows measurements with high

specificity that are tailored to one or more biomarkers of interest.

An accurate dynamical model of receptor-ligand interactions at the biochemical gate is a critical component in maximizing the sensitivity of FET-based measurements. Specifically, quantitative descriptions of the distribution of adsorbed ligands and their surface potentials can be combined with a model of the semi-conductor physics to allow predictions of the measured signal, which, in turn can be used to optimize sensor design, particularly the geometry of the biochemical gate.

A collection of models for receptor-ligand dynamics in FETs has been developed. Assuming uniform injection of ligand molecules along the top boundary, techniques from asymptotic analysis have been employed to reduce a coupled system of partial differential equations (PDE) to a nonlinear integrodifferential equation that describes the evolution of the concentration of adsorbed ligand molecules. Although this equation exhibits a convolution integral with a singular kernel, a first-order accurate numerical approximation has been found using the method of lines [6]. Furthermore, we have also studied sealed experiments wherein a drop of ligand molecules is injected at an instance of time. Owing to Neumann boundary conditions, the asymptotic reductions applied in the previous case result an elliptic equation that cannot satisfy its corresponding compatibility condition. This difficulty has been obviated by using Laplace transform theory to reduce a coupled PDE system to a singular nonlinear Integro-differential equation (IDE). These results provide insight into the origin of the signal in FET-based measurements, and form the foundation of a mathematical framework which may be used to optimize instrument sensitivity.

Numerical approximation of our model can be seen in Figure 24 and Figure 25 for various final times. A method of lines approximation was employed for physical constants that model the instruments being designed at NIST conditions.

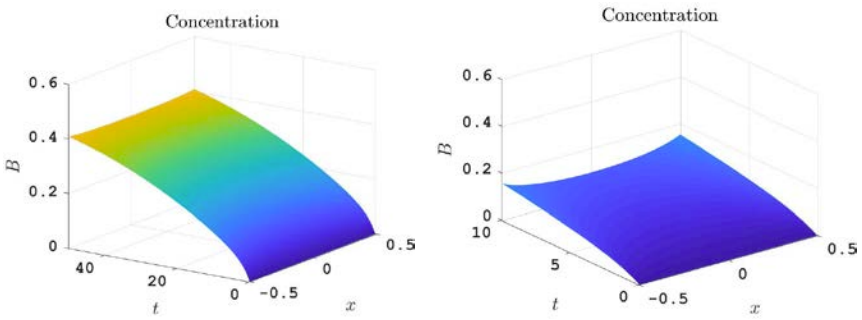

Figure 24. *Space time curves of B(x,t) for t in the intervals [0,1] (left) and [0,10] (right).*

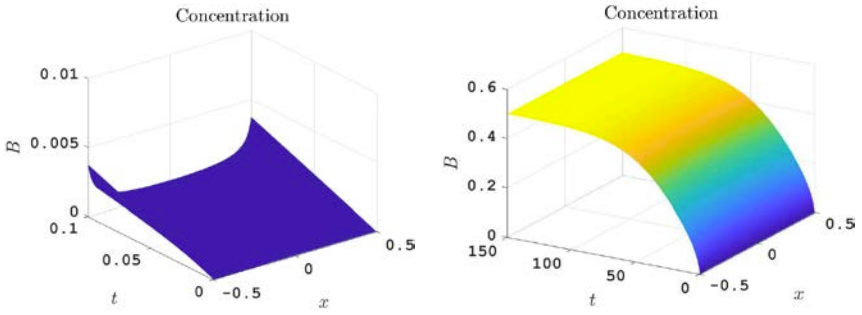

Figure 25: *Space time curves of B(x,t) for t in the intervals [0,50] (left), and [0,150] (right).*

[1] D. K. Armani, T. J. Kippenberg, S. M. Spillane and K. J. Vahala. Ultra-high-Q Toroid Microcavity on a Chip. *Nature* **421** (2003), 925-928.

[2] B. BK., Y.-L. Zheng, V. Shukla, N. D. Amin, P. Grant and H. C. Pant. TFP5, a Peptide Derived from P35, a CDK5 Neuronal Activator, Rescues Cortical Neurons from Glucose Toxicity. *Journal of Alzheimer's Disease* **39**:4 (2014), 899909.

[3] A. Cardone, H. Pant, and S. A. Hassan. Specific and Non-Specific Protein Association in Solution: Computation of Solvent Effects and Prediction of First-Encounter Modes for Efficient Configurational Bias Monte Carlo Simulations. *The Journal of Physical Chemistry B* **117**:41 (2013), 12360-12374.

[4] Y. Cui, Q. Wei, H. Park and C. M. Lieber. Nanowire Nanosensors for Highly Sensitive and Selective Detection of Biological and Chemical Species. *Science* **293** (2001), 1289-1292.

[5] P. K. Drain, L. Gounder, F. Sahid and M.-Y. Moosa. Rapid Urine LAM Testing Improves Diagnosis of Expectorated Smear-Negative Pulmonary Tuberculosis in an HIV-Endemic Region. *Scientific Reports* **6** (2016), 19992.

[6] R. M. Evans, A. Balijepalli and A. J. Kearsley. Diffusion-Limited Reaction in Nanoscale Electronics. In review.

[7] K. Fosgerau and T. Hoffmann. Peptide Therapeutics: Current Status and Future Directions. *Drug Discovery Today* **20** (2015), 122-128.

[8] B. Ilic, H. G. Craighead, S. Krylov, W. Senaratne, C. Ober and P. Neuzil. Attogram Detection using Nanoelectromechanical Oscillators. *Journal of Applied Physics* **95**:7 (2004), 3694-3703.

[9] W. Knoll. Interfaces and Thin Films as Seen by Bound Electromagnetic Waves. *Annual Review of Physical Chemistry* **49**:1 (1998), 569-638.

[10] P. Mohanty, Y. Chen, X. Wang, M. K. Hong, C. L. Rosenberg, D. T. Weaver, and S. Erramilli. Field Effect Transistor Nanosensos for Breast Cancer Diagnostics. ArXiv e-prints, 2014.

[11] F. Pouthas, C. Gentil, D. Cote and U. Bockelmann. DNA Detection on Transistor Arrays Following Mutation-specific Enzymatic Amplification. *Applied Physics Letters* **84**:9 (2004), 1594-1596.

Clustering Nuclear Magnetic Resonance Images of Proteins

Anthony Kearsley
Ryan M. Evans
Frank Delaglio (IBBR)
John Marino (IBBR)
Robert Brinson (IBBR)
Luke Arbogast (IBBR)

The expiration of originator biologic drug patent protection and the advent of biosimilars have created a dire need for advanced analytical methods to characterize the critical quality attributes (CQA) of these drug products that allow for robust demonstration of similarity. The higher order structure (HOS) of therapeutic proteins, which is directly linked to both efficacy and safety of biologic drugs, is one of the CQAs that needs to be well characterized [2, 5, 6, 9].

Originally proposed by Aubin and colleagues [1], it recently has been shown that NMR spectroscopy yields a precise and accurate assessment of the HOS of protein biotherapeutics. To date, quantitative analysis of NMR spectra has been primarily based upon principal component analysis (PCA) [3, 8], a method in which a matrix of spectral data is projected onto orthogonal axes of maximum variance. Results are visualized in a scatter plot, which can reveal HOS details without the need for baseline correction and peak analysis. Though PCA is often employed and highly successful, complementary techniques that rely on an objective dissimilarity measure are desired. One advantage of such techniques is that they may be applied directly to the spectra themselves, and do not require projecting data onto their principal component axes. Hence, dissimilarity measure-based methods can perform data analysis tasks such as classification on raw spectra.

The use of several metrics for estimating dissimilarity between NMR spectra of monoclonal antibodies has been investigated by pairing each of these metrics with a collection of candidate clustering algorithms. For the first time, the first Wasserstein metric has been introduced as a dissimilarity measure between spectra. When paired with the k-medoids clustering algorithm this metric does an outstanding job at classifying spectra that exhibit significant structural differences; a consequence of the fact that the Wasserstein metric uses global information. On the other hand, it has been shown that the chi-squared metric outperforms the Wasserstein metric

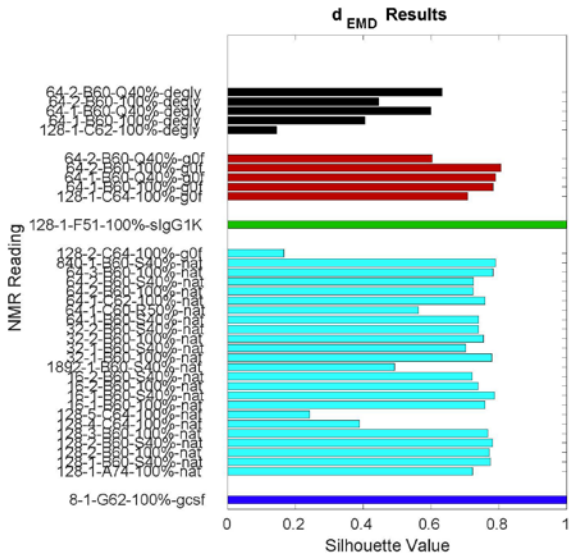

Figure 26. *Results of the EMD metric when paired with the k-medoids algorithm.*

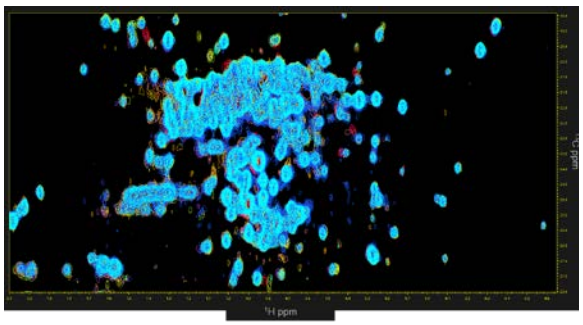

Figure 27. *Superimposed raw NMR data before clustering.*

when comparing spectra that correspond to proteins with a high degree of structural similarity. Since the chi-squared metric uses only local information, it is sensitive enough to detect minor perturbations in the spectra. In addition to establishing novel techniques for classifying monoclonal antibody spectra, these results show that one must seriously consider the choice of dissimilarity measure and clustering algorithm when devising unsupervised learning algorithms [4].

Furthermore, to further establish the precision and robustness of NMR as a biomolecular measurement technique, NMR spectra of monoclonal antibodies from twenty-six different laboratories, located in different countries across the world, have been collected under a variety of different experimental conditions by varying factors such as magnet strength and temperature. Using a novel hierarchical clustering method, we have peak tables i.e., compact representatives of these spectra– according to protein-type and temperature. These results contribute to the growing body of literature establishing the precision and robustness of two-dimensional NMR

spectroscopy as a tool for evaluating similarity between monoclonal antibodies [5].

[1] Y. Aubin, G. Gingras and S. Sauve. Assessment of the Three-Dimensional Structure of Recombinant Protein Therapeutics by NMR Fingerprinting: Demonstration on Recombinant Human Granulocyte Macrophage-Colony Stimulation Factor. *Analytical Chemistry* **80**:7 (2008), 2623–2627.

[2] O. V. Borisov, J. E. Schiel and D. Davis. Trends and Drivers for the Development of Next-Generation Biotherapeutic Characterization Tools. In *State-of-the-Art and Emerging Technologies for Therapeutic Monoclonal Antibody Characterization Volume 3*. Defining the Next Generation of Analytical and Bio-physical Techniques. ACS Publications, 2015, 1-16.

[3] R. G. Brinson, H. Ghasriani, D. J. Hodgson, K. M. Adams, I. McEwen, D. I. Freedberg, K. Chen, D. A. Keire, Y. Aubin and J. P. Marino. Application of 2D-NMR with Room Temperature NMR Probes for the Assessment of the Higher Order Structure of Filgrastim. *Journal of Pharmaceutical and Biomedical Analysis* **141** (2017), 229–233.

[4] R. G Brinson, J. P. Marino, L. W. Arbogast, R. M. Evans, A. J. Kearsley, *et al.* Benchmarking the Precision and Robustness of 2D-NMR for Higher-Order Structural of Protein Therapeutics: An International Inter-Laboratory Study. In preparation.

[5] A. J. Kearsley, R. M. Evans, R. G. Brinson, L. W. Arbogast and F. Delaglio. Classifying NMR Spectra of Monoclonal Antibodies. In preparation.

Chemical Spectroscopy for Illicit Drug Identification

Arun S. Moorthy (NIST MML)
William E. Wallace (NIST MML)
Anthony J. Kearsley
Dmitrii V. Tchekhovskoi (NIST MML)

A growing concern in the United States is the rapid introduction of illegal, so-called, *designer drugs*, substances that are chemical analogs of known illicit drugs, yet are different enough that they cannot be easily identified by traditional chemical identification technologies (e.g., mass spectrometry). One example is the designer Fentanyls. These opioid pain medications exhibit a rapid pain relief effect on those who ingest them, but over a very short duration, making them highly addictive. In some cases, these compounds are hundreds of times more potent than street heroin and are far more likely to lead to sudden respiratory depression. Deaths from fentanyl overdose has been declared a public health crisis in the United States (and in many other countries). The drug is extremely dangerous leading to easy cross-contamination, a problem that is facing law-enforcement and emergency rooms. Currently, simply identifying whether a given compound is a Fentanyl is an open problem.

Gas chromatography – mass spectrometry (GC-MS) is an analytical chemistry technique used in many industries. One of its primary purposes is chemical identification, which is done by searching the spectrum of an unknown chemical against a library of spectra with known origin. Typically, a "molecular fingerprint" is acquired and search is performed of known compounds in the NIST compound database. This similarity search very often is performed under less-than-ideal circumstances, and is complicated by the fact that many of these designer drugs are not yet represented in the database. There are enormous algorithmic, computational, and legal complications if the unknown compound is a designer drug not represented in the library.

A significant step toward identifying fentanyls is a mass spectral library search algorithm that identifies compounds that differ from library compounds by a single inert structural component [1]. This algorithm, the Hybrid Similarity Search, generates a similarity score based on matching both fragment ions and neutral losses. It employs a parameter called a *delta mass*, defined as the mass difference between query and library compounds, to shift neutral loss peaks in the library spectrum to match corresponding neutral loss peaks in the query spectrum. When the spectra being compared differ by a single structural feature, these matching neutral loss peaks should contain that structural feature.

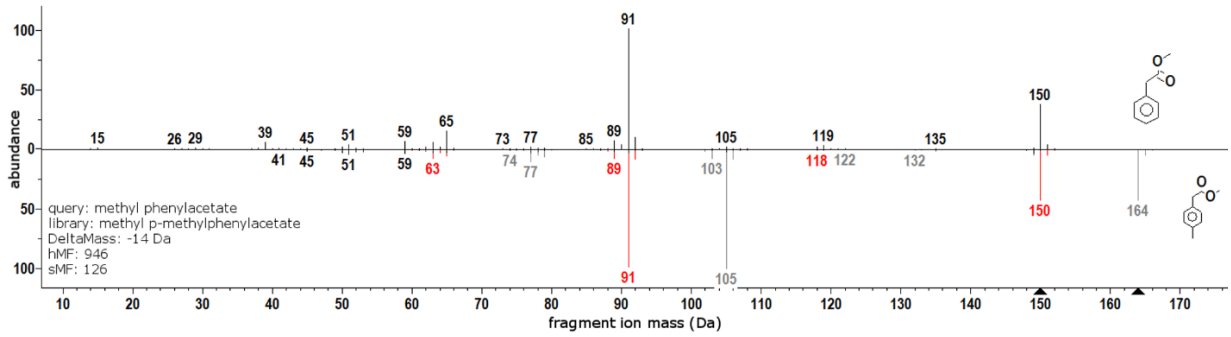

Figure 28. *Comparision of mass spectra for methyl phenylacetate (top) with methyl p-methylphenylacetate (black and gray peaks in bottom spectrum). The hybrid spectrum corresponds to the black and red peaks in the bottom spectrum.*

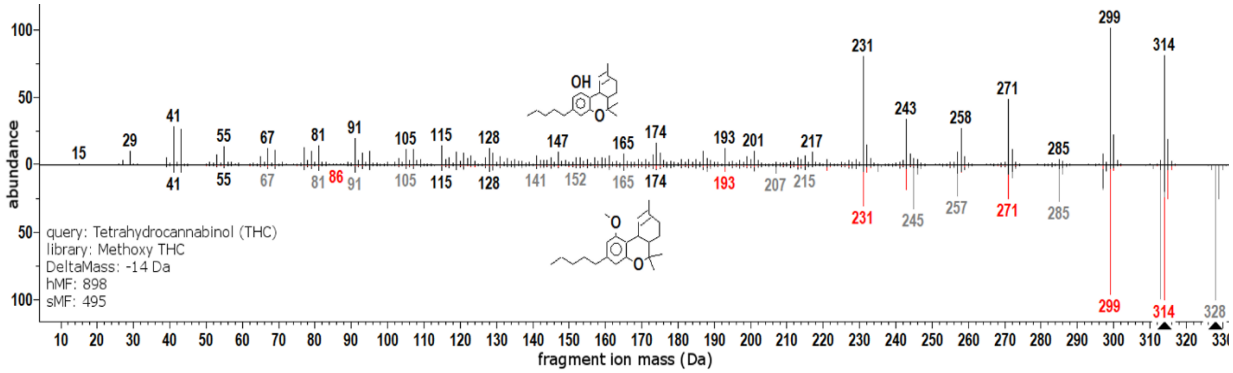

Figure 29. *Comparision of spectra for Tetrahydrocannabinol (top) and Methoxy Tetrahydrocannabinol (black and gray peaks in bottom spectrum). Hybrid spectrum corresponds to black and red peaks in the bottom spectrum.*

This method significantly extends the scope of the library to include spectra of "nearest-neighbor" compounds that differ from library compounds by a single chemical moiety. Additionally, determination of the structural origin of the shifted peaks can aid in the determination of the chemical structure and fragmentation mechanism of the query compound. A variety of examples are presented, including the identification of designer drugs and chemical derivatives not present in the library.

The mechanics of how the hybrid search employs a delta-mass parameter can be seen in Figure 28 and Figure 29. The method has outperformed currently available methods.

[1] A. S. Moorthy, W. E. Wallace, A. J. Kearsley, D. V. Tchekhovskoi and S. E. Stein. Combining Fragment-ion and Neutral-loss Matching During Mass Spectral Library Searching: A New General-Purpose Algorithm Applicable to Illicit Drug Identification. *Analytical Chemistry*, to appear.

Cryobiology Modeling

Daniel Anderson
James Benson (University of Saskatchewan)
Anthony Kearsley

Cryobiology, the study of organisms at low temperatures, broadly impacts medicine, agriculture and forensics and is important in the fight to maintain earth's biodiversity. An important application is cryopreservation, which involves the freezing of cells, tissues, organs and other, typically biological, compounds that are feared to be susceptible to damage caused by chemical kinetics. If correctly performed, cooling to very low temperatures (typically -80 °C using solid carbon dioxide or -196 °C using liquid nitrogen) can prevent damage. Cryoprotocols, laboratory procedures that cool and warm biospecimens, have a variety of objectives, ranging from preserving the viability of a cell as in assisted reproduction, to locally destroying cells or tissue in cryosurgery, and to optimally preserving chemical, genetic or proteomic information for archival and/or forensics applications.

Mathematical and computational sciences play a critical role as a means of effectively and efficiently exploring these complex bio-chemical and/or bio-physical systems and their overcrowded parameter spaces. There is now a growing interest in the development of mathematical models to aid in the explanation of phenomena, exploration of potential theories of damage or success, development of equipment, and refinement of optimal cryopreservation or cryoablation strategies.

Cryopreservation procedures permit the indefinite storage of cells using extremely cold temperatures to suspend all metabolic activities, therefore preserving the cell and its function. Loosely speaking, there are two main types of cryopreservation procedures: equilibrium (conventional slow freezing) and non-equilibrium or ultra-rapid freezing (vitrification). Both procedures employ the use of cryoprotectants, chemicals behaving like antifreeze to prevent cellular damage during the freezing process. After proper freezing, cells should be able to be stored for an indefinite amount of time, for example, by immersing them in liquid nitrogen, an extremely cold fluid with an approximate temperature of -196 ^{o}C. Cryoprotectants must be removed later during thawing, when the water balance in the cell can be slowly restored, and normal activity in the cell should return.

Procedures exist for the freezing of single cells, tissue comprised of many cells, and even entire organs. Size and amount of cytoplasm (or biofluid) structural complexity change the freezing procedures employed. For example, cells with less cytoplasm, like sperm cells, are generally considered to be less difficult to freeze than those cells with more cytoplasm, like eggs. Slow freezing or equilibration has been successfully employed to freeze and store a wide range cells, but research is ongoing to optimize cell cryopreservation.

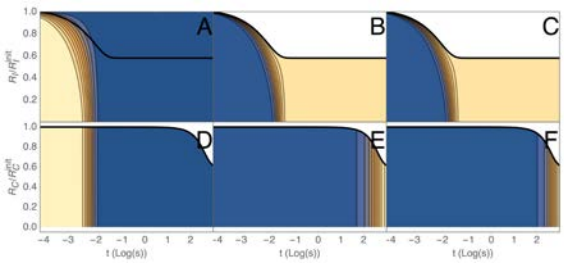

Figure 30. *Plots of numerical simulation of a cryobiology system beginning at equilibrium in mol/L and isosmotic NaCL when the temperature is abruptly changed to -25 Celsius.*

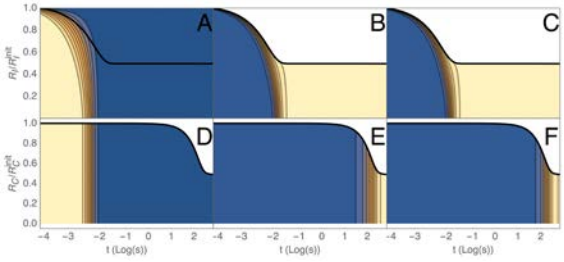

Figure 31. *Plots of numerical simulation of a cryobiology system beginning at equilibrium in 1 mol/L and isosmotic NaCL when the temperature is abruptly changed to -25 Celsius, however, freezing point depression and volume effects caused by differences in solid/liquid densities are ignored.*

Recently we studied the use of optimization techniques to determine or improve the equilibration of cryoprotectant. We considered the case of cells and tissues with high concentrations of permeating chemicals known as cryoprotective agents (CPAs). Despite their protective properties, CPAs can cause damage because of osmotically-driven cell volume changes, as well as chemical toxicity. In this study, data was used to determine a toxicity cost function, a quantity that represents the cumulative damage caused by toxicity. We then used this cost function to define and numerically solve the optimal control problem for CPA equilibration, using human oocytes as representative cell type, due to their high clinical relevance. The resulting toxicity-optimal procedures are predicted to yield significantly less toxicity than conventional procedures. Results showed that toxicity is minimized during CPA addition by inducing the cell to swell to its maximum tolerable volume and then loading it with CPA while in the swollen state. This counterintuitive result is considerably different from the conventional stepwise strategy, which involves exposure to successively higher CPA concentrations to avoid excessive shrinkage. The procedures identified are a first step in deriving protocols that significantly reduce toxicity damage [5].

Over the last half century there has been a considerable amount of work in bio-heat and mass-transport, and these models and theories have been readily and repeatedly applied to cryobiology with much success. However, there are significant gaps between experimental and theoretical results that suggest missing links in models. One source for these potential gaps is that cryobiology is at the intersection of several very challenging aspects of transport theory: it couples multicomponent, moving boundary, multiphase solutions that interact through a semipermeable elastic membrane with multicomponent solutions in a second time varying domain, during a two-hundred Kelvin temperature change with multimolar concentration gradients and multi-atmosphere pressure changes. We have been developing mathematical and computational models built on first principles to describe coupled heat and mass transport in cryobiological systems to account for these various effects [1, 2, 3]. Our efforts have advanced along three fronts. We have

(1) examined concentration variable relationships, their impact on choices of Gibbs energy models, and their impact on chemical potentials;
(2) developed heat and mass transport models that are coupled through phase-change and biological membrane boundary conditions;
(3) developed numerical methods for solving these multi-species multiphase free boundary problems.

Finally, employing these models together and building a new way to simulate these freezing procedures leads to an interesting free-boundary problem involving a spherically symmetric model of a biological cell separated by a ternary fluid mixture from an encroaching solid-liquid interface. The cell and liquid regions have associated with them intracellular and extracellular salts, respectively, that do not cross the cell membrane. The liquid surrounding the cell contains another solute, the CPA. The cell membrane is permeable to both water and the CPA. As cooling and solidification proceed the extracellular chemical environment evolves and leads to mass transport across the cell membrane. Consequently, both the solidification front and the cell membrane are free boundaries whose dynamics are coupled through transport processes in the solid, liquid and cell regions. We have described a new numerical procedure to solve this coupled free-boundary problem based on a domain transformation and a method of lines approach [4].

[1] D. M. Anderson, J. D. Benson and A. J. Kearsley. Foundations of Modeling in Cryobiology I: Concentration, Gibbs Energy, and Chemical Potential Relationships. *Cryobiology* **69**:3 (2014), 349-360.

[2] D. M. Anderson, J. D. Benson and A. J. Kearsley. Foundations of Modeling in Cryobiology II: Heat and Mass Transport in Bulk and at Cell Membrane and Ice-Liquid Interfaces. In review.

[3] D. M. Anderson, J. D. Benson and A. J. Kearsley. Foundations of Modeling in Cryobiology III: Inward Solidification of a Ternary Solution Towards a Permeable Spherical Cell in the Dilute Limit. In review.

[4] D. M. Anderson, J. D. Benson and A. J. Kearsley. Numerical Solution of Inward Solidification of a Dilute Ternary Solution Towards a Semi-Permeable Spherical Cell. In review.

[5] J. D. Benson, A. J. Kearsley and A. Z. Higgins. Mathematical Optimization Procedures for Cryoprotectant Equilibration using a Toxicity Cost Function. *Cryobiology* **64**:3 (2012), 144-151.

Enabling Large-Scale HVAC Simulations

Zhelun Chen (Drexel University)
Jin Wen (Drexel University)
Anthony Kearsley
Amanda Pertzborn (NIST MML)

A vast majority of electrical energy consumption in the United States comes from buildings' usage, most of which comes from lifecycle usage rather than from construction.Thus, optimal operational decisions are crucial to energy efficiency, especially considering a national push towards smart grid applications and optimized power grid use. For optimal operational decisions to take place, buildings need to interact with a smart electric grid as a function of energy demands (Figure 32).

This need poses a new computational challenge, as optimal decision-making for each building is governed by an automated cyber-physical system. As an example, heating, ventilation and air conditioning (HVAC) information provided to the building control system, as well as electrical pricing provided by the smart grid, can be used to make decisions about whether to use the power generated by solar panels in the building itself or to sell it to the utility for use elsewhere. This situation requires the development of algorithms for predicting usage, which in turn requires a large-scale HVAC simulation test bed that currently does not exist.

Previous work at NIST on this problem includes the development of HVACSIM+, a software package and computing environment for simulating HVAC systems originally developed in the 1980s. In HVACSIM+ and in other software packages available currently, the limitations of numerical solvers employed are apparent: the user must be adept at formulating the problem to achieve a meaningful solution, the methods are too sensitive to initial estimates for the state of the system, and the size of the problems that can be solved is limited due to abundant use of dense storage. There are many instances where small scale building simulations work well but when coupled to larger systems of buildings there is a failure to converge [1].

An example of this can be illustrated even in a "fan-coil'' unit (FCU), a simple but economically important structure appearing in commercial, institutional and

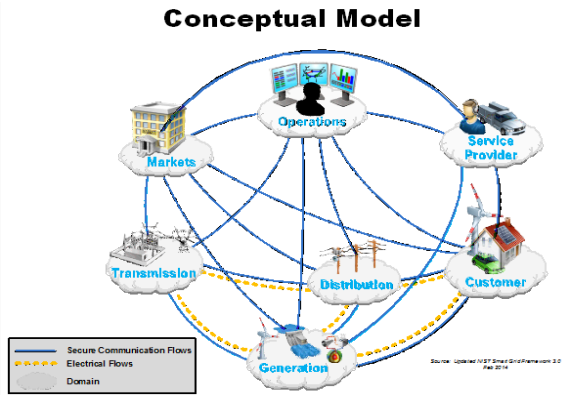

Figure 32. *General and conceptual model of energy flow.*

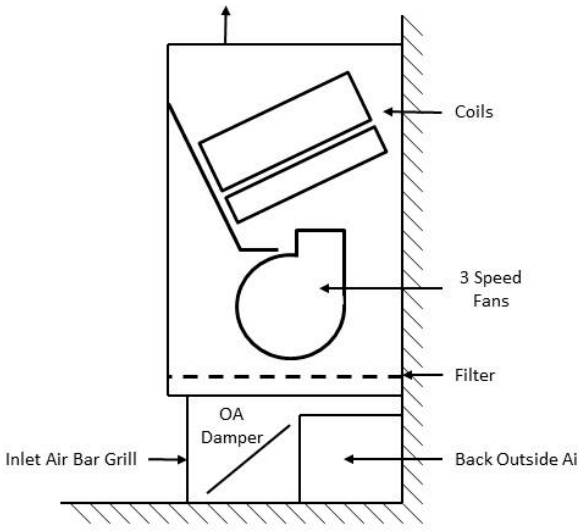

Figure 33. *Simple fan coil unit geometry.*

multifamily residential buildings. In Figure 33, a vertical floor-mounted four-pipe hydronic system, including three parallel fans run by two electric motors with three speeds (say, fast, medium and slow), would be used to modulate the amount of ventilation supplied by way of a motorized damper in the outside air connection at the back of the unit. If one were to simulate this scenario, variables would be typically grouped into blocks, control logic, actuators, air flow, thermal flow and a sensor block variable. These blocks are combined into a resulting nonlinear system which is solved at every time step and then matched with two exterior building zones. For the sake of this small example, east and south facing zones are selected on a summer day. The interior zones can be thought of as rooms in a building; the exterior zones can be thought of as the region adjacent to a building. In summer the outdoor air damper is fully closed and the fan speed is normally set on high. When the FCU is operating properly, the controller compares room temperature to the cooling set-point, 23.33 ^{o}C (74 ^{o}F), and heating set-point, 21.11 ^{o}C (70 ^{o}F). If the actual room temperature is 0.56 ^{o}C (1 ^{o}F) greater than the cooling set-

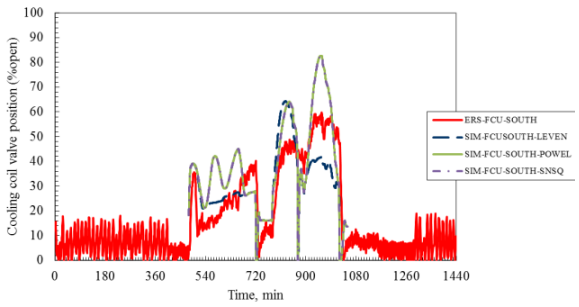

Figure 34. *Inconsistency in nonlinear solver solutions.*

point, the FCU is in cooling mode, and if it is 0.56 °C (1 °F) less than the heating set-point, the FCU is in heating mode. A dedicated proportional integral derivative (PID) loop is enabled for each mode to control the cooling or heating valve position. A PID loop is a means of regulating a process quantity (room temperature) by compensating it with closed-loop feedback of its error (the difference between the room temperature and set-point), with the compensation amount computed using three gain coefficients.

Figure 34 demonstrates that commonly employed numerical solution techniques give rise to sufficiently different solutions to raise serious concerns about simulation results, even in the very simple example of an FCU. While employing scaling techniques can mitigate this problem somewhat [2], the problem still persists especially for larger and more complicated simulations.

[1] S. Pourariana, A. Kearsley, J. Wen and Amanda Pertzborn. Efficient and Robust Optimization for Building Energy Simulation. *Energy and Buildings* **122** (2016), 53–62.

[2] Z. Chen, J. Wen, A. Kearsley and A. Pertzborn. Scaling Methods for Dynamic Building System Simulation in an HVACSIM+ Environment. In *Proceedings of IBPSA-USA Building Simulation Conference*, Building Simulation, August 7-9, 2017, San Francisco CA, 1984-1990.

Longitudinal Velocity Fluctuations and Dependence of the Integral Turbulence Scale on Wind Spectrum

Emil Simiu (NIST EL)
Florian A. Potra

Spectra of the longitudinal velocity fluctuations and integral scales of turbulence are of interest in structural engineering applications for several reasons. First, the resonant amplification of structural motions is induced in tall buildings by spectral components belonging to the inertial subrange and described by Kolmogorov's well known two-thirds law. Second, for other types of flexible structures the spectral components that produce resonant amplification typically belong to the low-frequency spectral range, for which mathematical descriptions fully consistent with both theory and measurements were heretofore unavailable. Third, low-frequency fluctuation components and integral scales of turbulence are of interest because they affect significantly the degree to which wind tunnel and computational fluid dynamics (CFD) simulations are realistic.

Our research has yielded expressions for the low-frequency content of the atmospheric boundary layer's longitudinal velocity fluctuations consistent with both theory and measurements [1], thus providing the first basis available in the literature for developing realistic wind tunnel and CFD simulations of low-frequency atmospheric boundary layer (ABL) turbulence.

More than three decades ago, Panofsky Dutton [2] said: "We recommend that integral scales be avoided in applications to atmospheric data. Many investigators have computed integral scales from atmospheric data, but the results are badly scattered and cannot be organized." Our paper [3] leverages the newly acquired knowledge of the low-frequency turbulence components to develop the following closed-form relation used to obtain stable and realistic estimates of the integral longitudinal turbulence length

$$L_u^x(z) = \frac{0.26a^{-5/3}}{4\beta(z)} \exp\left[\frac{\beta(z) - 0.65a - \frac{2}{3}}{0.26a - \frac{2}{3}}\right] z$$

where $L_u^x(z)$ is the integral scale of the longitudinal velocity fluctuations, z is the height above ground, $\beta(z)$ is a measure of the turbulence intensity, and a is the lower limit of the non-dimensional inertial frequency subrange.

[1] P. Drobinsky, *et al.* The Structure of the Near-Neutral Atmospheric Suface Layer. *Journal of Atmospheric Sciences* (March 2004), 699-714.

[2] H. A. Panofsky and J. A. Dutton. *Atmospheric Turbulence: Models and Methods for Engineering Applications*. Wiley-Interscience, 1984.

[3] E. Simiu and F. A. Potra. Low-Frequency Longitudinal Velocity Fluctuations and The Dependence of the Integral Turbulence Scale Upon Wind Spectrum. In review.

Figure 35. *Segmentation of the shoeprint in a crime scene image (rightmost) obtained by the phase field function evolution (left 1-4) of a checkerboard initialization.*

Computational Tools for Image and Shape Analysis

Günay Doğan (Theiss Research)
Javier Bernal
Charles R. Hagwood (NIST ITL)
Harbir Antil (George Mason University)
Marilyn Y. Vazquez (George Mason University)
Eve N. Fleisig (Thomas Wootton High School)
Kevin Su (Poolesville High School)
Gautham Venkatasubramanian (Birla Institute)

The main goal of this project is to develop efficient and reliable computational tools to detect geometric structures, such as curves, regions and boundaries, from given direct and indirect measurements (e.g., microscope images or tomographic measurements), as well as to evaluate and compare these geometric structures or shapes in a quantitative manner. This is important in many areas of science and engineering, in which practitioners obtain their data as images and would like to detect and analyze the objects in the data. Examples of such images are microscopy images for cell biology, micro-CT (computed tomography) images of microstructures in materials science, and shoeprint images in crime scenes for footwear forensics. In FY 2017, advances were made in the following two fronts: image segmentation and shape analysis, which are described separately below.

Image Segmentation. Image segmentation is the problem of finding distinct regions and their boundaries in given images. It is a necessary data analysis step for many problems in cell biology, forensics and materials science, as well as other fields in science and engineering. In recent years, we have been pursuing the active contours or deformable models approach to image segmentation [1, 2]. In this approach, the user starts with an initial guess of the region boundary in the image. Then the algorithm iteratively deforms the initial curve or surface in a manner to eventually converge to the region or object of interest. This iterative shape evolution process is guided by the shape energy, which is defined specifically for image segmentation application.

In FY2017, G. Doğan worked on an anisotropic weighted surface area energy to improve region boundary detection in images. The isotropic energy takes into account only the magnitude of the image intensity change, whereas the anisotropic model incorporates directionality as well, penalizing orientation deviations from the direction of the maximal intensity change. G. Doğan developed an efficient shape-Newton algorithm to compute segmentations using second order shape sensitivity of the anisotropic energy [3]. The total running time of the shape-Newton algorithm was significantly less than that of the previous gradient descent algorithm. Moreover, it was observed that the shape-Newton algorithm for the anisotropic model was much more robust with respect to the magnitude of the image gradients, in stark contrast with the gradient descent algorithm, whose performance deteriorated significantly as the image gradients got sharper.

In this period, Dr. Doğan started working on a different approach to image segmentation with his collaborator, H. Antil from George Mason University. In their approach, the regions and their boundaries were represented implicitly with a phase field function, and the segmentations were obtained by minimizing an associated cost functional. They implemented an efficient minimization algorithm for this cost functional. The phase field was represented in the Fourier domain, and then updated iteratively at a cost of a few FFT operations per iteration. The advantage of this algorithm was that it is concise, and easily implemented for 3D image data, as well as 2D image data. Doğan and Harbir are currently working on modifications of this model to improve the detection of fine geometric features around the regions, such as thin inclusions or protrusions. See Figure 35 for an example of the segmentation process with this method.

G. Doğan has been working with M. Y. Vazquez, a Ph.D. student at George Mason University, on using clustering algorithms to segment microstructure images. Vazquez had developed a powerful clustering algorithm that performs very well for nonlinear geometric structures or manifold-valued data. She built on this to implement a novel segmentation algorithm, which gave

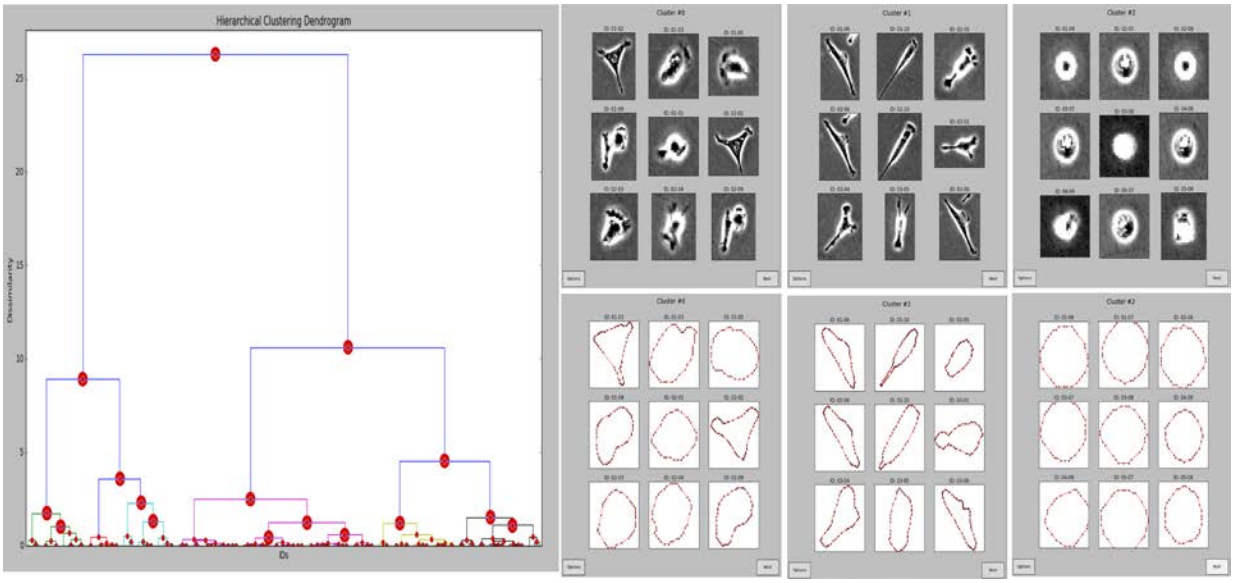

Figure 36. *Hierarchical clustering and grouping of cells using the shape dissimilarity measure.*

very promising results on the real microstructure images that were used for testing.

G. Doğan has also been collaborating with M. Herman's project in ITL on shoeprint forensics. For this, he developed specialized segmentation algorithms for semi-automatic detection of the features or patterns on shoeprints images. These specialized algorithms built on the segmentation principles that he developed previously. Doğan worked with undergraduate student volunteer, G. Venkatasubramanian to implement these algorithms in a user-friendly graphical user interface (GUI). Using this GUI, a forensics specialist can examine a shoeprint image and, mark geometric features manually or semiautomatically with the available segmentation options. Some preprocessing functionality, such as denoising, color adjustment, are also available.

Shape Analysis. In FY 2017, we made improvements to the optimization algorithm for elastic shape analysis. G. Doğan had previously developed a fast algorithm to compute an elastic shape distance between two given closed curves, working together with J. Bernal and C. Hagwood [5, 6, 7]. Elastic shape distance is a powerful metric to quantify the dissimilarity of two given closed curves, and is widely applicable to shape analysis problems in science and engineering [4]. It satisfies basic requirements for a shape distance, such invariance with respect to translation, rotation, scale, and reparameterization. Moreover, it is robust to changes in the relative locations of the features of the shapes. Thus, it matches a human's intuitive notion of shape well. However, the computation of the elastic shape distance is expensive, as it requires solving a difficult optimization problem. Another challenge of the optimization is that the theoretical shape distance definition requires finding the global minimum of the underlying energy, which is very difficult and expensive to do in practice.

To alleviate these challenges of the shape distance computation, we revised the underlying formulation and developed an optimization algorithm to compute a global minimum in reduced computation time. The key ingredients to this custom global optimization algorithm were an efficient reduced energy formulation, linear-time dynamic programming for reparameterization, FFT-based optimal alignment, and global optimization over starting point, and rotation with judicious selection of initial candidates.

In addition to improving the fundamental shape distance algorithm, Doğan worked on large-scale deployability to compute pairwise shape distance over large shape data sets, for example, one million shape distances for all pairs of one thousand cell shapes. He wrote Matlab scripts to distribute this computation to available computer nodes. Doğan is now developing a Python version of the shape distance algorithm with high school student volunteer K. Su. They implemented efficient Python versions of the dynamic programming algorithm for curve reparameterization. The complete shape distance code is still a work in progress. Once completed, it will be possible to deploy the code on a wide variety of computing configurations.

Once the pairwise shape distance matrix has been computed, users would like to use it for exploratory statistical analysis of shape populations. G. Doğan and high school student volunteer, E. Fleisig have been developing a GUI to enable such analyses. Currently, a user can view and browse shape data sets, cluster and group shapes, and view lower-dimensional visualizations with multidimensional scaling using this tool. See Figure 36 for an example of cell shape analysis using the GUI.

[1] G. Doğan. Fast Minimization of Region-based Active Contours using the Shape Hessian. In *Proceedings of the 4th International Conference on Scale Space and Variational Methods in Computer Vision (SSVM'15)*, May 2015.

[2] G. Doğan. An Efficient Curve Evolution Algorithm for Multiphase Image Segmentation. In *Proceedings of the International Conference on Energy Minimization Methods in Computer Vision and Pattern Recognition (EMMCVPR'15)*, January 2015.

[3] G. Doğan. An Efficient Lagrangian Algorithm for an Anisotropic Geodesic Active Contour Model. In *Proceedings of the 5th International Conference on Scale Space and Variational Methods in Computer Vision (SSVM'17)*, June 2017.

[4] A. Srivastava, E. Klassen, S. Joshi and I. Jermyn. Shape Analysis of Elastic Curves in Euclidean Space. *IEEE Transactions on Pattern Analysis and Machine Intelligence* **33**:7 (2011), 1415-1428.

[5] G. Doğan, J. Bernal and C. R. Hagwood. Fast Algorithms for Shape Analysis of Planar Objects. In *Proceedings of the IEEE Conference on Computer Vision and Pattern Recognition (CVPR'15)*, Boston, MA, June 2015.

[6] G. Doğan, J. Bernal and C. R. Hagwood. FFT-based Alignment of 2D Closed Curves with Application to Elastic Shape Analysis. In *Proceedings of the 1st International Workshop on Differential Geometry in Computer Vision for Analysis of Shapes, Images and Trajectories (DiffCV'15)*, Swansea, UK, September 2015.

[7] J. Bernal, G. Doğan and C. R. Hagwood. Fast Dynamic Programming for Elastic Registration of Curves. In *Proceedings of the 2nd International Workshop of Differential Geometry in Computer Vision and Machine Learning (DiffCVML'16)*, Las Vegas, NV, July 1, 2016.

Shape Analysis, Lebesgue Integration and Absolute Continutiy Connections

Javier Bernal
James F. Lawrence

Lebesgue integration and absolute continuity are of great importance in the development of shape analysis. Thus, it is advantageous to have a good grasp of these two notions. We are developing a set of notes that review basic concepts and results about these two subjects. In particular, we review fundamental results connecting them to each other and to shape analysis. Many results, especially well-known results, are presented without proof. In addition, definitions of well-known concepts, e.g., open and closed sets, are not included. Many such proofs and definitions can be found in Royden's *Real Analysis* [1] and Rudin's *Principles of Mathematical Analysis* [2] on which our notes are mostly based. However, if the proof of a result does not appear in these texts, nor in some other known publication, or if all by itself it could be of value to the reader, an effort is being made to present it accordingly. The fundamental ideas on shape analysis in these notes are mostly from Srivastava and Klassen's *Functional and Shape Data Analysis* [3].

[1] H. L. Royden. *Real Analysis*, 2nd edition. Macmillan, New York, 1968.

[2] W. Rudin, *Principles of Mathematical Analysis*, 2nd edition. McGraw-Hill, New York, 1964.

[3] A. Srivastava and E. P. Klassen. *Functional and Shape Data Analysis*. Springer, New York, 2016.

Explicit Stepwise Computation in Ill-Posed Time-Reversed 2D Burgers Equation

Alfred S. Carasso

An important methodology developed in ACMD allows effective numerical computation of a class of *retrospective* problems for time dependent partial differential equations (PDEs) that are generally considered intractable. Given the observed state of the physical system at time $T > 0$, can one reconstruct its past evolution from some unknown previous state at time $t = 0$? Ideally, that question might easily be answered by marching backward from the given state at $T > 0$, using negative time steps $\Delta t < 0$.

One important example of such time reversal is the recovery of the history of groundwater contaminant plumes, by solving an advection diffusion equation backward in time [1, 2]. In geophysics, the retrospective thermal evolution of the Earth's interior is of major interest [3, 4]. Another rich source of time reversed diffusion equations lies in the deconvolution problems that pervade measurement science. Commonly, the true physical signal must be deconvolved from the Gaussian-like point spread functions that typically characterize many measuring instruments. Such deconvolution problems can be reformulated into mathematically equivalent backward diffusion equations [5, 6, 7]. Using hat approach, we have produced high quality reconstructions in galactic scale Hubble telescope imagery, as well as in nanoscale scanning electron microscopy.

Although highly desirable because of their simplicity, stepwise schemes marching backward in time cannot be used on partial differential equation (PDE) systems involving dissipation. These are ill-posed initial value problems, and marching schemes consistent with such problems are necessarily *unconditionally unstable*, leading to explosive noise amplification.

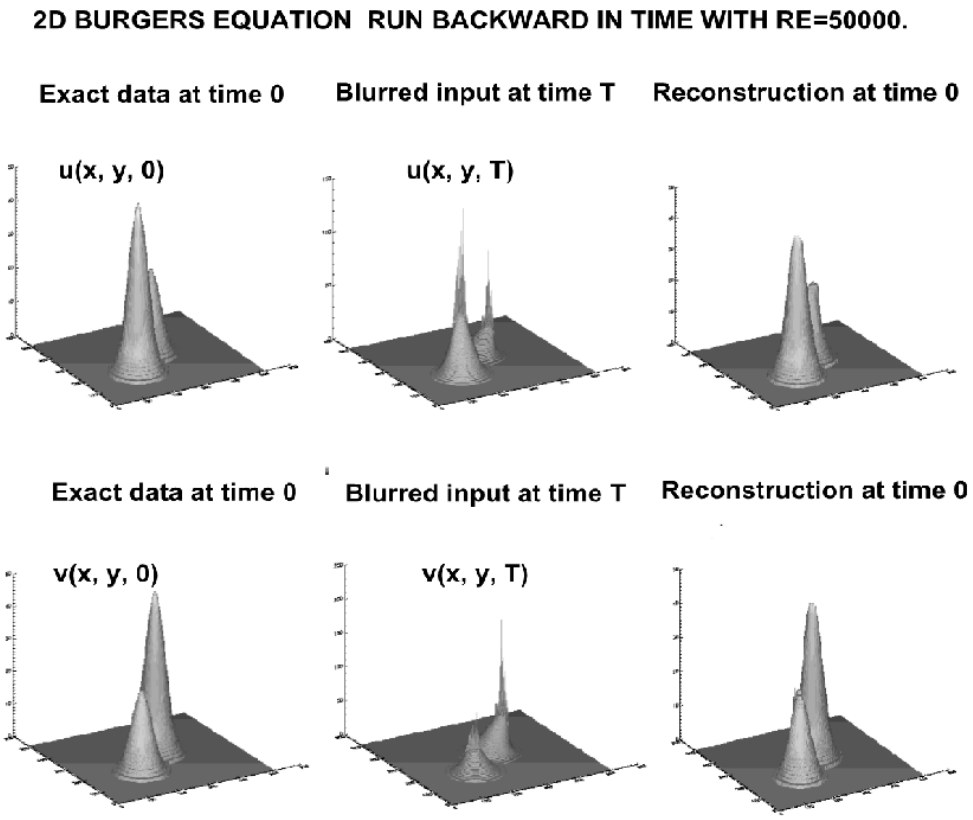

Figure 37. *Using the input data at T=0.0025 shown in the middle column, using Δt= -5.0 x 10^{-8}, with w = 1.0 x 10^{-9}, p = 3.0, in the compensating operator S in Eq. (7), and marching backward 50 000 time steps, produced the reconstruction at t=0 shown in the rightmost column. The maximum values in the recovered Gaussians are 46 and 23 respectively, rather than the correct values 50 and 25, shown in the leftmost column.*

Recently, we have developed a useful strategy that can stabilize ill-posed marching computations. A compensating smoothing operator is applied at each time step to quench the instability. Such stabilized schemes are slightly inconsistent, yet lead to useful results in numerous challenging nonlinear dissipative problems. In [8-12], such schemes were successfully applied in multidimensional time-reversed problems involving parabolic equations, wave propagation in viscous fluids, vibrating thermoelastic plates, and coupled sound and heat flow. Such successful reconstructions were not previously known in the literature.

2D Burgers Equation. Burgers' equation is an important PDE occurring in fluid mechanics, nonlinear acoustics, gas dynamics, and traffic flow. It is often used to provide useful insight into expected behavior in the incompressible 2D Navier-Stokes equations. The 1D time-reversed Burgers problem was considered in [13]. Theoretical stability estimates in the time-reversed Navier-Stokes equations are given in [14]. However, no time-reversed computations are known in the literature for either the Navier-Stokes equations or the 2D Burgers equation. The theoretical results in [14] indicate that accurate backward reconstructions with imprecise data is unlikely for either of these two PDEs. The time-reversed 2D Burgers problem would therefore provide a significant test of the viability of ACMD's compensated explicit schemes.

Let Ω be a bounded domain in $R^2$with a smooth boundary $\partial\Omega$. Let $<,>$ and $\| \|_2$, respectively denote the scalar product and norm on $\mathcal{L}^2(\Omega)$. With $(x,y) \in \Omega, t > 0$, we shall sudy the following system

$$\begin{aligned} u_t &= \nu\Delta u - uu_x - vu_y \\ v_t &= \nu\Delta v - uv - vv_y \end{aligned} \tag{1}$$

$$\begin{aligned} u(x,y,0) = u_0(x,y),\ v(x,y,0) = v_0(x,y),\ (x,y) \in \Omega \\ u(x,y,t) = v(x,y,t) = 0,\ (x,y) \in \partial\Omega,\ t \geq 0. \end{aligned} \tag{2}$$

In Eq. (1), $\nu > 0$ is the kinematic viscosity. With

$$\begin{aligned} L = \nu\Delta, \quad f(x,y,t) &= -uu_x - vu_y \\ g(x,y,t) &= -uv_x - vv_y, \end{aligned} \tag{3}$$

it is convenient to rewrite Eq. (1) in the form

$$\begin{aligned} u_t &= -Lu + f(x,y,t),\ 0 < t \leq T_{max} \\ v_t &= -Lv + g(x,y,t),\ 0 < t \leq T_{max} \end{aligned} \tag{4}$$

Let $\{\phi_m\}_{m=1}^{\infty}$be the complete set of orthonormal eigenfunctions for L on Ω, and let $\{\lambda_m\}_{m=1}^{\infty}$, satisfying

$$0 < \lambda_1 \leq \cdots \leq \lambda_m \leq \cdots \uparrow \infty, \tag{5}$$

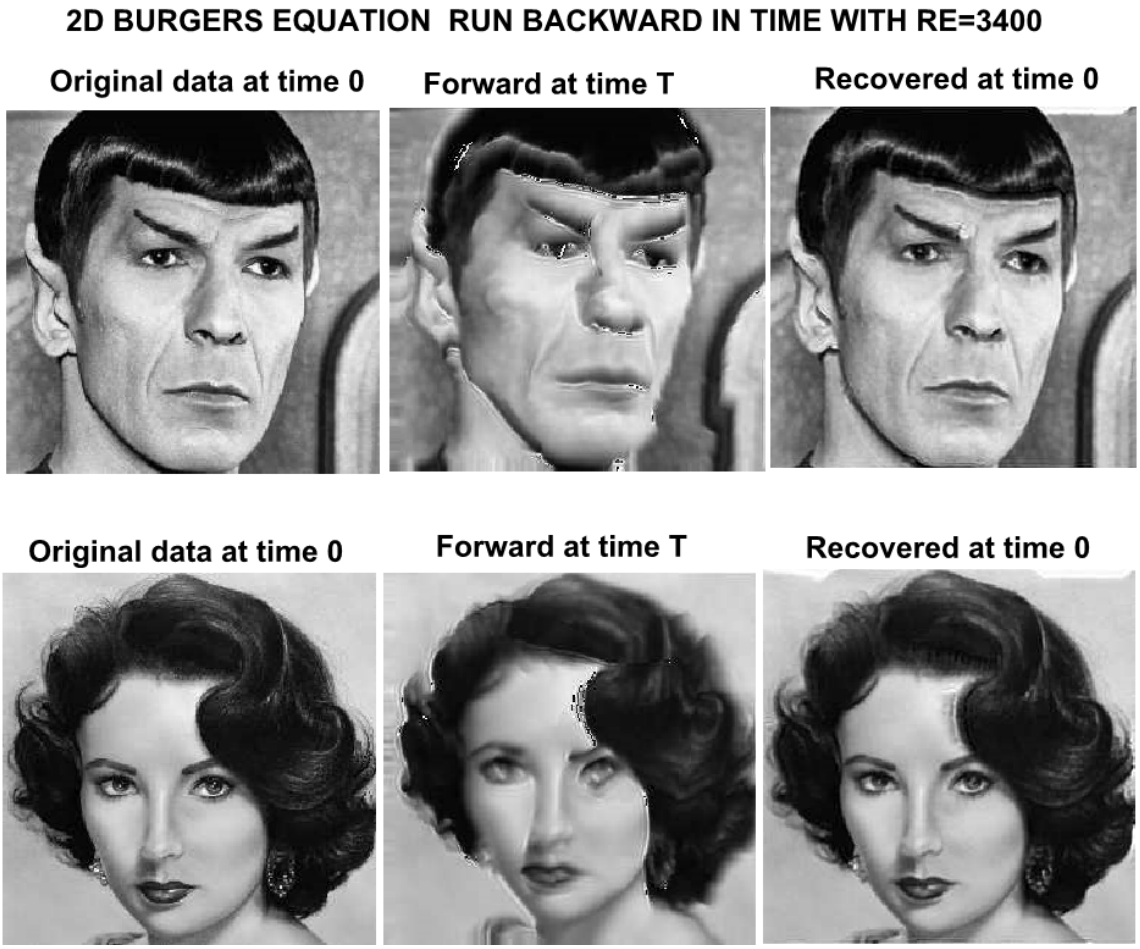

Figure 38. *Using the input data at T = 0.0002143 shown in the middle column, using Δt = -7.143 x 10⁻⁹, p = 3.25, in the compensating operator S in Eq. (7), and marching backward 30 000 time steps, produced the reconstruction at t = 0 shown in the rightmost column. Note the smudge on the left side of Liz Taylor's forehead.*

be the corresponding eigenvalues. The family $\{\lambda_m, \phi_m\}$ is assumed known or precomputed.

With a given positive integer N, let $|\Delta t| = T_{max}/(N+1)$ be the time step magnitude, and let $\tilde{u}^n = \tilde{u}(x, y, n\Delta t)$, $n = 1, \ldots, N+1$ denote the intended approximation to $u(x, y, n\Delta t)$, and likewise for $\tilde{v}^n$. Similarly, let $\tilde{f}^n \equiv -\tilde{u}^n\tilde{u}_x^n - \tilde{v}^n\tilde{u}_y^n$, denote the approximation to $f(x, y, n\Delta t),, 1, \ldots, N+1$, and likewise for $\tilde{g}^n$, where f and g are as in Eq. (3).

With given fixed $\omega > 0$, $p > 1$, define the linear operator S with eigenvalues q_m as follows

$$\begin{aligned} S &= \exp\{-\omega|\Delta t|L^P\} \\ q_m &= \exp\{\omega|\Delta t|\lambda_m^P\}, m > 1 \\ Su &= \Sigma_{m=1}^{\infty} q_m \langle u, \phi_m\rangle \phi_m, \ \ \forall u \in \mathcal{L}^2(\Omega) \end{aligned} \quad (6)$$

As in [8-12], the operator S is used as a stabilizing smoothing operator at each time step, in the following explicit time-marching finite difference approximation to Eq. (4), in which only the time variable is discretized, while the space variables remain continuous. We contemplate time-reversed computations by allowing for possible *negative* time steps Δt.

$$\begin{aligned} \tilde{u}^{n+1} &= S\tilde{u}^n - \Delta t S L\tilde{u}^n + \Delta t S\tilde{f}^n \\ \tilde{v}^{n+1} &= S\tilde{v}^n - \Delta t S L\tilde{v}^n + \Delta t S\tilde{g}^n \end{aligned} \quad n = 0,1, \ldots, N+1 \quad (7)$$

Analysis of the above scheme, along the lines discussed in [8-12], is currently in process. The smoothing operation at each time step leads to a distortion away from the true solution. However, in many problems of interest, that error is sufficiently small to allow for useful results.

Numerical experiments in rectangular regions. In a rectangular region, the eigenfunctions of the Laplacian with zero boundary conditions are known, and FFT algorithms can be used effectively to synthesize the compensating smoothing operator S in Eqs. (6, 7). Our first experiment, shown in Figure 37, involves initial data $u_0(x, y)$, $v_0(x, y)$, in the form of two Gaussians on the unit square, with maximum values of 50 and 25 respectively, as shown in the leftmost column. With a

kinematic viscosity $\nu = 0.001$ in Eq. (1), this leads to a Reynolds number $Re = 50\,000$. Using centered differencing for the space variables in Eq. (7) on a 512 × 512 mesh, with S chosen as the identity operator, stable forward computation for 250 000 time steps $\Delta t = 1.0 \times 10^{-8}$, up to time $T_{max} = 2.5 \times 10^{-3}$, produced the input data shown in the middle column of Figure 37. The maximum value at time T_{max} is almost double that at time 0, and the character of the solution has changed noticeably. These computed data are of unknown precision. However, using these data, and using $\Delta t = -5.0 \times 10^{-8}$, with $\omega = 1.0 \times 10^{-9}, p = 3.0$ in the compensating operator S in Eq. (7), and marching backward in time 50 000 time steps, produced the reconstruction at $t = 0$ shown in the rightmost column. This result is remarkable given the high value of Re. It should be noted that the maximum values in the recovered Gaussians are 46 and 23 respectively.

Our second experiment involves considerably more complicated initial data, namely, the intensity data associated with the 256 × 256 gray scale 8-bit images in the left column of Figure 38. As noted in [8, 12], most images are defined by highly nonsmooth intensity data, and nonlinear backward-in-time image reconstruction poses severe challenges. Here, the maximum value in the input data is 255, and the kinematic viscosity $\nu = 0.075$, leading to a Reynolds number $Re = 3\,400$. Using centered differencing for the space variables in Eq. (7) on a 256 × 256 mesh, with S chosen as the identity operator, stable forward computation for 300 000 time steps $\Delta t = 7.143 \times 10^{-10}$, up to time $T_{max} = 2.143 \times 10^{-4}$, produced the input blurred images shown in the middle column for Figure 38. Clearly, Burgers equation produces noticeable distortions, of a character distinctly different from typical optical aberrations. However, using these data, and marching backward in time with ten times larger $|\Delta t|$, and with $\omega = 2.0 \times 10^{-9}, p = 3.25$, in the compensating operator S in Eq. (7), results in the unexpectedly good reconstructions shown in the rightmost column in Figure 38. Note the smudge on the left side of Liz Taylor's forehead in the recovered image.
In both experiments, the optimal parameter pairs (ω, p) were found interactively.

[1] J. Atmadja and A. C. Bagtzoglou. State of the Art Report on Mathematical Methods for Groundwater Pollution Source Identification. *Environmental Forensics* **2** (2001), 205-214.

[2] R. N. Singh, Advection Diffusion Equation Models in Near-Surface Geophysical and Environmental Sciences. *Journal of the Indian Geophysical Union* **17** (2013), 117-127.

[3] A. Ismail-Zadeh, *et al.* Three-Dimensional Forward and Backward Numerical Modeling of Mantle Plume Evolution: Effects of Thermal Diffusion. *Journal of Geophysical Research* **111** (2006), B06401.

[4] A. Ismail-Zadeh, *et al.* Numerical Techniques for Solving the Inverse Retrospective Problem of Thermal Evolution of the Earth Interior. *Computers and Structures* **87** (2009), 802-811.

[5] G. Gilboa, *et al.* Forward-and-Backward Diffusion Processes for Adaptive Image Enhancement and Denoising. *IEEE Transactions on Image Processing* **11** (2002), 669-703.

[6] A. Carasso, D. S. Bright and A. E. Vladar. APEX Method and Real-Time Blind Deconvolution of Scanning Electron Microscope Imagery. *Optical Engineering* **41** (2002), 2499-2514.

[7] A. S. Carasso, Bochner Subordination, Logarithmic Diffusion Equations, and Blind Deconvolution of Hubble Space Telescope Imagery and Other Scientific Data. *SIAM Journal on Imaging Sciences* **3** (2010), 954-980.

[8] A. S. Carasso, Compensating Operators and Stable Backward in Time Marching in Nonlinear Parabolic Equations. *International Journal of Geomathematics* **5** (2014), 1-16.

[9] A. S. Carasso, Stable Explicit Time-Marching in Well-Posed or Ill-Posed Nonlinear Parabolic Equations. *Inverse Problems in Science and Engineering* **24** (2016), 1364-1384.

[10] A. S. Carasso, Stable Explicit Marching Scheme in Ill-Posed Timereversed Viscous Wave Equations. *Inverse Problems in Science and Engineering* **24** (2016), 1454-1474.

[11] A. S. Carasso, Stabilized Richardson Leapfrog Scheme in Explicit Stepwise Computation of Forward or Backward Nonlinear Parabolic Equations. *Inverse Problems in Science and Engineering* **25** (2017), 1719-1742.

[12] A. S. Carasso, Stabilized Backward in Time Explicit Marching Schemes in the Numerical Computation of Ill-Posed Time-Reversed Hyperbolic/Parabolic Systems. In review.

[13] A. Carasso, Computing Small Solutions of Burgers' Equation Backwards in Time. *Journal of Mathematical Analysis and Applications* **59** (1977), 169-209.

[14] R. J. Knops and L. E. Payne, On the Stability of Solutions of the Navier-Stokes Equations Backward in Time. *Archives of Rational Mechanics and Analysis* **29** (1968), 331-335.

Parallel Adaptive Refinement and Multigrid Finite Element Methods

William F. Mitchell
Eite Tiesinga (NIST PML)
Paul Julienne (NIST PML)
John Villarrubia (NIST PML)

http://math.nist.gov/phaml

Finite element methods using adaptive refinement and multigrid techniques have been shown to be very efficient for solving partial differential equations (PDEs). Adaptive refinement reduces the number of grid points by concentrating the grid in the areas where the

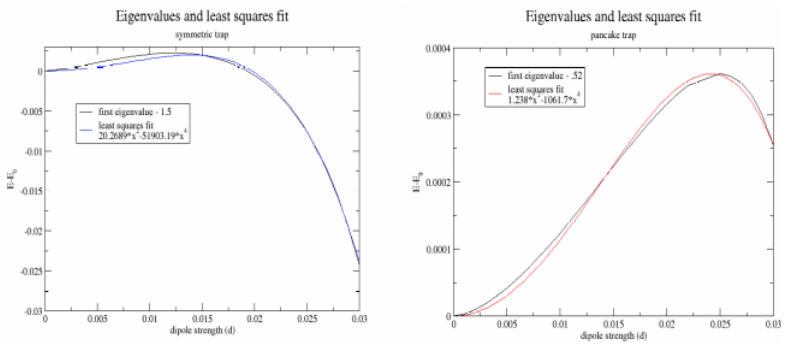

Figure 39. *Eigenvalues as a function of dipole strength, and least squares fits.*

action is, and multigrid methods solve the resulting linear systems in an optimal number of operations. Recent research has been with *hp*-adaptive methods where adaptivity is in both the grid size and the polynomial order of approximation, resulting in exponential rates of convergence. W. Mitchell has been developing a code, PHAML, to apply these methods on parallel computers. The expertise and software developed in this project has been applied to many NIST laboratory programs, including material design, semiconductor device simulation, the quantum physics of matter, and simulation of scanning electron microscopes.

We continue to improve the methods used for the parallel implementation of PHAML, in both the OpenMP shared-memory implementation and the MPI message-passing implementation. We developed a new refinement-edge-based approach to maintaining compatibility of the adaptively refined mesh which is more amenable to OpenMP than the previous element-based version. In this approach one selects a list of refinement edges and simultaneously refines all elements that contain a refinement edge, after recursively refining elements whose refinement edge is a different edge. This is implemented with task-based parallelism in OpenMP 3.0, and results in an implicit directed acyclic graph (DAG), which many consider to be the best approach for future high-performance computer architectures.

The MPI implementation was improved by replacing the expensive all-to-all communication for maintaining compatibility with nearest-neighbor communication. The recursion that maintains compatibility results in a so-called compatibility chain in 2D, or compatibility tree in 3D. This chain of elements may reach far across the domain to regions that could be owned by any processor. In the previous implementation, this requires all-to-all communication to inform all other processors of elements that must be refined for compatibility. In the new implementation, refined elements at the partition boundary are communicated to the neighboring processors, and the neighbor will continue the compatibility chain within its region, and, if it reaches another boundary, communicate that to its neighbors.

We are currently performing scalability studies to determine the effectiveness of these two new implementations. These computations are being performed on the Texas Advanced Computing Center (TACC) supercomputer Stampede, which is based on Intel Knight's Landing (KNL) processors.

We have created a Web site [4] to make available a collection of standard PDEs that are suitable for benchmarking and testing adaptive mesh refinement algorithms and error estimators. This year, we added a 2D advection dominated problem to this collection.

There are currently two major collaborative efforts with NIST PML to apply PHAML to their physical models. First, in a collaboration with E. Tiesinga and P. Julienne, we are using PHAML to study the interaction of atoms and molecules held in an optical trap. In particular, we are using 2D and 3D models to calculate the bound states, scattering properties and dynamics of two interacting dipolar molecules. Tiesinga has recently found a near-exact solution to the dipole problem using second-order perturbation theory. We are currently working to confirm this solution using computational solutions from PHAML. This requires very high accuracy solutions while varying the dipole strength over small values, using problems with a symmetric trap and with a "pancake" trap. Using PHAML, we obtained computational eigenvalues with 10 significant digits by using a mesh with 25 million vertices and 4th order elements. As a first step toward confirming the near-exact solution, the resulting eigenvalues were compared to a least-squares quartic+quadratic fit with fairly reasonable accuracy as shown in Figure 39.

We are also collaborating with J. Villarrubia to apply PHAML to the modeling of scanning electron microscope (SEM) images of samples containing a mixture of conducting and insulating regions. Villarrubia has a code, JMONSEL, that models electron scattering in materials, secondary electron production, and detection. We have coupled this code with PHAML which performs the finite element analysis to determine the electric fields that affect the image. We developed a new a posteriori error estimator suited to SEM simulations. The idea is to design an estimate that minimizes the error in the deflection of the electron path rather than minimizing some norm of the electric potential. We performed experiments [2] to compare the performance of the adaptive meshes from the new error estimator with those from a standard error estimator and with the fixed graded meshes currently used. For this experiment we used a simulation with 10 500 randomly placed point charges in a parallelpiped within a layer of

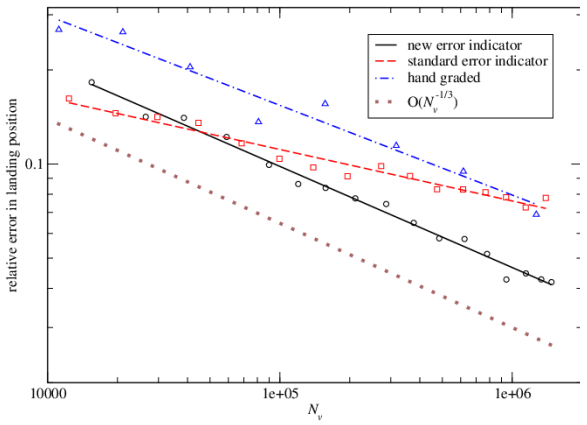

Figure 40. *For the SEM problem, comparision of the error in landing position as a function of mesh size.*

conducting material below the vacuum, for which an exact solution is known. This allows us to compute an error metric based on the trajectories of a collection of electrons using the computed electric field compared to using the exact electric field. The metric is the error in the landing position of an electron that escapes into the vacuum and returns to the surface, averaged over a collection of 193. The graph in Figure 40 shows the error as a function of the number of vertices, N_v, in the mesh. We expect to see $O(h)$ convergence, the slope of which is indicated by the dotted brown line. The new error estimate exhibits near-perfect $O(h)$ convergence. The hand graded mesh is also close to $O(h)$ but with a larger constant, and requires 4-5 times as many vertices to achieve a given error tolerance. The standard error estimate fails to achieve $O(h)$ convergence, which is not surprising since it is designed to optimize a different error metric.

Future work will continue to enhance PHAML with additional capabilities, robustness and efficiency, improve the parallel implementation with an emphasis on modern architectures such as the Intel Xeon Phi (Knight's Landing), and pursue NIST collaborations.

[1] W. F. Mitchell. Performance of *hp*-Adaptive Strategies for 3D Elliptic Problems. In *Proceedings of the Computation and Information Science and Engineering Conference*, 2016.

[2] W. F. Mitchell and J. S. Villarrubia. "Scanning Electron Microscope Simulation with Adaptive Finite Elements." *SIAM Conference on Computational Science and Engineering*, Atlanta, GA, March 2017.

[3] W. F. Mitchell. 30 Years of Newest Vertex Bisection. *Journal of Numerical Analysis, Industrial and Applied Mathematics* **11** (2017), 11-22.

[4] NIST Adaptive Mesh Refinement Benchmark Problems. URL: http://math.nist.gov/amr-benchmark

Numerical Solutions of the Time-Dependent Schrödinger Equation

Barry I. Schneider
Heman Gharibnejad
Mark Leadingham (WV Wesleyan College)
Luca Argenti (University of Central Florida)
Nico Douguet (University of Central Florida)
Jeppe Olsen (Aarhus University)

We have been developing numerically robust methods for solving the time dependent Schrödinger equation for several years. Luca Argenti, a new Assistant Professor from the University of Central Florida and his postdoc, Nico Douguet, joined the effort in 2016. Heman Gharibnejad, a NIST/NRC postdoctoral associate, joined the group in January of 2017.

There are two related research threads underway. The primary effort has been to develop a hybrid finite element discrete variable (FEDVR)-Gaussian approach to treat the interaction of attosecond (10^{-18} sec) radiation with molecular targets. In addition, we are examining the performance of various numerical time propagation techniques for the TDSE. This past summer, an undergraduate student intern, Mark Leadingham, worked with us to develop a simple one spatial dimension, time propagation code to test some of the numerical methods. While the model is simple, it serves well to illustrate the problems that would be faced in higher spatial dimensions while being simple enough for a talented undergraduate to tackle in a summer research program. A paper is being prepared for publication on this latter work.

The hybrid finite element approach that has been developed is quite general, but the applications to date have concentrated on describing the single and double ionization of electrons exposed to intense, ultrafast, laser radiation in many-body atomic and molecular systems. These attosecond (10^{-18} sec) pulses provide a new window to study the electronic motion in atoms and molecules on their natural timescale. To put this in context, the motion of electrons responsible for chemical binding and electron transfer processes in nature, have a characteristic timescale of about 100 attoseconds. (It takes an electron 152 attoseconds to go around the hydrogen atom.) These processes can only be described using time dependent quantum mechanics and, where appropriate, need to be coupled to Maxwell's equations to describe macroscopic phenomena. At the end of the day, we wish to image quantum phenomena with subfemtosecond temporal and sub-Angstrom spatial resolution. Eventually, one can contemplate producing "molecular movies" of this motion in much the same way as it is done in molecular dynamics simulations of heavy particle processes.

The basic methodology as applied to atoms and simple diatomic molecules, has been described in [1-3,

5-11] and [4] provides a detailed review of the work. The essential aspects have been

- Development of the finite element discrete variable method (FEDVR) to spatially discretize the coordinates of the electrons, and
- Use of the short iterative Lanczos method to propagate the wavefunction in time.

The method has been efficiently parallelized using MPI and scales linearly with the size of the FEDVR basis. Large scale calculations have been performed on a number of atoms and molecules using resources provided by the NSF Extreme Science and Engineering Discovery Environment (XSEDE) program. The group has received a competitively awarded allocation of more than 3 million service units for the current fiscal year.

We have begun a study to employ a mixed basis of Gaussian functions at short range and FEDVR functions at long range to extend our methods to complex polyatomic molecules. This approach has several important advantages over using a single basis over all of space. First, the use of nuclear centered Gaussians preserves the local atomic symmetry around each nucleus and avoids the poor convergence of using a single-center FEDVR basis at all distances. Second, once the electron is far enough away from the nuclear cusps, a single center expansion converges quickly and importantly, can represent the electrons out to very large distances using an approach that is very amenable to domain decomposition.

The major issue is to compute the one and two electron integrals between the two types of basis functions. Recently a new and efficient formalism, using transition density matrices, has been developed so that an optimal use can be made of existing quantum chemistry codes to extract the information required to compute the additional integrals. We have been lucky enough to interest Jeppe Olsen from Aarhus University, an extremely talented quantum chemist, to collaborate with us on the project. The NIST-UCF-Aarhus group has already met twice and substantial progress has been made. It should be noted that this is a very complex many-body problem, and even with the most talented of researchers, it is a long-term effort. We are in the process of implementing our approach and interfacing with the quantum chemistry code of Olsen. Computing the required hybrid one and two electron integrals is the major responsibility of the new NRC postdoctoral associate, Gharibnejad.

For the time propagation problem, Schneider, Gharibnejad and Leadingham have taken a simple one-dimensional model of the hydrogen atom in an intense electric field and examined the propagation of wave packets as the system evolved in time. The model uses a soft core to treat the interactions of the electron with the nucleus and a three-point finite difference approach to the second derivative operator. While this problem has been studied before, and the model is a reasonable representation of the three- dimensional hydrogen atom, our objective was to determine how various time propagation schemes perform as well as to suggest a new approach that might be more robust than those currently being used. The two senior researchers felt that this was an excellent problem for a summer student intern to tackle and indeed that turned out to be the case. Leadingham made excellent progress over the summer and Gharibnejad has worked to refine the initial research to the point where a publication will be forthcoming in the next few months. The study has found that while very simple propagation schemes such as the Crank-Nicholson (CN), variants of the split-operator (SO) method and real-space propagation (RSP) methods are very efficient per time step, the size of the time steps must be quite small to obtain accurate results. In contrast, more elaborate schemes, such as the short-iterative-Lanczos (SIL) method, are more expensive per time step but allow time steps two orders of magnitude larger than CN, SO or RSP for the same accuracy. While we suspected that might be the case, only a careful study confirmed the results. The conclusion was that the SIL performed much more efficiently in practice than the other methods. The basic reason is that the SIL only depends on the natural time scale of the laser field and not on issues of the spectrum of the operator being discretized. The SIL does not rely on a second order expansion to be accurate. We are now considering an integral equation approach that would combine the best of the SIL with perhaps even larger time steps for high accuracy.

In addition, we have given presentations [12] and published papers [13] on other aspects of our results.

[1] J. Feist, S. Nagele, R. Pazourek, E. Persson, B. I. Schneider, L. A. Collins and J. Burgdörfer. Nonsequential Two-Photon Double Ionization of Helium. *Physical Review A* **77** (2008), 043420.

[2] X. Guan, K. Bartschat and B. I. Schneider. Dynamics of Two-photon Ionization of Helium in Short Intense XUV Laser Pulses. *Physical Review A* **77** (2008), 043421.

[3] X. Guan, K. Bartschat and B. I. Schneider. Two-photon Double Ionization of H_2 in Intense Femtosecond Laser Pulses. *Physical Review A* **82** (2010), 041407.

[4] B. I. Schneider, J. Feist, S. Nagele, R. Pazourek, S. Hu, L. Collins and J. Burgdörfer. Recent Advances in Computational Methods for the Solution of the Time-Dependent Schrödinger Equation for the Interaction of Short, Intense Radiation with One and Two Electron Systems. In *Dynamic Imaging, Theoretical and Numerical Methods Series: CRM Series in Mathematical Physics XV*, (A. Bandrauk and M. Ivanov eds.), 2011.

[5] X. Guan, E. Secor, K. Bartschat and B. I. Schneider. Double-slit Interference Effect in Electron Emission from H_2^+ Exposed to X-Ray Radiation. *Physical Review A* **85** (2012), 043419.

[6] X. Guan, K. Bartschat, B. I. Schneider and L. Koesterk. Resonance Effects in Two-Photon Double Ionization of

H_2 by Femtosecond XUV Laser Pulses. *Physical Review A* **88** (2013) 043402.

[7] J. Feist, O. Zatsarinny, S. Nagele, R. Pazourek, J. Burgdörfer, X. Guan, K. Bartschat and B. I. Schneider. Time Delays for Attosecond Streaking in Photoionization. *Physical Review A* **89** (2014), 033417.

[8] X. Guan, K. Bartschat, B. I. Schneider and L. Koesterke. Alignment and pulse-duration effects in two-photon double ionization of H_2 by femtosecond XUV laser pulses, *Physical Review A* **90** (2014), 043416.

[9] B. I. Schneider, L. A. Collins, X. Guan, K. Bartschat and D. Feder. Time-Dependent Computational Methods for Matter Under Extreme Conditions. *Advances in Chemical Physics* **157**, Proceedings of the 240 Conference: Science's Great Challenges, (A. Dinner, ed.), John Wiley and Sons, Inc., 2015.

[10] B. I. Schneider, X. Guan and K. Bartschat. Time Propagation of Partial Differential Equations Using the Short Iterative Lanczos Method and Finite-Element Discrete Variable Representation. *Advances in Quantum Chemistry* **72** (2016).

[11] B. I. Schneider. How Novel Algorithms and Access to High Performance Computing Platforms Are Enabling Scientific Progress in Atomic and Molecular Physics. *IOP Journal of Physics Conference Series* **759** (2016).

[12] B. I. Schneider. 45 Years of Computational Atomic and Molecular Physics: What Have We (I) Learned. In Proceedings of the 30th International Conference on Photonic, Electronic and Atomic Collisions, August 2017, *IOP Journal of Physics Conference Series* **875**.

[13] B. I. Schneider, L. A. Collins, K. Bartschat, X. Guan and S. X. Hu. A Few Selected Contributions to Electron and Photon Collisions with H_2 and H_2^+. *Journal of Physics* (2017), 214004.

Modeling Magnetic Fusion

Geoffrey McFadden
Antoine Cerfon (New York University)

A future source of commercial energy may be based on the controlled fusion of a hot plasma of hydrogen isotopes that is confined by a strong magnetic field. Quite often, a toroidal geometry is envisioned in which the ions fuse to form helium and release energetic neutrons. Several computational methods to model such magnetic fusion devices have been developed by researchers at New York University (NYU) and elsewhere to allow effective numerical simulations of the most essential features of modern tokomak and stellarator experiments. G. McFadden and colleagues at NYU are currently participating in the continuing development of a code [1] that computes three dimensional equilibria of toroidal plasmas, and determines their nonlinear stability [2].

Recent work has extended the original iterative scheme that computes nonlinear solutions to the governing equations by implementing a quasi-Newton solver that computes solutions directly. This allows both stable and unstable solutions to be computed, in contrast to the iterative scheme that only produces stable solutions. This allows the construction of bifurcation diagrams that provide a more complete description of the solution space. In addition, an eigen-analysis of the approximate Jacobian allows the spatial structure of unstable modes to be determined, which is useful in providing guidance in choosing perturbations to high symmetry solutions in assessing the performance of the original iterative scheme. Another recent modification allows the computation of solutions that lack a mid-plane of symmetry, which will allow the assessment of tilted geometries with elongated and rotated wall perturbations [3].

[1] M. Taylor. A High Performance Spectral Code for Nonlinear MHD Stability. *Journal of Computational Physics* **110** (1994), 407-418.

[2] P. R. Garabedian and G. B. McFadden. Design of the DEMO Fusion Reactor Following ITER. *Journal of Research of the National Institute of Standards and Technology* **114** (2009), 229-236.

[3] J. Ball, F. I. Parra, M. Landreman and M. Barnes. Optimized Up-Down Asymmetry to Drive Fast Intrinsic Rotation in Tokomaks. *Nuclear Fusion* **58** (2018), 026003.

Advanced Materials

Delivering technical support to the nation's manufacturing industries as they strive to out-innovate and out-perform the international competition has always been a top priority at NIST. Mathematical modeling, computational simulation, and data analytics are key enablers of emerging manufacturing technologies. A clear case in point is the Materials Genome Initiative, an interagency program with the goal of significantly reducing the time from discovery to commercial deployment of new materials using modeling, simulation, and informatics. ACMD's role in advanced manufacturing centers on the development and assessment of modeling and simulation tools, with emphasis on uncertainty quantification, as well as support of efforts by other NIST Laboratories in materials modeling and smart manufacturing.

Micromagnetic Modeling

Michael Donahue
Don Porter
Robert McMichael (NIST CNST)
June Lau (NIST MML)
Justin Shaw (NIST PML)
Hans Nembach (NIST PML)

http://math.nist.gov/oommf/

Advances in magnetic devices such as recording heads, field sensors, spin torque oscillators, and magnetic nonvolatile memory (MRAM) are dependent on an understanding of magnetization processes in magnetic materials at the nanometer level. Micromagnetics, a mathematical model used to simulate magnetic behavior, is needed to interpret measurements at this scale. ACMD is working with industrial and academic partners, as well as with colleagues in the NIST CNST, MML, and PML, to improve the state-of-the-art in micromagnetic modeling.

We have developed a public domain computer code for performing computational micromagnetics, the Object-Oriented Micromagnetic Modeling Framework (OOMMF). OOMMF serves as an open, well-documented environment in which algorithms can be evaluated on benchmark problems. OOMMF has a modular structure that allows independent developers to contribute extensions that add to its basic functionality. OOMMF also provides a fully functional micromagnetic modeling system, handling three-dimensional problems, with extensible input and output mechanisms. In FY 2017 alone, the software was downloaded by more than 9000 users, and use of OOMMF was acknowledged in more than 170 peer-reviewed journal articles. OOMMF has become an invaluable tool in the magnetics research community.

Key developments over the last year include the following:

- The presence of OOMMF at the nanoHUB project [1] of Purdue University was enhanced by the addition of two related projects and a user group of 55 members. JOOMMF [2] integrates the computing capabilities of OOMMF with a Jupyter [3] notebook environment. The MAGE tool [4] creates input files for OOMMF simulations.
- Continued development of extended precision numerics and an alternative approach to the demagnetization energy calculation based on hybrid fine/coarse grid computations.
- Created multiple Git branches of development to pursue and integrate new features and interfaces while preserving a stable code base that supports third party extension code without disruption.
- Released OOMMF versions 1.2b1 [5] and 2.0a0 in September 2017 [6].

OOMMF is part of a larger activity, the Micromagnetic Modeling Activity Group (muMAG), formed to address fundamental issues in micromagnetic modeling through two activities: the development of public domain reference software, and the definition and dissemination of standard problems for testing modeling software. ACMD staff members are involved in development of the standard problem suite as well. A contributed solution to Standard Problem 5 [7] was received and published. [8]

In addition to the continuing development of OOMMF, the project also does collaborative research using OOMMF. M. Donahue provides technical guidance on micromagnetic modeling for the DARPA M3IC (Magnetic, Miniaturized, and Monolithically Integrated Components) project [9], which aims to integrate magnetic components into the semiconductor materials fabrication process. The goal is to improve electromagnetic systems for communications, radar, and related applications.

In total, the ACMD micromagnetic project produced two invited talks [10, 11] and two conference presentations [12, 13] during this past year.

[1] https://nanohub.org/
[2] https://nanohub.org/resources/oommfnotebooks
[3] https://jupyter.org
[4] https://nanohub.org/tools/mage
[5] https://math.nist.gov/oommf/software-12.html

[6] https://math.nist.gov/oommf/software-20.html
[7] https://www.ctcms.nist.gov/~rdm/std5/spec5.xhtml
[8] https://www.ctcms.nist.gov/~rdm/std5/Finnochio.html
[9] https://www.darpa.mil/program/magnetic-miniaturized-and-monolithically-integrated-components
[10] M. J. Donahue. "Quantifying Discretization Error in Micromagnetic Software." Magnetism 2017 Conference, University of York, York, UK, April 3, 2017.
[11] M. J. Donahue. "Tutorial: Introduction to Micromagnetics and OOMMF." OOMMF Workshop, University of York, York, UK, April 5, 2017.
[12] M. J. Donahue. "Fast Coarse Grid Demagnetization Tensor Computation with Local Refinement for Micromagnetics." Intermag 2017 Conference, Dublin, Ireland, April 27, 2017.
[13] M.J. Donahue. "Hybrid Fine/Coarse Stray Field Computation for Micromagnetics." 62nd Annual Conference on Magnetism and Magnetic Materials (MMM 2017), Pittsburgh, PA, November 10, 2017.

OOF: Finite Element Analysis of Material Microstructures

Stephen A. Langer
Andrew C.E. Reid (NIST MML)
Günay Doğan (Theiss Research)
Shahriyar Keshavarz (Theiss Research)
Marilyn Y. Vasquez (George Mason University)
Rachel Linder (University of Maryland)

http://www.ctcms.nist.gov/oof/

The OOF Project, a collaboration between ACMD and MML, is developing software tools for analyzing real material microstructure. The microstructure of a material is the (usually) complex ensemble of polycrystalline grains, second phases, cracks, pores, and other features occurring on length scales large compared to atomic sizes. The goal of OOF is to use data from a micrograph of a real or simulated material to compute its macroscopic behavior via finite element analysis.

The OOF user loads images into the program, assigns material properties to the features of the image, generates a finite element mesh that matches the geometry of the features, chooses which physical properties to solve for, and performs virtual experiments to determine the effect of the microstructural geometry on the material. OOF is intended to be a general tool, applicable to a wide variety of microstructures in a wide variety of physical situations. It is currently used by academic, industrial, and government researches worldwide.

There are two versions of OOF, OOF2 and OOF3D, each freely available on the OOF website. OOF2 starts with two dimensional images of microstructures and solves associated two dimensional differential equations, assuming that the material being simulated is either a thin freely suspended film or a slice from a larger volume that is unvarying in the third dimension (generalizations of plane stress and plane strain, respectively). OOF3D starts with three dimensional images and solves equations in three dimensions.

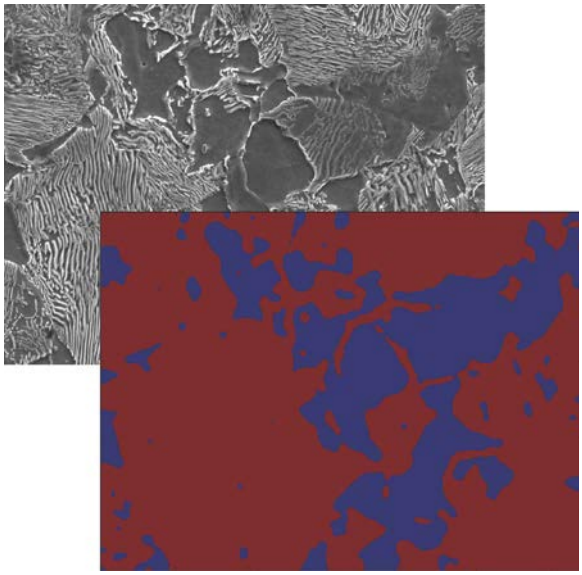

Figure 41. *A micrograph of pearlite steel (background) segmented into two phases (forground) by the Vazquez method.* [Photo credit: Steel image from M. Stoudt and S. Mates of NIST/MML].

During this year, S. Keshavarz and A. Reid made significant advances in incorporating crystal plasticity into the main OOF code. Plastic deformation occurs when a material is deformed so far that it doesn't spring back to its initial shape when the deforming forces are released. Crystal plasticity models describe plastic deformation materials, such as metals, whose plastic deformation is determined by their crystal structure. The models are complex and highly nonlinear. Keshavarz and Reid wrote a prototype code in Python, outside of OOF, and have been working to incorporate it into OOF. The current prototype code now accurately reflects the structure of the API used by OOF, and is proving to be a valuable step in adapting the crystal plastic algorithm to the OOF object structure and control flow. Success in this task will allow plasticity properties developed for the prototype, with quick turnaround and minimal overhead, to be easily adapted to the main OOF code.

A. Reid spoke about the OOF code at a number of conferences, most notably the 4th World Congress on Integrated Computational Materials Engineering, and the SIAM Conference on Computational Science and Engineering (CSE). At the former, a number of multiscale integrated materials modeling frameworks were identified, and informal conversations about integrating the OOF code into these larger frameworks were begun. At the SIAM CSE conference, a chance encounter with a field discretization algorithm used by cosmologists to model gas density fields lead to a useful strategic insight

into a long-standing problem in the OOF3D code, where the measurement of the partial volumes of microstructural features overlapping with elements had been a long-standing difficulty.

One of the measures that OOF2 and OOF3D use to determine whether a finite element mesh is a good representation of a micrograph is element homogeneity: the largest fraction of an element's area or volume that overlies the pixels or voxels (3D pixels) that represent each material component of the microstructure. In 3D, computing the homogeneity boils down to computing the intersection of a tetrahedral element with a set of voxels, which need not be either convex or simply connected. Computing the intersection of each voxel individually is computationally far too slow, so it is necessary to work with the surfaces of sets of voxels. Earlier efforts involved extracting the facets of the voxel set and computing the intersections of the facets with the cross sections of the tetrahedra. This work turned out to be surprisingly difficult, because round-off error in the (literal) corner cases could lead to ambiguous geometry, and microscopic errors in the position of an intersection point would create macroscopic errors in the computed intersection volume. This year S. Langer took the algorithm that A. Reid learned of at the SIAM CSE meeting and modified it to compute the voxel set/tetrahedron intersection quickly and robustly. Powell and Abel's "r3d" [1] algorithm was originally developed to remesh a grid while preserving integrals over the elements. It works by computing the edge graph of one convex polyhedron and clipping it sequentially with the faces of a second convex polyhedron. The core of the algorithm is the clipping method, which only relies on the topology of the graph and knowledge of which graph nodes are on which sides of the clipping plane. As such, it is immune to round-off error, because if a node appears to be infinitesimally on the wrong side of the clipping plane, the clipped polyhedron will only be infinitesimally different from the correct polyhedron.

A later modification of the r3d method [2] extended it to the case where one polyhedron was non-convex, which almost makes it applicable to arbitrary sets of voxels. However, the method also requires that the edge graph of the polyhedron be "three-vertex-connected", meaning that removing any two vertices will not split the graph into two disconnected pieces. It is easy to construct concave assemblies of voxels that do not meet this criterion, and r3d fails on them. Langer showed that an infinitesimal perturbation of the problem cases restores the required connectivity and indicates the correct clipping procedure.

The trickiest part of implementing r3d for voxels sets is to efficiently construct the edge graph for the voxels. Langer solved this by characterizing each corner in the voxel set by a byte indicating which of the 8 voxels at the corner are in the set. Taking advantage of rotational symmetry, the 256 possibilities resolve into 17 non-trivial cases, each of which is represented by a C++ "ProtoNode" class. The voxel set generates an array of ProtoNodes by simple table lookup, and then the ProtoNodes generate the actual graph nodes and edges by examining their nearest neighbors in each direction. There are subtleties, such as the double coincident graph edges required when two voxels touch along an edge, and the two graph edges must be connected consistently at both ends to ensure that the graph is well formed. These subtleties are handled by ProtoNode subclasses.

G. Doğan has been developing algorithms to automate segmentation and meshing of microstructure images. A mesh that is correctly aligned with the segmented regions and their boundaries in the microstructure is an essential ingredient for accurate finite element simulations of the microstructure physics. In the recent years, Doğan has been developing iterative segmentation algorithms based on shape optimization. These algorithms detect optimal region boundaries in microstructure images by minimizing specially designed image segmentation energies. Doğan has previously implemented edge-based and region-based segmentation energies, including a multiphase segmentation energy. Last year, he worked on improvement of the anisotropic edge-based energy, which gives better segmentations by aligning normals of the boundary curves with extended image gradients. He used the second shape derivative of the energy to implement a faster shape-Newton algorithm to compute better results in shorter time.

Microstructure images are very diverse, with widely-varying features and geometries. Therefore, any given class of segmentation algorithms cannot be expected to segment all microstructure images. An effective and user-friendly approach to this problem must be multi-pronged, and leverage several different classes of segmentation algorithms. Thus, Doğan has been exploring and pursuing other approaches as well. He has been investigating the use of data clustering algorithms for segmentation. For this, he has been working with Ph.D. student, M. Vazquez of George Mason University. Vazquez developed a novel clustering algorithm, and applied it to pearlite microstructure images. The results seem very promising; her algorithm produced good segmentations at different scales.

Doğan has also been collaborating with H. Antil of George Mason University to develop a new segmentation algorithm built on a phase field representation. The phase field representation is used to embed the regions and their boundaries. This approach contrasts with Doğan's previous work, which models the regions and the boundaries explicitly as curves. The advantage of the phase field segmentation algorithm is that it extends to 3D trivially. Moreover, each iteration of the solver requires only a few FFT operations executed on the image grid, both in 2D and 3D. This work is in preliminary stages, but is very encouraging so far.

[1] D. Powell and T. Abel. An Exact General Remeshing Scheme Applied to Physically Conservative Voxelization. *Journal of Computational Physics* **297** (2015), 340–356.

[2] D. Powell. r3d: Software for Fast, Robust Geometric Operations in 3D and 2D. LA-UR-15-26964, Los Alamos National Laboratory, 2015. URL: https://github.com/devonmpowell/r3d/blob/master/la-ur-15-26964.pdf

Numerical Methods for Reliable Computations with Equations of State

Ian Bell (NIST MML)
Bradley Alpert

Equations of state (EOS) provide quantitative relationships between thermodynamic variables of fluid mixtures, such as temperature, pressure, volume, and internal energy, that enable determination of key fluid properties, by exploiting statistical physics to interpolate or extrapolate beyond where laboratory measurements are economical or feasible. NIST provides data facilities REFPROP (Reference Fluid Thermodynamic and Transport Properties Database) and TDE (ThermoData Engine), widely accessed for a variety of chemical engineering needs, from critically evaluated laboratory data in combination with EOS.

Increasing reliance on, and automation of, retrieval of such thermodynamic property data imposes heightened demands on the reliability and generality of algorithms both for deriving and for exploiting the EOS. Calculation of the density of a mixture for a given temperature, pressure, and mixture composition from multiparameter mixture models sometimes fails, due to insufficiently accurate root finding, but also insufficiently robust algorithms that may miss certain roots entirely. The initial result of this collaboration has been to represent transcendental equations in one dimension with orthogonal polynomial (Chebyshev) expansions that enable reliable root finding. A concomitant requirement for very fast evaluations, achieved here, arises since typical applications may involve an extremely large number of root finding steps.

Near-term extension to two dimensions, where critical points and phase boundaries introduce significant geometric complications, is planned.

[1] I. H. Bell and B. K. Alpert. Exceptionally Reliable Density Solving Algorithms for Multiparameter Mixture Models from Chebyshev Expansion Rootfinding. in review.

Data Analysis and Uncertainty Quantification for Molecular Modeling of Advanced Materials

Paul Patrone
Anthony Kearsley
Andrew Dienstfrey

In a variety of manufacturing settings, advances in computer simulations have led to a dramatic paradigm shift in the way that new materials are created and tested. For example, molecular dynamics (MD) simulations are now routinely used to aid in the development of next-generation composites for passenger airplanes [1-4]. Similarly, chemical companies are exploiting MD to speed up discovery of lubricants with desirable properties, e.g., extended service-life in automobile engines. From an economic perspective, the motivations behind this trend are clear: every dollar spent on simulations yields as much as a $9 return-on-investment [5]. Moreover, the costs of more traditional "make-it-and-break-it" testing approaches can consume entire R&D budgets, so that there are significant incentives to develop cheaper alternatives. Given that MD can often replicate experimental procedures in an inexpensive, virtual environment, this tool has thus become a mainstay in materials modeling.

Despite their growing usefulness, however, simulations are often accompanied by distinct sources of uncertainty that can sometimes render predictions questionable. This issue largely arises from the fact that computers, while more powerful than ever, are still limited in their ability to model many degrees of freedom. Practically speaking, this limitation means that simulations cannot resolve bulk structures (e.g., airplane wings) with atomistic detail, so modelers are forced to simulate microscopic systems that may not be fully representative of the desired material. As a result, finite-size effects, thermal noise, and related issues manifest as noise in data, which confounds attempts to accurately predict materials' properties [3]. Scientists therefore need robust uncertainty-quantification tools if the full benefits, economic and otherwise, of simulations are to be realized.

Building on work from FY 2016, ACMD staff have collaborated with scientists from Boeing, Cytec/Solvay, ExxonMobil, and Schrödinger to develop uncertainty quantification (UQ) methods relevant to their associated modeling protocols. While the details cover a broad range of topics [4, 6], a key theme has emerged from this work: analysis and UQ of simulated predictions benefit from approaches that leverage the global behavior of data, especially when informed by physical principles. Generally speaking, this adage has long been observed by the scientific community, but in computational science it has more recently fallen victim to the belief that

larger computers obviate the need for systematic UQ. Thus, a large component of our work aims to not only develop methods that approach simulated data in a thoughtful manner, but also educate the community about such best-practices.

A typical problem that illustrates these points is the task of using MD to estimate the yield-strain ϵ_y of thermoset composites [4]. Roughly speaking, ϵ_y corresponds to the amount of deformation required to break a material. In the MD community, common practice estimates the yield strain by simulating a stress-strain curve and subsequently identifying ϵ_y as the first local extremum. However, a desire to more rapidly study complicated systems (especially in high-throughput industrial settings) often leads one to consider small systems with significant finite-size effects; see Figure 42 for a characteristic data set. Given that there is no known functional form for a generic stress-strain curve, data such as this has therefore confounded attempts to reliably estimate the ϵ_y in materials design studies.

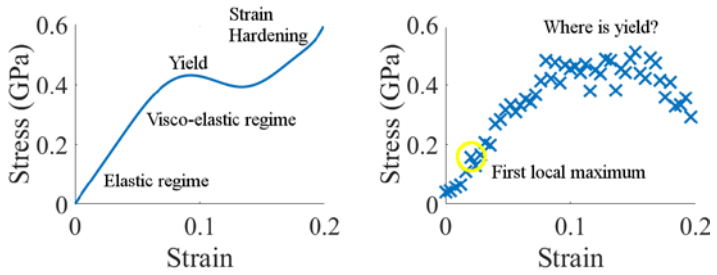

Figure 42. *Examples of an idealized (left) and simulated (right) stress-strain curves. The latter is so noisy that it is difficult to identify a global maximum, which corresponds to the yield-strain of the material.*

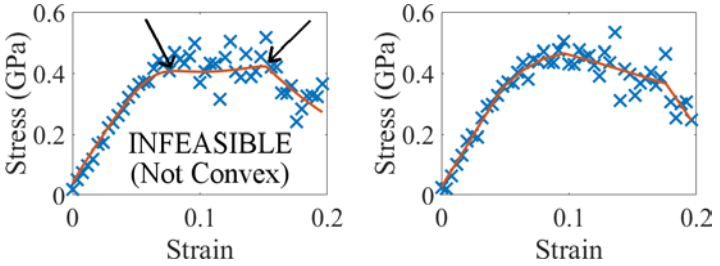

Figure 43. *Solutions to the quadratic program discussed in the main text. The left dataset yields an infeasible problem to within the noise-threshold. The orange curve is the algorithms best attemps at fitting a concave function to the data. The right dataset yields a fit that is concave.*

Despite these problems, however, deeper consideration of the underlying physics suggests a more generic description of yield that proves useful. In particular, it is well known that stress-strain curves exhibit four general regions with different behavior (see Figure 42):

(I) a linear regime;
(II) viscoelastic "softening";
(III) yield (i.e. the first local maximum); and
(IV) strain hardening.

Up to and somewhat beyond yield, it is reasonable to expect that the stress $\sigma(\varepsilon)$ is a concave function of strain, given that viscoelastic processes tend to dissipate energy. With this in mind, we therefore anticipate that a reasonable simulated stress-strain curve should be a superposition of a concave function with noise.

To make use of this observation, we recently proposed an analysis method that: (i) determines if a given dataset is concave to within a noise threshold, and (ii) if so, determines the closest concave function to the data. The method is essentially stated as a problem in convex optimization, with the solution determined by the quadratic program

$$\boldsymbol{\varsigma} = \min_{\hat{\boldsymbol{\varsigma}}} \left[\sum_i (\hat{\varsigma}_i - \sigma_i)^2 \right]$$

subject to the linear inequality constraints

$$\mathbf{A}\hat{\boldsymbol{\varsigma}}^T \leq \mathbf{0}$$
$$\mathbf{b}_l \leq \hat{\boldsymbol{\varsigma}} \leq \mathbf{b}_h$$

where inequalities are interpreted componentwise, $\mathbf{A}$ is the finite-difference matrix and σ_i is the simulated stress at the ith strain increment, and $\mathbf{b}_l$ and $\mathbf{b}_h$ are lower and upper bounds on the admissible values of the optimized stress. Notably, the quadratic program is not guaranteed to be feasible (i.e., have a solution), which thereby amounts to a test for the existence of a concave function that fits within the noise threshold. Figure 43 shows an example of this analysis applied to two different datasets, one for which there is a concave fit, and one for which there is not. Results have been published [4].

In addition to these more basic research tasks, we have also been engaging the MD community in an effort to better communicate best practices for MD and UQ thereof. To this end, Patrone and Dienstfrey authored an invited book chapter on UQ of MD for the series *Reviews in Computational Chemistry* [6]. The chapter (which is slated for publication in FY 2018) is intended to provide basic UQ tools to graduate-level modelers learning MD. In addition to this, Patrone has been involved in preparing a manuscript on best-practices in MD for the new journal *LiveCoMs*. Plans include extending our UQ tools to problems relevant to the petrochemicals industry.

[1] S. Christensen and J. Senger. Distortional Matrix of Epoxy Resin and Diamine. U.S. Patent 7,745,549 B2, filed December 20, 2006, and issued June 29, 2010.

[2] S. Christensen and J. Senger. Distortional Matrix of Epoxy Resin and Diamine. U.S. Patent 7,985,808 B2, filed April 23, 2010, and issued July 26, 2011.

[3] V. Sundararaghavan and A. Kumar. Molecular Dynamics Simulations of Compressive Yielding in Cross-Linked

Epoxies in the Context of Argon Theory. *International Journal of Plasticity* **47** (2013) 111-125.

[4] P. Patrone, A. Dientsfrey and A. Kearsley. The Role of Data Analysis in Uncertainty Quantification: Case Studies for Materials Modeling. In review.

[5] Gerhard Goldbeck. *The Economic Impact of Molecular Modelling: Impact of the Field on Research, Industry, and Economic Development*. Goldbeck Consulting Ltd., St. John's Innovation Centre, Cambridge, UK, 2012.

[6] P. Patrone and A. Dienstfrey. Uncertainty Quantification for Molecular Dynamics. In *Reviews in Computational Chemistry*.

Theory and Uncertainty Quantification of Coarse-Grained Molecular Dynamics

Paul Patrone
Geoffrey McFadden
Andrew Dienstfrey

In materials modeling, industrial R&D teams are increasingly reliant on computational tools such as molecular dynamics (MD) to speed up development and market insertion of next-generation materials. The ultimate dream of this strategy is to realize an "atoms-to-airplane" paradigm in which structural components such as wings can be designed in silico to meet certain strength requirements, given only knowledge of the underlying material composition. However, MD is generally limited to simulating systems with $O(10^6)$ atoms or less over timescales of nanoseconds, which is far short of the system sizes and timescales required for macroscopic component-level models. To overcome this problem, modelers have proposed a variety of coarse-graining strategies that attempt to "project-out" unnecessary degrees-of-freedom and thereby reach larger scales. But to date, no one technique has been accepted as a practical solution for coarse-grained (CG) modeling in high-throughput industrial settings.

From a fundamental standpoint, a key problem with many CG strategies is that they remove microscopic in-formation about systems in an ad-hoc manner and without any reference to limiting processes or quantitative error estimates. This removal of microscopic information has led to an untenable situation, in which the very definitions of material properties change in unpredictable ways, depending on the CG method being used. To address this so-called "representability" problem, ACMD staff are pursuing an alternate multipole-like CG strategy, in which: (i) rigid-like molecules are mapped onto a center-of-mass and inertia tensor; and (ii) the corresponding intermolecular force and torque fields are analytically derived as a series expansion in terms of their atomistic counterparts.

The benefits of this approach are two-fold. For one, the truncation of the multi-variate Taylor series for the intermolecular potential allows for systematic control in resolving the force fields between coarse-grained molecules. With sufficiently many terms in this expansion, the coarse-grain forces can be made to agree with the atomistic description to any desired accuracy. Common alternative formulations do not provide natural mechanisms for such convergence. Generally, one assumes a functional form for the intermolecular potential. Free parameters are determined by an indirect fitting process using ensemble quantities computed from dynamical simulation to assess quality of fit. Victory is declared if the agreement is satistfactory; otherwise, a new functional form is brought to the task. Another concern is that many approaches to coarse-graining assume that the multiple atoms within a grain may be collapsed to a point particle for the purposes of computing the quantities of interest. While this may be true in some cases, *a priori*, it is hard to anticipate the effects of removing rotational contributions to the dynamical energy balance that follow from this assumption.

Detailed simulations are required to explore the above ideas. Unfortunately, the large molecular dynamics code bases used by the community are difficult to modify so deeply within their core. In this past year we have developed our own simulation tools for this task. The code is written in Matlab and small systems may be computed natively in this environment. For systems on the order of hundreds of molecules, the Matlab scripts are compiled to C resulting in a 100-fold speed-up. Parallel scaling to 16 cores on a desktop was observed. We emphasize that this is an experimental code base designed for scientific computing and analysis. Large-scale simulations of tens of thousands of molecules would require a different approach.

Early results using this new simulation tool to explore our coarse-graining analysis are shown in Figure

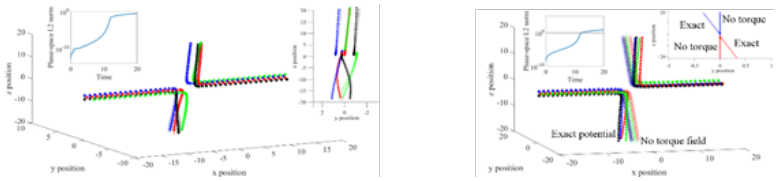

Figure 44. *Simulated collision between two rigid tetrahedral molecules using the atomistic and CG interaction potentials. Colors correspond to fixed vertices of the tetrahedra, whereas each point corresponds to the position of a given vertex at different timesteps. Solid dots are trajectories associated with the atomistic potential, open diamonds correspond to CG approximations. The left plot shows trajectories for the atomistic and CG model. The inset shows trajectory convergence in phase space. The plot on the right shows the same computation assuming a point particle. The loss of rotational energy results in an O(1) divergence of trajectories in phase space.*

44. The atomistic system consists of two rigid-body methane molecules in a near-collision. We compute the rigid-body dynamics using a complete description of all interatomic forces, and compare to the dynamics resulting from our coarse grain analysis. In the later we account for the first three terms in the generalized multipole expansion for the intermolecular potential. Furthermore, we can consider the molecules with and without angular moments of inertia. In the plot on the left we see that the trajectories agree visually. The inset shows that convergence in the phase space of the dynamics (48 dimensions in this case) can be achieved. Moreover, on the right, we demonstrate that omission of rotational energy can be significant under the assumption of a point particle for the coarse grain. Further analysis suggests that this may be a significant culprit contributing to the representability problem. This result is unexpected, since many body interactions have often been implicated instead. Results of this work are currently being written up in a manuscript that we anticipate submitting for publication in FY 2018. Future work aims to extend these results to systems of non-rigid molecules and further develop associated uncertainty quantification analyses.

[1] P. Patrone, A. Dienstfrey and G. McFadden. Multipole Coarse-Graining of Rigid-Body Dynamics: Exact and Approximate Solutions to the Transferability and Representability Problems. In preparation.

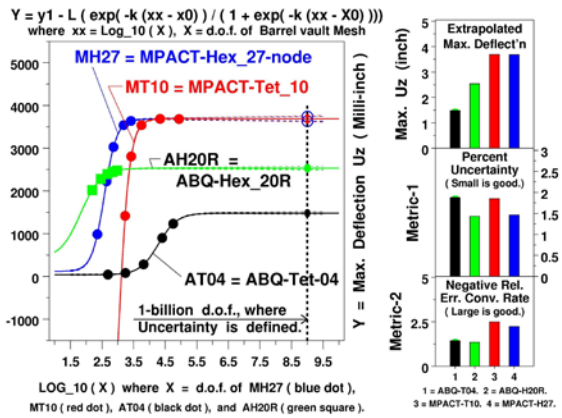

Figure 45. *Four sets of FEM solutions for a structural analysis problem of finding the maximum deflection of a cylindrical shell roof under snow load. Two FEM platforms, ABAQUS and MPACT, each with 2 different element types, were used to compute a least five runs at increasing mesh density or degrees of freedom to allow the estimation of a defection quanitiy, with uncertainty, at infinite degrees of freedom. Based on two a posteriori metrics, the winner is the MPACT Hexa-27 solution (blue) with the least uncertainty and greatest error convergence rate.*

Verification and Validation in the Finite Element Method

Jeffrey T. Fong
James J. Filliben (NIST ITL)
N. Alan Heckert (NIST ITL)
Stephen Freiman (NIST MML)
Li Ma (NIST MML)
Stephen Russek (NIST PML)
Karl Stupic (NIST PML)
Pedro V. Marcal (MPACT Corp.)
Robert Rainsberger (XYZ Scientific)

Errors and uncertainties in finite element method (FEM) [1] modeling and computing are known to originate from at least seven sources: (1) numerical algorithm of approximation for solving a system of partial differential equations with initial and boundary conditions; (2) the choice and design of the finite element mesh and element type; (3) the choice of when to stop computing before verification; (4) the uncertainty in the geometric parameters; (5) the uncertainty in the physical and material property parameters; (6) the uncertainty in the loading parameters, and (7) the uncertainty in the choice of a correct model. Examples of developing local and global validation metrics for specific classes of problems in scientific computing not using FEM have appeared in the literature (see, e.g., [3, 4]).

Using a fractional factorial orthogonal two-level design of experiments [5], we addressed in a 2008 paper [6] the FEM uncertainty problem for sources (4), (5), and (6). To address source (3), we used a nonlinear least squares algorithm and a mathematical function named the logistic distribution (after Verhulst [7]), that allows a user to fit a sequence of FEM solutions of increasing mesh density such that a "plateau" is predicted as the right horizontal asymptote representing the extrapolated solution at "infinite" degrees of freedom (see Figure 45, Figure 46, and Refs. [8, 9]). In addition, we developed three metrics (two *a posteriori* and one *a priori*) [9] to assess the accuracy of a finite element method-based solution in the absence of an experimental method of validation. To address sources (1) and (2), we recently expanded our 2008 experimental design [6] to check the "robustness" of FEM platform and element type in a new design involving both continuous and discrete factors. Source (7) is, of course, addressed by experiments.

[1] O. C. Zienkiewicz and R. L. Taylor. *The Finite Element Method, Volume 1: The Basis*, 5th ed. Butterworth-Heinemann, 2000.

[2] W. L. Oberkampf and C. J. Roy. *Verification and Validation in Scientific Computing*. Cambridge University Press, 2010.

[3] M. F. Barone, W. L. Oberkampf and F. G. Blottner. Validation case Study: Prediction of Compressible Turbulent Mixing Layer Growth Rate. *AIAA Journal* **44**:7 (2006), 1488-1497.

[4] W. L. Oberkampf and M. F. Barone. Measures of Agreement between Computation and Experiment: Validation

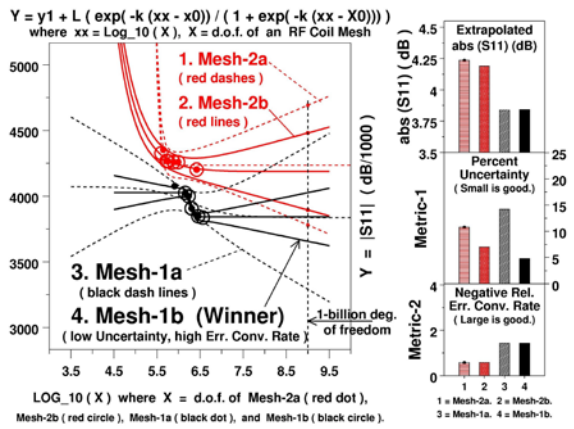

Figure 46. *Four sets of Nonlinear Least Squares Method-Extrapolated FEM solutions of a Magnetic Resonance Imaging (MRI) RF Birdcage Coil analysis problem, where the goal is to find the time-average reflection coefficient, S_{11}, at resonance, of a prototype coil used in a NIST MRI laboratory. Using one FEM platform, COMSOL, two mesh designs (Mesh-1-all tetra-10, and Mesh-2-mixed hexo-27 and tetra-10), and 15 mesh densities (or, degrees of freedom), we obtained four plausible solutions with estimates of S_{11} varying from -3.84 to 4.24 dB. The winner is (4) Mesh-1b, with the least Metric-1 and largest Metric-2 [9].*

Metrics. *Journal of Computational Physics* **217** (2006), 5-36.

[5] G. E. P. Box, W. G. Hunter and J. S. Hunter. *Statistics for Experimenters*, 1st ed. Wiley, 1978.

[6] J. T. Fong, J. J., Filliben, N. A. Heckert and R. deWit. Design of Experiments Approach to Verification and Uncertainty Estimation of Simulations based on Finite Element Method. In Proceedings of the Conference of the American Society for Engineering Education, Pittsburgh, PA, June 22-25, 2008, Paper AC2008-2725.

[7] P. F. Verhulst, 1845, Recherches Mathematiques sur la Loi d'Accroissement de la Population [Mathematical Research into the Law of Population Growth Increase], 1845. Re-published in *Nouveaux Memoires de l'Academie Royaledes Sciences et Belles-Lettres de Bruxelles* **18** (2013), 1-42.

[8] J. T. Fong, N. A. Heckert, J. J., Filliben, P. V. Marcal, R. Rainsberger and L. Ma. Uncertainty Quantification of Stresses in a Cracked Pipe Elbow Weldment Using a Logistic Function Fit, a Nonlinear Least Squares Algorithm, and a Super-parametric Method. *Procedia Engineering* **130** (2015), 135-149.

[9] J. T. Fong, N. A. Heckert, J. J., Filliben, P. V. Marcal, R. Rainsberger, K. F. Stupic and S. E. Russek. MRI Birdcage Coil Resonance with Uncertainty and Relative Error Convergence Rates. In *Proceedings of the International COMSOL Users' Conference*, Boston, MA, Oct. 4-6, 2017. URL: https://www.comsol.com/conference2017/view-paper-file/70832

Modeling of Emulsion Stability Using a Diffuse Interface Model

Sean Colbert-Kelly
Trevor Keller (NIST MML)
Geoffrey McFadden
Frederick Phelan, Jr. (NIST MML)

An outstanding problem in computational physics and important to emulsion science is the modeling of binary emulsions stabilized by a surfactant. The amphiphilic structure of surfactants results in their migration to the fluid interface in a binary mixture [1]. In general, this alters the interfacial tension, interfacial viscosity and diffusion between the two phases leading to greater emulsion stability. The lowering of the interfacial tension between the two fluids results in the rise of gradients in the surfactant concentration on the drop surface under flow, which, in turn, introduces Marangoni forces that alter drop shape, breakup and coalescence dynamics [2]. The altering of the stability, equilibrium properties, and the droplet dynamics of the mixture due to surfactants govern the long-time stability of emulsions. Surfactants are very low in overall composition, but have a dominant effect at the interface, which makes the modeling problem challenging.

Currently, the goal of this project is to develop an emulsion model that simulates the long-term stability of a predominantly binary fluid system stabilized by a surfactant. We take into consideration the effect that the composition of each component in the emulsion has on viscosity, as well as the relationship between the viscosity and the diffusion coefficients in the surfactant phase in the mathematical description of the system.

In this studt, a diffuse interface model is formulated to investigate binary emulsions with a ternary surfactant component. This formulation is accomplished by extending previous models [3] for the free energy of two-phase systems to include a third stabilizing surfactant phase, resulting, for example, in a modified three-phase Ginzburg-Landau formulation. Many of these models represent the two-phase fluid in terms of a conserved order parameter φ, with $\varphi \in [-1,1]$, where $\varphi = -1$ represents one phase and $\varphi = 1$ represents the second phase. In this work the surfactant phase is added by introducing a second conserved order parameter ψ, with $\psi \in (0,1)$, where $\psi = 0$ represents the surfactant-free system. The isothermal free energy density is then a double well function of both φ and ψ, $G = G(\varphi, \psi)$ plus a gradient energy term in φ, where the gradient energy coefficient, $(\kappa - \varepsilon\psi)$, is taken to depend on ψ to introduce a surface energy that depends on the level of surfactant.

Governing Equations. The hydrodynamic equations that govern this system are a fundamental diffuse interface model for the flow of two macroscopically immiscible viscous, incompressible Newtonian fluids with the same densities [4], with the addition of a surfactant component. This system consists of equations that govern the flow dynamics, which are the conservation of momentum and conservation of mass. The system also includes equations that govern the concentration dynamics, which are species balance equations for the two-phase fluid and surfactant components, respectively. The density and viscosity distributions both depend on the densities and viscosities of the bulk components. An explicit interfacial viscosity variable, η_I, is also introduced and the viscosity distribution also depends on this value. A mixing rule for the interfacial viscosity in the surfactant-free case [5] is generalized to include viscosity changes in the interfacial layer due to the decreased entanglement of polymers.

To complete the model, the dependence of the diffusion coefficients on composition and viscosity are introduced. Since surfactants migrate to the interface and stabilize emulsions, an increase in surfactant at the interface should decrease the diffusion of the two-phase fluid across the interface. Using the Stokes-Einstein relation, it can be argued that the diffusion coefficients, D_φ and D_ψ, are inversely proportional to the viscosity.

Results. In studying the effects of the model on emulsion stability, the average domain size is defined as

$$L(t) = 2\pi \sqrt{\frac{1}{< k_x^2 >} + \frac{1}{< k_y^2 >}}$$

where $\langle k_i^2 \rangle$ is the second moment of the structure factor in the i-th direction. Plotting the quantity $L(t)$ allows us to determine if the emulsion is stabilized, i.e., if no growth of domain size is observed after a set time.

The top plot in Figure 47 depicts a graph of the average domain size as a function of time where the viscosity has no dependency on the interfacial viscosity. The ratio ε/κ is increased from 0.1 to 0.7. This graph shows that the growth of the domain slows down with the introduction of surfactant in the system, but does not stabilize. This observation suggests that introducing a surfactant component alone does not lead to emulsion stability via surface tension. The bottom plot in Figure 47 shows the average domain size as a function of time, with ratio η_I/η_2.

Various concentration-dependent viscosity models are being formulated and studied. This formulation is expected to enable modeling of stable emulsions and the examination of droplet dynamics. Furthermore, the inclusion of simple velocity fields that influence droplet dynamics is planned, focusing on the effect of the flows on drop size distributions.

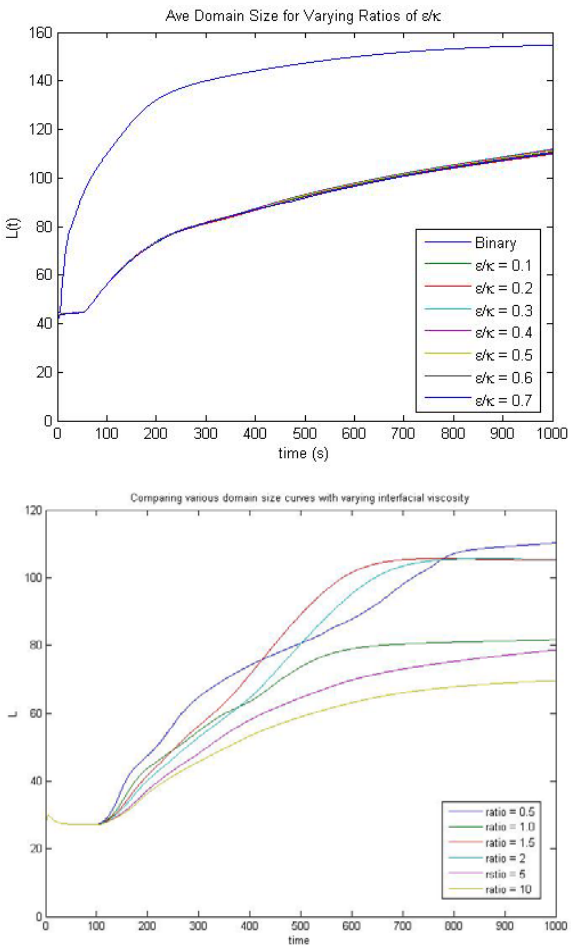

Figure 47. *Top: A graph of the average domain size as a function of time while increasing the ration between ε and κ with the viscosity varying by mole fraction values only. Bottom: A graph of the average domain size as a function of time while increasing the ratio η_I/η_2 of the viscosities in the bulk phases.*

[1] S. Engblom, M. Do-Quang, G. Amberg and A.-K. Tornberg. On Diffuse Interface Modeling and Simulation of Surfactants in Two-Phase Fluid Flow. *Communications in Computational Physics* **14**:4 (2013), 879-915.

[2] J. T. Schwalbe, F. R. Phelan, Jr., P. M. Vlahovska and S. D. Hudson. Interfacial Effects on Droplet Dynamics in Poiseuille Flow. *Soft Matter* **7** (2011), 7797–7804.

[3] C.-H. Teng, I.-L. Chern and M.-C. Lai. Simulating Binary Fluid-Surfactant Dynamics by a Phase Field Model. *Discrete and Continuous Dynamical Systems Series B* **17**:4 (2012), 1289–1307.

[4] P. C. Hohenberg and B. I. Halperin. Theory of Dynamic Critical Phenomena. *Reviews of Modern Physics* **49**:3 (1977), 435-479.

[5] W. Yu and C. Zhou. The Effect of Interfacial Viscosity on the Droplet Dynamics Under Flow Field. *Journal of Polymer Science Part B: Polymer Physics* **46**:14 (2008), 1505-1514.

Estimation of Shear Stress for the Modeling and Simulation of Machining Processes

Timothy Burns
Bert Rust
Steven Mates (NIST MML)
Richard Rhorer (NIST EL)
Eric Whitenton (NIST EL)
Debasis Basak (Orbital Sciences Corporation)

The rapid growth of additive manufacturing of metal components, commonly known as "3D printing," has not eliminated the need for subtractive processes, such as machining, which is still the go-to process used by US manufacturers of metal parts. During machining operations, thin layers of metal called chips are removed by the tool in a cutting process that involves large, rapid shearing deformation of the chip material. In materials which are difficult to machine, such as carbon steels and titanium alloys, this shearing deformation can lead to heating rates as high as 106 °C s^{-1}. Since excessive heating can lead to tool breakage, there is considerable interest in predicting optimal cutting parameters, i.e., speeds and feeds, which maximize material removal rates, while minimizing damage to the cutting tool.

Most attempts to model the material response for machining process simulations have been based on direct methods, which fit compression test data of small samples of the material of interest to a given highly nonlinear constitutive response model. Although some progress has been made in achieving more rapid heating rates in a material sample prior to loading a sample in a compression test [1], current experimental capabilities using this method are still nowhere near the extreme conditions of strain, strain-rate, and rate of heating that are present in a typical high-speed machining operation. As a result, finite-element simulations of machining processes using material models based on compression test data cannot yet predict peak temperatures along the tool-material interface.

One area of machining research in which significant progress has been made in the past few years has been in the measurement of the temperature distribution on the tool-chip interface, using infrared thermography. With a new type of transparent tool, Menon and Madhavan [2] have developed a method for obtaining high accuracy 1D temperature measurements along the tool-material interface in a controlled rapid machining experiment. Based on this work, we have been investigating a convection-diffusion model for steady-state chip flow near the tool-chip interface during a controlled machining process. Given a discrete set of temperature measurements on the tool face, which are contaminated by experimental noise, we have developed a method for estimating the flow stress in the material near the cutting face of the tool. The method involves solving Abel's integral equation [3]. Since this equation is improperly posed, we have developed a technique for regularizing the temperature data prior to estimating the flow stress [4], [5]. Future work will attempt to provide improved constitutive models for two materials of considerable interest to US manufacturers: AISI 1045 carbon steel, and the titanium alloy Ti–6Al–4V, using the estimated flow stress.

[1] S. P. Mates, R. L. Rhorer, E. P. Whitenton, T. J. Burns and D. Basak. A Pulse-Heated Kolsky Bar Technique for Measuring Flow Stress of Metals Subjected to High Loading and Heating Rates. *Experimental Mechanics* **48** (2008), 799–807.

[2] T. Menon and V. Madhavan. Infrared Thermography of the Chip-Tool Interface through Transparent Cutting Tools. In *Proceedings of the North American Manufacturing Research Institution/SME*, Ann Arbor, MI, June 2014.

[3] T. J. Burns, S. P. Mates, R. L. Rhorer, E. P. Whitenton and D. Basak. Inverse Method for Estimating Shear Stress in Machining. *Journal of the Mechanics and Physics of Solids* **86** (2016), 220–236.

[4] T. J. Burns and B. W. Rust. Estimation of Shear Stress in Machining Using the Temperature Distribution on the Tool Face. In *Proceedings of the 24th International Congress of Theoretical and Applied Mechanics* (ICTAM 2016), Montreal, Canada, August 21-26, 2016.

[5] T. J. Burns and B. W. Rust. Closed-Form Projection Method for Regularizing a Function Defined by a Discrete Set of Noisy Data and for Estimating its Derivative and Fractional Derivative. In review.

The Effect of Vacancy Creation and Annihilation on Grain Boundary Motion

Geoffrey McFadden
William Boettinger (NIST MML)
Yuri Mishin (George Mason University)

A crystalline solid typically consists of grains with given crystal orientations that are separated by grain boundaries where the orientation changes. Typical grain sizes can range from hundreds of micrometers to large single crystals that can be on the order of centimeters. A common technological problem in the electronics industry is that when metallic or semiconductor grains are subject to lateral mechanical stresses, diffusion along the grain boundary can lead to "whiskers'" that can extend normally to a substrate and provide unwanted electrical connections between neighboring components (see Figure 48). Often, whiskers can be prevented by the addition of various components to the substrate, such as

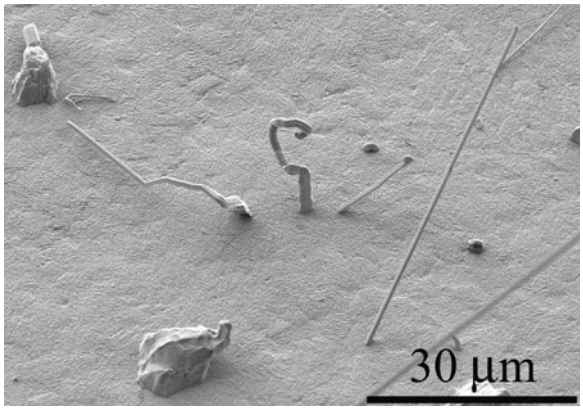

Figure 48. *Tin whiskers growing on a stressed substrate (from* https://www.nist.gov/programs-projects/lead-free-surface-finishes-electronic-components-tin-whisker-growth*).*

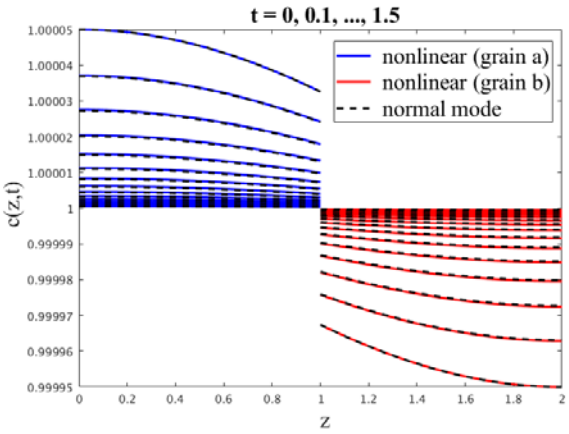

Figure 49. *Comparison of vacancy concentration profiles at various times. The diffusion takes place in a bi-crystal, with nonlinear simulation results shown as the solid blue and red curves, and corresponding normal mode solutions shown as dashed curves. The concentration is discontinuous at the grain boundary (which is fixed in these computational coordinates).*

lead, but these additives can be undesirable for environmental reasons. In particular, lead-free solder commonly has a high composition of tin, which is prone to the whisker development in high-stress conditions.

Modeling whisker growth involves the derivation of governing equations that couple the effects of mechanical stress and compositional diffusion in a multi-grain geometry. Of particular interest is the development of appropriate boundary conditions that apply at moving grain boundaries. In previous research, such derivations were carried out by using positive entropy production arguments that are based upon the second law of thermodynamics [1]. The resulting boundary conditions contain kinetic coefficients that relate vacancy diffusion across grain boundaries to thermodynamic driving forces such as jumps in chemical potential, and also include the effects of sources or sinks of vacancy concentrations at the grain boundary and their effect on conditions of thermodynamic equilibrium at the interface.

Recent research in this area has consisted of numerical simulations and theoretical stability studies for one-dimensional bi-crystals that illustrate the effects of the grain boundary boundary conditions [2]. The motion of grain boundaries is simulated using a mapping to a fixed computational domain which is computed along with the evolution of the diffusion fields from various initial conditions (see Figure 49). The dynamics can also be studied analytically by considering small-amplitude perturbations to equilibrium states which can described by a normal mode analysis of the linearized governing equations, illustrating the roles played by the various terms in the boundary conditions. Future work is anticipated to include the effects of surface energy and surface stress in curved geometries during grain growth, as well as the implementation of related phase-field models [3] that could aid in the description of whisker growth.

[1] Y. Mishin, G. B. McFadden, R. F. Sekerka and W. J. Boettinger. Sharp Interface Model of Creep Deformation in Crystalline Solids. *Physical Review B* **92** (2015) 064113. DOI: 10.1103/PhysRevB.92.064113

[2] G. B. McFadden, Y. Mishin, and W. J. Boettinger. The Effect of Vacancy Creation and Annihilation on Grain Boundary Motion. In preparation.

[3] Y. Mishin, J. A. Warren, R. F. Sekerka and W. J. Boettinger. Irreversible Thermodynamics of Creep in Crystalline Solids, *Physical Review B* **88** (2013) 184303. DOI: 10.1103/PhysRevB.88.184303

Shear Localization in Bulk Metallic Glasses

Timothy Burns

About forty years ago, the problem of the localization of rapid plastic deformation of polycrystalline metals into thin layers called adiabatic shear bands began to receive considerable attention, mainly due to its connection with military applications, such as armor penetration [1]. However, the phenomenon had been observed much earlier in the machining of titanium alloys [2]. At faster cutting speeds and larger depths of cut, the thin layers of work material removed by machining, called chips, exhibit a saw- tooth structure, when a bifurcation takes place in the material flow, from continuous, or fairly smooth chips, to serrated, or shear localized chips. The generally accepted explanation for the onset of shear localization in the cutting of polycrystalline metallic alloys is that the tendency of a metal to work- harden with increasing deformation is overcome by a competing tendency of the material to soften, due to heat production caused by the rapid shearing of the material

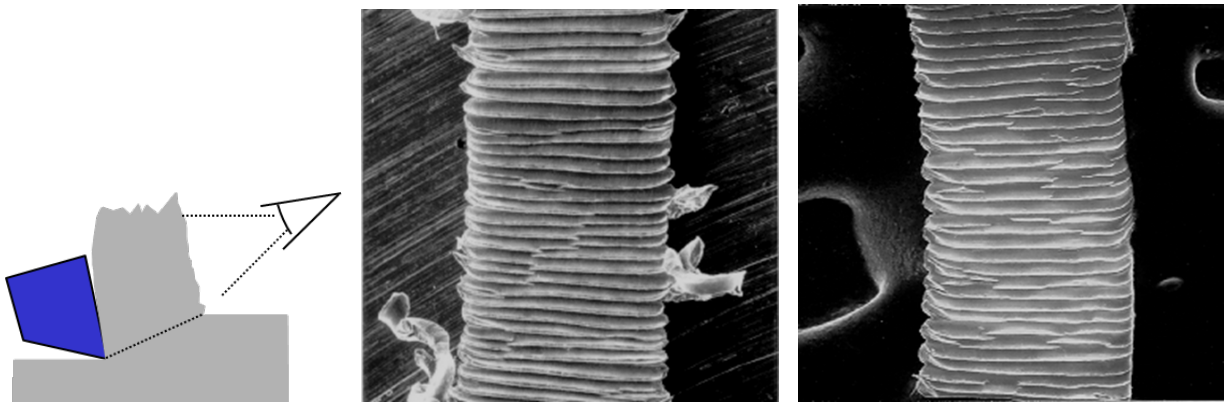

Figure 50. ***Shear-localized chips in (a) a polycrystalline metallic alloy, and (b) a BMG.***

[3]. Shear localization during machining can significantly degrade surface quality of the finished part, and it can also lead to unwanted tool vibrations, i.e. chatter.

Recently, there has been a growing interest in the use of amorphous metallic alloys, which are also called bulk metallic glasses (BMGs), as structural materials [4]. BMGs are a relatively young class of alloy materials, which have unique physical, mechanical, and chemical properties. For example, relative to more common structural alloys, some of these materials have very high elastic limits, as well as very large resilience, which is the capacity of a material to absorb energy when it is deformed elastically; this energy can be recovered upon unloading. Microscopically, BMGs are different from common polycrystalline metallic alloys, because their atoms do not assemble on a crystalline lattice [5]. What is interesting from a machining point of view is that several BMGs have been found to produce shear- localized chips; see Figure 50. Furthermore, some theoretical studies have argued that this strain localization is controlled not by rapid heating, but rather by a change in the concentration of free volume in the material [5, 6]; in other words, these shear bands are not adiabatic.

One way to approach the study of shear band formation in BMGs is to mimic the analysis that has been done to study the formation of adiabatic shear bands in polycrystalline metallic alloys, by analyzing the linear stability of a geometrically simple homogeneous shear flow of a BMG. Just as in the polycrystalline case, the difficulty here is that, because the reference shear flow solution is time-dependent, so is the matrix of the linearization of the model equations about the reference solution. An approach that has frequently been used in this field is to "freeze'' the coefficients in the time-dependent matrix at a fixed reference time, and to study the characteristic equation associated with determination of the eigenvalues of the matrix [1, 6]. Numerical analysis of the time-dependent linearized stability problem supports the free-volume concentration hypothesis, but it disagrees with the frozen coefficient analysis. A paper on this work is in preparation.

[1] R. J. Clifton, J. Duffy, K. A. Hartley and T. G. Shawki, On Critical Conditions for Shear Band Formation at High Strain Rates. *Scripta Metallurgica* **18** (1984) 443-448.

[2] M. C. Shaw, S. O. Dirke, P. A. Smith, N. H. Cook, E. G. Loewen and C. T. Yang. Machining Titanium. Mechanical Engineering Dept., MIT, Cambridge, MA, 1954.

[3] M. A. Davies and T. J. Burns. Thermomechanical Oscillations in Material Flow during High-speed Machining. *Philosophical Transactions of the Royal Society of London A* **359** (2001) 821-846.

[4] M. F. Ashby and A. L. Greer. Metallic Glasses as Structural Materials. *Scripta Materialia* **54** (2006) 321-326.

[5] R. Huang, Z. Suo, J. H. Prevost and W.D. Nix. Inhomogeneous Deformation in Metallic Glasses. *Journal of the Mechanics and Physics of Solids* **50** (2002) 1011-1027.

[6] L. H. Dai and Y. L. Bai. Basic Mechanical Behaviors and Mechanics of Shear Banding in BMGs. *International Journal of Impact Engineering* **35** (2008) 704–716.

High Performance Computing and Visualization

Computational capability has been advancing rapidly for some time. Modeling and simulation now can be done with greatly increased fidelity (e.g., higher resolution and more complex physics). However, developing the necessary large-scale parallel applications remains highly challenging, requiring expertise that application scientists rarely have. In addition, the hardware landscape is changing rapidly, so new algorithmic techniques must constantly be developed. We are developing such expertise for application to NIST problems. Such computations, as well as modern laboratory experiments, often produce large volumes of scientific data, which cannot be readily comprehended without some form of analysis. We are developing the infrastructure necessary for advanced interactive, quantificative visualization and analysis of scientific data, including the use of 3D immersive environments and applying this infrastructure to NIST problems. One of our goals is to develop the 3D immersive environment into an interactive measurement laboratory.

HydratiCA: A Parallelized Numeric Model of Cement Hydration

John Hagedorn
Afzal Godil (NIST ITL)
Wesley Griffin
Judith Terrill
Jeffrey Bullard (NIST EL)

HydratiCA is a stochastic reaction-diffusion model of cement hydration. Hydration transforms paste from a fluid suspension (e.g., cement powder mixed with water) into a hardened solid. This process involves complex chemical and microstructural changes. Understanding and predicting the rates of these changes is a longstanding goal.

Computational modeling of the hydration of cement is challenging because it involves many coupled nonlinear rate equations that must be solved in a highly irregular three-dimensional spatial domain. HydratiCA addresses these challenges with a computational model that has several advantages over other models of cement hydration. Parallelization of the model and the visualization of the output data are important components of this project. With parallelization, we can simulate systems that are large enough to be realistic, avoiding finite size effects, and still can complete the simulations in a reasonable amount of time. Visualization of the data volumes produced by HydratiCA is important both for validation and for understanding of the results.

This year we continued work on HydratiCA with significant improvements to the algorithm, the parallel implementation, and visualization. Large-scale runs have enabled us to make direct comparisons between simulations and experiments. We have an on-going series of runs that focus on calculating the time-dependent rate of heat release, and development of the percolating solid network responsible for the hardening of concrete. We are also investigating the effect of the size and spacing of the computational lattice.

Visualization. We have continued to pursue two avenues of visualization in this project. First, we have extended the 3D isosurface visualization tool to use a more intuitive desktop-based user interface. The new tool also has additional capabilities to allow the user to combine two columns of the simulation results using the four basic mathematical operations and then visualize the new column (Figure 51). This tool works both on the desktop and in the CAVE and is cross-platform to enable ease of use by the scientist.

Second, we have worked closely with a Ph.D. student at the University of Maryland to explore using a

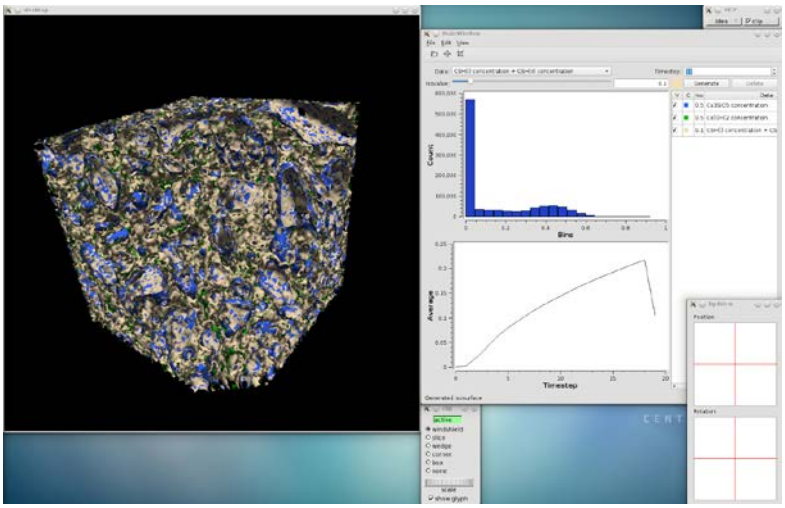

Figure 51. *HydratiCA visualization tool showing three isosurfaces: Ca_3SiO_5 concentration in blue, $Ca(OH)_2$ concentration in green, and CSH(I) + CSH(II) concentration (a computed column from the simulation dataset) in beige. The tool also shows a portion of the simulation volume clipped away to reveal the inside of the volume.*

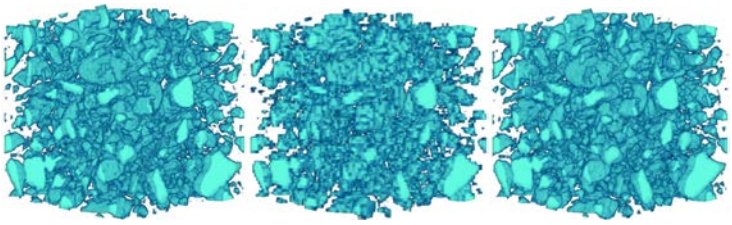

(a) Uncompressed Volume (b) Wavelet Compression (c) Learned Compression (ours)

Figure 52. *Comparison of volume rendering of Ca_3SiO_5 concentration at a single time step. The compressed representations (subfigures b and c) take 7% of the total memory. Rendering from our learned compression (c) is much closer in visual quality to the uncompressed volume (a) as compared to the best-performing wavelet compression algorithm (b).*

deep convolutional autoencoder network to compress the simulation data to enable in situ visualization. The results are promising as we found that the deep learning network could compress the original data by 93% (matching the best-performing wavelet compression algorithm) but provide better reconstruction quality (measured by peak-signal-to-noise) than the best-performing wavelet compression algorithm. (Figure 52).

Results. We have continued our large-scale runs on Stampede, a system at the Texas Advanced Computing Center, under a grant from NSF's XSEDE program. These runs have enabled us to continue our direct comparisons between experiments and HydratiCA simulations of the hydration of tricalcium silicate. In comparing experiment and simulation, some results are consistent but there are other points at which the experiment and simulation diverge. For example, the simulated and observed amounts of Ca_3SiO_5 dissolution agree to within the measurement uncertainty. At the same time, the number of observed moles, especially the apparent volume of hydration product phases, is greater than either what the simulations predict or what the observed amount of Ca_3SiO_5 dissolution can produce. This discrepancy, along with other discrepancies between experiment and simulation are a subject of ongoing investigation. These results are being reported in detail in a paper that is currently in preparation.

Using an additional XSEDE grant of time on Stampede, we are calculating the time-dependent rate of heat release and development of the percolating solid network responsible for the hardening of concrete. We are also investigating the effect of the size and spacing of the computational lattice. These runs are in progress.

Continuing Work. We are continuing our development of the HydratiCA code, which involves improvements to the algorithm, its implementation, and data visualization. We are currently enhancing the algorithm by adding new boundary conditions, and we are investigating improvements to our handling of adaptive time steps. Our efforts in improving the implementation are focusing on efficiency, communications, parallelization, and vectorization techniques. The visualization work will continue to focus on both improving the desktop/immersive isosurface visualization tool and continuing our research on in situ visualization methods. Specifically, we hypothesize that visualizing the layers of the convolutional network will provide scientific insight into the data.

We are proceeding with our investigation of rate of heat release and the evolution of the percolating network in concrete. These runs are continuing to produce data which we are analyzing as it becomes available. In addition, we are developing a series of simulations to characterize the sulfate-silicate interplay in concrete. We will model the full range of complexity found in real cementious materials validated by experimental measurements on materials that approximate those being simulated as closely as possible. We are submitting another application to XSEDE for time on Stampede to pursue these runs.

Acknowledgement. This work used the Extreme Science and Engineering Discovery Environment (XSEDE), which is supported by National Science Foundation grant number ACI-1053575.

[1] J. Bullard, E. Garboczi, P. Stutzman, P. Feng, A. Brand, L. Perry, J. Hagedorn, W. Griffin and J. Terrill. Measurement and Modeling Needs for Microstructure and Reactivity of Next-generation Concrete Binders. *Cement and Concrete Composites* (2017), in press. DOI: 10.1016/j.cemconcomp.2017.06.012

[2] J. Bullard, J. Hagedorn, T. Ley, Q. Hu, W. Griffin and J. Terrill. A Critical Comparison of 3D Experiments and Simulations of Tricalcium Silicate Hydration. *Journal of the American Ceramic Society* **101**:4 (2018), 1453–1470. DOI: 10.1111/jace.15323

Modeling of Suspension Flow in Pipes

William George
Nicos Martys (NIST EL)
Steven Satterfield
Judith Terrill

Understanding the flow of suspensions in pipes is important for a wide variety of technical applications. For example, in the construction industry, concrete is often placed by pumping it through extensive pipe systems. However, research into predicting the pumpability of concrete has been limited due to the heavy equipment and large amounts of material needed. Suspension flow is also important in the developing field of 3D additive manufacturing. It is challenging to predict the flow in this complex fluid which is composed of a non-Newtonian matrix fluid with suspended solid inclusions

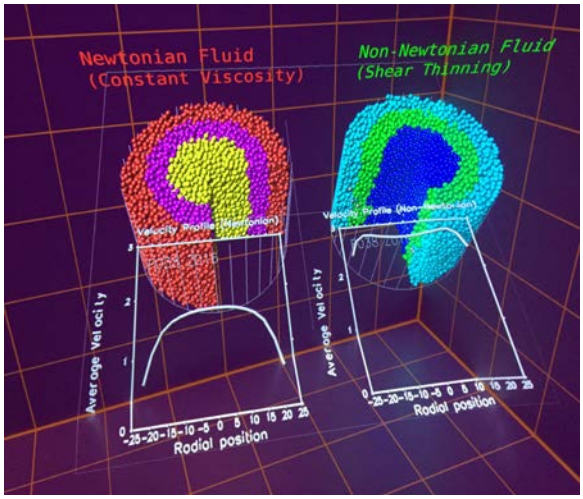

Figure 53. *A snapshot of two similar simulations showing the difference in the system velocity due primarily to slip at the wall.*

flowing under pressure. Flow in these systems is also complicated by variety of phenomena such as slip at the wall and shear induced migration which has only been studied for the simpler case of a suspensions with a Newtonian matrix fluid. A detailed discussion of this topic is available in a NIST Technical Note [1]. It is also the case, especially in the 3D additive manufacturing, that the placement of these materials is time sensitive, from the time the material is initially mixed to the time it is pumped and placed.

In order to develop predictive flow models of these materials and advance the measurement science needed in this field, we have been conducting detailed simulations of the flow of suspensions through pipes. Through quantitative analysis and visualization, we have gained insight into shear-induced migration and slip behavior in these systems. For example, Figure 53 shows a side-by-side comparison of an identical system with only the property of the matrix fluid changed, one being Newtonian and the other non-Newtonian (shear thinning).

Over this last year we have been conducting a suite of simulations of shear thinning and shear thickening suspensions, varying the properties of the matrix fluid and the driving force. Studying the flow velocity fields as a function of driving force we have discovered a useful scaling relationship. Given that the matrix fluids have a viscosity, μ, that relates to the strain rate $\dot{\gamma}$ such that $\mu \propto \dot{\gamma}^n$, we have determined that the system velocity in the pipe, v, is related to the driving force, g, as

$$v \propto g^{1/(1+n)}$$

So, for example, with a shear thinning matrix fluid with $n = -0.5$ we have

$$v \propto g^{1/(1-0.5)} = g^2$$

and with a matrix fluid which is shear thickening, with $n = 0.5$, we have

$$v \propto g^{1/(1+0.5)} = g^{2/3}$$

Notice that this scaling relation depends on the power law behavior of the non-Newtonian matrix fluid. As a consequence, given a few measurements of the flow velocity versus the driving force of the suspension, one can determine the power law behavior of the suspension, and indeed we can then also determine the power law behavior of the matrix fluid. Although our simulations have not yet completed, they appear to confirm this model to within about 15%. We will continue to examine this model in the coming year and expect to publish these findings.

In the coming year, in addition to continuing the simulation of these systems, collaborating researchers in NIST EL will perform experimental verification of these results. Other simulations of interest in the future will include the flow of these suspensions through a nozzle and simulating the placement of material in a 3D additive manufacturing device. It will likely be required, especially in the case of 3D additive manufacturing, to include in these simulations the changing of the material properties over time, including thixotropy, as this is very important in this setting.

[1] M. Choi, C. F. Ferraris, N. S. Martys, V. K. Bui, H. R. Trey Hamilton and D. Lootens. Research Needs to Advance Concrete Pumping Technology. Technical Note 1866, National Institute of Standards and Technology, 2015.

Nano-Structures, Nano-Optics, and Controlling Exciton Fine Structure

James Sims
Wesley Griffin
Garnett W. Bryant (NIST PML)
Jian Chen (UMBC)
Henan Zhao (UMBC)

Semiconductor nanoparticles, also known as nanocrystals and quantum dots (QDs), are one of the most intensely studied nanotechnology paradigms. Nanoparticles are typically 1 nm to 10 nm in size, with a thousand to a million atoms. Precise control of particle size, shape and composition enables tailoring charge distributions, while precise control of quantum effects enables tailoring properties completely different from the bulk and from small clusters. Due to enhanced quantum confinement effects, nanoparticles can act as artificial, man-made atoms with discrete electronic spectra exploitable as light sources for novel enhanced lasers, discrete components in nanoelectronics, qubits for quantum information processing, and enhanced ultrastable fluorescent labels for biosensors to detect, for example, cancers, malaria or other pathogens.

This is a joint project with the NIST PML to develop computationally efficient large-scale simulations of such nanostructures and developing novel visualization techniques and tools to allow analysis of the highly complex computational results from the simulations. This project is studying the electrical, mechanical, and optical properties of semiconductor nanocrystals and quantum dots. In the most complex scenarios, this entails modeling nanostructures on the order of a million atoms. Highly parallel computational and visualization platforms are critical for obtaining the computational speeds necessary for a systematic, comprehensive study.

Our current code analyzes wave functions, obtaining the function with maximum spin up, the function with maximum spin down, and two intermediate functions. The addition of a magnetic field provides a probe to split excitonic states, providing a more complete spectroscopy of quantum dot optics, which allows us to isolate contributions from spin-orbit coupling, Zeeman, and spatial motion. Magnetic field response depends sensitively on the QD size and shape.

The addition of a magnetic field allows for the intrinsic spins of the electrons to lead to different effects in a magnetic field depending on the quantum dot size and shape. As a result, it is necessary to be able to see the effect of spin in different QD arrangements. Without visualization, it becomes very difficult to understand what this distribution is and how it changes for different magnetic fields, electric fields or strain. This distribution is critical for understanding exchange interactions or electron/nucleus interactions in quantum devices. These properties influence the performance of these structures in quantum information processing.

As the device size in Si electronics continues to decrease, the devices are rapidly approaching the atomic scale where a change in only a few atoms can make a significant change in device performance. At the same time, the ability to make Si nanodevices with only a few deterministically placed dopant atoms opens the possibility to create quantum information processing devices with these structures. We are participating in a program to make, characterize and model both traditional and quantum Si devices at this few-dopant atom limit.

During the last year, we have been continuing to work to extend the atomistic tight-binding simulation tool to study systems made with random alloys and to develop tools to analyze results for many random configurations for the same structure. The use of random alloys allows for greater flexibility in engineering the electronic, optical and quantum properties of nanodevices. In particular, a random alloy has been modeled by replacing randomly chosen atoms in specified regions of the nanodevice with different atoms with different properties. Tools were developed to place new atoms at randomly chosen sites in and around the nanodevice. The current simulation tools were enhanced to treat this added complexity. Significant support from ITL made this possible. These simulation tools are also now being applied to atomic-scale dopant based Si electronic, quantum and photonic devices.

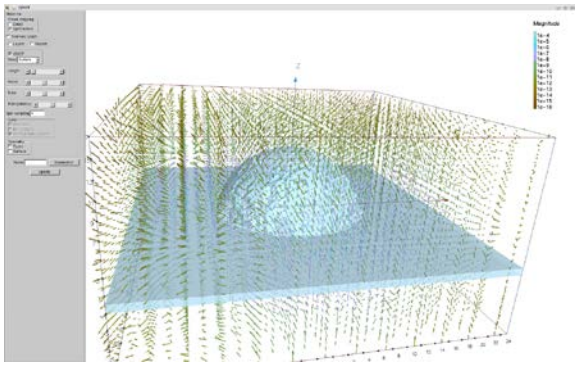

Figure 54. *Current visualization tool showing spin directions and magnitudes, where the length of the arrow encodes the digit of the magnitude and the color of the arrow encodes the exponent. The quantum dot geometry is visualized as the light-blue half-sphere.*

At the same time, ongoing analysis of results from the simulations of various nanodevices has been supported by a new visualization tool. The significant speedup of this tool makes it practical to use on data from million-atom device simulations both for visualization at the desktop and for immersive 3D visualization. This visualization tool will greatly facilitate analysis of systems with large amounts of data. The tool employs a novel visualization technique, which was developed by researchers at UMBC [1]. As part of their research effort, they designed and evaluated several clustering approaches for optimizing pattern detection on one or more cutting planes in the simulation data. Their evaluations found that k-means clustering was the best approach, and they have implemented that clustering algorithm in the visualization tool.

The user interface has undergone several iterations based on direct feedback from our collaborator in PML. The tool now supports symmetry pattern detection for both parallel- and anti-symmetries on and perpendicular to the symmetry plane. Additionally, the tool now renders the QD directly (Figure 54) which enables the user to see the atom types and spin behaviors inside and outside the geometry.

Finally, UMBC has been developing and evaluating different bivariate glyph strategies to encode magnitude values. Visualizing the spin magnitudes has been a difficult aspect of this project because the simulation results include magnitudes over a very large range (10^{12}). The bivariate glyph approach visualizes the magnitudes by separately encoding the digit and exponent of the magnitude.

[1] H. Zhao, G. W. Bryant, W. Griffin, J. E. Terrill, and J. Chen. Validation of SplitVectors Encoding for Quantitative Visualization of Large-Magnitude-Range Vector Fields. *IEEE Transactions on Visualization and Computer Graphics* **23**:6 (2017), 1691–1705.

High Precision Calculations of Fundamental Properties of Few-Electron Atomic Systems

James Sims
Stanley Hagstrom (Indiana University)
M. B. Ruiz (University of Erlangen, Germany)
Bholanath Padhy (Khallikote College, India)

NIST has long been involved in supplying critically evaluated data on atomic and molecular properties such as the atomic properties of the elements contained in the Periodic Table and the vibrational and electronic energy level data for neutral and ionic molecules contained in the NIST Chemistry WebBook. Fundamental to this endeavor is the ability to predict, theoretically, a property more accurately than even the most accurate experiments. It is our goal to be able to accomplish this for few-electron atomic systems.

While impressive advances have been made over the years in the study of atomic structure, in both experiment and theory, the scarcity of information on atomic energy levels is overwhelming, especially for highly ionized atoms. The availability of high precision results tails off as the state of ionization increases, not to mention higher angular momentum states. In addition, atomic anions have more diffuse electronic distributions, thus representing more challenging computational targets than the corresponding ground states.

In the past two decades, there has been breathtaking improvements in computer hardware and innovations in mathematical formulations and algorithms, leading to "virtual experiments" becoming a more and more cost-effective and reliable way to investigate chemical and physical phenomena. Our contribution in this arena has been undertaking the theoretical development of our hybrid Hylleraas-CI (Hy-CI) wave function method to bring sub-chemical accuracy to atomic systems with more than two electrons.

Hy-CI has from its inception been an attempt to extend the success of the Hylleraas (Hy) method to systems with more than three electrons, and hence is an attempt to solve not just the three-body problem but the more general *N*-body problem [1]. Fundamental to the method is the restriction of one r_{ij} per configuration state function (CSF). In the case of three electron lithium systems, we have computed four excited states of the lithium atom to two orders of magnitude greater than has ever been done before [2]. At the four-electron level, to get truly accurate chemical properties, like familiar chemical electron affinities and ionization energies, it is important to get close to the nanohartree level we achieved for the three-election atom, a significantly more difficult problem for four electrons than for three. By investigating more flexible atomic orbital basis sets and better configuration state function filtering techniques to control expansion lengths, we have been able to successfully tackle the four-electron case.

Progress to date has included computing the non-relativistic ground state energy of not only beryllium, but also many members of its isoelectronic sequence to 8 significant digit accuracy. With the results from our calculations and a least squares fit of the calculated energies, we have been able to compute the entire beryllium ground state isoelectronic sequence for Z = 4 through Z = 113 [3]. Li- (with Z=3), nominally the first member of this series, has a decidedly different electronic structure and was not included in those calculations and subsequent discussions. Work this past year has been to correct this "omission" and carry out a large, comparable calculation for the Li- ground state. A paper reporting the results of this study is in press [4].

The first member of the Be isoelectronic ground state sequence, the negative Li- ion, is also a four-electron system in which correlation plays a very important part in the binding. However due to the reduced nuclear charge, it is a more diffuse system in which one of its outer two L shell electrons moves at a greater distance from the nucleus than the other and hence its nodal structure is different from that of a coupled L shell with an identical pair of electrons. The ground state of the singlet S state of Li- is the same type of problem as the first excited state of Be; it is like Be(2s3s), not Be(2s2s). Completing this calculation has provided the necessary insight to complete the calculation of the Be first excited state of singlet S symmetry, Be(2s3s). This calculation has been completed and is an order of magnitude better than previous calculations. Armed with this result, it should be possible to improve the higher, more diffuse Rydberg states to something approaching this level of accuracy. Work is in progress to accomplish this for the Be 4 S through 7 S exited states. Current plans are to modify our parallel quadruple precision generalized eigenvalue problem solver to include pivoting, and then complete the calculation of the Be 4 S through 7 S excited states.

[1] J. S. Sims and S. A. Hagstrom. Combined Configuration Interaction – Hylleraas Type Wave Function Study of the Ground State of the Beryllium Atom. *Physical Review A* **4**:3 (1971), 908.

[2] J. S. Sims and S. A. Hagstrom. Hy-CI Study of the 2 Doublet S Ground State of Neutral Lithium and the First Five Excited Doublet S States. *Physical Review A* **80** (2009), 052507.

[3] J. S. Sims and S. A. Hagstrom. Hylleraas-Configuration Interaction Nonrelativistic Energies for the Singlet S Ground States of the Beryllium Isoelectronic Series up Through Z = 113. *Journal of Chemical Physics* **140** (2014), 224312.

[4] J. S. Sims. Hylleraas-Configuration Interaction Study of the Singlet S Ground State of the Negative Li Ion. *Journal of Physics B, Atomic, Molecular and Optical Physics*, in press.

MERSIV – Monitor, Explore, Review Simulations with Immersive Visualization

Steve Satterfield
Judith Terrill
Diana Chou (University of Maryland)
Margret Sauber (University of Maryland)
Aida Nurit Shumburo (Thomas Sprigg Wootton HS)

MERSIVE is a collection of commands/tools that allows a user within the ACMD High End Visualization (HEV) environment to Monitor, Explore, Review Simulations with Immersive Visualization.

The ACMD High Performance Computing and Visualization Group (HPCVG) collaborates with NIST EL to create computational models of various matter flows to simulate different rheology concepts. Some of these computations can take weeks, even months to complete. In the past, visualizations of these simulations were done at the end of computation. We are moving toward monitoring the simulation *in situ*, i.e. while it runs, which will enable deeper understanding of simulation parameters, and facilitate catching bugs and fixing them sooner. MERSIV is a toolkit that will allow scientists to run different visualizations on data that is periodically dumped from computations. This capability allows for a much more accessible way of monitoring the run.

Summer Project. MERSIV was started as a 2017 summer project with a team of SURF (Summer Undergraduate Research Fellowship), SHIP (Summer High School Intern Program) and volunteer students. The team built a prototype system and a skeleton set of commands sufficient for a proof-of-concept implementation. The prototype was successfully tested with a flow application. The team defined a software workflow for MERSIV; see Figure 57. Implementation Time is the work done by the visualization developer in to create the scripts/software necessary to visualize the data. Once the application specific software in place, each new data set must be transformed into displayable data structures (files). Depending on the size of the data, this step can be quick or lengthy. After the application scripts have been developed and tested, the Build Time is typically performed by the domain scientist. Run Time is the time spent by the domain scientist viewing and interacting with the data.

Future Work. Due to the limited time available during a typical summer session, MERSIVE was not developed beyond a prototype. However, the project was a successful experience for the students. The resulting SURF student presentation and SHIP student poster were very well received. The project provided an appropriate level of complexity and technical learning experience for the students.

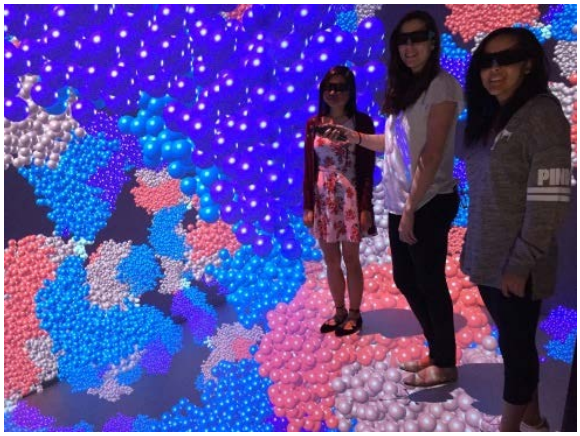

Figure 55. *The team views molecular data in the cave.*

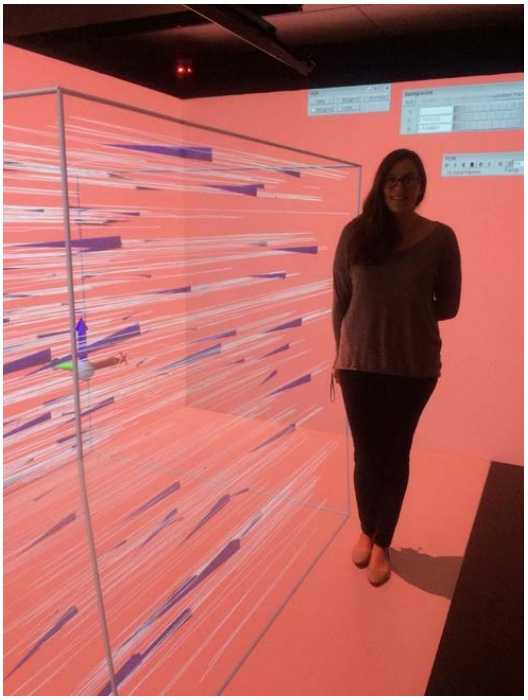

Figure 56. *MERSIV used for directional flow field.*

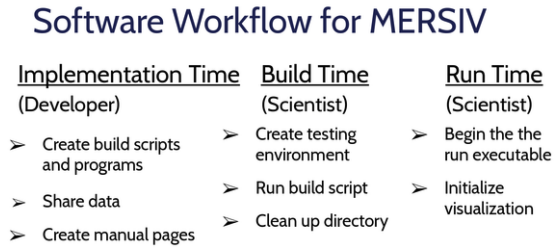

Figure 57. *Software workflow for MERSIV.*

We are planning to continue the project with similar summer student teams. Each year will build upon the previous work and produce a usable and functional software toolkit.

Testing an Immersive Visualization Environment

Judith Terrill
Steven Satterfield
Terence Griffin
Wesley Griffin
Dan Dunkers (Drexel University)
Alauna Jackson (Bowie State University)
Aleksander Psurek (Thomas S. Wootton High School)
Jeremy Rubin (UMBC)
Raef Youssef (UMBC)
Edwin Yu (Thomas S. Wootton High School)
Jason Zimmerman (Millersville University)

Our immersive visualization environment (IVE) consists of a three-wall cave as well as Linux desktops and laptops that all run the CentOS operating system. This environment is heterogenous and dynamic. The hardware is not the same everywhere, which includes different NVIDIA graphics cards This is likewise true for CentOS, which may be at different versions on different machines. Our IVE software consists of a combination of vendor supplied, open source, and locally written software [1] that run under CentOS. The IVE software stack outputs OpenGL [2].

In order to have confidence that our environment is functioning correctly, we have implemented three types of tests: hardware tests, software functional tests, and render tests. The render tests are necessary because the OpenGL standard does not guarantee that the pixels displayed will be exactly the same when displayed with different GPUs and different drivers. So, the images generated with identical inputs at two different times may both be correct, but not identical.

We have developed a software utility that enables us to run an application from a text file called a timeline file. Using this we can start and stop navigation, snap images, and issue commands to the application. The commands enable us to modify the visualization in various ways such as adding or deleting objects, or modifying object properties such as color. To create a test, we develop a timeline file to run the application and capture rendered images at specific times during the execution. To initialize the test, we run the timeline file and save the captured images as baseline images; see Figure 58. We run the test on multiple machines.

We have found that the primary reason for differences between images is anti-aliasing. Since there are many types of anti-aliasing and there are aspects that are proprietary to the cards and drivers, we have created two types of tests. One type of test is run with anti-aliasing turned off and has baseline images specific to that case. The second type of test is run with anti-aliasing turned on and compared to baseline images that were created on the CAVE host computer.

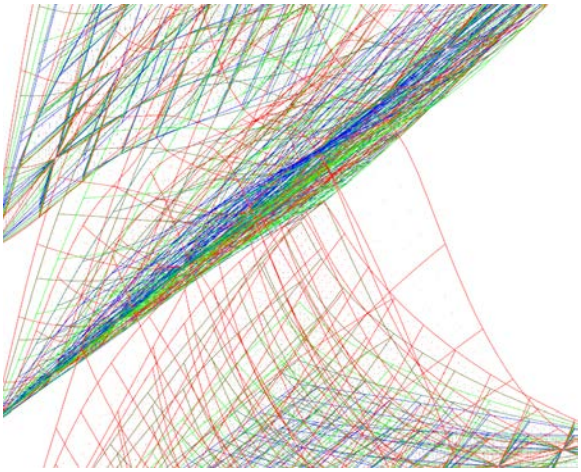

Figure 58. *A baseline for the 'moth' [3].*

The generated and baseline images are compared in three different ways. First, they are checked to see if they are identical. If they are not, they are evaluated for perceptual sameness [4], which uses a variety of image processing techniques to give us some information on the differences. After all the tests are run, they are published to a Web page where they can be examined.

In the coming year, we will continue to expand our render tests.

[1] W. Griffin, W. George, T. Griffin, J. Hagedorn, M. Olano, S. Satterfield, J. Sims and J. E. Terrill. Application Creation for an Immersive Virtual Measurement and Analysis Laboratory. In *Proceedings of the 9th Workshop on Software Engineering and Architectures for Realtime Interactive Systems* (SEARIS), March 20, 2016.

[2] https://www.opengl.org/

[3] https://www.nist.gov/itl/math/energy-spectrum-ultra-cold-atoms-synthetic-magnetic-field

[4] https://en.wikipedia.org/wiki/Spatial_anti-aliasing

[5] https://en.wikipedia.org/wiki/Structural_similarity

WebVR Graphics

Sandy Ressler
Emily Hobby (UMBC)
Amanda Malanowski (NIST Information Services)
Amy Trost (NIST Information Services)

WebVR is a technology that enables some types of virtual reality (VR) content to be displayed in a Web page. 2017 was a breakthrough year for WebVR, because prior versions of Web browsers required special "nightly" or "development" builds. Now the current production version of Firefox's Mozilla understands VR devices (Oculus Rift and HTC Vive) right out of the box. We expect other popular Web browsers to follow suit shortly. This major development means that it is now

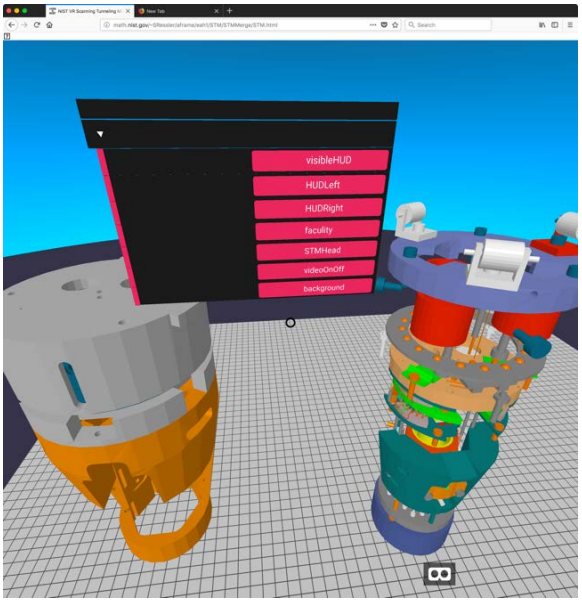

Figure 59. *STM with Menu.*

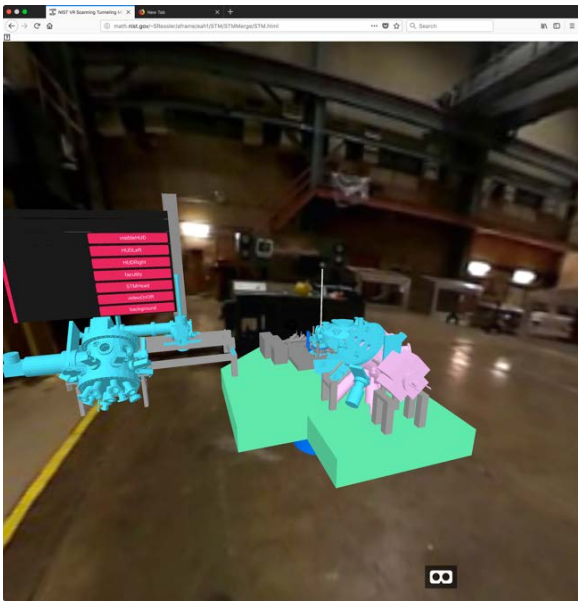

Figure 60. *STM facility in environment.*

possible to send someone the URL of a Web page that contains WebVR content, and, assuming that person has the hardware, he or she can experience the full 360-degree content with 6 degrees of freedom head tracking.

We continue work on two exemplar applications. The first is a navigable scanning tunneling microscope (STM) head, and the second is a walkthrough of the NIST Library using 360-degree images. As a multi-disciplinary agency, NIST performs research across a wide variety of domains. The techniques we are developing and exploring serve to expose NIST research in a simple yet powerful way.

STM head. Improvements this year include being able to use the STM head environment with both an Oculus Rift and HTC Vive. The Rift hand controllers have small joysticks, and using those to navigate is particularly effective. Figure 59 shows the STM with menu and the STM with several parts moved aside to allow viewing of the interior. Figure 60 shows the facility in which the STM is housed, put into the context of an image-based sphere which allows us to place the computer graphics object into a more realistic environment.

NIST Library Walkthrough. We placed a tripod at a dozen or so locations in the library and captured 360-degree videos. The videos were then made navigable by placing them into a WebVR page, which allows the user to select circular spots which take the user to that new location (another video sphere). For purposes of this initial prototype we extracted single frames from the video and simply used 360-images; however, the potential for using video has been demonstrated, enabling a guide or other video material presented rather than a static image.

The ability to present locations to the public is a capability quickly coming into high demand. Most demonstrations of this work and our poster/demo of the project now called “Public Access to Non-Public Spaces: A Virtual Reality Use Case,” indicate a high degree of interest in this method of presenting research spaces on the NIST campus. This coming year, we expect to create more extensive demonstrations of the NIST Library, the Net-Zero house and the NIST Machine Shop. In addition, the methodology and software will be packaged up to enable any NIST staff, or indeed the public, to create these types of VR virtual tours.

[1] S. Ressler, E. Hobby. “Immersive STM,” August 4, 2017, http://math.nist.gov/~SRessler/aframe/eah1/STM/STMMerge/STM.html

[2] S. Ressler, E. Hobby. “NIST Library 360,” August 4, 2017, http://math.nist.gov/~SRessler/aframe/eah1/imageLibrary/updatedLib.html

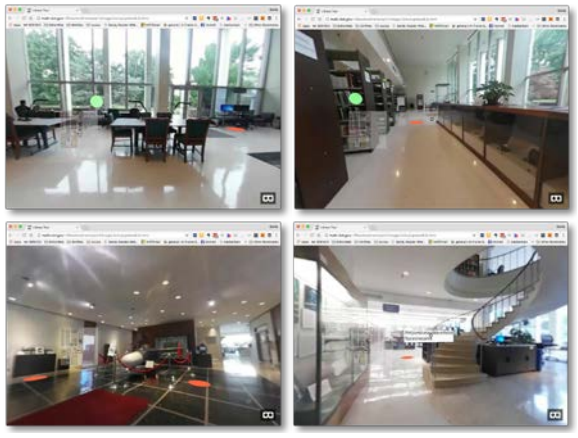

Figure 61. *Virtual Tour of NIST Library (example locations).*

Quantum Information

An emerging discipline at the intersection of physics and computer science, quantum information science is likely to revolutionize 21st century science and technology in the same way that lasers, electronics, and computers did in the 20th century. By encoding information into quantum states of matter, one can, in theory, exploit the unique properties of quantum systems to enable phenomenal increases in information storage and processing capability, as well as communication channels with high levels of security. Although many of the necessary physical manipulations of quantum states have been demonstrated experimentally, scaling these up to enable fully capable quantum computers remains a grand challenge. We engage in (a) theoretical studies to understand the power of quantum computing, (b) collaborative efforts with the multi-laboratory experimental quantum science program at NIST to characterize and benchmark specific physical implementations of quantum information processing, and (c) demonstration and assessment of technologies for quantum communication.

Quantum Information Science

Scott Glancy
Emanuel Knill
Peter Bierhorst (University of Colorado)
Adam Keith (University of Colorado)
Karl Mayer (University of Colorado)
Jim van Meter (University of Colorado)
Kevin Coakley (NIST ITL)
Cindy Regal (JILA and University of Colorado)
Ana Maria Rey (JILA and University of Colorado)
Gerardo Ortiz (Indiana University)
Yanbao Zhang (University of Waterloo, Canada)
Carlton Caves (University of New Mexico)

Quantum information technology has progressed to the point where one can routinely execute quantum programs on small numbers of qubits. Quantum advantages are being demonstrated for measurement while quantum information theory is increasingly influencing basic science in fields such as condensed matter and quantum field theory. ACMD researches are contributing to quantum information science by establishing basic protocols for quantum device characterization, improving statistical methods for certifying performance, and investigating the performance boundary for quantum technology.

A common problem in experiments involving quantum circuits is to determine the fidelity of the process implemented. ACMD researchers have determined that the minimum number of states required to verify that the fidelity of a process is close to one is the dimension of the state space, which is one less than previously believed. They determined and implemented a semidefinite program that can compute fidelity lower bounds given the fidelities on any given set of states.

These bounds can be used as a performance measure without full fidelity determination. A classification of sets of states for which these bounds converge to 1 as the process approaches fidelity 1 has been obtained. Beyond theoretical investigations of fidelity, the methods developed by ACMD researchers for device characterizations are being applied to a variety of quantum experiments, including experiments with trapped atoms [1] and experiments involving quantum mechanical oscillators [2]. See also "Quantum Estimation Theory and Applications" in this report.

ACMD researchers completed a detailed study [3] of the performance of test martingales on Bernoulli trials for estimating the probability of outcome 1 of biased random bits. Test martingale methods can robustly certify parameters even when the data is not independent and identically distributed. Unlike most other statistical methods for similar problems, they can adapt to changing conditions to verify fundamental properties. ACMD researchers have used these strategies for demonstrating the absence of local realism in quantum experiments and for quantum randomness generation. The study shows that although robustness involves some loss of sensitivity, the loss is within the range of statistical fluctuations for certificates.

With collaborators from Indiana University Bloomington, ACMD researchers have started to study the problem of how to benchmark proposed experiments for measuring Majorana modes. Majorana modes have been highly touted for use as robust qubits and are of fundamental interest in condensed matter physics. They have been claimed to be discovered anew multiple times in recent years, and Microsoft is investing significant resources in developing quantum computers based on Majorana modes. One test for Majorana behavior can be derived from the "magic square," originally proposed as a strong test of quantum contextuality. For testing Majorana behavior, it is desirable that the test is rigid and robust in the sense that if it succeeds with high probability, the underlying quantum system must be almost isomorphic to that expected for Majorana modes. Success then indicates "as if" Majorana behavior.

A fundamentally interesting question is what ultimately limits measurement precision when taking into consideration relativistic effects and the curvature of space-time. ACMD researchers and their collaborators

have completed work that establishes an algebraic framework for determining uncertainty bounds for measuring properties of space-time [4]. This work has consequences for interferometric measurements of relative length, such as those used for gravitational wave detection. The work includes extensions of known bounds on such measurements to the case of extremely broad-band probe light. Broad-band probes also play a role in verifying the ever-present entanglement of the quantum vacuum. The question of whether such a verification is feasible is of ongoing interest to ACMD researchers.

[1] B. J. Lester, Y. Lin, M. O. Brown, A. M. Kaufman, R. J. Ball, E. Knill, A. M. Rey and C. A. Regal. Measurement-Based Entanglement of Non-Interacting Bosonic Atoms. arXiv:1712.06633, 2017.

[2] A. P. Reed, K. H. Mayer, J. D. Teufel, L. D. Burkhart, W. Pfaff, M. Reagor, L. Sletten, X. Ma, R. J. Schoelkopf, E. Knill, and K. W. Lehnert. Faithful Conversion of Propagating Quantum Information to Mechanical Motion. *Nature Physics* **13** (2017), 1163-1167. DOI: 10.1038/nphys4251

[3] P. Wills, E. Knill, K. Coakley and Y. Zhang. Performance of Test Supermartingale Confidence Intervals for the Success Probability of Bernoulli Trials. arXiv:1709.04078, 2017.

[4] T. G. Downes, J. R. van Meter, E. Knill, G. J. Milburn and C. M. Caves. Quantum Estimation of Parameters of Classical Spacetimes. *Physical Review D* **96** (2017), 105004. DOI: 10.1103/PhysRevD.96

Quantum Estimation Theory and Applications

Arik Avagyan (University of Colorado)
Charles Baldwin
Scott Glancy
Emanuel Knill
Karl Mayer (University of Colorado)
Hilma Vasconcelos (Federal Univ. of Ceara, Brazil)
Stephen Erickson (NIST PML)
Alexey Gorshkov (NIST PML)
Daniel Kienzler (NIST PML)
Dietrich Leibfried (NIST PML)
Alan Migdall (NIST PML)
Trey Porto (NIST PML)
Kartik Srinivisan (NIST PML)
Yong Wan (NIST PML)
David Wineland (NIST PML)
Leonardo Silva (Federal University of Ceara, Brazil)

Many emerging technologies will exploit quantum mechanical effects to enhance metrology, computation, and communication. Developing these technologies requires improved methods to measure the states of quantum systems. Quantum estimation is a statistical problem of estimating an underlying quantum state, measurement, or process by using a collection of measurements made on independently prepared copies of the state or applications of the measurement or process. Accurate quantum estimation allows experimentalists to answer the question "What is happening in my quantum experiment?" and to characterize uncertainty in that answer.

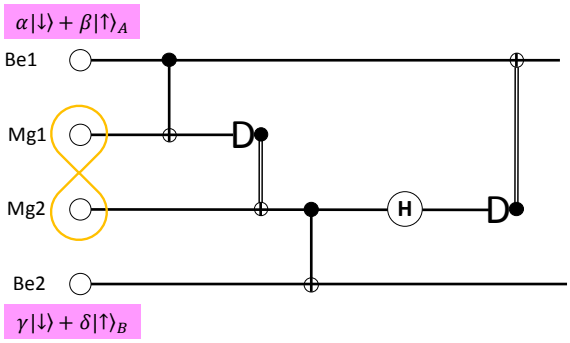

Figure 62. *Simplified diagram of CNOT teleportation. The Magnesium qubits Mg1 and Mg2 are prepared in an entangled state, and the two Berillium qubits Be1 and Be2 are prepared in arbitrary logical states. Each Be ion interacts with its partner Mg ion through conventional quantum CNOT operations. Then the Mg ions are measured, and depending on the measurement results, single qubit operations are applied to the Be ions. After these corrections, the action of the circuit is equivalent to application of CNOT between the Be ions.*

NIST's Ion Storage Group has pioneered one of the world's most successful quantum computer development projects. To keep pace with their recent advances in qubit preparation, logical operation, and measurement fidelities, ACMD researchers have developed more advanced statistical techniques to characterize trapped ion quantum computers. In particular, in collaboration with the Ion Storage Group, ACMD researchers have developed tools to estimate properties of quantum states for experiments with extremely high fidelity. These tools include a single procedure for both calibrating measurements (using data from qubits with known states) and estimating the quantum state (of qubits in an unknown state) [1]. This year these tools have been expanded to also estimate unknown quantum processes, such as quantum logic operations performed in a quantum computer. ACMD researchers are preparing this software for public release on GitHub.

ACMD researchers are collaborating with the Ion Storage Group to demonstrate a controlled-NOT (CNOT) quantum logic operation that is transferred from two magnesium ion qubits to two beryllium ion qubits through quantum teleportation. As shown Figure 62, a CNOT is first applied to entangled magnesium ions, which are then used to teleport the beryllium ions. After teleportation, the beryllium ions have received the CNOT operation, even though they do not directly interact with one another. ACMD's tools for estimating

quantum states and processes are being used to diagnose errors and improve the fidelity of the CNOT operation.

ACMD researchers are contributing to the Metrology with Interacting Photons project, which is funded by the NIST Innovations in Measurement Science program. Its goals are to demonstrate photon-photon interactions that are mediated by Rydberg atoms, and to exploit those for metrology. ACMD researchers are adapting traditional homodyne detection so that it can verify that the photons have actually interacted with one another despite noise, loss, and a strict limit on the power of the homodyne reference field (or "local oscillator").

When measuring the state of a quantum harmonic oscillator (such as a nano-mechanical resonator or a quantum optical field), the natural measurements are continuous variables that are phase variants of position and momentum. The fact that every measurement outcome may be unique can cause estimation of the quantum state to be computationally expensive. ACMD researchers have designed a scheme for discretizing the measurement outcomes, which allows much faster estimation while keeping high fidelity of the estimate [2].

[1] C. Keith, C. H. Baldwin, S. Glancy and E. Knill. Partial Quantum Tomography Using Maximum Likelihood Estimation. In preparation.

[2] J. L. E. Silva, H. M. Vasconcelos and S. Glancy. Quadrature Histograms in Maximum Likelihood Quantum State Tomography. In preparation.

Phase Retrieval and Quantum Tomography

Yi-Kai Liu
Shelby Kimmel (Middlebury College)
Felix Krahmer (Technical University of Munich)
Martin Kliesch (University of Gdansk)
Ingo Roth (Free University of Berlin)
Jens Eisert (Free University of Berlin)
Richard Kueng (Caltech)

Phase retrieval is the task of learning an unknown n-dimensional vector $\boldsymbol{x}$ from measurements of the form

$$y_i = |\langle a_i, x\rangle|^2 \quad i = 1, 2, \ldots, m,$$

where the vectors a_i are chosen by the observer. Such measurements arise in a variety of applications, including optical imaging (where one measures the intensity of the light field, but not the phase), and quantum tomography (where one measures the probability, but not the complex amplitude, of the wave function).

We have studied the performance of PhaseLift, a well-known algorithm for phase retrieval that is based on convex relaxation, using different kinds of structured measurements, i.e., different choices for the vectors a_i.

First, we studied random Bernoulli measurements, where the a_i are sampled at random from the hypercube $\{1, -1\}^n$. In this case, there exist vectors x that cannot be recovered uniquely. However, we showed that these failures are rare, and, in fact, there is a large class of vectors that can be recovered successfully using PhaseLift [2]. This result is interesting because it is obtained without relying on any of the small-ball probability assumptions that were used in previous work.

Second, we studied the situation where the unknown vector x belongs to the unitary group, and the measurement vectors a_i are sampled at random from the Clifford group. This situation arises in quantum process tomography, when one wants to characterize an unknown unitary quantum process using robust measurements derived from randomized benchmarking.

In [3], we proved approximate, average-case recovery guarantees when the a_i are sampled from a unitary 2-design, and we proved exact, worst-case recovery guarantees when the a_i are sampled from a unitary 4-design. We are now working to strengthen the latter result when the a_i are sampled from the Clifford group.

Finally, we are developing a method called quantum system tomography, which tries to discover the sources of noise in quantum information processors. At a high level, quantum system tomography consists of two steps. First, measure all the relevant environmental parameters (sometimes called side information) that can affect the internal quantum state of the device under investigation. Second, use machine learning techniques to construct a mathematical model that describes the correlations between the side information and the internal quantum state. These correlations can provide a human-interpretable explanation of the noise processes occurring in the device.

[1] F. Krahmer and Y.-K. Liu. Phase Retrieval Without Small-Ball Probability Assumptions. *IEEE Transactions on Information Theory* **64**:1 (January 2018), 485-500.

[2] S. Kimmel and Y.-K. Liu. Phase Retrieval Using Unitary 2-Designs. In *Proceedings of the 2017 International Conference on Sampling Theory and Applications (SampTA)*, Tallin, Estonia, July 3-7, 2017, 345-349.

Quantum Reinforcement Learning

Yi-Kai Liu
Vedran Dunjko (Max Planck Institute-Quantum Optics)
Jacob Taylor (NIST PML)
Xingyao Wu (University of Maryland)

The field of quantum machine learning – using quantum computers to discover patterns in complex data sets – has seen rapid progress in recent years. Thus far, most of this work has focused on data analysis tasks, such as supervised learning (e.g., for classification) and unsupervised learning (e.g., for clustering). In this project, we investigate quantum speedups for another class of machine learning tasks, namely reinforcement learning.

Reinforcement learning is concerned with situations where an agent interacts with an environment. The goal of the agent is to learn how to extract "rewards" from the environment, given some minimal prior information. This involves challenges that go beyond data analysis. For instance, there is a tension between the need to explore the environment (to discover which actions are rewarding), and the need to exploit the environment (to earn rewards). Reinforcement learning is linked to robotics and game theory, and can be viewed as a step beyond data analysis towards full-blown artificial intelligence.

When applying quantum computers to reinforcement learning, an obvious difficulty arises: the environment may cause decoherence effects that transform an agent's quantum strategy into a merely classical strategy. This problem cannot be solved using techniques for fault-tolerant quantum computation, because the environment is not fully under the agent's control. However, it turns out that one can get quantum speedups for reinforcement learning, in certain situations where the agent has partial control over the environment.

In our recent work [1], we showed the first super-polynomial speedups for quantum reinforcement learning, improving on previous work that showed quadratic speedups. Specifically, we showed a super-polynomial quantum speedup for an interactive learning task that is based on the Recursive Fourier Sampling problem. While this example is somewhat contrived, we conjecture that a similar quantum speedup can be achieved for a much broader class of recursive reinforcement learning tasks. Finally, we showed an exponential quantum speedup for an interactive learning task that is based on Simon's problem.

[1] V. Dunjko, Y.-K. Liu, X. Wu and J. M. Taylor. Super-polynomial and Exponential Improvements for Quantum-enhanced Reinforcement Learning. arXiv: 1710.11160, 2017.

Computational Complexity of Quantum and Classical Field Theory

Stephen Jordan
Ning Bao (University of California, Berkeley)
Raphael Bousson (University of California, Berkeley)
Pedro Costa (Brazilian Center for Res. in Physics)
Keith Lee (University of Toronto)
John Preskill (Caltech)
Hari Krovi (Raytheon/BBN)
Ali Moosavian (University of Maryland)
Troy Sewell (University of Maryland)

Field theories are ubiquitous in physics, describing quantities, such as the electromagnetic field, which vary continuously in space. From a computational complexity point of view, field theories, both classical and quantum, pose unique challenges due to the formally infinite set of degrees of freedom present even within a finite volume. Our recent and ongoing work applies tools from quantum information to develop new algorithms by which quantum computers (once they become available) can efficiently simulate field theories, and to develop the fundamental computational complexity theory of field theories. This project has several aspects, described below.

Quantum and Classical Algorithms for Simulating Quantum Field Theories. Our prior work has yielded quantum algorithms which can approximate scattering cross-sections in certain quantum field theories using numbers of qubits and quantum gates that scale polynomially with the desired precision and the energy of the process being simulated. Our recent and ongoing work focuses on improving these quantum algorithms in terms of their speed and generality.

The most challenging step in our quantum algorithms for simulating quantum field theories is the initial step in which a quantum state representing the initial conditions for the simulation is prepared. This step is the most time-consuming part of the algorithm, and also the key bottleneck limiting the generality of the algorithm. In recent work [1], we have developed a completely different approach to this step, which achieves a much faster runtime, at least asymptotically, and can be applied to simulate the symmetry broken phase of the Gross-Neveu quantum field theory, a task which was out of reach for our earlier quantum algorithms for simulating quantum field theories. In related work we are developing novel classical algorithms for computing correlation functions in quantum field theories by formulating the problem as a semidefinite program.

Quantum Algorithms for Simulating Classical Field Theories. A large fraction of scientific computing is devoted to solving partial differential equations (PDEs) describing classical fields, such as electromagnetic fields, acoustic waves, flow fields in fluid dynamics, and

mechanical stress fields. It is natural to ask whether quantum computers have any potential to more efficiently solve these problems. In recent work [2], we have obtained a new quantum algorithm for simulating the dynamics of classical wave equations. This quantum algorithm uses a number of qubits that scales only logarithmically with the number of lattice points in the spatial mesh used to discretize the PDEs and also runs quadratically faster than prior quantum algorithms as a function of the lattice spacing. We are now exploring the applicability of preconditioners to improve the performance of quantum algorithms for linear algebra problems arising in the context of scientific computing.

Computational Complexity of the Dynamics of Quantum Fields. While developing quantum algorithms to simulate quantum field theories the question arises as to whether classical algorithms could be developed to solve the same problems without the need for exotic and expensive quantum computing hardware. Presently known classical algorithms for simulating quantum field theories break down when applied to the dynamics of strongly coupled quantum field theories, particularly in settings with a high density of fermions. Decades of effort have not succeeded in fully overcoming this problem, but how do we know a new and better classical algorithm won't soon be discovered?

In recent work [3], we have obtained formal complexity-theoretic evidence that the inability of classical computers to efficiently solve all instances of the quantum field theory simulation problem is not a result of lack of imagination but rather due to a fundamental barrier. Specifically, we have shown that the input-output behavior of any quantum circuit can always be encoded into a corresponding quantum field theory scattering amplitude. Therefore, if any efficient classical algorithm could compute these scattering amplitudes in complete generality, it could efficiently solve all the problems that quantum computers can solve, including for example integer factorization. Complexity theorists generally consider this scenario (BQP=P) to be highly unlikely. Thus, our result constitutes evidence for the fundamental intractability of simulating quantum field theory on classical computers. Interestingly, our construction applies even in a setting with weak coupling and no fermions.

Another setting in which computational complexity theory and quantum field theory meet is cosmology. In an influential 2007 paper, Denef and Douglas pointed out that, according to certain models, the problem of finding a vacuum solution with cosmological constant compatible with observation is a large instance of an NP-hard problem called number partitioning. How then did the universe solve it? In recent work [4], we have pointed out that, though NP-hard in general, the number partitioning problem arising in cosmology can nevertheless be efficiently solved in certain parameter regimes, specifically if the number of fields is very large.

[1] H. Moosavian and S. Jordan. Faster Quantum Algorithm to Simulate Fermionic Quantum Field Theory. arXiv:1711.04006, 2017.

[2] P. C. S. Costa, S. Jordan and A. Ostrander. Quantum Algorithm for Simulating the Wave Equation. arXiv:1711.05394, 2017.

[3] S. P. Jordan, H. Krovi, K. S. M. Lee and J. Preskill. BQP-Completeness of Scattering in Scalar Quantum Field Theory. *Quantum*, in press. arXiv:1703.00454.

[4] N. Bao, R. Bousso, S. Jordan and B. Lackey. Fast Optimization Algorithms and the Cosmological Constant. *Physical Review D* **96** (2017), 103512.

Quantum and Stochastic Optimization Algorithms

Stephen Jordan
Alan Mink (Theiss Research)
Aniruddha Bapat (University of Maryland)
Jake Bringewatt (University of Maryland)
Bill Dorland (University of Maryland)
Brad Lackey (University of Maryland)

Discrete optimization problems are widespread in industry and form the heart of the theory of NP-completeness. Although exact solutions to worst case instances of NP-complete optimization problems probably cannot be obtained in polynomial time by classical or quantum computers, the development of powerful approximation algorithms and heuristics is an active area of research in both classical and quantum computing.

Many proposed quantum algorithms for optimization problems are based on stoquastic adiabatic quantum computing, in which all of the quantum amplitudes are real and positive. Quantum states with positive amplitudes are similar to probability distributions, although normalized differently, and do not give rise to the destructive interference effects that one can obtain using more general wavefunctions. This property of quantum states with positive amplitudes has led to the question of whether stoquastic adiabatic computations can be efficiently simulated by classical stochastic algorithms. Our recent work in collaboration with Michael Jarret and Brad Lackey has shown that classical diffusion Monte Carlo algorithms cannot always efficiently simulate stoquastic adiabatic computation. Our work gave examples on which diffusion Monte Carlo takes exponential time to converge. However, our examples involved Hamiltonians with many-body interactions, which are physically unrealistic and not used in practice in stoquastic adiabatic computations. In a recent collaboration [1], we constructed examples of stoquastic processes that diffusion Monte Carlo takes exponential time to simulate, but which do not involve many-body interactions.

In both quantum and classical optimization heuristics, the algorithms themselves have a lot of adjustable parameters. Choosing these parameters to ensure good performance of the algorithms is a daunting problem. In the last few years, people have begun applying optimal control theory to the design of quantum optimization algorithms. In ongoing work, we are generalizing this framework to apply simultaneously to quantum optimization heuristics such as adiabatic optimization, the Quantum Approximate Optimization Algorithm (QAOA), and to classical stochastic optimization heuristics such as simulated annealing. So far, we have discovered one example problem for which an optimized annealing schedule via "bang-bang" control yields exponentially improved performance of simulated annealing relative to standard quasi-static annealing. Currently we are investigating the degree to which such speedups are achievable more generally.

[1] J. Bringewatt, W. Dorland, S. P. Jordan and A. Mink. Diffusion Monte Carlo Versus Adiabatic Computation for Local Hamiltonians. arXiv:1709.03971M.

Contextualtiy as a Resource for Efficient Classical Algorithms of Quantum Simulation

Lucas Kocia

There is great interest currently in developing quantum computers that outperform modern classical computers. Many, particularly in industry, are competing to build quantum machines that have limited potential as they lack error-correction capabilities, but are able to nevertheless solve some target problems faster than current top-of-the-line classical computers. This approach is known as the search to establish "quantum supremacy," in the sense that a quantum computer outperforms its classical competitors in actual practice.

For this to be achieved, one must establish:

(1) the limit of today's classical computers to simulate particular quantum gate-sets in terms of qubit number, circuit depth and runtime, etc. and,

(2) classical algorithms that simulate the purported quantum machine efficiently so that the machine can be validated to be quantum mechanical.

Many approaches are being taken to tackle the both goals by developing efficient classical algorithms of quantum simulation. They include quantum Monte Carlo techniques [1], Feynman path methods [2] and novel tensorial decompositions [3]. Another line of approach is in using quasiprobability distributions [4] and leveraging contextuality as a resource wisely [5]. This is an effort to enable an algorithm running on a classical computer to efficiently handle quantum corrections. Contextuality is related to the negativity in the quasiprobability representations of the quantum states, unitary gates or measurements involved in a quantum process. It is an ingredient necessary for a classical process to attain quantum universality.

We have recently shown that contextuality is also equivalent to higher order hbar corrections in a particular quasiprobability distribution related to the Wigner-Weyl-Moyal formalism [5-7]. We are attempting to use this formalism as a framework to efficiently add contextuality to a non-contextual backbone that is known to be efficiently simulable classically. This formalism is a new approach to this problem that attempts to bridge efficient algorithms developed for continuous infinite-dimensional systems and bring them to bear in discrete Hilbert spaces.

[1] S. Bravyi and D. Gosset. Improved Classical Simulation of Quantum Circuits Dominated by Clifford Gates. *Physical Review Letters* **116**:25 (2016), 250501.

[2] S. Boixo, *et al.* Simulation of Low-Depth Quantum Circuits as Complex Undirected Graphical Models. arXiv:1712.05384, 2017)

[3] E. Pednault, *et al.* Breaking the 49-Qubit Barrier in the Simulation of Quantum Circuits. arXiv:1710.05867, 2017.

[4] H. Pashayan, J. J. Wallman and S. D. Bartlett. Estimating Outcome Probabilities of Quantum Circuits Using Quasiprobabilities. *Physical Review Letters* **115**:7 (2015), 070501.

[5] C. Duarte and B. Amaral. Resource Theory of Contextuality for Arbitrary Prepare-and-Measure Experiments. arXiv:1711.10465, 2017.

[6] L. Kocia, Y. Huang and P. Love. Semiclassical Formulation of the Gottesman-Knill Theorem and Universal Quantum Computation. *Physical Review A* **96**:3 (2017), 032331.

[7] L. Kocia and P. Love. Measurement Contextuality and Planck's Constant. arXiv:1711.08066, 2017.

[8] L. Kocia, and P. Love. Discrete Wigner Formalism for Qubits and the Non-Contextuality of Clifford Operations on Qubit Stabilizer States. arXiv:1705.08869, 2017.

One-Time Programs and Pseudo-Random Quantum States

Yi-Kai Liu
Zhengfeng Ji (University of Technology Sydney)
Fang Song (Portland State University)

A one-time program is a type of trusted computing hardware that performs a pre-programmed computation exactly once, and then self-destructs. One-time programs can be used to perform actions that should not be repeated, such as spending a set amount of money, or casting a vote in an election. They can also be used to

protect mobile devices, such as smartphones or autonomous drones, from being stolen and reverse-engineered by an adversary.

In previous work, we developed techniques for constructing one-time programs based on solid-state quantum systems, such as nuclear spins. These constructions have been proven secure in the isolated qubits model. However, while these constructions are efficient in the sense of being polynomially bounded, they are still too inefficient for practical use.

To address this issue, we are now investigating a new construction for one-time programs that uses program obfuscation, in concert with isolated qubits. This construction uses fewer qubits, and is more robust to noise. In addition, this construction only requires obfuscation for a weak class of functions, which is possible under fairly mild complexity-theoretic assumptions. We are now developing new techniques for proving the security of this construction.

In related work, we have also developed new techniques for constructing pseudorandom quantum states [1]. These are quantum states that look "random" to an observer that is computationally bounded. These states can be used to construct cryptographically secure quantum money, and to perform numerical simulations of quantum statistical mechanics. Pseudorandom quantum states are related to quantum *t*-designs, which have been studied previously. Such states differ from quantum *t*-designs in two ways: they are only computationally secure (not information-theoretically secure), and they can be constructed more efficiently using log-depth (rather than poly-depth) quantum circuits.

[1] Z. Ji, Y.-K. Liu and F. Song. Pseudorandom States, Non-Cloning Theorems and Quantum Money. arXiv:1711.00385, 2017.

Post-Quantum Cryptography

Stephen Jordan
Yi-Kai Liu
Gorjan Alagic (NIST ITL)
Jacob Alperin-Sheriff (NIST ITL)
Larry Bassham (NIST ITL)
Lily Chen (NIST ITL)
Carl Miller (NIST ITL)
Dustin Moody (NIST ITL)
Rene Peralta (NIST ITL)
Ray Perlner (NIST ITL)
Daniel Smith-Tone (NIST ITL)

In December 2016, NIST published a call for proposals which marked the beginning of a formal process to develop standards for post-quantum cryptosystems [1]. The goal of this process is to standardize one or more cryptosystems that could replace currently used schemes, such as RSA, Diffie-Hellman and elliptic curve cryptosystems, that are vulnerable to attack using quantum computers. These cryptosystems play a crucial role in Internet commerce and cybersecurity. While large quantum computers have not yet been built, it is prudent to begin preparing for that possibility.

The NIST call for proposals focuses on three main functionalities: public-key encryption, key exchange, and digital signatures. These are fundamental cryptographic primitives that enable a variety of applications, including secure Web browsing, digital certificates, and secure software updates.

There are a number of candidate cryptosystems that are believed to be quantum-secure. These cryptosystems are based on a variety of mathematical techniques, including high-dimensional lattices, coding theory, systems of multi-variate polynomial equations, elliptic curve isogenies, hash-based signatures, and many others. However, further research is needed to build confidence in the security of these schemes, and to improve their practical performance.

The NIST standards development process involves an open call for proposals, followed by multiple rounds of public review, involving experts and stakeholders in academia, government and industry. This process is intended to foster the development of post-quantum cryptosystems that will be suitable for standardization, as well as basic research on related topics, such as quantum algorithms and quantum cryptanalysis.

In 2017, NIST worked with the post-quantum cryptography community to refine NIST's guidelines in the call for proposals. NIST received a total of 82 proposals by the submission deadline in November 2017. NIST is now beginning the review process, which includes both internal review and public discussions. In April 2018, NIST will hold a workshop, collocated with the PQCrypto conference in Fort Lauderdale, Florida, to discuss the proposed cryptosystems.

NIST is also carrying out research in several areas in post-quantum cryptography, including quantum-secure symmetric cryptography [2], multivariate cryptography [3, 4, 5], and quantum cryptanalysis [6, 7]. In addition, NIST is engaging with the community through conference presentations [8-11], online mailing lists, and technical magazine articles [12, 13].

[1] Announcing Request for Nominations for Public-Key Post-Quantum Cryptographic Algorithms. Federal Register, 81 FR 92787, December 20, 2016.

[2] G. Alagic and A. Russell. Quantum-Secure Symmetric-Key Cryptography Based on Hidden Shifts. In *Proceedings of EUROCRYPT 2017*, Paris, France, April 30–May 4, 2017.

[3] R. Cartor and D. Smith-Tone. An Updated Security Analysis of PFLASH. In *Proceedings of PQCrypto 2017*, Utrecht, the Netherlands, June 26–28, 2017.

[4] D. Moody, R. Perlner and D. Smith-Tone. Improved Attacks for Characteristic-2 Parameters of the Cubic ABC

Simple Matrix Encryption Scheme. In *Proceedings of PQCrypto 2017*, Utrecht, the Netherlands, June 26–28, 2017.

[5] D. Cabarcas, D. Smith-Tone and J. A. Verbel. Practical Key Recovery Attack for ZHFE. In *Proceedings of PQCrypto 2017*, Utrecht, the Netherlands, June 26–28, 2017.

[6] B. Amento-Adelmann, M. Grassl, B. Langenberg, Y.-K. Liu, E. Schoute and R. Steinwandt. Quantum Cryptanalysis of Block Ciphers: A Case Study. Manuscript, 2017.

[7] R. Perlner and Y.-K. Liu. Thermodynamic Analysis of Classical and Quantum Search Algorithms. arXiv:1709.10510, 2017.

[8] R. Peralta. "NIST's Post-Quantum Cryptography Project." Real World Crypto 2017, New York, USA, January 10-12, 2017.

[9] D. Smith-Tone, R. Perlner and D. Moody. "Q&A Session on the NIST Call for Proposals." PQCrypto 2017, Utrecht, the Netherlands, June 26–28, 2017.

[10] L. Chen. "Updates on the NIST Post-Quantum Cryptography Standardization Process." ETSI / IQC Quantum Safe Workshop, London, UK, September 13-15, 2017.

[11] D. Moody. "The Ship Has Sailed: the NIST Post-Quantum Cryptography Competition." Asiacrypt 2017, Hong Kong, China, December 3-7, 2017.

[12] L. Chen. Cryptography Standards in Quantum Time: New Wine in an Old Wineskin? *IEEE Security & Privacy* 15:4 (July/August 2017), 51-57.

[13] S. Jordan and Y.-K. Liu. Quantum Cryptanalysis: Shor, Grover, and Beyond. *IEEE Security & Privacy*, to appear.

Quantum Repeater R & D

Lijun Ma
Oliver Slattery
Xiao Tang

Quantum information science (QIS) is expected to open entirely new vistas of technological development. In July 2016, the National Science and Technology Council's Subcommittee on Physical Sciences released a report [1] recommended a gradual increase in QIS R&D funding to maintain US scientific leadership and to reap the societal benefits of QIS technologies. In that report, quantum communication, along with sensing and metrology, quantum simulation and quantum computing, were predicted to have the greatest impact to the society. The further stated that "Solutions that build on current experimental work to develop reliable photon sources and technology to allow long-distance transmission of quantum information as well as ongoing theoretical work on protocols for sharing data, for example between quantum processors, could, with consistent attention and support, appear within 5 to 10 years." It is clear that quantum communication science and technology has become a priority research area for the nation.

Quantum communication, which transmits information encoded in quantum states of light or matter, is a challenging technical problem because the information stored in quantum states is irrevocably altered when the quantum system is disturbed. This property has the advantage that eavesdroppers are easily detected, leading to quantum-secure methods of communication. At the same time, this property has the disadvantage that signals cannot be replicated or amplified due to their quantum nature.

Quantum-secured communication or quantum key distribution (QKD) is currently an active area of development world-wide. However, a fiber-based QKD system can only be operated between two partners (point-to-point) and the operating distance is limited to within a couple of hundred kilometers. These two limitations are due to unavoidable loss of photons in optical fiber, and to the fact that the signal carried by the photons cannot be replicated or amplified. The development of quantum repeaters aims to resolve this problem without violating the fundamental laws of quantum mechanics. In principle, a quantum repeater can relay the information encoded in quantum states from one system to another by using a so-called Bell state measurement without reading the information. In this way it can extend the QKD operation distance. More importantly, quantum repeaters can be used as network nodes to connect future quantum computers to form quantum networks. In the longer term, quantum networks will connect distributed quantum systems used, for example, for global seismic monitoring, andwill allow quantum information to flow coherently between the internal components of quantum simulators and quantum computers. As essential building blocks, quantum repeaters will play a central role in future quantum information science and technology.

Previous work. The quantum communication research project in ITL was established at the beginning of the 21st century as a part of a NIST-wide quantum key distribution collaboration. This collaboration resulted in the fastest QKD systems in the world at that time, and the demonstration of a 3-node QKD network for secure exchange of cryptographic keys, enabling transmission of video signals between one "Alice" and two "Bobs" using real-time "one-time pad" encryption and decryption [2]. Our team then worked on single photon frequency conversion systems based on engineered nonlinear materials [3]. These systems can be used, in principle, for entangled photon pair generation, single-photon detection and as an interface between wavelengths of transmission and storage, which are essential components for quantum repeaters.

In FY 2015, we demonstrated a single-photon-pair source in which one photon in the pair is at 1310 nm (telecommunication wavelength) and the other is at 894.6 nm (matching the Cs atomic D1 line) [4]. A narrow linewidth of 28 MHz was achieved, suitable for so-

called cold atomic quantum memory based on a magneto-optic trap (MOT). In FY 2016, we demonstrated single-photon pair generation based on four wave mixing (FWM) in a silicon-based micro-toroid device also at a wavelength suitable for atomic interaction.

In FY 2015, we also demonstrated a quantum memory based on electromagnetically-induced transparency (EIT) in a warm cesium (Cs) atomic vapor cell [5]. The EIT quantum memory with Cs atomic vapor provides an inexpensive and scalable scheme for quantum repeaters. To provide higher fidelity for the quantum system, we focused our 2016 research on reducing noise for the EIT quantum memory. By combining specialized etalon and atomic filters with a high extinction ratio polarization filter, we successfully reduced the noise from a residual control beam by 125 dB, thus greatly improving the performance of the quantum memory. We have made recent research progress in quantum memories, photon pair sources and quantum interfaces.

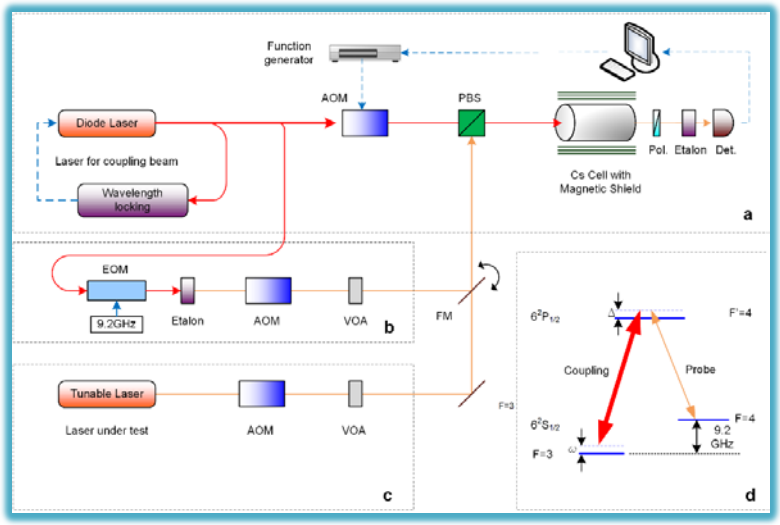

Figure 63. *Schematic diagram of the experiment setup for an EIT-based spectrometer.*

Quantum Memory. In recent years, a variety of quantum memory schemes based on different principles and working conditions have been reported worldwide. The research community in this area needs a comprehensive review to provide an overall profile and clear snapshot of state of the art in quantum memories. We were invited to write a review article [6] on quantum memory technologies by the *Journal of Optics*. The paper was listed as an "article of the week" by the journal editor when it appeared in February 2017.

In an optically controlled quantum memory, the quantum signal carried by single photons can be stored in an atomic ensemble, which needs to be controlled by strong laser beams for storage and retrieval. In this case, the residual control beams become a serious source of noise in the single photon signal band carrying the quantum information. Therefore, noise reduction is an important requirement and is a common challenge in the development of quantum memories. Many research groups, including ours, have developed novel noise reduction techniques. We were invited to write a review article on noise reduction in optically controlled quantum memory by the editor of *Modern Physics Letters B*. This paper [7] shares our experience and summarizes all reported noise reduction techniques.

Based on the previous work in FY 2016, we developed a spectral characterization method for single photon sources with an ultra-high resolution, accuracy and sensitivity based on the electromagnetically induced transparency (EIT) phenomenon. In future quantum communication systems, single photons, as the information carriers, are required to possess very narrow linewidths and accurate wavelengths for an efficient interaction with quantum memories. Spectral characterization of such single photon sources must be performed with very high spectral resolution, wavelength accuracy and detection sensitivity. In general, an atomic vapor cell is opaque to a photon if its frequency is at or near by an atomic transition line. According to the principle of EIT, when the atomic cell is illuminated by a strong laser at a frequency near the atomic transition line, the atoms in the cell will open a very narrow transparent frequency window, where a photon with the same frequency can pass through. By tuning the frequency of the pump laser, the position of the frequency window can be precisely determined. Our team has experimentally demonstrated an optical spectral resolution of better than 150 kHz, an absolute optical wavelength accuracy of within 50 kHz and an exceptional detection sensitivity suitable for optical signals as weak as -117 dBm. Figure 63 shows the experiment setup for spectral characterization of single photons with ultra-high resolution, accuracy and sensitivity. The related results were recently published in *Optics Express* [8].

The storage time for a quantum memory based on a warm atomic vapor cell is mainly limited by collisions among atoms and between atoms and the inner wall of the cell, since these collisions destroy the coherence of the atomic energy level where the quantum information is stored. In FY 2017, we designed a new atomic cell and coated the inner wall of the cell with a chemical called Alpha Olefin. Based on existing knowledge, the coherence time of such a system can be extended even if the collisions between atoms and the inner wall of the cell occur. We will test this new type of quantum memory in

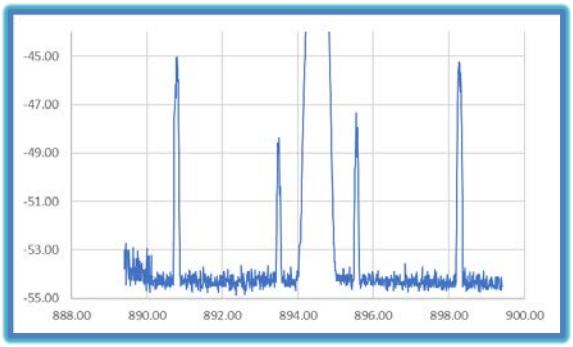

Figure 64. *The measured Four Wave Mixing signal from the micro resonator made of calcium fluoride. Y-axis: Intensity (dBm), X-axis: Wavelength (nm).*

FY 2018, and we expect that the storage time could be extended by two orders of magnitude in the best case.

In F Y2016, we started to build a magneto-optic trap (MOT) for Cesium (Cs) atoms. In FY2017, our team continuously worked on the MOT, and now Cs atoms can be trapped in a small volume at millikelvin temperature. In FY 2018, we will improve its performance by upgrading it to a 2D MOT for a higher quantum memory efficiency. The MOT will be ready for more quantum memory experiments in FY 2018.

Photon Pair Source. In the previously developed photon pair source, a narrow linewidth of 28 MHz was achieved. This linewidth is suitable for quantum memories based on cold atoms in a MOT. For a quantum memory based on warm atoms in a cell, a linewidth of just a few MHz is more desirable. The linewidth is determined by quality factor (Q value) of the cavity or resonator used. The higher the Q value, the narrower the linewidth will be. To generate photon pairs with a narrower linewidth, we used a commercial micro-resonator made of calcium fluoride. The Q value of this device is two orders of magnitude higher than that of the silicon based micro-toroid. However, the unpackaged micro-resonator is very fragile and requires near clean room conditions to avoid dust contamination. To overcome this challenge, in FY 2016-2017, we spent a lot of effort to renovate the laboratory for an improved experimental environment. In 2017, we started work with a commercially packaged micro-resonator made of calcium fluoride with an extremely high Q value (as high as 109), which should be able to generate signals based on four-wave mixing (FWM) with a linewidth of sub-megahertz. Figure 64 shows our initial results. The shown linewidth was broadened by the measuring instrument. The actual linewidth is so narrow that we do not have suitable tools in the lab to characterize it at present. But we will find a way to measure it in the future. We are now working to achieve single photon level signals from this source.

Quantum Interface. Photon pairs generated via FWM are spectrally nearly degenerate, meaning that both photon's wavelengths are close to the atomic transition (near 895 nm) we are targeting. In this case, a quantum interface is needed to convert the wavelength of one of the photons in the pair to the telecommunication wavelength band for long distance transmission in an optical fiber. We have been working on this for many years, and have developed single-photon frequency conversion technology and applications [2]. Some techniques have been adopted for potential commercialization through the SBIR programs of NIST and DARPA. In 2017, we worked with a company (HC Photonics) to jointly design a new quantum interface unit. The unit should be able to convert the wavelength of single photons from near 895 nm to the telecommunication wavelengths near 1550 nm by using a powerful pump laser at 2118 nm. The pump laser is ready to use and new interface unit will be shipped to NIST soon. The quantum interface experiment is now in preparation.

Future research. The implementation of a quantum repeater is a very challenging research project. So far, there is no quantum repeater existing in the world. So far, we have completed a very small part of the research and development on the path to a quantum repeater. In FY 2018, we will continue the efforts in three aspects:

(a) Further development and improvement of the essential elements necessary for practical quantum repeaters including quantum memories, narrow linewidth photon sources and quantum interfaces.

(b) Conversion of the single photon wavelength from the memory wavelength (near 895 nm) to the telecom wavelength (near 1550 nm) for long distance transmission.

(c) Possible integration of quantum memory with a single photon source and /or with a quantum interface.

[1] Advancing Quantum Information Science: National Challenges and Opportunities, A Joint Report of The Committee on Science and Committee on Homeland and National Security of the National Science and Technology Council, July 2016. URL: https://obamawhitehouse.achives.gov/sites/whitehouse.gov/files/images/Quantum_Info_Sci_Report_2016_07_22%20final.pdf

[2] L. Ma, A. Mink and X. Tang. High Speed Quantum Key Distribution Over Optical Fiber Network System. *Journal of Research of the National Institute of Standards and Technology*, **114**:3 (2009), 149.

[3] L. Ma, O. Slattery and X. Tang. Single Photon Frequency Up-Conversion and its Applications. *Physics Reports* **521**:2 (2012), 69-94.

[4] O. Slattery, L. Ma, P. Kuo and X. Tang. Narrow-linewidth Source of Greatly Non-Degenerate Photon Pairs for Quantum Repeaters from a Short Singly Resonant Cavity. *Applied Physics B* **121** (2015), 413-419.

[5] L. Ma, O. Slattery, P. Kuo and X. Tang. EIT Quantum Memory with Cs Atomic Vapor for Quantum Communication. *Proceedings of the SPIE* **9615** (2015), 96150D–1.

[6] L. Ma, O. Slattery, and X. Tang. Optical Quantum Memory Based on Electromagnetically Induced Transparency. *Journal of Optics* **19** (2017), 043001.

[7] L. Ma, Oliver Slattery and Xiao Tang. Noise Reduction in Optically Controlled Quantum Memory *Modern Physics Letters B*, to appear.

[8] L. Ma, O. Slattery and X. Tang. Spectral Characterization of Single Photon Sources with Ultra-High Resolution, Accuracy and Sensitivity. *Optics Express* 25:23 (2017), 28898.

Quantum Interfaces for Hybrid Quantum Networks

Paulina Kuo
Thomas Gerrits (NIST PML)
Varun Verma (NIST PML)
Sae Woo Nam (NIST PML)
Carsten Langrock (Stanford University)
Martin Fejer (Stanford University)

Future quantum networks will consist of a heterogeneous mix of qubit technologies, from superconducting qubits to trapped ion qubits to qubits based on quantum dots, nitrogen-vacancy centers or atomic ensembles. These different qubits operate at different wavelengths, which will require quantum interfaces for interconnectivity and transport. This work focuses on developing interfaces that preserve quantum information and convert a qubit at one optical wavelength to another wavelength. This conversion can be accomplished by (1) using quantum frequency conversion or (2) distributing entanglement using entangled photon pairs.

In FY 2017, we developed new tools to evaluate the quality of entangled photon pairs [1]. In a collaboration with researchers in the NIST PML, we characterized our entangled-photon-pair source using fiber-assisted single-photon spectroscopy. We also investigated indistinguishability in this source by studying how it can be erased and restored by rotating the polarizations of the photons. We performed spectrally resolved measurements near the so-called "Hong-Ou-Mandel dip" and observed an interference signature when the entangled photon source had indistinguishability. We presented this work at a conference in 2017 [2].

We also continued development of tools for quantum frequency conversion (QFC). Our QFC is performed using highly efficient periodically poled $LiNbO_3$ (PPLN) waveguides, which are fabricated by our collaborators at Stanford University. Our long-term goal is to demonstrate QFC between a telecommunications band photon (at 1550 nm wavelength) and a ≈850 nm photon. This conversion is mediated by a pump near 1900 nm. The 1550 nm wavelength is interesting because ultra-low-loss optical fibers operate at this wavelength, while the 850 nm range photons are interesting because the Cesium D2 line at 852 nm may be used for quantum memory and 854 nm photons interact with transitions in trapped Calcium ion qubits.

[1] P. S. Kuo, T. Gerrits, V. B. Verma and S. W. Nam. Spectral Correlation and Interference in Non-Degenerate Photon Pairs at Telecom Wavelengths. *Optics Letters* **41** (2016), 5074-5077.

[2] P. S. Kuo, T. Gerrits, V. Verma and S. W. Nam, "Spectral Correlation and Interference in Continuous-wave Non-Degenerate Photon Pairs at Telecom Wavelengths," SPIE Photonics West, San Francisco, CA, February 1, 2017.

Quantum Key Distribution Standards

Alan Mink
Thomas Chapuran (Applied Communication Sciences)

Quantum key distribution (QKD) is a unique security primitive that builds on quantum physics, telecommunications and information theory [1]. It employs a multi-stage protocol over an insecure quantum channel and a public authenticated and an integrity-protected classical channel to generate information theoretically secure cryptographic key between two parties, even in the presence of an unconstrained eavesdropper. QKD contrasts with current techniques, based on public key cryptography, which derive their security from believed computational complexity. The dynamically measured quantum bit error rate (QBER) bounds the information attainable over the quantum channel by an eavesdropper, even though the errors are normally caused by the non-ideal behavior of system devices.

A number of demonstration and testbed systems were implemented in the early 21st century, but none of these systems could be proven secure because existing security proofs relied on a generic theoretically perfect design and not the actual design using real non-ideal devices. In addition, most side channels are not part of the security proof and some were unknown at that time.

Following this implementation effort, a world-wide endeavor to develop standards for QKD systems was formed through the European Telecommunication Standards Institute (ETSI) QKD Industry Specification Group (ISG) [2, 3]. Its focus is to combine QKD security analysis with details of practical implementations to develop standards that could be used by companies developing QKD products. The ultimate goal is to develop a certification framework that bridges the gap between theoretical security proofs and practical implementations with imperfect devices. In some cases, this

has stimulated further theoretical research, in order to make the theoretical assumptions easier to meet in practice. In other cases, it consists of defining the best engineering practice to approach existing theoretical assumptions. This framework is considered a "forward looking standard". Most standards are based on a few existing methods already in commercial use. Forward looking standards anticipate the emerging technology and attempt to provide the needed operational guidance, testing methods and verification to help advance new technology to broad commercial adoption.

Standardization is fundamental to promoting broad commercialization of QKD by building trust and consistency leading to certification. The standardization process also highlights areas of QKD research needed to support the development of standards. Well-established standards would be beneficial both to potential QKD users, as it provides definition to what they might consider buying, and to QKD vendors, as it provides a framework for requirements and how to specify them.

NIST has partnered with Applied Communication Sciences (formerly Telcordia Technologies), an ETSI member, to participate in the ETSI ISG QKD effort. The group has focused on the security of the quantum channel, since that is the only channel where secret information is developed. (No secret information is communicated over the classical channel.) The group realized that a vital missing element was the metrics necessary to characterize quantum devices. As a result, an effort was initiated with group members from the UK National Physics Laboratories (NPL) and the National Institute for Metrological Research (INRIM) of Italy to develop the necessary metrology for needed characteristics. [4] This quantum device characterization was not just significant for QKD but for all quantum science.

A QKD certification framework requires a security proof and countermeasures for side channel attacks. A security proof for a generic theoretical system is a difficult task. Development of such proofs continue to be more robust with relaxation of the underlying assumptions. But a security proof that applies to practical systems and their imperfections is significantly more difficult. Some proofs may require numerical solutions, rather than analytic, and application of engineering best practices. Theoreticians from this group have been pursuing these avenues and are making some headway.

Side channel attacks are an additional consideration and are normally thought of being addressed separately. After significant study of some side channels on a real QKD system, this group is developing a QKD side channel analysis framework. Such a framework includes listing all known side channel attacks, identifying the source of the information leakage, and eliminating it through re-engineering/re-design when possible. Otherwise, one must determine the source of the leakage and how to measure the amount of leakage, establish a limit on the leakage, develop means to mitigate that leakage, and determine if additional privacy amplification can compensate on what remains. But, in some cases, the countermeasure may affect the quantum channel and in those cases the security proof must be revised. For side channel attacks that are not currently feasible, partial or no countermeasures may be acceptable.

In summary, a QKD certification framework is being developed by this ETSI QKD group through theory, analysis, measurement, and experimentation. A massive QKD development project in China, covering 2000+ km, encompassing more than 60 nodes using trusted node networking and a satellite link, has revived interest in QKD. But to date, commercialization of QKD has suffered from scalability (networking is limited to multi-hops over trusted nodes), distance limitations (quantum signals can't be amplified) and the lack of a certification process.

[1] N. Gisin, G. Ribordy, W. Tittel and H. Zbinden. Quantum Cryptography. *Reviews of Modern Physics* **74** (2002), 145.

[2] T. Langer and G. Lenhart. Standardization of Quantum Key Distribution and the ETSI Standardization Initiative ISG-QKD. *New Journal of Physics* **11** (2009), 055051. URL: http://www.etsi.org/technologies-clusters/technologies/quantum-key-distribution

[3] R. Alléaume, T. Chapuran, C. Chunnilall, I. Degiovanni, N. Lutkenhaus, V. Martin, A. Mink, M. Peev, M. Lucamarini, M. Ward and A. Shields. Worldwide Standardization Activity for Quantum Key Distribution. In *Proceedings of the IEEE GlobeCom Workshop on Telecom Standards – From Research to Standards*, December 8, 2014, 741-746.

[4] ETSI GS QKD 011. Quantum Key Distribution (QKD); Component Characterization: Characterizing Optical Components for QKD Systems. V1.1.1, May (2016). URL:http://www.etsi.org/deliver/etsi_gs/QKD/001_099/011/01.01.01_60/gs_QKD011v010101p.pdf

Joint Center for Quantum Information and Computer Science

Stephen Jordan
Yi-Kai Liu
Jacob Taylor (NIST PML)
Carl Williams (NIST PML)
Andrew Childs (University of Maryland)

http://quics.umd.edu/

Established in October 2014, the Joint Center for Quantum Information and Computer Science (QuICS) is a cooperative venture of NIST and the University of Maryland (UMD) to promote basic research in understanding how quantum systems can be effectively used to store, transport and process information. QuICS brings together researchers from the University of Maryland Institute for Advanced Computer Studies

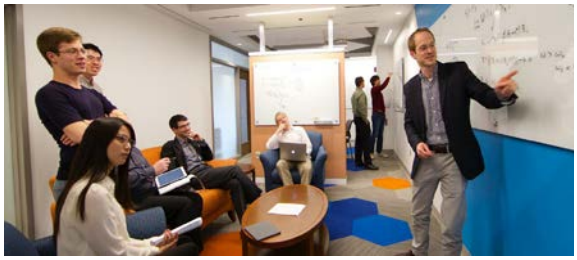

Figure 65. *Co-Director Andrew Childs in a technical discussion with QuICS fellows, postdocs and students in the QuICS offices at the University of Maryland.*

(UMIACS) and the UMD Departments of Physics and Computer Science with NIST's Information Technology and Physical Measurement Laboratories, together with postdocs, students and a host of visiting scientists.

QuICS has quickly established itself as a premier center for research in quantum information science. Fifteen Fellows, 11 postdocs and 22 students are currently associated with the center. In CY 2017 a total of 88 research papers were produced by those associated with the center. Some 70 seminars were held through the year, many by visiting researchers. Stephen Jordan and Yi-Kai Liu of ACMD serve as QuICS Fellows, holding research appointments at the University.

In FY 2017 QuICS hosted two major events. On July 31 – August 2, the Workshop on Computational Complexity and High Energy Physics was held; Stephen Jordan was the main organizer. The 4th International Conference on Quantum Error Correction was held in College Park, MD on September 11-15.

Machine Learning Approach to Quantum Dot Experiments

Sandesh S. Kalantre (University of Maryland)
Justyna P. Zwolak (University of Maryland)
Stephen Ragole (University of Maryland)
Xingyao Wu (University of Maryland)
Neil M. Zimmerman (NIST PML)
M. D. Stewart, Jr. (NIST PML)
Jacob M. Taylor (NIST PML)

There is a myriad of quantum computing approaches, each having its own set of challenges to understand and effectively control their operation. Electrons confined in arrays of nanostructures, called quantum dots, is one such approach. Quantum dots are defined by electrostatically confining electrons in a two-dimensional electron gas present at the interface of semiconductor heterostructures [1]. For semiconductor-based methods, realization of good qubit performance is achieved via electrostatic confinement, band-gap engineering, and dynamically adjusted voltages on nearby electrical gates (see Figure 66(a) for a generic model of quantum dots in a nanowire). Current experiments set the input voltages heuristically in order to reach a stable few electron configuration. With growing array sizes, however, it is desirable to have an automated protocol to achieve a target electronic state.

In recent years, machine learning (ML) has emerged as a "go-to" technique for automated classification, giving reliable output when trained on a representative, comprehensive data set [2]. This suggest that such techniques may be used to assist the experimental effort, replacing the gross-scale heuristics developed by experimentalists. In our work, we take this data classification approach to determine the dot configuration. Artificial neural networks (ANNs), and, in particular convolutional neural networks (CNNs), turned out to be especially suitable for this task. ANNs — a ML approach inspired by analogous biological units — were originally intended to mimic the workings of the human brain. They are composed of "artificial neurons" organized in multiple fully-connected layers—thus the term "deep neural networks"—with each layer performing a specific transformation of the data. In CNN architecture, a set of convolutional and pooling layers precedes the series of hidden layers. To learn larger scale features in the input more efficiently, each convolutional layer is generally followed by a pooling layer, which takes a sub-region in the input and replaces it by an effective element (e.g., the maximum element) in that region.

We use tools from machine learning to develop good heuristics for the gate voltages from a training set and to design an effective and efficient neural network for the characterization of experimental data in semiconductor quantum dot experiments. The three main steps in our workflow were as follows:

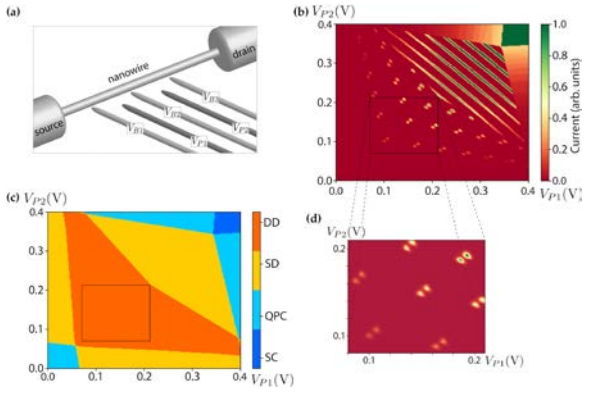

Figure 66. *(a) A generic model of a nanowire with 5 gates. The barrier voltages are set to V_{B1} = V_{B2} = V_{B3} = -200 mV. For plungers, voltages varied between 0mV and 400 mV. (b) An example of full 2D map (100×100 points) from the space of plunger gate voltages (V_{P1}, V_{P2}) to current. (c) A state map corresponding to the current map presented in (b). (d) A sample sub-region with double dot configuration.*

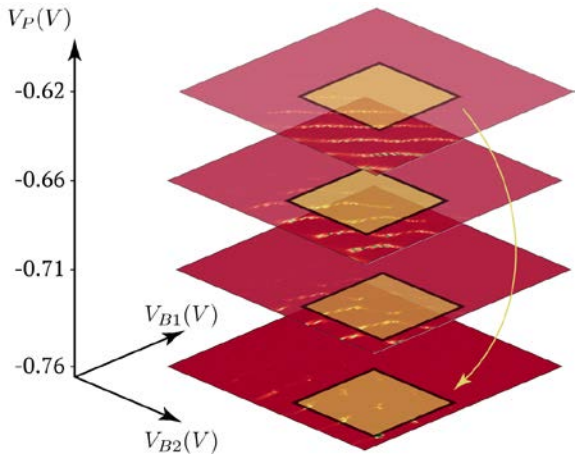

Figure 67. *The idea behind auto-tuning in the three-dimensional space of two barrier and plunger gate voltages. The successive squares represent the sub-regions encountered in the tuning process which are fed as input to the CNN. The arrow represents the direction of movement in going from an initial region to a final region.*

Step 1: Establishing reliable training and evaluation data sets, based on simulated data. We used a modified Thomas-Fermi approximation to model a reference semiconductor system comprising of a quasi-1D nanowire with a series of depletion gates whose voltages determine the number of islands and the charges on each of those islands, as well as the conductance through the wire. We generated 1000 gate configurations averaging over different possible realizations of the same type of quasi-1D device. Each sample data was stored as a 100×100-pixel map from plunger voltages to current (see Figure 66(b)) and a state map (see Figure 66(c)). The training and evaluation set was then generated by taking 25 random 30×30 pixels sub-images of each map to go from 1000 realizations to 25000 effective realizations (see Figure 66(d)).

Step 2: Training of the CNNs to "recognize" the electronic state within quantum dot arrays. The labels for each subregion were assigned based on the current data and state map data. We found > 95 % agreement between the CNN characterization and the Thomas-Fermi model predictions for nanowires. Having the network trained, we tested it on the experimental data and found that it correctly identifies single and double dot state configurations, as well as the intermediate cases.

Step 3: Auto-tuning of the multidimensional gate voltage space to obtain a required configuration. By formulating auto-tuning as an optimization problem over the nanowire state in the space of gate voltages, i.e., optimizing the parameter space to achieve a desired configuration of the array, we exhibit automated tuning of single and double quantum dot devices to a given state for both, simulated and experimental data (see Figure 67).

Results of this work are detailed in a paper that has been submitted for publication [3]. Future directions for this project include extending the machine learning methodology to charge sensor data as well as to multiple dot devices [4].

[1] R. Hanson, L. P. Kouwenhoven, J. R. Petta, S. Tarucha and L. M. K. Vandersypen. Spins in Few-electron Quantum Dots. *Reviews of Modern Physics* **79**:4 (2007), 1217-1265.

[2] A. Krizhevsky, I. Sutskever and G. E. Hinton. Imagenet Classification with Deep Convolutional Neural Networks. In *Advances in Neural Information Processing Systems* **25** (F. Pereira, C. J. C. Burges, L. Bottou and K. Q. Weinberger, eds.), Curran Associates, Inc., 2012, 1097-1105.

[3] S. S. Kalantre, J. P. Zwolak, S. Ragole, X. Wu, N. M. Zimmerman, Jr., M. D. Stewart and J. M. Taylor. Machine Learning Techniques for State Recognition and Auto-tuning in Quantum Dots. arXiv:1712.04914, 2018.

[4] D. M. Zajac, T. M. Hazard, X. Mi, E. Nielsen and J. R. Petta. Scalable Gate Architecture for a One-dimensional Array of Semiconductor Spin Qubits. *Physical Review Applied* **6** (2016), 054013.

Foundations of Measurement Science for Information Systems

Modern information systems are astounding in their complexity. Software applications are built from thousands of interacting components. Computer networks interconnect millions of independently operating nodes. Large-scale networked applications provide the basis for services of national scope, such as financial transactions and power distribution. Despite our increasing reliance on such systems, our ability to build far outpaces our ability to ensure security and reliability. Protocols controlling individual nodes can lead to unexpected macroscopic system behavior. Local power anomalies propagate in unexpected ways leading to large-scale outages. Computer system vulnerabilities are exploited in viral attacks resulting in widespread loss of data and system availability. The actual resilience of our critical infrastructure is largely unknown. Measurement science has long provided a basis for the understanding and control of physical systems. Such deep understanding and insight is lacking for complex information systems. We seek to develop the mathematical foundations for a measurement science for complex networked information systems.

Deep Learning and Neuromorphic Computing

Yi-Kai Liu
Alan Mink (Theiss Research)
Oleg Aulov (NIST ITL)
Vincent Stanford (NIST ITL)

In recent years there has been dramatic progress in machine learning, particularly "deep learning," where deep neural networks have been shown to achieve or sometimes exceed human-level accuracy on a range of tasks in handwriting recognition, image classification, and other domains. One drawback of these methods is that training each network requires extremely large data sets and a computationally expensive optimization process.

This has motivated many researchers to investigate alternative hardware architectures that might achieve better performance on deep learning tasks. These alternative architectures include graphics processing units (GPUs), many-integrated-core (MIC) processors, field-programmable gate arrays (FPGAs), and neuromorphic processors based on spiking neural networks. This research is gaining in importance, as it is becoming more difficult to extract higher performance from today's underlying silicon semiconductor technology, often referred to as the "end of Moore's Law."

In collaboration with colleagues in the ITL Information Access Division, ACMD researchers are investigating several questions in this area. In the following, we report on the work being done in ACMD, which focuses on FPGAs and spiking neural networks.

We acquired a state-of-the-art Xilinx FPGA accelerator chip, and worked with the vendor to overcome several bugs and deployment issues. We then implemented a simple neural network for recognizing handwritten digits on the FPGA. This neural network was trained on a conventional computer, using the well-known MNIST data set. The network was then deployed on the FPGA to perform classification of unknown handwritten digits.

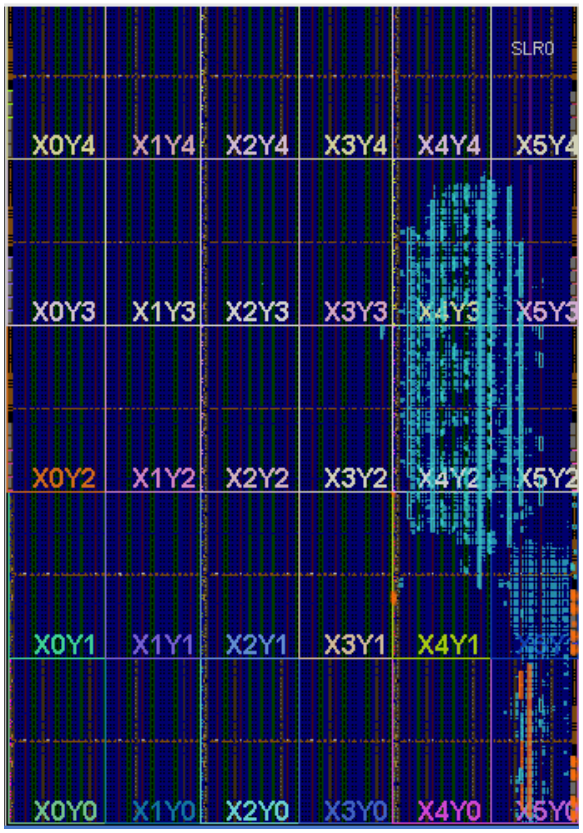

Figure 68. *Layout of a small neural network on an FPGA. The network consists of 784 input connections, a hidden layer with 100 neurons, and an output layer with 10 neurons. The layout of the neural network on the FPGA is constrained by the number of logic elements available in each region of the chip, and by the capacity of the interconnections between the different regions. Overall, the neural network uses fewer than 10% of the logic elements on the chip. This diagram only shows the lower half of the chip; the upper half is not being used.*

Our initial investigation of the FPGA platform showed limited promise for capacity and computational

robustness, but a strong result for speed and accuracy. Current FPGAs have a moderate amount of resources that can be applied to computational models, but those resources have a wide range of potential parallelism. We were easily able to implement a deployable neural network with over 100 neurons, which processed the MNIST data set with the same accuracy as a similar model running on a CPU. The FPGA implementation was 10 times faster than the CPU implementation.

However, any FPGA implementation would be limited to a few thousand hardware neurons, and the associated model would need to be mapped to fixed point arithmetic, preferably integers, rather than the more common floating-point arithmetic, in order to optimize resources. Also, an implementation that included the training procedure, to determine the necessary weights and other parameters, would require a good deal more hardware resources on the FPGA.

We are now investigating spiking neural networks, which can be implemented using low-power analog circuits. We are experimenting with spiking neural networks that are first trained and optimized on a CPU or GPU, and then deployed on an FPGA, using state-of-the-art commercial software for high-level synthesis of FPGA designs. This work is motivated by emerging applications that require low-power machine learning, such as computer vision on mobile robots.

In addition, we are investigating recently developed mathematical tools, such as the "Semantic Pointer Architecture" and "Neural Engineering Framework" (from Chris Eliasmith's group at the University of Waterloo). These tools can be used to design a spiking neural network that can approximate a given functionality. These techniques will be useful for programming future neuromorphic computers, such as IBM's TrueNorth, and next-generation neuromorphic devices based on silicon memristors and superconducting optoelectronics, which are currently being developed at NIST. In the long term, these techniques will also be useful for tackling fundamental research problems in machine learning, such as the development of "explainable AI."

A New Metric for Externalities in Interdependent Security – A Case Study of Cybersecurity

Richard J. La (University of Maryland)

Understanding the security of large, complex systems with many interdependent components has emerged as one of key challenges that information system engineers face today. Examining the system-level security of complex networks or systems is hindered by the fact that security measures adopted by various agents or organizations or lack thereof produce either positive or negative externalities as well as what is known as "network externalities" on others, leading to so-called interdependent security (IDS).

Many, if not most, of existing studies on IDS fail to consider the fact that agents can adapt and employ security measures that are best suited for their needs. Instead, our efforts aimed at examining the scenarios where the agents are strategic entities that are only interested in optimizing their own objectives. The goal of this project is two-fold: (a) to understand how the underlying network properties affect the security choices made by strategic agents and, in the process, influence the ensuing network-level security, and (b) to improve system-level security via internalization of externalities, where the externalities produced by an agent are the costs it imposes on other agents in the system. Internalizing externalities requires that the policy makers alter the private costs of agents to reflect their "true" costs to the system, including any externalities they cause to other agents in the system. The first necessary step to realizing this is to correctly estimate the externalities produced by agents in various systems.

In the first part of the project, we studied how the underlying network properties influence security choices, in particular, investments in security measures and insurance. It is well documented that many natural and engineered networks exhibit non-negligible correlations in the degrees of end nodes. Furthermore, these degree correlations (also known as networking mixing or assortativity) have significant impact on network security and the effectiveness of botnet takedown strategies. We investigated how such degree correlations observed in real networks affect network-level security with strategic agents.

There are two key findings from our study: (i) When agents with larger degrees see higher risks (per neighbor) than those with smaller degrees, the overall network-level security degrades in that the total number of attacks or infections that spread through the network (from infected agents to their neighbors) rises; and (ii) somewhat surprisingly, the overall effects of degree correlations on network security depend very much on the (cost) effectiveness of security measures available to agents; when the security measures are ineffective in protecting the agents against attacks, increasing degree correlations (resp. decreasing degree correlations) leads to deteriorating network security (resp. improving network security). On the other hand, when the security measures are effective, degree correlations have the opposite effects. In other words, as a network becomes more assortative (resp. disassortative), network security improves (resp. degrades) instead.

In the second part, we investigated the important problem of estimating the externalities produced by agents in IDS, without requiring the topological information of the underlying network, which is hard to

obtain in practice. While computing the externalities exactly in real networks is difficult, if possible at all, even with topological information, our study suggested that it is possible to approximate the true costs of each agent to the overall system. To be more precise, we demonstrated that any local minimizer of the overall social cost (i.e., the aggregate cost of all agents) can be obtained as a (Nash) equilibrium of a population game for which we alter the costs of agents based on the average number of attacks they suffer from neighbors. Based on this observation, we first showed that the selfish nature of strategic agents indeed leads to under-investments in security and degraded network-level security measured by the average or total number of attacks suffered by the agents. More importantly, we proved under a mild condition that there exists a unique minimizer of the social cost, which coincides with the unique (Nash) equilibrium of the population game. This finding suggests that we can view the difference between the agents' costs in the population game and their private costs as the externalities they impose on the others.

[1] R.J. La. Interdependent Security with Strategic Agents and Global Cascades. *IEEE/ACM Transactions on Networking* **24**:3 (June 2016), 1378-1391.

[2] R.J. La. Effects of Degree Correlations in Interdependent Security: Good or Bad? *IEEE/ACM Transactions on Networking* **25**:4 (August 2017), 2484-2497.

[3] R.J. La. Influence of Network Mixing on Interdependent Security: Local Analysis. in *Proceedings of IEEE Globecom*, Washington D.C., December 2016.

[4] R.J. La. Estimation of Externalities in Interdependent Security: A Case Study of Large Systems. in *Proceedings of IEEE Conference on Decision and Control*, Melbourne, Australia, December 2017.

A New Metric for Robustness of Complex Systems - Effects of Dependence Structure

Richard J. La (University of Maryland)

Many critical systems (e.g., smart grids, manufacturing systems, transportation systems) comprise multiple heterogeneous systems whose agents depend on other agents belonging to different component systems (CSes). For instance, a modern power system not only includes an electrical grid/network, but also relies on an information and communication network (ICN) to monitor the state of the electrical network and to take appropriate actions based on the observed state.

Intricate interdependence among agents in CSes makes the analysis of these complex systems difficult. Moreover, in many cases, a local failure of a small number of agents in one CS can cause unexpected widespread failures of many agents in multiple CSes. In the previous example of a modern power system, a failure in the ICN can hamper the collection of crucial sensor measurements regarding the state of the electrical network (e.g., phase or voltage measurements) in a timely manner. This failure to gather critical information can in turn lead to an outage in parts of the electrical network or even a large-scale blackout, affecting millions of people (e.g., Northeast blackout of 2003 and India blackouts of 2012).

With increasing reliance of modern societies on such complex yet fragile systems for critical services and greater interdependence among CSes, there is a growing interest in modeling and understanding the interaction between CSes and the robustness of the overall systems. The goal of this project is three-fold: (i) develop a new sound model for capturing the interdependence among CSes; (ii) investigate the likelihood of suffering widespread failures in large complex systems; and (iii) identify more vulnerable agents and CSes that will serve as the "weak" links in critical systems. The expected outcomes will help researchers and engineers to better understand the fragility/robustness of critical systems and develop a new guideline for improving their resilience against attacks and failures.

To achieve these goals, borrowing advanced tools from random graphs and multi-type branching process theory, we first developed a novel model that allows us to estimate the likelihood that a large system will experience widespread failures, beginning with local failures in different CSes. We call this the Probability of Cascading Failures (PoCF). Because the PoCF depends on the CS in which the initial failure originates, it helps us identify the CSes that are more vulnerable in that localized failures in these CSes are more likely to result in widespread failures throughout the entire system spanning multiple CSes. Using the new model, we investigated how the underlying structure of interdependence among the agents in the CSes affects the PoCF.

Some of our key findings are: (i) The higher variability of interdependence among the agents leads to smaller PoCF and, hence, more robust systems; (ii) Positive correlations in the interdependence of agents across different CSes lower the PoCF and improve the resilience of the system; (iii) There is an intriguing relationship between the clustering (also known as transitivity) exhibited by real networks and the PoCF. But, in the critical regime where a large system can suffer widespread failures, clustering tends to help keep failures localized in a small neighborhood, thus diminishing the PoCF in large systems; and (iv) The higher variability of interdependence among the agents lessens the influence of clustering on PoCF. As a result, scale-free networks with power law degree distributions enjoy less

positive benefits of clustering (which tends to keep failures contained in a small neighborhood).

Our study illustrates the complexity of how the interdependence structure among the agents affects the robustness of large complex systems. Furthermore, some of our findings are surprising in view of a common belief that more widespread degree distributions, such as power laws in scale-free networks, which allow the existence of large-degree hubs in the systems, are good for disseminating failures, information or rumors. They instead suggest that more concentrated degree distributions, such as Poisson distributions, are in fact more conducive to disseminating failures or information in complex systems, starting with randomly chosen nodes.

[1] R.J. La. Cascading Failures in Interdependent Systems: Impact of Degree Variability and Dependence. *IEEE Transactions on Network Science and Engineering*, in press. DOI 10.1109/TNSE.2017.2738843

[2] R.J. La. Effects of Degree Variability and Dependence on Cascading Failures: A Case Study of Two Interdependent Systems. In *Proceedings of Conference on Information Sciences and Systems*, Baltimore, MD, March 2017.

[3] R.J. La. Influence of Clustering on Cascading Failures in Interdependent Systems, in review.

Toward Resilient yet Economically Viable Networked Infrastructures

Vladimir Marbukh

DHS's 2013 National Infrastructure Protection Plan [1] defined resilience as

> *The ability to prepare for and adapt to changing conditions and withstand and recover rapidly from disruptions; includes the ability to withstand and recover from deliberate attacks, accidents, or naturally occurring threats or incidents.*

While for military systems, resilience is the primary requirement, large-scale and especially nationwide critical infrastructures, such as power grid, communication networks, computing clouds, etc., must combine resilience with economic viability. Managing the resilience vs. economic viability tradeoff involves (a) keeping the system on the corresponding Pareto frontier, and (b) the ability to adjust the system operating point on the Pareto frontier according to the current exogenous risks due to either adverse natural events or malicious actions.

Project goals. While economics incentivizes the current trend for interconnectivity, recent numerous systemic failures in various critical networked infrastructures have demonstrated the risks of interconnectivity due to enabling undesirable contagion. The goal of this project is to propose and justify quantitative metrics for the resilience and economic viability for a wide range of networked infrastructures to be used for optimization of the corresponding tradeoffs.

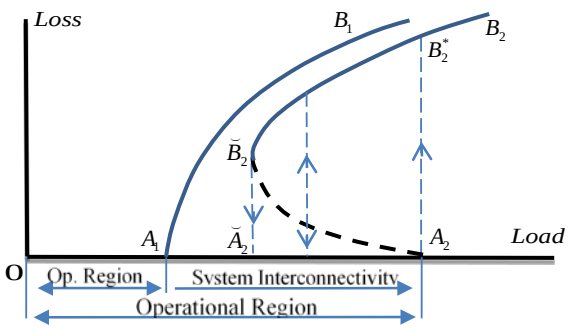

Figure 69. *Interconnectivity vs. size of operational region vs. systemic instability.*

The Scientific Approach. Our approach, which is based on Perron-Frobenius (P-F) theory, assumes that undesirable contagion in the networked infrastructure has self-reinforcing dynamics, which is described by a non-negative evolutionary operator. This assumption holds for a wide range of contagion phenomena, including systemic overload. P-F theory allows us to define the point of systemic instability in terms of the P-F eigenvalue of the linearized evolutionary operator, and describe the emergence of the systemic contagion in one-dimensional space associated with the corresponding P-F eigenvector.

Main findings [2-4]. We propose a quantitative metric for the resilience vs. economic viability tradeoff in networked infrastructures. The economic benefits of interconnectivity are quantified by the system operational region with respect to all possible combinations of exogenous demand and system resources which can sustain this demand. Interconnectivity, which enables dynamic resource sharing, increases the system operational region by allowing for the exogenous load to be shifted from overloaded to underloaded system segments. Resilience is characterized by the type of systemic instability. System interconnectivity may induce hard/discontinuous instability associated with the existence of undesirable metastable states, and thus may negatively affect system resilience by increasing system fragility and inhibiting the system's ability to recover. Based on these metrics, we suggest a concept of systemic risk-aware networked infrastructure design, which maximizes the economic benefits of interconnectivity subject to constraining the risk of abrupt systemic instability. Figure 69 illustrates the effect of system interconnectivity on the tradeoff between size of the system operational region and systemic instability.

Future work. Future research should address the practical viability of the proposed concept of systemic risk-

aware networked infrastructure design. Our preliminary results indicate that practical implementation of this concept requires a combination of (a) anomaly detection to generate warning signals as risk of systemic instability exceeds certain threshold, and (b) controlling system interconnectivity by identifying and cutting the most likely paths of the undesirable contagion spreading.

[1] https://www.dhs.gov/publication/nipp-2013-partnering-critical-infrastructure-security-and-resilience.

[2] V. Marbukh. Fragility Risks of Low Latency Dynamic Queuing in Large-Scale Clouds: Complex Systems Perspective. In *Proceedings of the Workshop on Future of Internet Transport*, IFIP Networking Conference, Stockholm, Sweden, 2017.

[3] V. Marbukh. "Towards Classification, Evaluation, and Quantification of Systemic Risks of Dynamic Resource Sharing in Networked Systems." The International Conference on Network Science 2017 (NetSci X 2017), Tel Aviv, Israel, January 15-18, 2017.

[4] V. Marbukh. Towards Resilient Yet Economically Viable Networked Infrastructures: Quantitative Metrics and Systemic Risk-Aware Design. International Conference on Infrastructure Resilience, ETH Zurich, February 2018.

An Algebraic Formulation for the Analysis and Visualization of Network Graphs

Roldan Pozo

Characterizing the topological structure of large graphs remains an important problem in network science. While it is straightforward to visualize small networks of hundreds or a few thousands of vertices and edges using conventional graph visualization packages, attempting to render large real networks is nearly impossible. This problem is particularly true for information networks and social networks, where the graph sizes number into the millions and billions. Also, with the ever-increasing amount of data being generated and gathered from large social media sites, characterizing larger and larger networks is becoming more challenging.

Conventional algorithms for graph visualization result in a rendering of very large networks as a solid blot of color from which it is difficult to obtain meaningful information. This difficulty is strongly influenced by the sheer volume of nodes and edges which makes rendering into a reasonable image size for viewing and printing impractical. It is exacerbated by the presence of high-degree nodes (hubs) which entangle many parts of the graph with itself.

An alternate approach is to visualize important network properties, rather than the actual network itself. Such network portraits attempt to capture interesting attributes of a large graph, such as degree distribution,

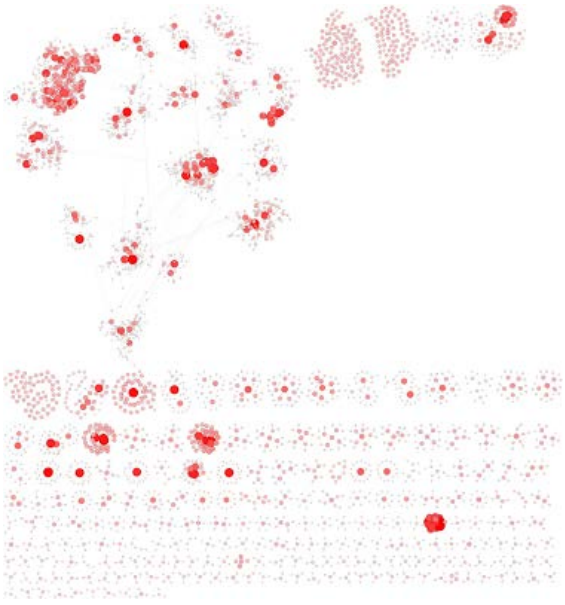

Figure 70. *Non-trivial components math.nist.gov Web graph, restricted to nodes with combined degree less than or equal to 25.*

or its connective properties. In this research area, we focus on the distribution of "fringe" communities, i.e., connected components of a graph in the absence of high-degree hubs. In a social science context, for example, they represent independent or rogue groups, highly connected amongst themselves, but which are often lost with the inclusion of more popular nodes.

Our approach, the Q-matrix of a network, in its fundamental form, is a connected component size distribution matrix for a series of degree-limited subgraphs of the original network (or weakly-connected component for directed networks.) Thus, Q(*i, j*) is the number of connected components of size *j* in a subgraph where the maximum degree is equal to or less than i. Consider, for example, a Web graph, where nodes are individual pages, and edges are directed hyperlinks between two Web pages. Figure 70, for example, illustrates connected components of the math.nist.gov Web graph, where nodes of degree greater than 25 have been removed. The result is a collection of non-trivial components of math.nist.gov Web graph, restricted to nodes with combined degree less than or equal to 25. The image reveals various structures, such as ladder, star, and cluster patterns, representing tightly coupled webpages. These form the nucleus of fringe communities of Web pages, and by varying the degree parameter we can direct the size and granularity of groups revealed.

As the degree threshold is increased from 1 to the largest degree in the original graph, we can form a connected component size distribution, which can be encoded as a row of a matrix. This sparse matrix may still be too large to view directly, but can be compactly rendered by projecting its nonzero values onto the *z*-axis

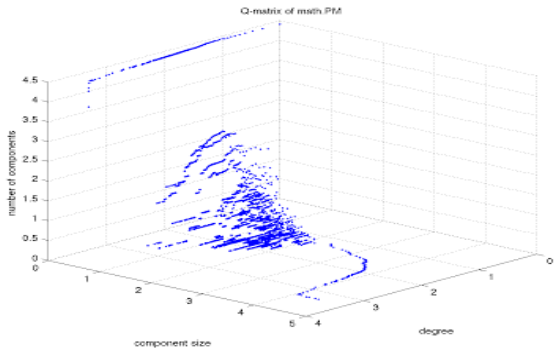

Figure 71. *Q-matrix plot of math.nist.gov webgraph (29K vertices, 62K edges) showing the componenet size distribution of degree-limited subgraphs.*

and displaying it as a three-dimensional plot, as shown in Figure 71. This Q-matrix plot of the math.nist.gov webgraph (29K vertices, 62K edges) shows the component size distribution of degree-limited subgraphs.

The Q-matrix of a graph can be considered as a generalization of its degree distribution. However, it encodes other properties, such as the formation and growth of its giant component, its connected subparts, as well as its size parameters. In fact, common network metrics (e.g., degree distribution, number of connected components, number of vertices and edges) can be extracted from the Q-matrix using simple linear algebra operations.

Among the interesting characteristics of the Q-matrix formulation is that network graphs from similar application areas (e.g., social networks, email networks, Web graphs, peer-to-peer networks, road networks, citation graphs) share similar visual characteristics, creating a potential framework for network identification and classification. Indeed, we have used the Q-matrix formulation to generate meaningful thumbnail images for network data collections. The computation of the Q-matrix is relatively efficient; graphs with millions of vertices and edges can be processed in less than one minute.

We have extended this framework by developing a measure that compares Q-matrices of networks in varying sizes and scale. This measure is critical in developing the theory, because it allows one to compare vastly different networks and provides a numerical similarity between them, while establishing a taxonomy based on these characteristics. We have also provided an extended measure formulated on second and third-generation degree distributions, which provides a refined fingerprint of network graphs. To each vertex we assign not just its degree (d), but the average degree of all its neighbors (d_1), average degree of all its neighbor's neighbors (d_2), and so on. This refined fingerprint of network graphs replaces a single vertex value with a finite vector (d, d_1, d_2, ..., d_k). Such vectors can be arranged in lexicographical order along one dimension, creating a much richer profile than the conventional degree distribution.

The Q-matrix decomposition is being used to aid the study of communication and information spreading through graph topologies. (See joint project summary below.) Identifying critical nodes in the network structure is an important, but computationally expensive problem. New multi-stage heuristics have been developed to compute these in large graphs with millions of elements, but this class of algorithms require cut-off parameters for hub and central nodes to limit the evaluation of candidate vertices. The Q-matrix decomposition finds natural fracture points in the graph, which help identify nodes as effective information spreaders.

[1] R. Pozo. Q-matrix: An Algebraic Formulation for the Analysis and Visual Characterization of Network Graphs. *Journal of Research of NIST* **121**:1 (2016), 16 pages.

Algorithms for Identifying Important Network Nodes for Communication and Spread

Fern Y. Hunt
Roldan Pozo

The identification of nodes in a network that will enable the fastest spread of information is an important if not fundamental problem in network control and design. It is applicable to the optimal placement of sensors, the design of secure networks and the problem of control when network resources are limited. Our approach to this problem has its origins in models of opinion dynamics and the spread of innovation in social networks. The mode of communication between nodes is described by simple models of random or deterministic propagation of information from a node to its neighbors.

During the past few years, we have made progress in understanding the structural requirements for sets of nodes for effective spread in networks and have developed scalable algorithms for constructing these sets in real world networks. Following Borkar et al. [1], consider a discrete time model of information spread (represented by a variable assigned to each node) in a network with a set of nodes V and a subset $A \subseteq V$ of k nodes representing leaders or stubborn agents that are initially assigned a single value. Propagation occurs by iterated averaging or diffusion defined by a stochastic matrix P. All node values will eventually converge to the single value at a speed determined by the sub-stochastic matrix $P_{\sim A}$, the matrix P restricted to the complement of A. An effective spreader in this situation

is, then, a set of nodes for which convergence to this single value is fastest, i.e., the set A for which the Perron-Frobenius eigenvalue of $P_{\sim A}$ is the largest.

Using a classical result of Markov chain theory, the problem can be recast in terms of finding the set A of cardinality k that minimizes the mean first hitting time, i.e., the average expected time a random walker reaches the target set A for the first time. As stated, solution of this minimization problem requires an examination of all subsets of cardinality k. The essence of our approximation method is to vastly reduce the search space using the supermodularity property of the first hitting time function (see [2] for details). We developed a polynomial time algorithm for finding an approximation to the optimal set. It is an extension of the classic greedy algorithm and it begins with a class of optimal and near optimal starter sets of cardinality $m < k$, rather than the best singleton set. The complexity of the method is $O(N^{m+3})$, where N is the number of nodes. In actual computations we find that $m \leq 2$. Our method, as implemented on smaller graphs ($N \leq 300$), demonstrates that optimal spreaders can deviate significantly from approximations based on degree-based methods or even the classical greedy method. Despite its (rigorously proved) accuracy, we must use another approach for realistic networks.

In the past year, we have developed a new set of fast heuristics that employ multi-stage optimization modules for identifying candidate vertices. Multi-neighborhood expansions and closeness metrics are used. The aggregate random walk arrival times are computed using high-resolution Monte Carlo sampling. As a result, finding near-optimal and optimal spreaders in networks with millions of vertices and edges takes a few seconds on a conventional laptop. To check the validity of these results, comparisons between the theoretical and heuristic approaches outlined here are underway on smaller networks and selected subsets of larger ones. Favorable comparability has been obtained for real world examples such as the C. Elegans neural network, the reduced Abilene network, and a business network from downtown Bethesda Maryland.

Other measures of effective spread are possible but the first hitting time, particularly in the case of the uniform random walk, allows a structural, i.e., topological, description of the node sets of optimal spreaders. This year we obtained upper bounds on the first hitting time that demonstrate the connection between the optimal sets we approximate and other subsets whose importance in the control of large complex networks has been demonstrated recently, in particular, vertex covers, partial vertex covers and dominating sets.

[1] V.S. Borkar, J. Nair and N. Sanketh. Manufacturing Consent. In *48th Annual Allerton Conference*, Allerton House, UIUC, Illinois, September 2010, 1550-1555.

[2] F. Hunt. An Algorithm for Identifying Optimal Spreaders in a Random Walk Model of Network Communication. *Journal of Research of the National Institute of Standards and Technology* **121** (2016), 180-195.

[3] F. Hunt and R. Pozo. Algorithms for Effective Spread and Communication in Real Complex Networks. In preparation.

Algorithmic Tools for Network Modeling and Analysis

Brian Cloteaux

Studying interactions within systems, such as biological, social or communications, is an active area of pursuit in the research community. Commonly, such interactions are modeled as networks or graphs. As these areas of investigation mature, researchers increasingly need to be domain specialists, not experts in programming and graph algorithms. Providing such researchers with a tool set of fast and efficient algorithms for network modeling and analysis is the central idea behind this project. As a byproduct of this research, there have been a number of theoretical discoveries.

Recent results coming from this project have given extremely efficient algorithms for testing if a sequence is graphic [1], and for generating random instances of a network with a given degree sequence [2]. In addition to these new algorithms, we have been looking at approaches to improving existing algorithms. We found several new bounds that have direct algorithmic application [3, 4], leading to to faster modeling algorithms, and interesting applications in graph theory.

As an example of the results from this project, we recently worked on the problem of random graph generation. The most common approach used for this problem is to create a non-random instance and then to modify it using a Monte Carlo Markov chain approach. A serious problem with this approach is that it requires holding an entire graph in memory. For random graph generation, sequential importance sampling methods have also been developed, but suffer from slow run times. We introduced a new algorithm for creating random instances [2], which overcomes the space and speed limitations of earlier methods. At the same time, we also published results that can be used to speed-up some instances of the traditional Monte Carlo Markov chain approach [4].

This year we gave attention to the problem of generating random graphs created using a graphic degree sequence selected from some given probability distribution. More specifically, how do we deal with a randomly drawn integer sequence that is not graphic (i.e., a degree distritution that is not realized in any graph)? There have been two approaches to this problem. The first is to simply discard the sequence and repeatedly select a new sequence until a graphic sequence is found. This approach is used by the NetworkX graph library. A

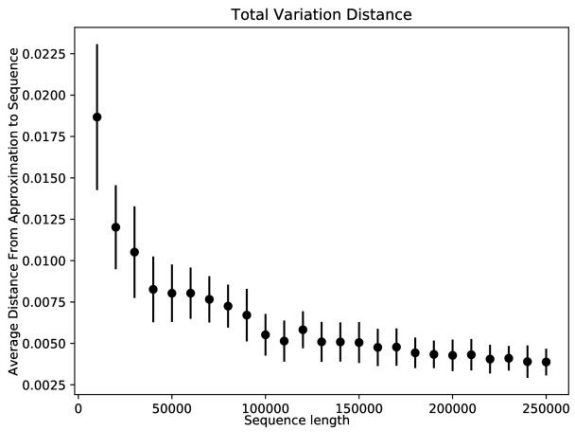

Figure 72. *This figure represents the average difference between a non-graphic sequence selected from a power-law distribution with exponent of 2 and its approximation created from our new algorithm. Each point represents the average distance for 30 sequences created at a given lenfth. The error bars represent one standard deviation.*

disadvantage to this approach is that for some probability distributions, such as a power-law distribution, the probability of selecting a graphic sequence can be very small. For these distributions, we have a very small chance of finding a graphic sequence in reasonable time.

In response to this difficulty, an alternative is to find the closest graphic sequence to the original non-graphic degree sequence using a given distance measure. We contributed to the problem by introducing a new algorithm that is extremely fast, requiring only one pass through the sequence in order to give a graphic approximation [5]. We then examined our method in the context of minimizing the probability distribution distance, and specifically the total variation distance, between the original sequence and the approximation. We showed that under the total variation distance, the quality of the result from our approximation algorithm for many sequences actually improves as the size of the sequences increases. In fact, this distance goes to zero as the length of the sequence increases. Figure 72 shows how the average total variation distance between the original sequences and their approximations from the algorithm approach zero as the sequence length grows. Our work is the first practical approximation for extremely large sequence generation.

We are currently publishing this new algorithm and enhancements for the benefit of the public. We are further looking to see if we can parallelize some of these algorithms for even greater speed up. In addition, we are continuing to examine other fundamental algorithms needed by the network research community.

[1] B. Cloteaux. Is This for Real? Fast Graphicality Testing. *Computing in Science & Engineering* **17**:6 (2015), 91-95.

[2] B. Cloteaux. Fast Sequential Creation of Random Realizations of Degree Sequences. *Internet Mathematics* **12**:3 (2016), 205-219.

[3] B. Cloteaux. A Sufficient Condition for Graphic Lists with Given Largest and Smallest Entries, Length and Sum. In review.

[4] B. Cloteaux. Forced Edges and Graph Structure. In review.

[5] B. Cloteaux. One-pass Graphic Approximation of Integer Sequences. In review.

Using Sequential Importance Sampling to Speed up the Monte Carlo Markov Chain Method

Isabel Beichl
Francis Sullivan

The Monte Carlo Markov Chain Method (MCMC) is widely used in simulations of all types. But getting reliable answers to real-world problems is still difficult because MCMC can be slow, even when the theory provides assurance of polynomial time convergence, because: (1) the convergence rate guaranteed by the theory is often much slower than the actual rate and cannot be determined exactly and, (2) the fugacity, which dictates where samples will concentrate, must be guessed by examining partial results. Sequential Importance Sampling (SIS) can be quite efficient on the same problems, but there are very few analytic results.

We applied both methods to the monomer-dimer problem [1, 2]. The solution to this problem gives first principles thermodynamic information for a physical system modeled by a grid graph which allows monomers and dimers to exist in specific grid locations. The problem reduces to counting the number of ways to put k dimers onto an $n \times n$ grid. The problem is provably hard. We approximate solutions with MCMC and SIS. The first MCMC solution was proposed in [1]. In [2] we have a more efficient solution. in [3] we showed SIS can give a faster solution.

To address problems (1) and (2) of MCMC, we present two applications of sequential importance sampling (SIS). To determine an approximation to the "true" convergence rate, we use aggregation which approximates the transition matrix by a much smaller condensed matrix whose eigenvalues can be determined. Here SIS generates the entries of the aggregated matrix. For deciding on fugacity, we use SIS to generate an approximation to the solution. This approximation is sufficient to determine appropriate fugacities for MCMC. Because SIS and MCMC have been applied to a class of problems we suspect that other MCMC methods may be amenable to this method.

[1] C. Kenyon, D. Randall and A. Sinclair. Approximating the Number of Monomer-Dimer Coverings of a Lattice. *Journal of Statistical Physics* 83 (1996), 637-659.

[2] I. Beichl, D. P. O'Leary and F. Sullivan. Approximating the Number of Monomer-Dimer Coverings in Periodic Lattices. *Physical Review E* **64** (2001), 016701.

[3] I. Beichl and F. Sullivan. Applications of Sinkhorn Balancing: The Monomer-Dimer Problem. Stochastic Processes and Functional Analysis. In *Dekker Lecture Notes in Pure and Applied Mathematics*, ed. (A. C. Krinik and R. J. Swift, eds.), 2004, 53-65.

Counting the Number of Linear Extensions of a Partially Ordered Set

Isabel Beichl
Alathea Jensen (George Mason University)
Francis Sullivan (IDA Center for Computing Sciences)

Given a partially ordered set (P,lt) a *linear extension* is a linear ordering (P,<) of the elements of P that is consistent with (P,lt), i.e. if p_1 .lt. p_2 then $p_1 < p_2$. The ability to count the number of linear extensions is central to the theory of sorting which in turn is extremely important in the design of algorithms for advanced computers. A count of linear extensions is also important in ranking alternatives in scheduling problems where one might want to keep options open as long as possible, and in applications that arise in the social sciences where one wants to rank products or job candidates from a given partial order. It also appears in big data applications where one might need to set priorities and yet keep as many options open as possible. The number of linear extensions is also a measure of the entropy of a graph.

While it is computationally easy to generate a single linear extension of (P,lt) it is known that counting the number of linear extensions is #P-complete, and so one must resort to approximation. One Monte Carlo technique, called Monte Carlo Markov Chain (MCMC), has been devised and investigated extensively in the literature of theoretical computer science [1]. It has been proved that the method does give an accurate approximation for this problem. However, the method is not helpful for practical computation because it still requires work (n^5) for an n-element partially ordered set.

Because the aim of our work is practical computational methods, we decided to investigate an alternative Monte Carlo method that has been used with success in other #P-hard counting problems. The alternate method, called sequential importance sampling (SIS), is based on non-uniform sampling based on an importance function. In this case, the importance function is derived from the famous Möbius inversion formula. A second importance function has been invented that changes dynamically as the problem is run. Another sampling method for this problem was developed in the last year based on a technique called *Stochastic Enumeration* (SE), which has been proven in this work to reduce variance. SE chooses several linear extensions probabilistically which interact with one another in each sample. These SIS and SE based algorithms have been found to work extremely well in test cases.

[1] G. Brightwell and P. Winkler. Counting Linear Extensions. *Order* **8** (1991), 225-242.

A Simulation Platform to Study Ultra-WideBand Propagation for Wireless Capsule Endoscopy

Katjana Krhac (University of Zagreb)
Wesley Griffin
Kamran Sayrafian
Judith Terrill

Ingestible Wireless Capsule Endoscopy (WCE) is the only painless, effective, and novel diagnostic technology for inspecting the entire gastrointestinal (GI) tract for various diseases such as obscure gastrointestinal bleeding, tumors, cancer, Crohn's disease, and celiac disease. A typical WCE includes a miniature-sized camera that periodically transmits images as it passes through the human GI tract. The images are captured by several receivers that are usually embedded in a belt worn by the patient for the duration of the procedure. The long sequence of images is later analyzed to investigate possible abnormalities inside the patient's GI tract. WCE is the only non-invasive procedure that allows physicians to look into the small intestine.

The next generation of endoscopy capsules (i.e., medical micro-robots) is expected to deliver higher quality images or even videos, as well as more diagnosis and therapeutic functionality. This level of performance will require a communication link with higher data rates, which in turn necessitates higher bandwidth transmission mechanisms. Despite the possibility of high attenuation, Ultra-Wideband (UWB) technology is an attractive candidate to deliver sufficient bandwidth for future WCE applications. The low complexity of a UWB transceiver also implies less power consumption which is critical for these capsules [1, 2].

A comprehensive study of radio wave propagation for ingestible electronics is a very challenging task. Obtaining physical measurements is nearly impossible. And, although limited experimentation on animals, or liquid phantom measurements, are possible, the results are not quite reflective of the complex and inhomogeneous human body environment.

Computational phantoms are another alternative; however, they require sophisticated human body models along with verified transmitter and receiver antenna models [3]. Commercially available human body models do not usually have a sufficient model of the GI tract

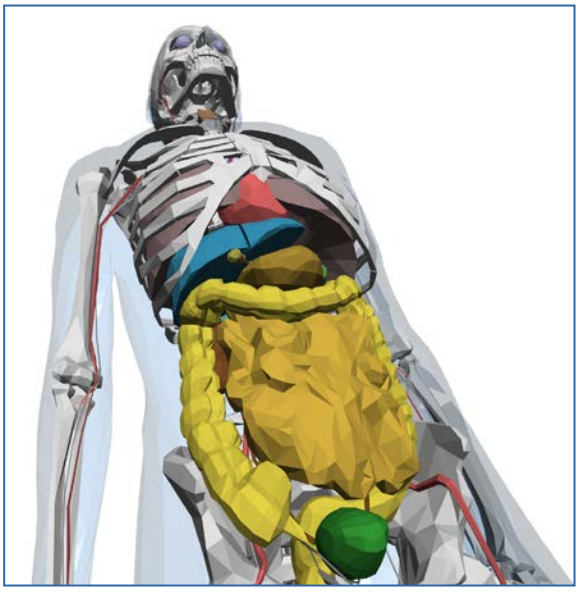

Figure 73. *Computational human body model.*

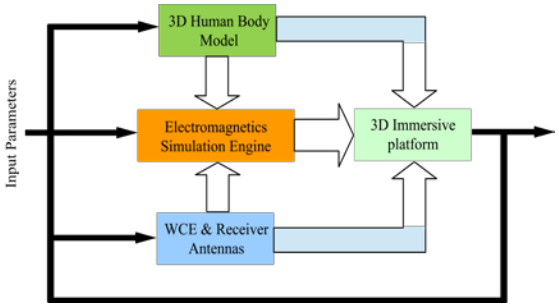

Figure 74. *System block diagram.*

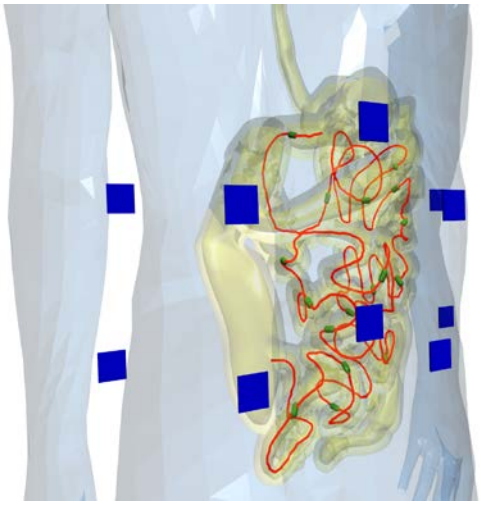

Figure 75. *Computational body model with enhanced GI tract.*

(Figure 73). But a detailed model of the GI tract is necessary to consider accurate placement of the WCE as it traverses through the GI tract. To initiate the study on UWB propagation from a WCE, a flexible and interactive immersive platform containing an enhanced 3D body model and accurate antennas is a desirable solution [4].

We have developed a novel 3D immersive platform to emulate the communication link between a WCE and several on-body sensors (Figure 74). A 3D human body model has been enhanced to include an accurate model of the GI tract with interior surfaces. Validated models of practical antennas have also been incorporated in the system to better characterize the wireless link.

A high-resolution 3D GI tract model without self-intersections or other "non-manifold" features has been developed and integrated with the ACMD computational human body model. The center line that passes through this tract in 3D space has been calculated and used as the reference line for the capsule placement within the GI tract. Multiple receivers (indicated with blue squares) have been considered around the stomach area (Figure 75). The collection of the received signal strength at these receivers can be used to characterize the UWB propagation from the WCE [5, 6]. The placement of the capsule should be carefully chosen such that there are enough measurement samples for the entire range of transmitter-receiver separation.

This platform enables researchers to conduct a comprehensive study of the UWB propagation channel for WCE applications. For example, using the immersive platform, the first UWB statistical path loss (i.e., attenuation versus distance) model for the small intestine can be characterized. The scatter plot shown in Figure 76 (highlighting the mean value obtained by fitting a least square linear regression line) indicate a path loss model for 3.6 GHz frequency. Such models will provide important information to physical layer designers who are interested in using UWB technology for the next generation of WCE.

The random shadowing effect of the propagation channel which is due to inhomogeneity of the body tissues as well as non-omnidirectionality of the transmitting and receiving antennas and possible multipath fading can be modeled by a lognormal distribution as shown in Figure 77.

Enhancing communication and control capabilities of medical microbots (micro-robots) will enable a revolutionary set of diagnosis and therapeutic tools without the need for costly and invasive procedures. The immersive platform that has been developed in this project is a powerful, one-of-a-kind metrology tool to study wireless communication for such microbots. It could also be used as a virtual platform to investigate positioning technologies that can track the movement and location of ingestible electronics as they travel through the GI tract. With such information building a personalized 3D map of the patient's GI tract could be a possibility.

[1] R. Chavez-Santiago, I. Balasingham and J. Bergsland. Ultrawideband Technology in Medicine: A Survey. *Journal of Electrical and Computer Engineering* **2012** (2012), 716973.

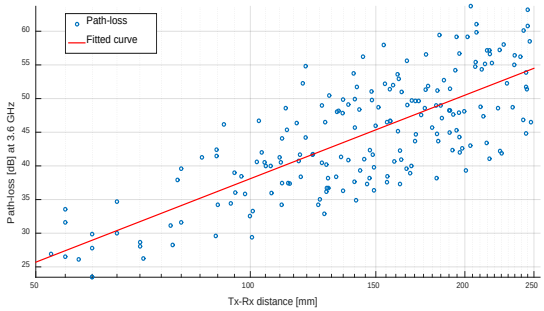

Figure 76. *Pathloss scatter plot at 3.6 GHz.*

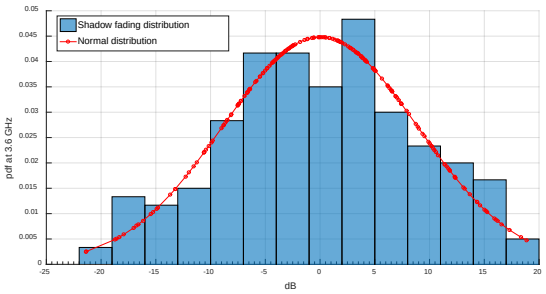

Figure 77. *Shadow fading distribution at 3.6 GHz.*

[2] V. Niemela, J. Haapola, M. Hamalainen and J. Iinatti. An Ultra-Wideband Survey: Global Regulations and Impulse Radio Research Based on Standards. *IEEE Communications Surveys & Tutorials* **19**:2, (2017).

[3] K. Sayrafian, J. Hagedorn, J. Terrill and M. Alasti. A Simulation Platform to Study Cross-Interference in Multiple Body Area Networks. In *Proceedings of the 4th IEEE International Conference on Cognitive Infocommunications (CogInfoCom)*, Budapest, Hungary, December 2-5, 2013.

[4] K. Y. Yazdandoost. Antenna for Wireless Capsule Endoscopy at Ultra-WideBand Frequency. In *Proceedings of the 27th Annual IEEE Symposium on Personal Mobile Radio Communications (PIMRC)*, September 4-7, 2016.

[5] K. Sayrafian, W. Yang, J. Hagedorn, J. Terrill and K. Yazdandoost. Simulation Study of Body Surface RF Propagation for UWB Wearable Medical Sensors. In *Proceedings of IEEE ISABEL*, 2009.

[6] K. Sayrafian, W. Yang, J. Hagedorn, J. Terrill and K. Yazdandoost. A Statistical Path Loss Model for Medical Implant Communication Channels. In *Proceedings of the 20th Annual IEEE International Symposium on Personal Indoor and Mobile Radio Communications*, 2009.

Mathematical Knowledge Management

We work with researchers in academia and industry to develop technologies, tools, and standards for representation, exchange, and use of mathematical data. Of particular concern are semantic-based representations which can provide the basis for interoperability of mathematical information processing systems. We apply these representations to the development and dissemination of reference data for applied mathematics. The centerpiece of this effort is the Digital Library of Mathematical Functions, a freely available interactive and richly linked online resource, providing essential information on the properties of the special functions of applied mathematics, the foundation of mathematical modeling in all of science and engineering.

Visualization of Complex Functions Data

Bonita Saunders
Brian Antonishek (NIST EL)
Qiming Wang
Bruce Miller
Sandy Ressler

A desire for clear and informative graphical representations of complex mathematical functions in the NIST Digital Library of Mathematical Functions (DLMF) provided the impetus for this work, but important byproducts are the development and exploitation of new technologies for viewing and manipulating 3D graphics on the web, and the creation of codes for generating computational grids to accurately plot key function features such as zeros, poles, and branch cuts.

Our work has led to continuous improvement of the graphs and visualizations in the DLMF since its launch in 2010. Our first visualizations used a Web 3D format called VRML (Virtual Reality Modeling Language) that required users to download a special graphics plugin, but our latest format, X3DOM/WebGL [1], can be viewed directly in most internet browsers on major platforms. WebGL [2] is a JavaScript API (application programming interface) for rendering 3D graphics in a Web browser without a plugin. X3DOM, a special framework for creating graphics applications on the Web, allowed us to quickly build our WebGL applications around our earlier graphics codes. The new format significantly improves the look and maneuverability of our visualizations. We did notice that the WebGL surface color maps were more sensitive to the quality of the underlying grid, but in most surface regions the problem was lessened or eliminated by refining the grid, that is, adding more grid points. However, since we would like to keep the size of the grid data files as small as possible, we are currently working to solve the problem by adapting the underlying grids to function curvature and gradient data.

Feedback on DLMF graphs and visualizations has been positive, but more needs to be done to improve visibility. Many users see the static images, but are unaware

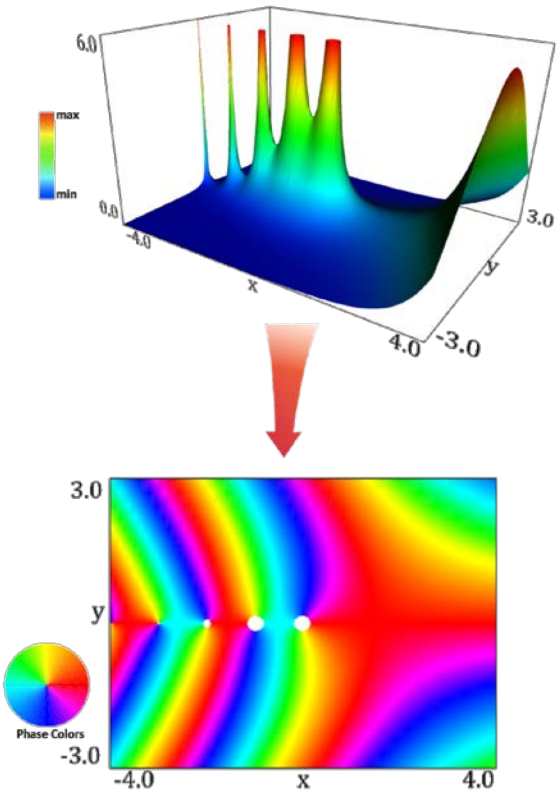

Figure 78. *DLMF visualizations provide several control options for exploring mathematical functions surfaces. The complex gamma function surface, $|\Gamma(x+iy)|$, shown at the top with a height based color map, can be transformed into a density plot by viewing the surface from above and scaling it down to 0 in the vertical direction. Going a step further by changing the color map to one based on phase, or argument, yields the phase density plot below it. The progression of phase values around the poles is analogous to what one would see in fluid flow generated by a semi-infinite line of vortices.*

that there are interactive visualizations that can be rotated and otherwise manipulated. We have added more visual cues to the static images and to the visualizations themselves, but we are also looking at other possibilities, such as a strategically located animation. For example, in Figure 78 we describe how a user might create a phase based density plot. Information of this type could be provided in a popup window on the DLMF site or illustrated in a short animation. We have also tried to

take advantage of external options for publicizing the work. We provided an image based on the DLMF phase density plots for the gamma and digamma function as part of a two-month display sponsored by the NIST Public Affairs Office at the Johns Hopkins University Montgomery County Campus [7]. DLMF graphics were also discussed in a post to the NIST Taking Measure Blog for Mathematics and Statistics Awareness Month [5] and an extensive discussion, along with several images, will be in our *Physics Today* article [3]. In addition to these efforts, we continue to generate publications, and present talks and displays at a variety of venues to publicize our work [4-13].

[1] J. Behr, P. Eschler, Y. Jung and M. Zollner. X3DOM: a DOM-based HTML5/X3D Integration Model. In *Proceedings of the 14th International Conference on 3D Web Technology (Web3D '09)*, (S. N. Spencer, ed.), Darmstadt, Germany, June 16-17, 2009, 127–135.

[2] https://www.khronos.org/webgl/

[3] B. Schneider, B. Miller and B. Saunders, NIST's Digital Library of Mathematical Functions. *Physics Today*, in press.

[4] B. Saunders. "Adaptive Grids for Accurate Visualizations of Complex Function Data." SIAM Conference on Industrial and Applied Geometry (GD17), Pittsburgh, PA, July 12, 2017.

[5] B. Saunders. Plotting a Path from NASA Grids to NIST Graphics. NIST Taking Measure Blog, April 27, 2017.

[6] B. Saunders. "Grid Generation: From NASA to the NIST Digital Library of Mathematical Functions." Women's History Month Celebration, African American History Club, Riderwood, Silver Spring, MD, March 22, 2017.

[7] C. Clark and B. Saunders. DLMF Gamma, Digamma Phase Plot Display. MICRO/MACRO: Big Images of Small Things from NIST Labs, Johns Hopkins University Montgomery County Campus, Rockville, MD, September 6 – November 11, 2016.

[8] B. Saunders, B. Antonishek, B. Miller and Q. Wang. "Adaptive Curvature-Based Composite Grid Generation Techniques Applied to 3D Visualizations." 9th International Conference on Mathematical Methods for Curves and Surfaces, Tonsberg, Norway, June 23, 2016.

[9] B. Saunders. "Slices of 3D Surfaces on the Web Using Tensor Product B-Spline Grids." SIAM Conference on Geometric and Physical Modeling (GD/SPM15), Salt Lake City Utah, Utah, October 12, 2015.

[10] B. Saunders. "Cutting Edge Information Technology Applied to the NIST Digital Library of Mathematical Functions." MAA MathFest 2015, Washington, D.C., August 8, 2015.

[11] B. Saunders. "X3DOM/WebGL Visualizations in the NIST DLMF, Web3D Showcase." 20th International Conference on 3D Web Technology (Web3D 2015), Heraklion, Crete, Greece, June 20, 2015.

[12] B. Saunders, B. Antonishek, Q. Wang and B. Miller. "State of the Art Visualizations of Complex Function Data." International Conference on Orthogonal Polynomials, Special Functions and Applications, NIST, June 4, 2015.

[13] B. Saunders, B. Antonishek, Q. Wang and B. Miller. Dynamic 3D Visualizations of Complex Function Surfaces Using X3DOM and WebGL. In *Proceedings of the 20th International Conference on 3D Web Technology (Web3D 2015)*, Crete, Greece, June 18-21, 2015, 219-225.

DLMF Standard Reference Tables on Demand

Bonita Saunders
Bruce Miller
Marjorie McClain
Daniel Lozier
Andrew Dienstfrey
Annie Cuyt (University of Antwerp)
Stefan Becuwe (University of Antwerp)
Franky Backeljauw (University of Antwerp)
Chris Schanzle

http://dlmftables.uantwerpen.be/

The original NBS *Handbook of Mathematical Functions* (A&S) [1] has served as a comprehensive source of information on functions arising in the mathematical and physical sciences, but its main purpose was to be a compendium of tables of function values. Today, manual interpolation in tables has been superseded by software for evaluating special functions at any argument. Thus, exhaustive tables of function values were not included in the follow-on NIST Digital Library of Mathematical Functions (DLMF) [2].

Nevertheless, a reliable source of function values that are certifiably accurate is still needed. This need was made even more clear by recent DLMF feedback. An email message from a Boeing Research & Technology scientist expressed his desire for a system that would allow him to test a table of function values against reference values. Another user said the following:

> *It is no longer useful to include large tables of function values for the purpose of interpolation. But a set of test values for each function with various decimal precisions would be useful for developers as they try to test implementations of special functions. This could be the beginning of a benchmark for numeric software. [9]*

Comments like these make it clear that there is a need for tables, but the size of the potential user base is hard to ascertain. The DLMF Standard Reference Tables on Demand Project (DLMF Tables) is designed to address this need. The goal is to develop an online service

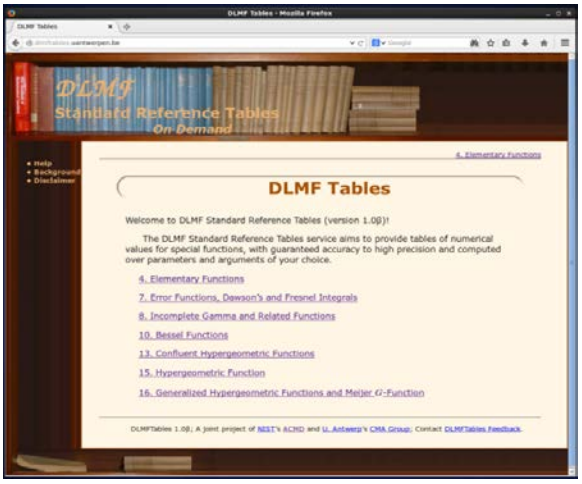

Figure 79. *Table of contents for DLMF Tables website.*

Computed values of $I_\nu(x)$

Computed using MpIeee+R(on odd lines), compared to ν, x, $I_\nu(x)$ (on even lines), for ν, x, $I_\nu(x)$ from file Iv_user_valus.txt; output to 12 digits, using interval mode; computation and output in base 10 .

ν	x	$I_\nu(x)$	Relative Error
0	1	1.26606 58777 5 20085±5	
		1.26606 58777 5	1.6×10^{-12}
1	2	1.59063 68546 3 73295±5	
		1.59063 68546 3 ‡	4.7×10^{-12}
2	5	$1.75056\ 14966\ 6\ 24235\pm5 \times 10^{1}$	
		$1.75056\ 14966\ 6 \times 10^{1}$	1.4×10^{-12}
3	5	$1.03311\ 50169\ 1\ 51135\pm5 \times 10^{1}$	
		$1.03311\ 50169\ 3 \times 10^{1}$ ‡	1.5×10^{-11}

Figure 80. *Output for comparision of DLMF Tables computations with table of function values submitted by user. Differences between reference values and uploaded values are highlighted in either yellow (warning) or red (error).*

where users can generate tables of special function values with an error certification. The project is a collaboration between ACMD and the University of Antwerp Computational Mathematics Research Group (CMA).

ACMD is working on the front-end interface while CMA, under the direction of Professor Annie Cuyt, is developing the system's computational engine based on their MpIeee library. MpIeee is an IEEE 754/854 compliant C++ library for mixed precision floating point arithmetic in base 2^n or 10^m. IEEE compliance implies, among other things, that basic arithmetic operations, as well as remainder and square root operations, are rounded correctly, that is, the result of the operation is the floating-point value that would be obtained by first computing the exact mathematical value and then rounding it to its floating-point representation. IEEE compliance provides a solid foundation for building reliable software [4-8].

A challenging, but critical, part of creating a system such as DLMF Tables is determining the likely users and assessing their needs. To help us address this problem, we have built and publicly released a beta version that includes design features we feel are crucial. By publicizing this fully operational site, we hope to obtain feedback that can be considered as we expand and enhance the service.

The importance of communicating with potential users was driven home after a meeting with a NIST physicist to discuss the testing of his Bessel function software. After just a few minutes of discussion, several issues were apparent:

(a) *The name of our site may mask its intended use for software testing.*

Still a devoted user of A&S, the physicist associated our site name with the tables in A&S which were primarily used to compute function values through interpolation. He saw no use for tables in his work.

(b) *Reference values can be computed in several well-known computer algebra packages. Users often accept these values without any claims about accuracy.*

The physicist wrote a modified algorithm for computing certain Bessel functions after he obtained disappointing results using an A&S algorithm based solely on asymptotic expansions. He tested his code by computing the function using both his software and a computer algebra package. If the first "*n*" consecutive digits agreed, they were assumed to be correct. However, for some parameters his results agreed more with the result obtained using his original A&S-based algorithm. This observation prompted us to ask him how he knew which software was providing the most correct result and point out the benefit of obtaining a certified result with error-bound information.

(c) *Large digits of precision or extreme parameter values? Which do users want?*

Surprisingly, for the problem the physicist was solving, very large values for the Bessel function parameters were needed more than extremely large digits of precision. A precision of around 20 digits was fine, but Bessel function parameters of more than our current onsite restriction of 1000 were needed.

All these issues produced interesting discussions and raised questions still being sorted out, but the last issue may have the most immediate effect on technical aspects of the project. Many of the size restrictions currently in place are to ensure that a user can obtain a result in a reasonable length of time. If this restriction prevents the computation of function values of interest to users, we may have to re-think our design. Perhaps we might allow the user to increase the size limits on some parameters with a warning that the computations may take more time, or offer the option of submitting a batch job.

The question is how long a user would be willing to wait with the knowledge that the result will be certifiably correct? Of course, we must also look at how this affects CMA's software. Will it be able to handle much larger parameter values? How large is too large? In any case, this example shows the importance of feedback and working closely with potential users to ensure that we are creating a product they not only want but can use.

To encourage more feedback, we continue to publicize the site through talks and publications [10-14]. A brief overview of the project appears in a forthcoming *Physics Today* article on the DLMF [11]. In addition to publicizing the site, we continue to work with CMA on developing and expanding it to more functions, and we are looking at what changes are necessary to address the issues noted. We are also looking at additional high precision codes that might be relevant to our project [15,16].

[1] M. Abramowitz and I. Stegun, eds. *Handbook of Mathematical Functions*, Applied Mathematics Series **55**, National Bureau of Standards, Washington, DC, 1964.

[2] NIST Digital Library of Mathematical Functions. http://dlmf.nist.gov/, Release 1.0.17 of 2017-12-22. Online companion to [3].

[3] F. W. J. Olver, D. W. Lozier, R. F. Boisvert and C. W. Clark, eds. *NIST Handbook of Mathematical Functions*. Cambridge University Press, New York, NY, 2010. Print companion to [2].

[4] F. Backeljauw, S. Becuwe, A. Cuyt, J. Van Deun and D. Lozier. Validated Evaluation of Special Mathematical Functions. *Science of Computer Programming* **10** (2013), 1016.

[5] M. Colman, A. Cuyt and J. Van Deun. Validated Computation of Certain Hypergeometric Functions. *ACM Transactions on Mathematical Software* **38**:2 (January 2012), Article 11.

[6] F. Backeljauw. A Library for Radix-independent Multiprecision IEEE-compliant Floating-point Arithmetic. Technical Report 2009-01, Department of Mathematics and Computer Science, Universiteit Antwerpen, 2009.

[7] A. Cuyt, V. B. Petersen, B. Verdonk, H. Waadeland and W. B. Jones. *Handbook of Continued Fractions for Special Functions*. Springer, New York, 2008.

[8] A. Cuyt, B. Verdonk and H. Waadeland. Efficient and Reliable Multiprecision Implementation of Elementary and Special Functions. *SIAM Journal of Scientific Computing* **28** (2006), 1437-1462.

[9] E. Smith-Rowland. Personal communication. DLMF Feedback, September 20, 2016.

[10] B. Saunders, B. Miller, F. Backeljauw, S. Becuwe, M. McClain, D. Lozier, A. Cuyt and A. Dienstfrey. DLMF Tables: A Computational Resource Inspired by the NIST Digital Library of Mathematical Functions. In review.

[11] B. Schneider, B. Miller and B. Saunders. NIST's Digital Library of Mathematical Functions. *Physics Today*, February 2018.

[12] B. Saunders. "Who Needs Standard Reference Tables on Demand?" Mathematical Association of America, MD-DC-VA Section Meeting, Frostburg State University, Frostburg, MD, April 29, 2017.

[13] B. Saunders, B. Miller, M. McClain, D. Lozier, A. Dienstfrey, A. Cuyt, S. Becuwe and F. Backeljauw. "DLMF Standard Reference Tables on Demand (DLMF Tables)." Minisymposium on Orthogonal Polynomials and Special Functions: Computational Aspects, 2015 International Conference on Orthogonal Polynomials, Special Functions and Applications, NIST, June 1, 2015.

[14] B. Saunders. "NIST Projects: Graphics in the Digital Library of Mathematical Functions (DLMF) and DLMF Standard Reference Tables on Demand (DLMF Tables)." Careers in Mathematical Sciences Workshop for Underrepresented Groups, Institute for Mathematics and Its Applications, University of Minnesota, Minneapolis, MN, March 29, 2015.

[15] J. Le Maire, N. Brunie, F. de Dinechin and J. Muller. Computing Floating-point Logarithms with Fixed-point Operations. In *Proceedings of the IEEE 23nd Symposium on Computer Arithmetic (ARITH)*, 2016, 156-163.

[16] N. Brunie, F. de Dinechin, O. Kupriianova and C. Lauter. Code Generators for Mathematical Functions. In *Proceedings of the IEEE 22nd Symposium on Computer Arithmetic* (ARITH), 2015, 66-7.

Mathematical Knowledge Management

Bruce Miller
Tom Wiesing (University of Erlangen, Germany)

Providing a collection of useful information about the special functions of applied is, of course, the purpose of the Digital Library of Mathematical Functions (DLMF) project. We might call it tactical that our initial focus was to put these definitions, relationships, properties and other data into a form readable by the scientists and engineers who make up our readership. But the longer-term strategy calls for the data to be machine-readable. When appropriately indexed by either major search engines, or special purpose ones, this will support richer search and discoverability. Most important is the goal that DLMF's formula can be imported directly into other software systems and used within the computations of those systems.

The first, most fundamental question immediately reveals itself: Are the functions treated in DLMF actually the same as those in Mathematica, or Maple or the NAG libraries? As it turns out, usually they are, but sometimes they are not, and the differences can be subtle. Establishing these correspondences is exactly the purpose of the Special Function Concordance activity of the International Mathematical Knowledge Trust (IMKT) established by the Global Digital Mathematical Library (GDML) working group of the International Mathematical Union. We are participating in this effort

to establish this concordance between the various special functions, in all their flavors, as used within various handbooks, such as the DLMF, and software systems, such as Mathematica, Maple and NAG, to assure interoperability.

For our part, we are developing a catalog of the special functions as defined in DLMF. Obviously, we start by listing those formulas which we consider to be the defining ones for each function. However, the key is to focus on those aspects, those choices, that potentially distinguish our version of a particular function from those of other systems. Choices of argument conventions (e.g., elliptic functions sn(u,k) vs. sn(u,m)) are significant. Patterns of singularities and type signatures help distinguish different extensions and generalizations of functions. A trickier class of difference are the choices made for the location of branch-cuts or which value is taken on the cuts, or indeed the choice made to avoid them entirely as multi-valued functions.

Given this set of distinguishing features, we are now proceeding to collect and encode that information for each of the functions treated in DLMF and present the result in the form of OpenMath Content Dictionaries.

Part-of-Math Tagging

Abdou Youssef

Simply, stated, a part-of-math (POM) tagger determines the mathematical category/role (called tag) of every symbol in a given mathematical expression or equation. In addition, the POM tagger should often be able to determine the mathematical meaning of a symbol by using the symbol's expression-level context and manuscript-level context, as well as broad domain-level and sub-domain-level knowledge.

To that end, a tagset for math terms and expressions has been created, and a tagger has been developed in this project. The current state of the tagger takes as input mathematical expressions, and tags each math term and some sub-expressions with a number of tags, some certain while others tentative needing further disambiguation. Also, the tagger needs to extract definite semantics about the math terms and expressions from the expressions themselves and from surrounding contexts. The disambiguation and context-driven semantics extraction will be will carried out using the deep learning techniques described below.

[1] Abdou Youssef. Part-of-Math Tagging and Applications. *Lecture Notes in Artificial Intelligence* **10383** (2017), 10th Conference on Intelligent Computer Mathematics (CICM), Edinburgh, Scotland, UK, 2017.

Deep Learning for Math & Science Knowledge Processing

Abdou Youssef
Bruce Miller

The amount of literature in STEM fields is growing so rapidly that it is impossible to keep current, thus causing many lost opportunities for advances, and much wasted time in re-inventing the wheel. Therefore, automated semantic-processing of math and science documents is essential for future progress in knowledge discovery and reuse, and for the synthesis of large and exponentially growing volumes of technical text. Many researchers are now using automated techniques to mine the scientific literature. Success in doing this relies on being able to determine the meaning, i.e., semantics, of the literature in an automated way.

In this newly established project, we plan to apply (design and train) deep neural network (DNNs) to perform semantic-processing of math and science documents for several foundational tasks, such as automated translation from informal/LaTeX form to machine understandable forms such as computer programs, to semantic math markup language (e.g., Content MathML), and/or to formal logic languages suitable for automated reasoning. In the process, considerable disambiguation of symbols, and semantic extraction, will be performed by the DNNs, and large datasets (of math and science documents) will be created for training and testing of DNNs on such tasks. Also, traditional NLP and machine learning techniques will be applied to our tasks, and optimal synergistic combinations of those techniques with DNNs will be derived.

Automated Presentation-to-Computation Conversion

Abdou Youssef
Howard S. Cohl
Moritz Schubotz (University of Konstanz, Germany)
André Greiner-Petter (Technische Universität Berlin)

For increased efficiency and productivity, maximum convenience, and more reliability of software, it is desirable to have computer systems algorithmically convert math expressions into procedures for computing math functions and equations. In this collaboration, using the part-of-math tagger described above, we developed automated presentation-to-computation (P2C) techniques and software to convert a large set of mathematical expressions (written in LaTeX and some pre-defined macros) to Maple software, with considerable success. Performance evaluation of our conversion

techniques have been conducted and have shown that the output (Maple code) is quite accurate. Further advancement is planned using more sophisticated versions of the part-of-math tagger that will result from applying deep learning techniques to MLP in this project.

[1] H. Cohl, M. Schubotz, A. Youssef, A. Greiner-Petter, J. Gerhard, B. V. Saunders, M. A. McClain, J. Bang and K. Chen. Semantic Preserving Bijective Mappings of Mathematical Formulae between Word Processors and Computer Algebra Systems. *Lecture Notes in Artificial Intelligence* **10383** (2017), 10th Conference on Intelligent Computer Mathematics (CICM), Edinburgh, Scotland, UK, 2017.

NIST Digital Repository of Mathematical Formulae

Howard S. Cohl
Marjorie A. McClain
Bonita V. Saunders
Abdou Youssef
Moritz Schubotz (University of Konstanz, Germany)
André Greiner-Petter (Technische Universität Berlin)
Jurgen Gerhard (Maplesoft)
Claude Zou (Poolesville High School)
Joon Bang (Poolesville High School)
Kevin Chen (Poolesville High School)
Edward Bian (Poolesville High School)
Jagan Prem (Poolesville High School)
Kevin Shen (Poolesville High School)
Philip Wang (Poolesville High School)
Parth Oza (Poolesville High School)
Kaitlyn Yang (Poolesville High School)
Sahil Sinha (Poolesville High School)
Andrew Mao (Richard Montgomery High School)

http://drmf.wmflabs.org/wiki/Main_Page

The NIST Digital Repository of Mathematical Formulae (DRMF) is a Wiki-based compendia of formulae for orthogonal polynomials and special functions (OPSF) designed to (1) facilitate interaction among a community of mathematicians and scientists interested in OPSF; (2) be expandable, allowing the input of new formulae from the literature; (3) provide information for related linked open data projects; (4) represent the context-free full semantic information concerning individual formulas; (5) have a user friendly, consistent, and hyperlinkable viewpoint and authoring perspective; (6) contain easily searchable mathematics; and (7) take advantage of modern MathML tools for easy-to-read, scalably rendered content-driven mathematics.

Our DRMF implementation is built using MediaWiki, the wiki software used by Wikipedia. See Figure 81 for a sample DRMF formula home page. The

Figure 81. *Sample DRMF formula home page.*

DRMF has been described in a series of publications and talks [1-5].

A key asset in the development of DRMF semantic content is the utilization of a set of LaTeX macros, originally created by Bruce Miller of ACMD, to achieve the encapsulation of semantic information within the NIST Digital Library of Mathematical Functions (DLMF) [6]. These macros give us the capability to tie LaTeX commands in a mostly unambiguous way to mathematical functions defined in an OPSF context. There are currently 533 DLMF LaTeX macros, as well as an additional 156 which have been created specifically for the DRMF. All DLMF macros have at least one DLMF Web page associated with them, and the goal is to have definition pages for all additional DRMF macros. The use of DLMF and DRMF macros guarantees mathematical and structural consistency throughout the DRMF. We refer to LaTeX source with incorporated DLMF and DRMF macros as semantic LaTeX. DRMF formula seeding is currently focused on

(1) DLMF chapters 5 (Gamma Functions), 15 (Hypergeometric Function), 16 (Generalized Hypergeometric Functions and Meijer G-Function), 17 (q-Hypergeometric and Related Functions), 18 (Orthogonal Polynomials), and 25 (Zeta and Related Functions);

(2) Koekoek, Lesky, and Swarttouw (KLS) chapters 1 (Definitions and Miscellaneous Formulas), 9 (Hypergeometric Orthogonal Polynomials), and 14 (Basic Hypergeometric Orthogonal Polynomials [7];

(3) Koornwinder KLS addendum LaTeX data [8];

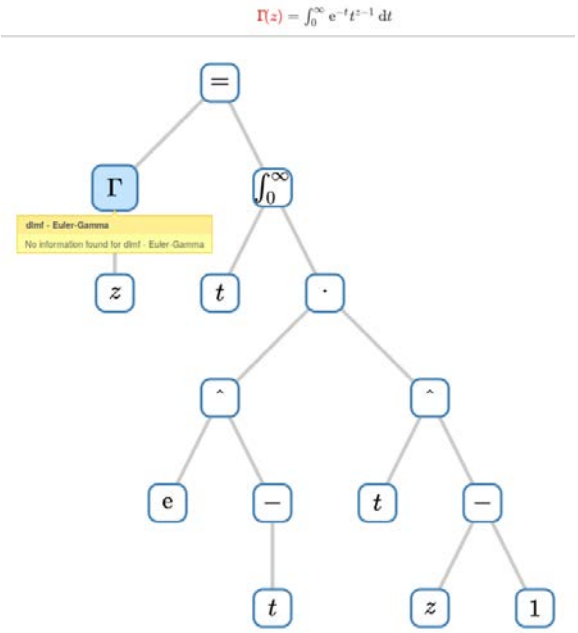

Figure 82. *VMEXT visualization of (5.2.1) in the DLMF. The corresponding MathML XML file is 89 lines and 6293 characters long.*

(4) Wolfram Computational Knowledge of Continued Fractions Project (eCF) [3];

(5) Continued Fractions for Special Function (CFSF) Maple dataset hosted by the University of Antwerp [3,10]; and

(6) Bateman Manuscript Project (BMP) books [9].

With regard to the seed project (1), the DLMF source already has DLMF macros inserted. However, for seed projects (2-6), we are developing Python and Java software to incorporate DLMF and DRMF macros into the corresponding LaTeX source. Our coding efforts have also focused on extracting formula data from LaTeX source as well as generating DRMF Wikitext. We have developed Java software for the seeding of the eCF and CFSF projects which involve conversion from Mathematica and Maple format to DLMF and DRMF macro incorporated LaTeX [3]. Moreover, in [4] we developed the VMEXT visualization that helps us to investigate the content structure of MathML expressions without reading the verbose parallel MathML markup; see Figure 82.

In August 2014, the DRMF Project obtained permission and license to use BMP material as seed content for the DRMF from Caltech. Caltech has loaned us copies of the BMP. We have forwarded these copies to Alan Sexton, Scientific Document Analysis Group, School of Computer Science, University of Birmingham, UK. Sexton has scanned the BMP and is developing software to perform mathematical optical character recognition to obtain LaTeX source. To enhance the development process of the OCR software, we have developed an automated testing framework that uses visual diffs of the original scanned source and the rendering of the generated LaTeX source.

Current and future DRMF MediaWiki development projects include the production of formula output representations (such as semantic LaTeX, MathML, Mathematica, Maple, and Sage); incorporation of sophisticated DLMF and DRMF macro related formula search; and the development of capabilities for user community formula input. In this vein, Abdou Youssef has written a grammar-based mathematical language processor (MLP) that uses JavaCC to parse mathematical LaTeX expressions. Based on the MLP, André Greiner-Petter has developed a Java tool to convert mathematical LaTeX expressions, which contains DLMF and DRMF macros, to a given computer algebra system source format. This Java tool provides further information of the conversion about possible ambiguities and differences in definitions, domains and branch cuts between the semantic LaTeX source and the CAS source. Furthermore, it is designed to be easily extendable to other computer algebra systems and currently supports Maple and Mathematica input sources.

Our current DRMF server, both public and development instances, have been deployed using the Wikitech server of the Wikimedia Foundation. We use the vagrant virtualization service and configure our machines using puppet roles, which fully automates the installation of new testing or deployment instances. For an efficient data import, we rely on the standard MediaWiki XML Dump format. Our LaTeXML server is located on an instance of the XSEDE Jetstream cloud computing environment.

The DLMF Chapter 25 source has been uploaded to the Wikitech instances as well as the KLS and KLSadd datasets, which have been uploaded for a total of 1842 Wikitext pages [3]. These pages include 1 Main page, 1 Bibliography page, 1 Common.css page, 1 DRMF Requirements page, 2 Table of Contents Pages, 76 Lists of Formulas Pages, 124 Definition Pages, and 1636 Formula Home Pages.

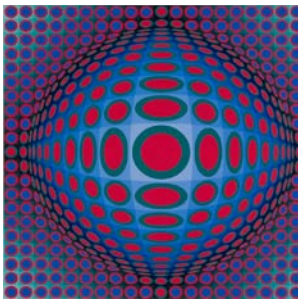

Figure 83. *DRMF logo.*

By working with the Artists Rights Society, New York, NY, we have received permission from Foundation Vasarely, to use an image of one of Victor Vasarely's paintings as the DRMF logo; Figure 83.

[1]H. S. Cohl, M. A. McClain, B. V. Saunders, M. Schubotz and J. C. Williams. Digital Repository of Mathematical Formulae. *Lecture Notes in Artificial Intelligence* **8543** (2014), Proceedings of the Conferences on Intelligent Computer Mathematics 2014, Coimbra, Portugal, July 7-11, 2014, (S. M.

Watt, J. H. Davenport, A. P. Sexton, P. Sojka and J. Urban, eds.), Springer, 419-422.

[2] H. S. Cohl, M. Schubotz, M. A. McClain, B. V. Saunders, C. Y. Zou, A. S. Mohammed and A. A. Danoff. Growing the Digital Repository of Mathematical Formulae with Generic LaTeX Sources. *Lecture Notes in Artificial Intelligence* **9150** (2015), Proceedings of the Conference on Intelligent Computer Mathematics 2015, Washington DC, USA, July 13-17, 2015, (M. Kerber, J. Carette, C. Kaliszyk, F. Rabe and V. Sorge, eds.), Springer, 280-287.

[3] H. S. Cohl, M. Schubotz, A. Youssef, A. Greiner-Petter, J. Gerhard, B. V. Saunders, M. A. McClain, J. Bang, and K. Chen. Semantic Preserving Bijective Mappings of Mathematical Formulae between Word Processors and Computer Algebra Systems. *Lecture Notes in Computer Science* **10383** (2017), Proceedings of the Conference on Intelligent Computer Mathematics 2017, Edinburgh, Scotland, U.K., July 17-21, 2017, (H. Geuvers, M. England, O. Hasan, F. Rabe, O. Teschke, eds.), Springer, 115-131.

[4] M. Schubotz, N. Meuschke, T. Hepp, H. S. Cohl. and B. Gipp. VMEXT: A Visualization Tool for Mathematical Expression Trees. *Lecture Notes in Computer Science* **10383** (2017), Proceedings of the Conference on Intelligent Computer Mathematics 2017, Edinburgh, Scotland, U.K., July 17-21, 2017, (H. Geuvers, M. England, O. Hasan, F. Rabe, O. Teschke, eds.), Springer, 340-345.

[5] M. Schubotz and H.S. Cohl. Content Dictionary Description: Select Symbols from Chapter 9 of the KLS Dataset in the DRMF. OpenMath Workshop, Conference on Intelligent Computer Mathematics 2017, Edinburgh, Scotland, U.K., July 17-21, 2017.

[6] B. Miller. "Drafting DLMF Content Dictionaries." OpenMath Workshop, 9th Conference on Intelligent Computer Mathematics, CICM 2016, Bialystok, Poland.

[7] R. Koekoek, P. A. Lesky and R. F. Swarttouw. *Hypergeometric Orthogonal Polynomials and their q-Analogues*. Springer Monographs in Mathematics, Springer-Verlag, Berlin, 2010.

[8] T. H. Koornwinder. Additions to the Formula Lists in Hypergeometric Orthogonal Polynomials and their q-analogues by Koekoek, Lesky and Swarttouw. arXiv:1401.0815, June 2015.

[9] A. Erdelyi, W. Magnus, F. Oberhettinger and F. G. Tricomi. *Higher Transcendental Functions*, Vols. I, II, III, Robert E. Krieger Publishing Co., Melbourne, FL, 1981.

[10] M. Cuyt, V. Petersen, H. Waadeland, W. B. Jones, F. Backeljauw, C. Bonan-Hamada and S. Becuwe. *Handbook of Continued Fractions for Special Functions*. Springer, New York, 2008.

Fundamental Solutions and Expansions for Special Functions and Orthogonal Polynomials

Howard S. Cohl
Roberto S. Costas-Santos (University of Alcalá, Spain)
Hans Volkmer (University of Wisconsin-Milwaukee)
Gestur Olafsson (Louisiana State University)
T. Mark Dunster (San Diego State University)
Mourad E. H. Ismail (University of Central Florida)
Michael A. Baeder (Citigroup Inc.)
Jessica E. Hirtenstein (University of California Davis)
Philbert R. Hwang (University of Maryland)
Wenqing Xu (Caltech)
Justin Park (Poolesville High School)
Tanay Wakhare (University of Maryland)
Thinh H. Dang (George Washington University)
Jason Zhao (University of California Lost Angeles)
Naveen Raman (Richard Montgomery High School)

The concept of a function expresses the idea that one quantity (the input) completely determines another quantity (the output). Our research concerns special functions and orthogonal polynomials. A special function is a function that has appeared in the mathematical sciences so often that it has been given a name. Green's functions (named after the British mathematician George Green, who first developed the concept in the 1830s) describe the influence of linear natural phenomena such as electromagnetism, gravity, heat and waves. For example, in electrostatics, a Green's function describes the influence of a point charge, called the source, over all of space. The inputs for Green's functions are all of space (with the exception of a singular region), and the output is the "force" exerted from the point throughout space. Green's functions are fundamental to the study of partial differential equations and are powerful mechanisms for obtaining their solutions.

We investigate fundamental solutions (Green's functions) of linear partial differential equations on highly symmetric Riemannian manifolds (harmonic, rank-one symmetric spaces) such as real, complex, quaternionic, and octonionic Euclidean, hyperbolic, and projective spaces. Our recent focus has been on applications of fundamental solutions for linear elliptic partial differential operators on spaces of constant curvature. We have constructed closed-form expressions of a fundamental solution for the Helmholtz equation in d-dimensional spaces of constant positive and negative curvature. These were in the hyperboloid model of hyperbolic geometry, in terms of associated Legendre functions, and on the d-dimensional hypersphere, in terms of Ferrers functions [1]. With Gestur Olafsson, we are also preparing work on fundamental solutions for the Laplace-Beltrami operator on rank one symmetric spaces of compact and noncompact type [2].

Cohl is working with J. E. Hirtenstein on deriving Gegenbauer expansions and addition theorems for binomial and logarithmic fundamental solutions of the polyharmonic equation in even-dimensional space with powers of the Laplacian greater than or equal to the dimension divided by two [3]. In conjunction with J. Park and H. Volkmer, Cohl is computing all Gauss hypergeometric representations of Ferrers functions of the second kind by starting with the full list 18 Gauss hypergeometric representations for the associated Legendre function of the second kind [4].

In the following works, we derive and use properties of hypergeometric orthogonal polynomials. In particular, we compute specializations and generalizations of generalized and basic hypergeometric orthogonal polynomial generating functions as well as corresponding definite integrals using orthogonality. We present the power collection method for hypergeometric orthogonal polynomials, and summarize for which orthogonal polynomials in the Askey and q-Askey schemes, it can be applied [5]. Here, we apply the power collection method to Meixner polynomials and compute a series of connection and connection-type relations for these orthogonal polynomials. We also apply these connection and connection-type relations to generating functions for Meixner and Krawtchouk polynomials.

Our series-rearrangement technique is extended to generalizations of generating functions for basic hypergeometric orthogonal polynomials in [6]. Here, we derive generalizations of generating functions for Askey-Wilson, q-ultraspherical/Rogers, q-Laguerre, and little q-Laguerre/Wall polynomials, and also derive a new quadratic transformation for basic hypergeometric series, and a Wilson polynomial expansion which corresponds to the generalized Rogers generating function given by Ismail.

We give contour integral orthogonality relations for the Al-Salam-Carlitz polynomials which is valid for arguments in the complex plane and complex-valued parameters in [7]. Here, we compute generalized generating functions for the Al-Salam-Carlitz polynomials using connection relation for these polynomials.

We obtain q-analogues of the Sylvester, Cesaro, Pasternack, and Bateman polynomials in [8]. Here, we also derive generating functions for these polynomials. We derive generalized linearization formulas for generalized and basic hypergeometric orthogonal polynomials by applying connection relations to them in [9]. Here, in conjunction with student Naveen Rahman, we generalize linearization formulae for Laguerre, Gegenbauer, continuous q-ultraspherical/Rogers, Jacobi, and continuous q-Jacobi polynomials. Cohl also worked with S. Casey in a recent project which uses the projection method with a basis system designed to work with Ultra-Wideband Signals, implementing modified Gegenbauer functions designed specifically for these signals in [10].

Cohl served on the Scientific and Local Organizing committees for the Orthogonal Polynomials and Special Functions Summer School 6 (OPSF-S6) workshop which was held on June 17-23, 2016 at the Norbert Wiener Center for Harmonic Analysis and Applications at the University of Maryland. The OPSF-S6 lecture notes will be published by Cambridge University Press, edited by H. S. Cohl and M. E. H. Ismail, including lecture notes by A. Duran, M. E. H. Ismail, E. Koelink, H. Rosengren, and J. Zeng [11].

[1] H. S. Cohl, T. H. Dang and T.M. Dunster. Fourier and Gegenbauer Expansions for a Fundamental Solution of the Helmholtz Operator in Riemannian Spaces of Constant Curvature. In preparation.

[2] G. Olafsson and H. S. Cohl. Fundamental Solutions for the Laplace-Beltrami Operator on the Rank One Symmetric Spaces. In preparation.

[3] H. S. Cohl and J. E. Hirtenstein. Binomial and Logarithmic Gegenbauer Expansions for the Even-dimensional Polyharmonic Equation. In preparation.

[4] H. S. Cohl, J. Park and H. Volkmer. Gauss Hypergeometric Representations of Ferrers Functions of the Second Kind. In preparation.

[5] M. A. Baeder, R. S. Costas-Santos and W. Xu. The Power Collection Method for Connection Relations: Meixner Polynomials. *Journal of Classical Analysis* **11**:2 (2017).

[6] H. S. Cohl, R. S. Costas-Santos, P. R. Hwang and T. V. Wakhare. Generalizations of Generating Functions for Basic Hypergeometric Orthogonal Polynomials. In review.

[7] H. S. Cohl, R. S. Costas-Santos and W. Xu. The Orthogonality of Al-Salam-Carlitz Polynomials for Complex Parameters. In *Frontiers in Orthogonal Polynomials and q-Series* (Z. Nashed and X. Li, eds.), World Scientific Publishing (2017).

[8] H. S. Cohl, R. S. Costas-Santos and T. V. Wakhare. Some Generating Functions for q-Polynomials. In review.

[9] H. S. Cohl, R. S. Costas-Santos and J. Zhao. Generalizations of Linearization Formulae for Continuous Hypergeometric Orthogonal Polynomials. In preparation.

[10] S. D. Casey and H. S. Cohl. Sampling Architectures for Ultra-Wideband Signals. In Sampling Theory and Applications, 12th International Conference 2017, Tallinn, Estonia, July 3-7, 5 pages.

[11] *Lecture Notes from the Sixth Orthogonal Polynomials and Special Functions Summer School 2016* (M. E. H. Ismail and H. S. Cohl, eds.), Cambridge University Press, in preparation.

Part IV

Activity Data

Publications

Note: Names of authors with a Division affiliation during this reporting period are underlined.

Appeared

Refereed Journals

1. M. A. Baeder, H. S. Cohl, R. S. Costas-Santos and W. Xu. The Power Collection Method for Connection Relations: Meixner Polynomials. *Journal of Classical Analysis* **11**:2 (2017), 107-128. DOI: 0.7153/jca-2017-11-02
2. N. Bao, R. Bousso, S. Jordan and B. Lackey. Fast Optimization Algorithms and the Cosmological Constant. *Physical Review D* **96** (2017), 103512. DOI: 10.1103/PhysRevD.96.103512
3. W. J. Boettinger, M. E. Williams, K. W. Moon, G. B. McFadden, P. N. Patrone and J. H. Perepezko. Interdiffusion in the Ni-Re System: Evaluation of Uncertainties. *Journal of Phase Equilibria and Diffusion* **38**:5 (2017), 750-763. DOI: 10.1007/s11669-017-0562-7
4. J. Bullard, E. Garboczi, P. Stutzman, P. Feng, A. Brand, L. Perry, J. Hagedorn, W. Griffin and J. Terrill. Measurement and Modeling Needs for Microstructure and Reactivity of Next-Generation Concrete Binders. *Cement and Concrete Composites* (2017). DOI: 10.1016/j.cemconceomp.2017.06.012
5. J. Bullard, J. Hagedorn, T. Ley, Q. Hu, W. Griffin and J. Terrill. A Critical Comparison of 3D Experiments and Simulations of Tricalcium Silicate Hydration. *Journal of the American Ceramic Society* **101**:4 (2018), 1453-1470. DOI: 10.1111/jace.15323
6. H. S. Cohl, S. J. Nair and R. M. Palmer. Some Dual Definite Integrals for Bessel Functions. *Scientia, Series A, Mathematical Sciences*, **27** (2016), 15-30.
7. S. Colbert-Kelly, G. B. McFadden, D. Phillips and J. Shen. Numerical Analysis and Simulation for a Generalized Planar Ginzburg-Landau Equation in a Circular Geometry. *Communications in Mathematical Sciences* **15**:2 (2017), 329-357. DOI: 10.4310/CMS.2017.v15.n2.a3
8. R. Denlinger, L. Greengard, Z. Gimbutas and V. Rokhlin. A Fast Summation Method for Oscillatory Lattice Sums. *Journal of Mathematical Physics* **58**:023511 (2017), arXiv: 1609.08523. DOI: 10.1063/1.4976499
9. W. B. Doriese, P. Abbamonte, B. K. Alpert, D. A. Bennett, E. V. Denison, Y. Fang, D. A. Fischer, C. P. Fitzgerald, J. W. Fowler, J. D. Gard, J. P. Hays-Wehle, G. C. Hilton, C. Jaye, J. L. McChesney, L. Miaja-Avila, K. M. Morgan, Y. I Joe, G. C. O'Neil, C. D. Reintsema, F. Rodolakis, D. R. Schmidt, H. Tatsuno, J. Uhlig, L. R. Vale, J. N. Ullom and D. S. Swetz. A Practical Superconducting-Microcalorimeter X-ray Spectrometer for Beamline and Laboratory Science. *Review of Scientific Instruments* **88** (2017), 053108. DOI: 10.1063/1.4983316
10. T. G. Downes, J. R. Van Meter, E. Knill, G. J. Milburn and C. M. Caves. Quantum Estimation of Parameters of Classical Spacetimes. *Physical Review D* **96** (2017), 105004. DOI: 10.1103/PhysRevD.96.105004
11. D. A. Edwards, R. M. Evans and W. Li. Measuring Kinetic Rate Constants of Multiple Component Reactions with Optical Sensors. *Analytical Biochemistry* **533** (2017), 41-47. DOI: 10.1016/j.ab.2017.06.009
12. R. M. Evans, David A. Edwards. Transport Effects on Multiple-Component Reactions in Optical Biosensors. *Bulletin of Mathematical Biology* **79** (2017), 2214-2241. DOI: 10.1007/s11538-017-0327-9
13. J. W. Fowler, B. K. Alpert, W. B. Doriese, J. Hayes-Wehle, Y. I. Joe, K. M. Morgan, G. C. O'Neil, C. D. Reintsema, D. R. Schmidt, J. N. Ullom and D. S. Swetz. When Optimal Filtering Isn't. *IEEE Transactions on Applied Superconductivity* **27**:4 (2017), 2500404. DOI: 10.1109/TASC.2016.2637359
14. J. W. Fowler, B. K. Alpert, W. B. Doriese, G. C. Hilton, L. T. Hudson, T. Jach, Y. I. Joe, K. M. Morgan, G. C. O'Neil, C. D. Reintsema, D. R. Schmidt, D. S. Swetz, C. Szabo-Foster and J. N. Ullom. A Reassessment of Absolute X-ray Line Energies for Lanthanide Metals. *Metrologia* **54**:4 (2017), 494-511. DOI: 10.1088/1681-7575/aa722f
15. P. Guba and D. M. Anderson. Pattern Selection in Ternary Mushy Layers. *Journal of Fluid Mechanics* **825** (2017), 853-886. DOI: 10.1017/jfm.2017.382
16. T. Hoft and B. K. Alpert. Fast Updating Multipole Coulombic Potential Calculation. *SIAM Journal on Scientific Computing* **39**:3 (2017), A1038-A1061. DOI: 10.1137/16M1096189
17. C. L. Holloway, M. T. Simons, J. A. Gordon, A. Dienstfrey, D. A. Anderson and G. Raithel. Electric Field Metrology for SI Traceability: Systematic Measurement Uncertainties in Electromagnetically Induced Transparency in Atomic Vapor. *Journal of Applied Physics* **121**:233106 (2017). DOI: 10.1063/1.4984201
18. M. Jarret and S. Jordan. Modulus of Continuity Eigenvalue Bounds for Homogeneous Graphs and Convex Subgraphs with Applications to Quantum Hamiltonians. *Journal of Mathematical Analysis*

and Applications **452**:2 (2017), 1269-1290. DOI: 10.1016/j.jmaa.2017.03.030

19. M. Jarret, S. P. Jordan and B. Lackey. Adiabatic Optimization Versus Diffusion Monte Carlo Methods. *Physical Review A* **94** (2016), 042318. DOI: 10.1103/PhysRevA.94.042318

20. S. Jordan. Fast Quantum Computation at Arbitrarily Low Energy. *Physical Review A* **95** (2017), 032305. DOI: 10.1103/PhysRevA.95.032305

21. S. Keshavarz, Z. Molaeinia, A. C. E. Reid and S. A. Langer. Morphology Dependent Flow Stress in Nickel Based Superalloys in the Multi-Scale Crystal Plasticity Framework. *Crystals* **7**:334 (2017). DOI: 10.3390/cryst7110334

22. S. Keshavarz, S. Ghosh, A. C. E. Reid and S. A. Langer. A Non-Schmid Crystal Plasticity Finite Element Approach to Multi-Scale Modeling of Nickel-Based Superalloys. *Acta Materialia* **114**:106 (2016). DOI: 10.1016/j.actamat.2016.05.016

23. F. Krahmer and Y. K. Liu. Phase Retrieval Without Small-Ball Probability Assumptions. *IEEE Transactions on Information Theory* **64**:1 (2018), 1-16. DOI: 10.1109/TIT.2017.2757520

24. P. S. Kuo, T. Gerrits, V. Verma and S. W. Nam. Spectral Correlation and Interference in Non-Degenerate Photon Pairs at Telecom Wavelengths. *Optics Letters* **41**:21 (2016), 5074. DOI: 10.1364/OL.41.005074

25. R. J. La. Effects of Degree Correlations in Interdependent Security: Good or Bad? *IEEE/ACM Transactions on Networking* **25**:4 (2017), 2484-2497. DOI: 10.1109/TNET.2017.2691605

26. Y. Lin, J. P. Gaebler, F. Reiter, T. R. Tan, R. Bowler, Y. Wan, A. Keith, E. Knill, S. Glancy, K. Coakley, A. S. Sorensen, D. Leibfried and D. J. Wineland. Preparation of Entangled States by Hilbert Space Engineering. *Physical Review Letters*, **117** (2016), 140502. DOI: 10.1103/PhysRevLett.117.140502

27. L. Ma, O. Slattery and X. Tang. Optical Quantum Memory Based on Electromagnetically Induced Transparency. *Journal of Optics* **19**:4 (2017), 043001. DOI: 10.1088/2040-8986/19/4/043001

28. L. Ma, O. Slattery and X. Tang. Spectral Characterization of Single Photon Sources with Ultra-High Resolution, Accuracy and Sensitivity. *Optics Express* **25**:23 (2017), 28898. DOI: 10.1364/OE.25.028898

29. F. Maggioni, F. A. Potra and M. Bertocchi. A Scenario-Based Framework for Supply Planning Under Uncertainty: Stochastic Programming Versus Robust Optimization Approaches. *Computational Management Science* **14**:1 (2017), 5-44. DOI: 10.1007/s10287-016-0272-3

30. H. Mahboubi, K. Moezzi, A. Aghdam and K. Sayrafian. Distributed Sensor Coordination Algorithms for Efficient Coverage in a Network of Heterogeneous Mobile Sensors. *IEEE Transactions on Automatic Control* **62**:11, 5954-5961. DOI: 10.1109/TAC.2017.2714102

31. H. Mahboubi, W. Masoudimansour, A. Aghdam and K. Sayrafian. An Energy-Efficient Target-Tracking Strategy for Mobile Sensor Networks. *IEEE Transactions on Cybernetics* **47**:2, 511-523. DOI: 10.1109/TCYB.2016.2519939

32. W. Mitchell. 30 Years of Newest Vertex Bisection. *Journal of Numerical Analysis, Industrial and Applied Mathematics* **11** (2017), 11-22. URL: http://www.jnaiam.org/index.php?/archives/125-30-Years-of-Newest-Vertex-Bisection.html

33. G. O'Neil, L. Miaja-Avila, Y. Joe, B. Alpert, M. Balasubramanian, S. Dodd, W. Doriese, J. Fowler, W. Fullagar, G. Hilton, R. Jimenez, B. Ravel, C. Reintsema, D. Schmidt, K. Silverman, D. Swetz, J. Uhlig and J. Ullom. Ultrafast time-resolved X-ray Absorption Spectroscopy of Ferrioxalate Photolysis with a Laser Plasma X-ray Source and Microcalorimeter Array. *The Journal of Physical Chemistry Letters* **8** (2017), 1099-1104. DOI: 10.1021/acs.jpclett.7b00078

34. P. N. Patrone and T. W. Rosch. Beyond Histograms: Efficiently Estimating Radial Distribution Functions via Spectral Monte Carlo. *The Journal of Chemical Physics* **146**:9 (2017), 094107. DOI: 10.1063/1.4977516

35. P. N. Patrone, S. Tucker and A. Dienstfrey. Estimating Yield-Strain via Deformation-Recovery Simulations. *Polymer* **116**:5 (2017), 295-303. DOI: 10.1016/j.polymer.2017.03.046

36. F. A. Potra. A Superquadratic Variant of Newton's Method. *SIAM Journal on Numerical Analysis* **55**:6 (2017), 2863-2884. DOI: 10.1137/17M1121056

37. A. P. Reed, K. H. Mayer, J. D. Teufel, L. D. Burkhart, W. Pfaff, M. Reagor, L. Sletten, X. Ma, R. J. Schoelkopf, E. Knill and K. W. Lehnert. Faithful Conversion of Propagating Quantum Information to Mechanical Motion. *Nature Physics* **13** (2017), 1163-1167. DOI: 10.1038/nphys4251

38. B. I. Schneider, L. A. Collins, K. Bartschat, X. Guan and S. X. Hu. A Few Selected Contributions to Electron and Photon Collisions with H_2 and H^+_2. *Journal of Physics* **50** (2017), 214004. DOI: 10.1088/1361-6455/aa8e6d

39. R. F. Sekerka, G. B. McFadden and W. J. Boettinger. Analytical Derivation of the Sauer-Freise Flux Equation for Multicomponent Multiphase Diffusion Couples with Variable Partial Molar Volumes. *Journal of Phase Equilibria and*

Diffusion **37** (2016), 640-650. DOI: 10.1007/s11669-016-0500-0

40. C. Shen, R. W. Heeres, P. Reinhold, L. Jiang, Y. K. Liu, R. J. Schoelkopf and L. Jiang. Optimized Tomography of Continuous Variable Systems Using Excitation Counting. *Physical Review A* **94** (2016), 052327. DOI: 10.1103-PhysRevA.94-052327

41. G. B. Silva, H. M. Vasconcelos and S. Glancy. Investigating Bias in Maximum Likelihood Quantum State Tomography. *Physical Review A* **95** (2017), 022107. DOI: 10.1103/PhysRevA.95.022107

42. J. S. Sims. Hylleraas-Configuration Interaction Study of the Singlet S Ground State of the Negative Li Ion. *Journal of Physics B: Atomic, Molecular and Optical Physics* **50**:24 (2017), 245003. DOI: 10.1088/1361-6455-aa961e

43. T. R. Tan, Y. Wan, S. Erickson, P. Bierhorst, D. Kienzler, S. Glancy, E. Knill, D. Leibfried and D. J. Wineland. Chained Bell Inequality Experiment with High-Efficiency Measurements. *Physical Review Letters*, **118** (2017), 130403. DOI: 10.1103/PhysRevLett.118.130403

44. J. C. Wu, A. F. Martin, C. S. Greenberg and R. N. Kacker. Impact of Data Dependence on Speaker Recognition Evaluation. *IEEE/ACM Transactions on Audio, Speech and Language Processing* **25** (2017) 5-18. DOI: 10.1109/TASLP.2016.2614725

45. J. C. Wu, M. Halter, R. N. Kacker, J. T. Elliott and A. L. Plant. A Novel Measure and Significance Testing in Data Analysis of Cell Image Segmentation. *BMC Bioinformatics* **18**:168 (2017). DOI: 10.1186/s12859-017-1527-x

46. H. Zhao, G. W. Bryant, W. Griffin, J. E. Terrill and J. Chen, Validation of Split Vectors Encoding for Quantitative Visualization of Large-Magnitude-Range Vector Fields. *IEEE Transactions on Visualization and Computer Graphics* **23**:6 (2017), 1691-1705. DOI: 10.1109/TVCG.2016.2539949

Journal of Research of NIST

1. D. Juba, D. J. Audus, M. Mascagni, J. F. Douglas and W. Keyrouz. ZENO: Software for Calculating Hydrodynamic, Electrical and Shape Properties of Polymer and Particle Suspensions**.** *Journal of Research of the NIST* 122 (2017), 20. DOI: 10.6028/jres.122.020

2. V. Sriram and W. Griffin. A Sampling-Agnostic Software Framework for Converting Between Texture Map Representations of Virtual Environments. *Journal of Research of the NIST* **122** (2017), 25. DOI: 10.6028/jres.122.025

Book Chapters

1. H. S. Cohl, R. S. Costas-Santos and W. Xu. The Orthogonality of Al-Salam-Carlitz Polynomials for Complex Parameters. *Orthogonal Polynomials and q-Series* (Z. Nashed and X. Li, eds.), World Scientific Publishing, 2017, 155-167.

In Conference Proceedings

1. M. Barbi, K. Sayrafian and M. Alasti. Low Complexity Adaptive Schemes for Energy Detection Threshold in IEEE802.15.6 CSMA/CA. In *Proceedings of the 2016 IEEE Conference on Standards for Communications & Networking (CSCN'16)*, Berlin, Germany, October 31-November 2, 2016. DOI: 10.1109/CSCN.2016.7785182

2. S. D. Casey and H. S. Cohl. Sampling Architectures for Ultra-Wideband Signals. In *Proceedings of the 12th International Conference on Sampling Theory and Applications*, Tallinn, Estonia, July 3-7, 2017, 246-250. DOI: 10.1109/SAMPTA.2017.8024452

3. J. Chandrasekaran, H. Feng, Y. Lei, D. R. Kuhn and R. N. Kacker. Applying Combinatorial Testing to Data Mining Algorithms. In *Proceedings of the 10th IEEE International Conference on Software Testing, Verification and Validation Workshops (ICSTW)*, Tokyo, Japan, March 13-17, 2017, 253-261. DOI: 10.1109/ICSTW.2017.46

4. Z. Chen, J. Win, A. Kearsley and A. Pertzborn. Scaling Methods for Dynamic Building System Simulation in an HVACSIM+Envirnoment. In *Proceedings of Building Simulation 2017*, San Francisco, CA, August 7-9, 2017, 1984-1990. URL: http://www.ibpsa.org/proceedings/BS2017/BS2017_534.pdf

5. H. S. Cohl, M. Schubotz, A. Youssef, A. Greiner-Petter, J. Gerhard, B. V. Saunders, M. A. McClain, J. Bang and K. Chen. Semantic Preserving Bijective Mappings of Mathematical Formulae Between Word Processors and Computer Algebra Systems. In: H. Geuvers, M. England, O. Hasan, F. Rabe and O. Teschke, eds. *Intelligent Computer Mathematics. CICM 2017*. Lecture Notes in Computer Science **10383**. Springer, 115-131. DOI: 10.1007/978-3-319-62075-6_9

6. G. Doğan. An Efficient Lagrangian Algorithm for an Anisotropic Geodesic Active Contour Model. In *Scale Space and Variational Methods in Computer Vision*, SSVM 2017. (F. Lauze, Y. Dong and A. Dahl, eds.) *Lecture Notes in Computer Science* **10302** (2017). Springer. DOI: 10.1007/978-3-319-58771-4_33

7. F. Duan, Y. Lei, L. Yu, R. N. Kacker and D. R. Kuhn. Optimizing IPOG's Vertical Growth with

Constraints Based on Hypergraph Coloring. In *Proceedings of the 10th IEEE International Conference on Software Testing, Verification and Validation Workshops (ICSTW)*, Tokyo, Japan, March 13-17, 2017, 181-188, DOI: 10.1109/ICSTW.2017.37

8. J. T. Fong, N. A. Heckert, J. J. Filliben, P. V. Marcal, R. Rainsberger, K. Stupic and S. Russek. MRI Birdcage RF Coil Resonance with Uncertainty and Relative Error Convergence Rates. In *Proceedings of 2017 COMSOL Users' Conference*, Boston, MA, October 4-6, 2017.

9. H. Guan, P. Y. Lee, C. L. Lamp, A. M. Dienstfrey, M. F. Theofanos, B. C. Stanton and M. Schwarz. Analysis, Comparison, and Assessment of Latent Fingerprint Preprocessing. In *Proceedings of the IEEE Conference on Computer Vision and Pattern Recognition Workshops (CVPRW)*, Honolulu, HI, July 22-25, 2017. DOI: 10.1109/CVPRW.2017.91

10. A. Gueye, C. Mahmoudi, O. I. Elmimouni, M. L. Gueye and S. O. Ndiaye. An Opportunistic Connectivity Network for Rural Areas in Senegal. In *Proceedings of the 1st EAI International Conference on Innovation and Interdisciplinary Solutions for Underserved Areas (InterSol2017)*, Dakar-Senegal, April 11-12, 2017.

11. S. Kimmel and Y. K. Liu. Phase Retrieval Using Unitary 2-Designs. In *Proceedings of the 2017 International Conference on Sampling Theory and Applications (SampTA)*, Tallinn, Estonia, July 3-7, 2017. DOI: 10.1109/SAMPTA.2017.8024414

12. D. R. Kuhn, R. N. Kacker and Y. Lei. A Model for T-Way Fault Profile Evolution During Testing. In *Proceedings of the 10th IEEE International Conference on Software Testing, Verification and Validation Workshops (ICSTW)*, Tokyo, Japan, March 13-17, 2017, 162-170. DOI: 10.1109/ICSTW.2017.35

13. D. R. Kuhn, M. S. Raunak and R. N. Kacker. An Analysis of Vulnerability Trends, 2008-2016. In *Proceedings of the IEEE International Conference on Software Quality, Reliability, and Security (QRS 2017)*, Prague, Czech Republic, July 25-29, 2017. DOI: 10.1109/QRS-C.2017.106

14. P. S. Kuo, T. Gerrits, V. Verma and S. W. Nam. Spectral Correlation and Interference in Continuous-wave Non-Degenerate Photon Pairs at Telecom Wavelengths. In *Proceedings of the SPIE*, San Francisco, CA, January 28 - February 2, 2017. DOI: 10.1117/12.2263389

15. R. J. La. Influence of Network Mixing on Interdependent Security: Local Analysis. In *Proceedings of the 2016 IEEE Global Communications Conference (GLOBECOM)*, Washington, DC, December 4-8, 2016. DOI: 10.1109/GLOCOM.2016.7841901

16. R. J. La. Effects of Degree Variability and Dependence on Cascading Failures: A Case Study of Two Interdependent Systems. In *Proceedings of the 51st Conference on Information Sciences and Systems (CISS)*, Johns Hopkins University, Baltimore, MD, March 22-24, 2017.

17. R. J. La. Estimation of Externalities in Interdependent Security: A Case Study of Large System. In *Proceedings of the 56th IEEE Conference on Decision and Control (CDC)*, Melbourne, Australia, December 12-15, 2017.

18. D. Li, L. Hu, R. Gao, W. E. Wong, D. R. Kuhn and R. N. Kacker, Improving MC/DC and Fault Detection Strength Using Combinatorial Testing. In *Proceedings of the IEEE International Conference on Software Quality, Reliability, and Security (QRS 2017)*, Prague, Czech Republic, July 25-29, 2017. DOI: 10.1109/QRS-C.2017.131

19. V. Marbukh. Towards Cross-Layer Design of Communication Network for Smart Grid with Real-Time Pricing. In *Proceedings of the IEEE SmartGridComm*, Sydney, Australia, November 2016.

20. V. Marbukh and K. Sayrafian. Regret Minimization Based Adaptation of the Energy Detection Threshold in Body Area Networks. In *Proceedings of Global Internet of Things Summit (GIoTS)*, Geneva, Switzerland, June 6-9, 2017, 1-6. **DOI:** 10.1109/GIOTS.2017.8016231

21. V. Marbukh. Fragility Risks of Low Latency Dynamic Queuing in Large-Scale Clouds: Complex Systems Perspective. In *Proceedings of the IFIP Networking Conference*, Stockholm, Sweden, June 2017.

22. P. V. Marcal, J. T. Fong, R. Rainsberger and L. Ma. Error Norm vs. Uncertainty Metric in Assessing Accuracy of the Finite Element Method. In *Proceedings of ASME 2017 Pressure Vessels and Piping Conference*, Kawaii, HI, July 17-21, 2017.

23. D. G. Porter. Introduction to the HAMT and Tcl. In *Proceedings of the 24th Annual Tcl/Tk Conference*, Houston, TX, October 16-20, 2017.

24. L. Rabieekenari, K. Sayrafian and J. S. Baras. Autonomous Relocation Strategies for Cells on Wheels in Public Safety Networks. In *Proceedings of the 14th IEEE Annual Consumer Communications & Networking Conference*, Las Vegas, NV, January 8-11, 2017, 41-44. DOI: 10.1109/CCNC.2017.7983079

25. L. Rabieekenari, K. Sayrafian. and J. Baras. Autonomous Relocation Strategies for Cells on Wheels in Environments with Prohibited Areas. In *Proceedings of the IEEE International Conference on*

Communications (ICC'17), Paris, France, May 21-25, 2017, 1-6. DOI: 10.1109/ICC.2017.7997091

26. L. Rabieekenari, K. Sayrafian and J. Baras. Autonomous Relocation of Mobile Base Stations in Emergency Scenarios. In *Proceedings of the Workshop on Dependable Wireless Communications and Localization for the IoT*, Graz, Austria, September 12, 2017. URL: https://www.tugraz.at/fileadmin/user_upload/Projekte/Dependablethings/IRACON_WS_17/19_Rabieekenari.pdf

27. Z. B. Ratliff, D. R. Kuhn, R. N. Kacker, Y. Lei and K. S. Trivedi. The Relationship Between Software Bug Type and Number of Factors Involved in Failures. In *Proceedings of the 27th IEEE International Symposium on Software Reliability Engineering (ISSRE) Workshops*, Ottawa, Canada, October 23-27, 2016, 119-124. DOI: 10.1109/ISSREW.2016.26

28. M. S. Raunak, D. R. Kuhn and R. N. Kacker. Combinatorial Testing of Full Text Search in Web Applications. In *Proceedings of the IEEE International Conference on Software Quality, Reliability, and Security (QRS 2017)*, Prague, Czech Republic, July 25-29, 2017. DOI: 10.1109/QRS-C.2017.24

29. B. I. Schneider, How Novel Algorithms and Access to High Performance Computing Platforms are Enabling Scientific Progress in Atomic and Molecular Physics. In *Journal of Physics Conference Series* **759**:1 (2016), 012002. DOI: 10.1088/1742-6596/759/1/012002

30. M. Schubotz, N. Meuschke, T. Hepp, H. S. Cohl and B. Gipp. VMEXT: A Visualization Tool for Mathematical Expression Trees. In: H. Geuvers, M. England, O. Hasan, F. Rabe and O. Teschke, eds. *Intelligent Computer Mathematics. CICM 2017*. Lecture Notes in Computer Science **10383**. Springer, 340-355. DOI: 10.1007/978-3-319-62075-6_24

31. D. Simos, D. R. Kuhn, R. N. Kacker and S. Mekesis. Combinatorial Coverage Measurement of Test Vectors Used in Cryptographic Algorithm Validation. In *Proceedings of the 28th IEEE Software Technology Conference (STC 2017)*, Gaithersburg, MD, September 25-28, 2017.

32. F. Sullivan and I. Beichl. Merging Data Science and Large Scale Computational Modeling. In *Proceedings of the New Frontiers in High Performance Computing and Big Data*, (G. Fox, V. Getov, L. Grandinetti, G. Joubert and T. Sterling, eds.), *Advances in Parallel Computing* **30** (2017), 227-234. DOI: 10.3233/978-1-61499-816-7-227

33. S. Vilkomir, A. Alluri, D. R. Kuhn and R. N. Kacker. Combinatorial and MC/DC Coverage Levels of Random Testing. In *Proceedings of the IEEE International Conference on Software Quality, Reliability, and Security (QRS 2017)*, Prague, Czech Republic, July 25-29, 2017. DOI: 10.1109/QRS-C.2017.19

34. A. Youssef. Part-of-Math Tagging and Applications. In: H. Geuvers, M. England, O. Hasan, F. Rabe and O. Teschke, eds. *Intelligent Computer Mathematics. CICM 2017*. Lecture Notes in Computer Science **10383**. Springer. DOI: 10.1007/978-3-319-62075-6_25

Technical Magazine Articles

1. R. F. Boisvert. Incentivizing Reproducibility. *Communications of the ACM* **50** (October 2016), 5. DOI: 10.1145/2294031

2. D. R. Kuhn, A. G. Voyiatzis and R. N. Kacker. D. E. Simos. Combinatorial Methods in Security Testing. *IEEE Computer* **49** (2016), 80-83. DOI: 10.1109/MC.2016.314

3. R. Kuhn, M. Raunak and R. Kacker. It Doesn't Have to be Like This: Cybersecurity Vulnerability Trends. *IT Professional* **19**:6 (2017), 66-70. DOI: 10.1109/MITP.2017.4241462

Technical Reports

1. R. F. Boisvert (ed.). Applied and Computational Mathematics Division, Summary of Activities for Fiscal Year 2016. NISTIR 8175, March 2017, 132 pages. DOI: 10.6028/NIST.IR.8175

2. E. Knill, Y. Zhang and P. Bierhorst. Quantum Randomness Generation by Probability Estimation with Classical Side Information. arXiv:1709.06159 (2017).

3. A. Olivas, C. F. Ferraris, N. S. Martys, W. L. George, E. J. Garboczi and B. Toman. Certification of SRM 2493: Standard Reference Mortar for Rheological Measurements, NIST Special Publication 260-187 (2017).

4. A. Olivas, M. A. Helsel, N. S. Martys, C. F. Ferraris, W. L. George and R. Ferron. Rheological Measurement of Suspensions without Slippage: Experiment and Model. NIST Technical Note 1946 (2016).

5. P. Wills, E. Knill, K. Coakley and Y. Zhang. Performance of Test Supermartingale Confidence Intervals for the Success Probability of Bernoulli Trials. arXiv:1709.04078 (2017).

NIST Blog Posts

1. B. Saunders. Plotting a Path from NASA Grids to NIST Graphics. Taking Measure Blog, NIST Public Affairs Office, April 27, 2017.

Accepted

1. C. Abellán, A. Acín, A. Alarcón, O. Alibart, C. K. Andersen, F. Andreoli, A. Beckert, F. A. Beduini, A. Bendersky, M. Bentivegna, P. Bierhorst, D. Burchardt, A. Cabello, J. Cariñe, S. Carrasco, G. Carvacho, D. Cavalcanti, R. Chaves, J. Cortés-Vega, A. Cuevas, A. Delgado, H. de Riedmatten, C. Eichler, P. Farrera, J. Fuenzalida, M. García-Matos, R. Garthoff, S. Gasparinetti, T. Gerrits, F. Ghafari Jouneghani, S. Glancy, E. S. Gómez, P. González, J.-Y. Guan, J. Handsteiner, J. Heinsoo, G. Heinze, A. Hirschmann, O. Jiménez, F. Kaiser, E. Knill, L. T. Knoll, S. Krinner, P. Kurpiers, M. A. Larotonda, J.-Å. Larsson, A. Lenhard, H. Li, M.-H. Li, G. Lima, B. Liu, Y. Liu, I. H. López Grande, T. Lunghi, X. Ma, O. S. Magaña-Loaiza, P. Magnard, A. Magnoni, M. Martí-Prieto, D. Martínez, P. Mataloni, A. Mattar, M. Mazzera, R. P. Mirin, M. W. Mitchell, S. Nam, M. Oppliger, J.-W. Pan, R. B. Patel, G. J. Pryde, D. Rauch, K. Redeker, D. Rieländer, M. Ringbauer, T. Roberson, W. Rosenfeld, Y. Salathé, L. Santodonato, G. Sauder, T. Scheidl, C. T. Schmiegelow, F. Sciarrino, A. Seri, L. K. Shalm, S.-C. Shi, S. Slussarenko, M. J. Stevens, S. Tanzilli, F. Toledo, J. Tura, R. Ursin, P. Vergyris, V. B. Verma, T. Walter, A. Wallraff, Z. Wang, H. Weinfurter, M. M. Weston, A. G. White, C. Wu, G. B. Xavier, L. You, X. Yuan, A. Zeilinger, Q. Zhang, W. Zhang and J. Zhong. Challenging Local Realism with Human Randomness. *Nature*, The BIG Bell Test Collaboration.
2. M. Barbi, K. Sayrafian and M. Alasti. Application of Link Adaptation in Body Area Networks. 28th Annual IEEE International Symposium on Personal, Indoor and Mobile Radio Communications (IEEE PIMRC 2017), Montreal, Canada, October 8-13, 2017.
3. P. Bierhorst, E. Knill, S. Glancy, Y. Zhang, A. Mink, S. Jordan, A. Rommal, Y. K. Liu, B. Christensen, S. W. Nam, M. J. Stevens and L. K. Shalm. Experimentally Generated Random Numbers Certified by the Impossibility of Superluminal Signaling. *Nature.*
4. R. Brinson, F. Delaglio, L. Arbogast, R. Evans and A. Kearsley, + 49 additional co-authors. Benchmarking the Precision and Robustness of 2D-NMR for Protein Therapeutics: An International Inter-Laboratory NMR Study. *Nature Biotechnology*.
5. H. S. Cohl, R. S. Costas-Santos and W. Xu. The Orthogonality of Al-Salam-Carlitz Polynomials for Complex Parameters. *Frontiers in Orthogonal polynomials and q-Series.*
6. R. M. Evans and D. A. Edwards Receptor Heterogeneity in Optical Biosensors. *Journal of Mathematical Biology*. DOI: 10.1007/s00285-017-1158-x
7. J. T. Fong, N. A. Heckert, J. J. Filliben and S. W. Freiman. Uncertainty in Multi-Scale Fatigue Life Modeling and a New Approach to Estimating Frequency of In-Service Inspection of Aging Components, *IOS Journal of Strength, Fracture and Complexity.*
8. S. P. Jordan and Y. K. Liu. Quantum Cryptanalysis: Shor, Grover, and Beyond. *IEEE Security & Privacy.*
9. S. Jordan, H. Krovi, K. M. Lee and J. Preskill. BQP-Completeness of Scattering in Scalar Quantum Field Theory. *Quantum.*
10. Y. Kemper and J. Lawrence. The Odd-Even Invariant and Hamiltonian Circuits in Tope Graphs. *European Journal of Combinatorics.*
11. R. J. La. Cascading Failures in Interdependent Systems: Impact of Degree Variability and Dependence. *IEEE Transactions on Network Science and Engineering.* DOI: 10.1109/TNSE.2017.2738843
12. L. Ma, O. Slattery and X. Tang, Noise Reduction in Optically Controlled Quantum Memory. *Modern Physics Letters B.*
13. V. Marbukh. Towards Resilient Yet Economically Viable Networked Infrastructures: Quantitative Metrics and Systemic Risk-Aware Design. International Conference on Infrastructure Resilience, ETH Zurich, February 2018.
14. W. Mitchell. Performance of hp-Adaptive Strategies for 3D Elliptic Problems. In *Proceedings of the Computational and Information Science and Engineering Conference,* University of Thessaly Press.
15. A. Moorthy, W. E. Wallace, A. Kearsley, D. Tchekhovskoi and S. Stein. Combining Fragment-ion and Neutral-loss Matching During Mass Spectral Library Searching: A New General-Purpose Algorithm Applicable to Illicit Drug Identification. *Analytical Chemistry.*
16. P. N. Patrone and A. Dienstfrey. Uncertainty Quantification for Molecular Dynamics. *Reviews in Computational Chemistry.*
17. B. I Schneider, B. R. Miller and B. V. Saunders. NIST's Digital Library of Mathematical Functions. *Physics Today.*
18. B. I. Schneider, J. Segura, A Gil, X. Guan and K. Bartschat. A New Fortran 90 Program to Compute Regular and Irregular Associated Legendre Functions. *Journal of Computational Physics*.

19. M. Schubotz and H. S. Cohl. Content Dictionary Description: Select Symbols for Chapter 9 of the KLS Dataset in the DRMF. In *Proceedings of the OpenMath Workshop,* Conference on Intelligent Computer Mathematics, Edinburgh, UK, July 17-21, 2017.

In Review

1. D. M. Anderson, J. D. Benson and A. J. Kearsley. Foundations of Modeling in Cryobiology II: Heat and Mass Transport in Bulk and at Cell Membrane and Ice-Liquid Interfaces.
2. D. M. Anderson, J. D. Benson and A. J. Kearsley. Foundations of Modeling in Cryobiology III: Heat and Mass Transport in a Ternary System.
3. D. M. Anderson, J. D. Benson and A. J. Kearsley. Numerical Solution of Inward Solidification of a Dilute Ternary Solution Towards a Semi-Permeable Spherical Cell.
4. I. Beichl, A. Jensen and F. Sullivan. A Sequential Importance Sampling Algorithm for Estimating Linear Extensions.
5. I. Bell and B. K. Alpert. Exceptionally Reliable Density Solving Algorithms for Multiparameter Mixture Models from Chebyshev Expansion Root-finding.
6. J. Bernal and J. F. Lawrence. Shape Analysis, Lebesgue Integration and Absolute Continuity Connections.
7. M. Boss, A. Dienstfrey, Z. Gimbutas, K. E. Keenan, J. D. Splett, K. F. Stupic and S. E. Russek. MRI Biomarker Calibration Service: Proton Relaxation Times.
8. J. Bringewatt, W. Dorland, S. Jordan and A. Mink. Diffusion Monte Carlo Versus Adiabatic Computation for Local Hamiltonians.
9. T. J. Burns and B. W. Rust. Closed -Form Projection Method for Regularizing a Function Defined by a Discrete Set of Noisy Data and for Estimating its Derivative and Fractional Derivative.
10. A. S. Carasso. Stabilized Backward in Time Explicit Marching Schemes in the Numerical Computation of Ill-Posed Time-Reversed Hyperbolic/Parabolic Systems.
11. B. Cloteaux. A Sufficient Condition for Graphic Lists with Given Largest and Smallest Entries, Length and Sum.
12. B. Cloteaux. Forced Edges and Graph Structure.
13. B. Cloteaux. One-Pass Graphic Approximation of Integer Sequences.
14. H. S. Cohl, R. S. Costas-Santos, P. R. Hwang and T. V. Wakhare. Generalizations of Generating Functions for Basic Hypergeometric Orthogonal Polynomials.
15. H. S. Cohl, R. S. Costas-Santos and T. V. Wakhare. Some Generating Functions for q-Polynomials.
16. P. Costa, S. Jordan and A. Ostrander. Quantum Algorithm for Simulating the Wave Equation.
17. V. Dunjko, Y. K. Liu, X. Wu and J. M. Taylor. Super-Polynomial Separations for Quantum-Enhanced Reinforcement Learning.
18. R. Evans, A. Balijepalli and A. Kearsley. Diffusion-limited Reaction in Nanoscale Electronics.
19. C. F. Ferraris, W. L. George and N. S. Martys. Modeling of Suspension Flow in a Pipe Geometry and Rheometers.
20. J. T. Fong, N. A Heckert, J. J. Filliben, P. V. Marcal and S. W. Freiman. Estimating with Uncertainty Quantification a Minimum Design Allowable Strength for a Full-Scale Component or Structure of Engineering Materials.
21. J. W. Fowler, C. Pappas, B. K. Alpert, W. B. Doriese, G. C. O'Neil, J. N. Ullom and D. S. Swetz. Approaches to the Optimal Nonlinear Analysis of Microcalorimeter Pulses.
22. H. Gharibnejad, M. Leadingham and B. Schneider. Comparison of Several Numerical Approaches to the Time Dependent Schrodinger Equation.
23. C. Hagwood, G. Doğan and J. Bernal. Optimality of a Class of Variations Problems Occurring in Shape Analysis.
24. Z. Ji, Y. K. Liu and F. Song. Pseudorandom States, Non-Cloning Theorems and Quantum Money.
25. R. N. Kacker. True Value and Uncertainty in Measurement.
26. L. Kocia and P. Love. Measurement Contextuality and Planck's Constant.
27. M. Kovarek, L. Amatucci, K. A. Gillis, F. A. Potra, J. Ratino, M. L. Levitan and D. Yeo. Calibration of Dynamic Pressure in a Tubing System and Optimized Design of Tube Configuration: A Numerical and Experimental Study.
28. D. R. Kuhn, D. Yaga, R. N. Kacker, Y. Lei, V. C. T. Hu and D. F. Ferraiolo. Pseudo-exhaustive Verification of Rule Based Systems.
29. R. J. La. Influence of Clustering on Cascading Failures in Interdependent Systems.

30. G. Lesaja and F. A. Potra. Adaptive Full Newton-Step Infeasible Interior-Point Method for Sufficient Horizontal LCP.
31. A. Moosavian and S. Jordan. Faster Quantum Algorithm to Simulate Fermionic Quantum Field Theory.
32. N. Mouha, M. S. Raunak, D. R. Kuhn and R. N. Kacker. Finding Bugs in Cryptographic Hash Function Implementations.
33. S. Papanikolaou, M. Tzimas, H. Song, A C. E. Reid and S. A. Langer. A Machine Learning Approach for Plastic Deformation History Using Spatial Strain Correlations.
34. R. Perlner and Y. K. Liu. Thermodynamic Analysis of Classical and Quantum Search Algorithms.
35. A. L. Plant, C. A. Becker, R. J. Hanisch, R. F. Boisvert and A. Possolo. Reproducibility and the Components of Research: A Systematic Approach to High Quality Research Studies.
36. D. R. Schultz, H. Gharibnejad and T. E. Cravens. Data for Secondary Electron Production for Ion Precipitation at Jupiter II: Simultaneous and Non-Simultaneous Target and Projectile Processes in Collisions of Oq++H2 (q=0-8).
37. F. Sullivan and I. Beichl. Using Sequential Importance Sampling to Speed up MCMC.

Presentations

Invited Talks

1. I. Beichl. "Sequential Importance Sampling for Counting Linear Extensions." Center for Scientific Computing and Mathematical Modeling, University of Maryland, College Park, MD, November 9, 2016.
2. P. Bierhorst. "Experimentally Generated Random Numbers Certified by the Impossibility of Superluminal Signaling." Trustworthy Quantum Information Conference, Paris, France, June 19, 2017.
3. R. F. Boisvert. "Computational Science in a Federal Lab." Career Lecture Series, Keene State College, Keene, NH, February 21, 2017.
4. R. F. Boisvert. "Computational Science in a Federal Lab." NIST / Center for Scientific Computation and Mathematical Modeling Workshop, University of Maryland, College, Park, MD, February 24, 2017.
5. R. F. Boisvert. "ACM Reproducibility Taxonomy." Workshop on Reproducibility Taxonomies for Computing and Computational Science, National Science Foundation, Arlington, VA, July 25, 2017.
6. R. F. Boisvert. "How We Got Here." Third ACM Workshop on Data, Software and Reproducibility, New York, December 7, 2017.
7. B. Cloteaux. "Graph Generation for Fun and Profit." Computer Science Seminar, University of Texas, El Paso, TX, October 28, 2016.
8. H. S. Cohl. "Convergence of Magnus Integral Addition Theorems for Confluent Hypergeometric Functions." International Conference on Special Functions: Theory, Computation, and Applications, City University of Hong Kong, Hong Kong, China, June 9, 2017.
9. A. Dienstfrey and P. Patrone. "Uncertainty Quantification, Molecular Dynamics, and the Glass-Transition Temperature of Aerospace Polymers." International Workshop on Mathematics and Statistics for Metrology, Physikalisch-Technische Bundesanstalt, Berlin, Germany, November 7-9, 2016.
10. G. Doğan. "Detecting and Analyzing Objects and Shapes in Images." NIST / Center for Scientific Computation and Mathematical Modeling Workshop, University of Maryland, College Park, MD, February 24, 2017.
11. G. Doğan, J. Bernal and C. R. Hagwood. "A Fast Algorithm for Elastic Shape Distances Between Closed Planar Curves." Georgia Tech, Atlanta, GA, February 27, 2017.
12. M. J. Donahue. "Quantifying Discretization Error in Micromagnetic Software." Magnetism 2017 Conference, University of York, York, UK, April 3, 2017.
13. M. J. Donahue. "Tutorial: Introduction to Micromagnetics and OOMMF." OOMMF Workshop, University of York, York, UK, April 5, 2017.
14. R. M. Evans. "Measuring Reaction Rate Constants with Optical Biosensors." Applied and Computational Mathematics Seminar, George Mason University, Fairfax, VA, October 7, 2016.
15. R. M. Evans. "Measuring Reaction Rate Constants with Optical Biosensors." Applied Mathematics Colloquium, University of Maryland Baltimore County, October 28, 2016.
16. R. M. Evans. "Measuring the Speed of Biochemical Reactions." DuestoTech Laboratory Seminar, University of Deusto, Bilbao, Spain, March 2, 2017.
17. R. M. Evans. "Measuring the Speed of Biochemical Reactions." Computational Mathematics Seminar,

University of Pittsburgh, Pittsburgh, PA, April 11, 2017.

18. R. M. Evans. "Applications of Mathematics to Biology and Medicine." SIAM Student Seminar, University of Delaware, Newark, DE, April 21, 2017.
19. R. M. Evans. "Measuring the Speed of Biochemical Reactions." NIST Microfluidics Seminar. Gaithersburg, MD, May 3, 2017.
20. R. M. Evans. "Measuring Reaction Rate Constants with Optical Biosensors." Mathematical Sciences Departmental Colloquium, Michigan Tech, Houghton, MI, November 10, 2017.
21. J. T. Fong. "Uncertainty as a Metric in Finite Element Simulations for Accuracy and Optimization." Department of Aerospace and Mechanical Engineering, Texas Tech University, Lubbock, TX, November 11, 2016.
22. J. T. Fong. "An Uncertainty Quantification Approach to Solving Continuum Physics Problems Using the Finite Element Method." Department of Electrical Engineering, University of Texas at Arlington, Arlington, TX, November 15, 2017.
23. J. T. Fong. "Uncertainty Quantification (UQ) Software Tools for Engineering Risk Analysis, and Risk-Informed NDE of Components." ASME Boiler & Pressure Vessel (BPV) Code Committee – Subcommittee XI on Nuclear Inservice Inspection (SC XI) – Special Working Group on Reliability Integrity Management (RIM), Atlanta, GA, February 13, 2017.
24. J. T. Fong. "Uncertainty Quantification (UQ) Software Tools for Engineering Risk Analysis, and Risk Informed NDE of Components." ASME Boiler & Pressure Vessel (BPV) Code Committee – Subcommittee V on Nondestructive Evaluation Methods (SC V) – Subgroup on Surface Examination Methods, Atlanta, GA, February 15, 2017.
25. J. T. Fong. "Uncertainty Quantification (UQ) Software Tools for Engineering Risk Analysis, and Risk Informed NDE of Components." ASME Boiler & Pressure Vessel (BPV) Code Committee – Subcommittee V on Nondestructive Evaluation Methods (SC V) – Subgroup of Volumetric Methods, Atlanta, GA, February 15, 2017.
26. J. T. Fong. "A Finite Element Analysis with Uncertainty Quantification of the Resonance and S11 Parameter of a Prototype MRI RF Coil." Electromagnetics Division Seminar, NIST, Boulder, CO, February 23, 2017.
27. J. T. Fong. "Introduction of Software Tools for Expert Knowledge Elicitation Based on an Open-Source Package Named SHELF (Sheffield Elicitation Framework)." Applied Physics Division, Pacific Northwest National Laboratory, Richland, WA, March 22, 2017.
28. J. T. Fong. "Uncertainty in Fatigue Crack Growth Life Modeling and a New Approach to Estimating Frequency of In-Service Inspection of Aging Components." Taplin Symposium, 14th International Conference of Fracture (ICF-14), Rhodes, Greece, June 19, 2017.
29. J. T. Fong. "A New Approach to Crack-Growth-Rate-Exponent-based Statistical Fatigue Life Modeling." Symposium in Honor of Professor Kenneth Reifsnider, International Conference on Computational and Experimental Sciences and Engineering (ICCES-2017), Madeira, Portugal, June 26, 2017.
30. J. T. Fong. "Finite Element Analysis, with Uncertainty Quantification and Verification, of a Birdcage RF Coil Design Problem for Magnetic Resonance Imaging (MRI) Systems." International Conference on Computational and Experimental Sciences and Engineering (ICCES-2017), Madeira, Portugal, June 27, 2017.
31. J. T. Fong. "Uncertainty as a Metric to Assess Correctness of Finite Element Simulations." International Conference on Computational and Experimental Sciences and Engineering (ICCES-2017), Madeira, Portugal, June 27, 2017.
32. J. T. Fong. "Introduction of Software Tools for Expert Knowledge Elicitation Based on an Open-Source Package Named SHELF (Sheffield Elicitation Framework)." ASME Boiler & Pressure Vessel (BPV) Code Committee-Subcommittee XI on Nuclear Inservice Inspection (SC XI) – Task Team on NDE Performance Qualifications, Minneapolis, MN, Aug. 6, 2017.
33. J. T. Fong. "Uncertainty Quantification (UQ) Software Tools for Engineering Risk Analysis, and Risk-Informed NDE of Components." ASME Boiler & Pressure Vessel (BPV) Code Committee – Subcommittee XI on Nuclear Inservice Inspection (SC XI) – Special Working Group on Reliability Integrity Management (RIM), Minneapolis, MN, Aug. 7, 2017.
34. J. T. Fong. "Uncertainty Quantification (UQ) Software Tools for Engineering Risk Analysis, and Risk Informed NDE of Components." ASME Boiler & Pressure Vessel (BPV) Code Committee – Subcommittee XI on Nuclear Inservice Inspection (SC XI) – Working Group on Personnel Qualification SV and ECE, Minneapolis, MN, Aug. 9, 2017.
35. J. T. Fong. "Uncertainty Quantification (UQ) Software Tools for Engineering Risk Analysis, and

Risk-Informed NDE of Components." ASME Boiler & Pressure Vessel (BPV) Code Committee – Subcommittee XI on Nuclear Inservice Inspection (SC XI) – Working Group on Procedure Qualification and Volumetric Examination, Minneapolis, MN, Aug. 9, 2017.

36. J. T. Fong. "Introduction of Software Tools for Expert Knowledge Elicitation Based on an Open-Source Package Named SHELF (Sheffield Elicitation Framework)." ASME Boiler & Pressure Vessel (BPV) Code Committee – Subcommittee V on Nondestructive Evaluation Methods (SC V) – Subgroup on Volumetric Methods, Minneapolis, MN, Aug. 10, 2017.
37. J. T. Fong. "Uncertainty Quantification (UQ) Software Tools for Engineering Risk Analysis, and Risk-Informed NDE of Components." ASME Boiler & Pressure Vessel (BPV) Code Committee – Subcommittee XI on Nuclear Inservice Inspection (SC XI), Minneapolis, MN, Aug. 11, 2017.
38. Z. Gimbutas and A. Dienstfrey. "Fast Summation Algorithms for Decaying Exponentials Arising in MRI Simulations." Modern Advances in Computational and Applied Mathematics, Yale University, New Haven, CT, June 9, 2017.
39. S. Glancy. "Chained Bell Inequality Experiment with High-Efficiency Measurements." Foundations of Quantum Mechanics and Technology, Vaxjo, Sweden, June 12, 2017.
40. W. Griffin. "Scientific Discovery Through Visualization." CSIRO/Data61, Sydney, Australia, August 22, 2017.
41. W. Griffin. "Scientific Discovery Through Visualization." University of New South Wales, Sydney, Australia, August 16, 2017.
42. W. Griffin. "Watching Cement Cure: Using a CAVE to Advance Cement Metrology." SIGGRAPH Immersive Visualization for Science, Research, and Art Birds of a Feather, Los Angeles, CA, August 1, 2017.
43. A. Gueye. "Science-Based Metrics for Network Topology Resilience Against Attacks." Carnegie Mellon University Africa, Kigali, Rwanda, March 30, 2017.
44. A. Gueye. "Challenges of Science Education in Africa." Carnegie Mellon University Africa, Kigali, Rwanda, March 30, 2017.
45. A. Gueye. "Security of Nations' Critical Infrastructures: Threats and Solutions." Senegalese Army Conference on Cybersecurity and Cyberdefense, Dakar-Senegal, July 20, 2017.
46. S. Jordan. "BQP-Completeness of Scattering in Quantum Field Theory." Conference on Theory of Quantum Computation, Communication, and Cryptography (TQC2017), Paris, France, June 15, 2017.
47. S. Jordan. "Quantum Algorithms for Quantum Field Theories." Turing Workshop on Near Term Quantum Computation, Calistoga, CA, Aug. 22, 2017.
48. S. Jordan. "Quantum and Stochastic Optimization." Adiabatic Quantum Computing (AQC2017), Tokyo, Japan, June 28, 2017.
49. S. Jordan. "Measuring Complexity with Simulations." It-From-Qubit Complexity Workshop, Stanford Institute for Theoretical Physics, Palo Alto, CA, March 21, 2017.
50. S. Jordan. "High Complexity at Low Energy." Simons Center Workshop of Entanglement in Field Theory and Gravity, Stony Brook, NY, December 5, 2016.
51. S. Jordan. "Topological Quantum Field Theory and Quantum Computing." Caltech High Energy Theory Seminar, Pasadena, CA, October 28, 2016.
52. S. Jordan. "Adiabatic Optimization Versus Monte Carlo." CQCS Conference, Center for Quantum Coherent Science, Berkeley, CA, June 11, 2017.
53. S. Jordan. "Adiabatic Optimization Versus Monte Carlo." Institute for Quantum Information Seminar (IQI), California Institute of Technology, Pasadena, CA, October 25, 2016.
54. S. Jordan. "Quantum Computation: From Philosophy to Technology in One Generation." US Patent Trademark Office Tech Fair, Alexandria, VA, Aug. 3, 2017.
55. Y. K. Liu. "Quantum System Tomography." Army Research Office / Laboratory for Physical Sciences Workshop on Quantum Characterization, Verification and Validation (QCVV), Annapolis, MD, July 24, 2017.
56. Y. K. Liu. "Quantum Algorithms for Testing Graph Bipartiteness and Expansion." MIT / Lincoln Labs Workshop on Graph Analysis and Exploitation (GraphEx), Boston, MA, May 17, 2017.
57. Y. K. Liu. "Phase Retrieval Using Unitary 2-Designs." MIT Optics and Quantum Electronics Seminar, March 1, 2017.
58. L. Ma (panelist). "Quantum Communications Programs Around the World," Optical Fiber Communication (OFC) Conference, Los Angeles, CA, March 19, 2017.
59. L. Ma, O. Slattery and X. Tang. "Noise Reduction in EIT Quantum Memories Based Cs Atoms."

American Physical Society March Meeting, March 2017.

60. L. Ma, O. Slattery and X. Tang. "Towards Long Distance Quantum Communication." OFC: The Optical Networking and Communications Conference, March 2017.
61. V. Marbukh. "Towards Unified Perron-Frobenius Framework for Managing Systemic Risk in Networked Systems." Department of Mathematics of Macquarie University, Sydney, Australia, November 2016.
62. W. Mitchell. "Fundamental Research and Application of Adaptive Mesh Refinement at NIST/ACMD" NIST / Center for Scientific Computation and Mathematical Modeling Workshop, University of Maryland, College Park, MD, February 24, 2017.
63. P. N. Patrone. "A Tale of Rho: Open Questions About Computational Methods for the Radial Distribution Function." NIST / Center for Scientific Computation and Mathematical Modeling Workshop, University of Maryland, College Park, MD, February 24, 2017.
64. P. N. Patrone. "From Probability to PDEs: Modeling the Physics of Polymerization." University of Maryland, College Park, MD, April 12, 2017.
65. D. G. Porter (panelist). "Tcl Core Team." 23rd Annual Tcl/Tk Conference, Houston, TX, November 17, 2016.
66. D. G. Porter. "Tcl Core Team Year in Review." 24th Annual Tcl/Tk Conference, Houston, TX, October 20, 2017.
67. F. A Potra. "Equilibria and Weighted Complementarity Problems." 4th International Conference on Numerical Analysis and Optimization, Muskat, Oman, January 2-5, 2017.
68. B. Saunders. "Grid Generation: From NASA to the NIST Digital Library of Mathematical Functions." Women's History Month Celebration, African American History Club, Riderwood Senior Living Community, Silver Spring, MD, March 22, 2017.
69. K. Sayrafian (panelist). "5G for Medical Information & Communication Technology." 11th International Symposium on Medical Information & Communication Technology (ISMICT 2017), Lisbon, Portugal, February 6, 2017.
70. K. Sayrafian. "Introduction and Body Environment Communications System Aspects." Training School on Antennas and Propagation Modeling for Body Environment Communications, Dresden University, Dresden, Germany, March 1-3, 2017.
71. K. Sayrafian. "Human Body, the Other Final Frontier." Stevens Innovation Expo, Stevens Institute of Technology, May 3, 2017.
72. K. Sayrafian. "IoT Health: Body Area Networks for Pervasive Health Monitoring. R&D 100 Conference, Orlando, FL, November 16, 2017.
73. B. Schneider. "40 Years of Computational Atomic and Molecular Physics; What Have We Learned." International Conference on Photonic Electronic and Atomic Collisions (ICPEAC XXX), Cairns, Australia, July 25, 2017.
74. B. Schneider. "NSCI at NIST." National Strategic Computing Initiative Update Birds of a Feather, The International Conference for High Performance Computing, Networking Storage and Analysis (SC17), Denver, CO, November 5, 2017.

Conference Presentations

1. C. Baldwin. "Joint Quantum State and Measurement Tomography with Incomplete Measurements." 1st North American Conference on Trapped Ions, Boulder, CO, Aug. 17, 2017.
2. P. Bierhorst. "Experimentally Generated Random Numbers Certified by the Impossibility of Superluminal Signaling." Southwest Quantum Information and Technology Workshop, Baton Rouge, LA, February 24, 2017.
3. P. Bierhorst. "Experimentally Generated Random Numbers Certified by the Impossibility of Superluminal Signaling." American Physical Society March Meeting, New Orleans, LA, March 13, 2017.
4. P. Bierhorst. "Device-Independent Random Number Generation with Photons." Single Photon Workshop, Boulder, CO, Aug. 2, 2017.
5. S. Colbert-Kelly. "Modeling of Stable Emulsions Using a Diffuse Interface Model with a Surfactant Phase and Interfacial Viscosity." American Physical Society March Meeting, New Orleans, LA, March 13-17, 2017.
6. H. S. Cohl. "Semantic Preserving Bijective Mappings of Mathematical Formulae Between Semantic LaTeX and Computer Algebra Systems." 10th Conference on Intelligent Computer Mathematics, University of Edinburgh, Edinburgh, Scotland, UK, July 18, 2017.
7. H. S. Cohl. "Binomial and Logarithmic Gegenbauer Expansions for the Even-Dimensional Polyharmonic Equation." 14th International Symposium on Orthogonal Polynomials, Special Functions and Applications, University of Kent, Canterbury, UK, July 4, 2017.

8. G. Doğan. “Fast Algorithms for Elastic Shape Analysis.” SIAM Annual Meeting, Pittsburg, PA, July 12, 2017.
9. M. J. Donahue. “Fast Coarse Grid Demagnetization Tensor Computation with Local Refinement for Micromagnetics.” Intermag 2017 Conference, Dublin, Ireland, April 27, 2017.
10. M. J. Donahue. “Hybrid Fine/Coarse Stray Field Computation for Micromagnetics.” 62nd Annual Conference on Magnetism and Magnetic Materials (MMM 2017), Pittsburgh, PA, November 10, 2017.
11. R. M. Evans. “Cluster Analysis of Biological medicine.” SIAM Conference on Optimization, Vancouver, BC, Canada, May 22, 2017.
12. R. M. Evans. “Measuring the Speed of Biochemical Reactions.” Society for Mathematical Biology Annual Meeting, Salt Lake City, UT, July 20, 2017.
13. R. M. Evans. “Precision Medicine and Nonlinear Partial Differential Equations.” Eastern Pennsylvania and Delaware Section of the Mathematical Association of America Fall Meeting, Shippensburg University, Shippensburg, PA, November 18, 2018.
14. J. T. Fong. “Uncertainty Quantification (UQ) of a Finite Element Analysis of a Prototype MRI Birdcage RF Coil.” 2016 COMSOL Users’ Conference, Boston, MA, October 6, 2017.
15. J. T. Fong. “MRI Birdcage RF Coil Resonance with Uncertainty and Relative Error Convergence Rates.” 2017 COMSOL Users’ Conference, Boston, MA, October 5, 2017.
16. Z. Gimbutas. “Generalized Gaussian Quadratures for Singular and Hypersingular Kernels.” SIAM Conference on Computational Science and Engineering (CSE17), Atlanta, GA, March 2, 2017.
17. Z. Gimbutas and A. Dienstfrey. “Modeling Scanning Microwave Impedance Microscopy/Spectroscopy.” Frontiers in Applied and Computational Mathematics (FACM 17), New Jersey Institute of Technology, Newark, NJ, June 25, 2017.
18. A. Gueye, C. Mahmoudi, O. I. Elmimouni, M. L. Gueye, S. O. Ndiaye. “An Opportunistic Connectivity Network for Rural Areas in Senegal.” 1st EAI International Conference on Innovation and Interdisciplinary Solutions for Underserved Areas (InterSol2017), Dakar-Senegal, April 11-12, 2017.
19. R. J. La. “Effects of Degree Variability and Dependence on Cascading Failures: A Case Study of Two Interdependent Systems.” Conference on Information Sciences and Systems (CISS), Johns Hopkins University, Baltimore, MD, March 22-24, 2017.
20. R. J. La. “Estimation of Externalities in Interdependent Security: A Case Study of Large System.” IEEE Conference on Decision and Control (CDC), Melbourne, Australia, December 12-15, 2017.
21. Y. K. Liu. “Quantum Cryptanalysis of Block Ciphers: A Case Study.” Dagstuhl Workshop on Quantum Cryptanalysis, Wadern, Germany, October 2, 2017.
22. V. Marbukh. “Towards Classification, Evaluation, and Quantification of Systemic Risks of Dynamic Resource Sharing in Networked Systems.” NetSci X, Tel Aviv, Israel, January 2017.
23. V. Marbukh. “Towards Cross-Layer Design of Communication Network for Smart Grid with Real-Time Pricing.” IEEE SmartGridComm, Sydney, Australia, November 2016.
24. V. Marbukh and K. Sayrafian. “Regret Minimization Based Adaptation of the Energy Detection Threshold in Body Area Networks.” Global Internet of Things Summit (GIoTS), Geneva, Switzerland, June 2017.
25. V. Marbukh. “Fragility Risks of Low Latency Dynamic Queuing in Large-Scale Clouds: Complex Systems Perspective.” Workshop on Future of Internet Transport (FIT 2017), IFIP Networking Conference, Stockholm, Sweden, June 2017.
26. N. S. Martys, W. L. George, S. G. Satterfield and C. F. Ferraris. “Modeling and Visualizing the Flow of Standard Reference Materials for the Calibration of Rheometers Used in the Cement and Concrete Industries.” 89th Annual Meeting of the Society of Rheology, Denver, CO, October 8, 2017.
27. K. Meyer. “Faithful Conversion of Propagating Quantum Bits to Mechanical Motion.” Southwest Quantum Information Technology Workshop, Baton Rouge, LA, February 23, 2017.
28. W. Mitchell and J. Villarrubia. “Scanning Electron Microscope Simulation with Adaptive Finite Elements.” SIAM Conference on Computational Science and Engineering, Atlanta, GA, March 2, 2017.
29. N. Mouha, M. S. Raunak, D. R. Kuhn and R. N. Kacker. “Finding Bugs in Cryptographic Hash Function Implementations.” 28th IEEE Software Technology Conference (STC 2017), Gaithersburg, MD, September 25-28, 2017.
30. P. N. Patrone. “Uncertainty Quantification of Atomistic Materials Modeling for Composites.” The

Composites and Advanced Materials Expo (CAMX), Orlando, FL, December 12, 2017.

31. D. G. Porter. "Tcl Values-Past, Present and Tales from the Future." 23rd Annual Tcl/Tk Conference, Houston, TX, Nov 16, 2016.
32. D. G. Porter. "Introduction to the HAMT; Opportunity for Tcl." 24th Annual Tcl/Tk Conference, Houston, TX, October 19, 2017.
33. F. A. Potra. "Complementarity Problems and Multibody Dynamics with Contacts, Joints, and Friction." EUROMECH Colloquium 578 on Rolling Contact Mechanics for Multibody System Dynamics, Funchal, Madeira, Portugal, April 10-13, 2017.
34. F. A. Potra. "A Superquadratic Variant of Newton's Method." 15th EUROPT Workshop on Advances in Continuous Optimization, Montreal, Canada, July 12-14, 2017.
35. F. A. Potra. "Interior Point Methods for Sufficient Horizontal LCP in a Wide Neighborhood of the Central Path with Best Known Iteration Complexity." 21st Conference of the International Federation of Operational Research Societies (IFORS 2017), Quebec City, Canada, July 17-21, 2017.
36. M. S. Raunak, D. R. Kuhn and R. N. Kacker. "Trends in Vulnerabilities." 28th IEEE Software Technology Conference (STC 2017), Gaithersburg, MD, September 25-28, 2017.
37. S. Ressler. "Pragmatic WebVR." Birds of Feather on Immersive Visualization for Science, Research, and Art, 44th International Conference & Exhibition on Computer Graphics and Interactive Techniques (SIGGRAPH 2017), Los Angeles, CA, August 1, 2017.
38. B. Saunders. "Adaptive Grids for Accurate Visualizations of Complex Function Data." SIAM Conference on Industrial and Applied Geometry (GD17), Pittsburgh, PA, July 12, 2017.
39. B. Saunders. "Who Needs Standard Reference Tables on Demand?" MAA MD-DC-VA Section Meeting, MAA, Frostburg State University, Frostburg, MD, April 29, 2017.
40. K. Sayrafian. "Application of Link Adaptation in Body Area Networks." 28th Annual IEEE International Symposium on Personal, Indoor and Mobile Radio Communications (IEEE PIMRC 2017), Montreal, Canada, October 8-13, 2017.
41. K. Sayrafian. "Autonomous Relocation of Mobile Base Stations in Emergency Scenarios." Workshop on Dependable Wireless Communications and Localization for the IoT, Graz, Austria, September 12, 2017.
42. K. Sayrafian. "Adaptive Energy Detection Threshold in Body Area Networks." COST 15104 (IRACON), Lund, Sweden, May 29-31, 2017.
43. K. Sayrafian. "Autonomous Relocation Strategies for Cells on Wheels in Environments with Prohibited Areas." IEEE International Conference on Communications (ICC'17), Paris, France, May 21-25, 2017.
44. K. Sayrafian. "An Adaptive Algorithm for the Energy Detection Threshold in IEEE802.15.6 CSMA/CA." 2016 IEEE Conference on Standards for Communications & Networking (CSCN'16), Berlin, Germany, October 31 – November 2, 2016.
45. K. Sayrafian. "A Study of the Energy Detection Threshold in the IEEE802.15.6 CSMA/CA." COST 15104 (IRACON) 2nd Technical Meeting, Durham, UK, October 3-6, 2016.
46. W. E. Wong, R. Gao, L. Hu, D. R. Kuhn and R. N. Kacker. "Automated Test Generation for High MC/DC Using Guided Concolic Testing." 28th IEEE Software Technology Conference (STC 2017), Gaithersburg, MD, September 25-28, 2017.
47. A. Youssef. "Part-of-Math Tagging and Applications." 10th Conference on Intelligent Computer Mathematics (CICM), Edinburgh, Scotland, July 20, 2017.

Poster Presentations

1. B. Alpert. "A Framework for Analyzing Events at High Rates in TES Microcalorimeters." 17th International Workshop on Low Temperature Detectors, July 17-21, 2017, Kurume, Fukuoka, Japan.
2. J. Bernal, G. Doğan and C. Hagwood. "Fast Dynamic Programming for Elastic Registration of Curves." Workshop on Applications-Driven Geometric Functional Data Analysis, Florida State University, October 8-11, 2017.
3. Z. Chen, J. Wen, A. Kearsley and A. Pertzborn. "Scaling Methods for Dynamic Building System Simulation in an HVACSIM+." Building Simulation 2017, San Francisco, CA, August 8, 2017.
4. S. Colbert-Kelly. "Modeling of Stable Emulsions Using a Diffuse Interface Model with a Surfactant Phase and Interfacial Viscosity." Society of Rheology 88th Annual Meeting, Tampa, FL, February 12-16, 2017.

5. G. Doğan. "Scikit-Shape: A Python Package for Shape Optimization and Analysis." SIAM Conference on computational Science and Engineering, Atlanta, GA, February 28, 2017.
6. G. Doğan. "An Efficient Lagrangian Algorithm for an Anisotropic Geodesic Active Contour Model." 6th International Conference on Scale Space and Variational Methods in Computer Vision (SSVM'17), Kolding, Denmark, June 17, 2017.
7. G. Doğan. "Open-Source Python Package for Easy and Flexible Shape Optimization and Analysis." SIAM Annual Meeting, Pittsburgh, PA, July 12, 2017.
8. G. Doğan, J. Bernal, C. R. Hagwood and E. Fleisig. "Tools for Exploratory Shape Analysis of Cell Populations." Workshop for Computer Vision in Microscopy Imaging, Honolulu, HI, July 17, 2017.
9. S. Glancy. "Statistical Framework for 'Chained Bell Inequality Experiment with High-Efficiency Measurements'." Southwest Quantum Information Technology Workshop, Baton Rouge, LA, February 23, 2017.
10. P. S. Kuo, T. Gerrits, V. Verma and S. W. Nam. "Spectral Correlation and Interference in Continuous-Wave Non-Degenerate Photon Pairs at Telecom Wavelengths." San Francisco, CA, February 1, 2017.
11. R. J. La. "Influence of Network Mixing on Interdependent Security: Local Analysis." IEEE Globecom, Washington, DC, December 4-8, 2016.
12. K. Mayer. "Bounding the Quantum Process Fidelity with a Minimal Set of Input States." 1st North American Conference on Trapped Ions, Boulder, CO, Aug. 14-18, 2017.
13. A. Moorthy, A. Kearsley, W. E. Wallace, D. Tchekhovskoi and S. Stein, "Drugs – A Case Study Using Fentanyl." ASMS Annual Meeting, Indianapolis, IN, June 6, 2017.
14. L. Ma, O. Slattery and X. Tang. "Towards the Integration of Single Photon Source and Cesium Based Quantum Memory." Single Photon Workshop 2017.
15. L. Ma, O. Slattery and X. Tang. "Narrow Linewidth Single Photon Source and Low Noise Cesium Based Quantum Memory for Quantum Repeater Applications." Workshop on Quantum Repeaters and Networks (WQRN) 2017.
16. Y. Zhang. "Quantum Randomness from Probability Estimation with Classical Side Information." QCRYPT 2017, Cambridge, UK, September 18-22, 2017.

Web Services

Note: ACMD provides a variety of information and services on its website. Below is a list of major services provided that are currently under active maintenance.

1. *Digital Library of Mathematical Functions:* a repository of information on the special functions of applied mathematics.
2. *Digital Repository of Mathematical Formulae*: a repository of information on special function and orthogonal polynomial formulae.
3. *DLMF Standard Reference Tables on Demand*: an online software testing service providing tables of values for special functions, with guaranteed accuracy to high precision.
4. *muMAG*: a collection of micromagnetic reference problems and submitted solutions.
5. *NIST Adaptive Mesh Refinement Benchmark Problems*: a collection of benchmark partial differential equations for testing and comparing adaptive mesh refinement algorithms.
6. *Quantum Algorithm Zoo*: A repository of quantum algorithms.

Software Released

Note: ACMD distributes many software packages that have been developed during its work. Listed below are packages which have seen new releases during the reporting period.

1. *Combinatorial Coverage Measurement*: (Java version with support of constraints), R. N. Kacker.
2. *Itcl*: C++ inspired object-oriented commands for Tcl. Version 4.1.0 (8/9/2017), D. G. Porter.
3. *LaTeXML*: A LaTeX to XML Converter, continuous access from svn/git repository, B. R. Miller.
4. *OOF2*: Image-Based Analysis of Materials with Complex Microstructures, Versions 2.1.13 (12/21/16), and 2.1.14 (9/15/17), S. A. Langer, A. C. E. Reid, G. Doğan and R. Linder.
5. *OOF3*: Three-Dimensional Analysis of Materials with Complex Microstructures, Versions 3.1.0 (8/9/17) and 3.1.1 (9/1/17), S. A. Langer, A. C. E. Reid, G. Doğan and R. Linder.
6. *OOMMF*: Micromagnetics software suite. Versions 1.2b1 and 2.0a0. M. J. Donahue and D. G. Porter.
7. *PHAML*: solution of elliptic boundary value and eigenvalue problems, using finite elements, hp-adaptive refinement, and multigrid, on distributed

memory and shared memory parallel computers. Versions 1.17.0 (11/22/2016), 1.18.0 (9/28/2017), 1.18.1 (10/10/2017), W. Mitchell.

8. *Tcl/Tk*: Extensible scripting language and GUI toolkit. Versions 8.6.7 (8/9/2017) and 8.7a1 (9/7/2017), D. G. Porter.
9. *TDBC*: Database connection commands for Tcl. Version 1.0.5 (8/9/2017), D. G. Porter.
10. *Combinatorial Test Suite Generation*: (t-way with constraints) Version 3.01, R. N. Kacker.
11. *Thread*: Thread management commands for Tcl. Version 2.8.1 (8/9/2017), D. G. Porter.
12. *Sqlite3*: bindings to the SQLite database engine for Tcl. Versions 3.15.0, 3.16.2, 3.17.0, 3.18.0, 3.20.0, 3.21.0. D. Porter.

Conferences, Minisymposia, Lecture Series, Courses

ACMD Seminar Series

Wesley Griffin served as Chair of the ACMD Seminar Series. There were 23 talks presented during this period; all talks are listed chronologically.

1. T. Goldstein (University of Maryland). "Large Scale, Highly Parallel Methods for Machine Learning and Sparse Signal Recovery." October 19, 2016.
2. E. W. Bethel (Lawrence Berkeley National Laboratory). "Management, Analysis, and Visualization of Experimental and Observational Data – The Convergence of Data and Computing." October 24, 2016.
3. I. Beichl (NIST ACMD). "Sequential Importance Sampling for Counting Linear Extensions." November 8, 2016.
4. J. Rezack (University of Delaware). "Obstacle Detection Using Limited Measurements of Scattered Waves." January 10, 2017.
5. E. Jonckheere (University of Southern California). "Data-Driven Fractal Modeling for Blackout and Malicious Threat Detection." January 24, 2017.
6. E. L. Shirley (NIST PML). "Methods of Mathematical Physics Applied to Practical Radiometry." March 31, 2017.
7. K. Okoudjou (University of Maryland). "Analysis on Fractals: An Introduction." April 11, 2017.
8. S. Leyffer (Argonne National Lab). "Mixed-Integer Nonlinear Optimization: Applications and Methods." April 18, 2017.
9. B. Schneider (NIST ACMD). "45 Years of Computational Atomic and Molecular Physics: What Have We Learned." April 20, 2017.
10. I. Yotov (University of Pittsburgh). "Multiscale Stochastic Domain Decomposition Methods for Multiphysics Problems." May 16, 2017.
11. H. Shen (Ohio State University). "Large Scale Distribution-based Data Analysis and Visualization." May 23, 2017.
12. V. Sorge (University of Birmingham, UK). "Towards Fully Accessible Data Visualization." June 8, 2017.
13. A. Lindsey (University of Notre Dame). "Modeling Diffusion and Capture." June 13, 2017.
14. J. Weare (University of Chicago). "Stratification for Markov Chain Monte Carlo Sampling." June 27, 2017.
15. P. Plechac (University of Delaware). "Information-Theoretic Tools for Uncertainty Quantification of High Dimensional Stochastic Models." July 28, 2017.
16. H. Cohl (NIST ACMD). "Binomial and Logarithmic Gegenbauer Expansions for the Even-Dimensional Polyharmonic Equation." August 7, 2017.
17. A. Youssef (George Washington University and NIST ACMD). "Part-of-Math Tagging and Applications." August 10, 2017.
18. George Sherwood (Tescover.com). "Embedded Functions in Combinatorial Testing: Progress in Automating Test Design." October 11, 2017.
19. Aron Laszka (University of Houston). "Designing Resilient Cyber-Physical Systems." October 25, 2017.
20. Matthew Brown (Virginia Tech). "A Statistical Approach for Ill-Posed Inverse Problems." November 3, 2017.
21. Peter Guba (Comenius University). "Convective Instabilities During Solidification of Binary and Tertiary Alloys." November 15, 2017.
22. Andrew Ray (Radford University). "Examining the Latest Resurgence of Interest in Virtual Reality." December 1, 2017.
23. Alathea Jensen (George Mason University). "Stochastic Enumeration with Importance Sampling." December 11, 2017.

Figure 84. *ACMD has a presence in the exhibit hall in the yearly supercomputing conference. At SC17, held in Denver, CO on November 12-17, 2017, Division staff members Wesley Griffin, Lochi Orr and William George helped to staff the booth. To the left is Mark Williams of the NIST Office of Information Systems Management, who was also in attendance.*

Short Courses

1. G. Doğan and H. Antil. "PDE-Based Approaches to Image Denoising." Mason Modeling Days, Arlington, VA, June 28-July 1, 2017.
2. J. T. Fong, "Uncertainty Quantification (UQ) in Finite Element Method (FEM)." NIST Engineering Laboratory, Gaithersburg, MD, December 7, 2016.

Conference Organization

Leadership

1. I. Beichl, Organizer, NIST / Center for Scientific Computation and Mathematical Modeling Workshop, University of Maryland, College, Park, MD, February 24, 2017.
2. J. T. Fong, Chair, Finite Element Method Symposium in Honor of Dr. Pedro Marcal, International Conference on Computational & Experimental Engineering and Sciences, Madeira, Portugal, June 25-30, 2017.
3. W. Griffin, Co-Organizer, Immersive Visualization for Science, Research, Birds of a Feather Session, and Art, 44th International Conference & Exhibition on Computer Graphics and Interactive Techniques (SIGGRAPH 2017), Los Angeles, CA, August 1, 2017.
4. W. Griffin, Co-Organizer, Software Engineering and Architectures for Realtime Interactive Systems (SEARIS) Working Group.
5. A. Gueye, Co-Chair, 1st EAI International Conference on Innovation and Interdisciplinary Solutions for Underserved Areas (InterSol2017), Dakar-Senegal, April 11-12, 2017.
6. S. Jordan, Organizer, Workshop on Computational Complexity and High Energy Physics, College Park, MD, July 31 – August 2, 2017.
7. S. Jordan, Co-Organizer, Program on Quantum Physics of Information, Kavli Institute for Theoretical Physics (KITP), Santa Barbara, CA, September 1 – December 15, 2017.
8. S. Jordan, Co-Organizer, Frontiers of Quantum Information Physics, Santa Barbara, CA, October 9-13, 2017.

9. R. N. Kacker, Co-Organizer and Member, Program Committee, 6th International Workshop on Combinatorial Testing (IWCT 2017), Tokyo, Japan, March 13-17, 2017.
10. R. N. Kacker, Member, Program Committee, 10th IEEE International Conference on Software Testing, Verification and Validation, (ICST 2017), Tokyo, Japan, March 13-18, 2017.
11. F. A. Potra, Minisymposium Organizer, SIAM Conference on Optimization, Vancouver, Canada, May 22-25, 2017.
12. B. Saunders, Chair, Session on Geometry in Finite Elements and Optimization, SIAM Conference on Industrial and Applied Geometry (GD17), Pittsburgh, PA, July 12, 2017.
13. K. Sayrafian, Chair, IEEE Globecom 2016 Conference, Washington, DC, December 2016.
14. K. Sayrafian, Co-Chair, IoT Health Group, European Cooperation in Science and Technology (COST), Action IC1004: Cooperative Radio Communications for Green Smart Environments.
15. K. Sayrafian, Co-Organizer, Training School on Antennas and Propagation Modeling for Body Environment Communications, Dresden University, Dresden, Germany, March 1-3, 2017.
16. K. Sayrafian, Co-Chair, IEEE International Symposium on Personal, Indoor and Mobile Radio Communications (PIMRC) 2017, Montreal, Canada, October 9-13, 2017.
17. K. Sayrafian, Co-Chair and Organizer, IoT Health 2018: Workshop on IoT Enabling Technologies in Healthcare, Barcelona, Spain, April 15, 2018.
18. K. Sayrafian, Co-Chair, IEEE International Symposium on Personal, Indoor and Mobile Radio Communications (PIMRC) 2018, Bologna, Italy, September 9-12, 2018.
19. B. Schneider, Lead Organizer, Institute for Theoretical, Atomic, Molecular and Optical Physics (ITAMP) Workshop on Developing Flexible and Robust Software in Computational Atomic and Molecular Physics, Cambridge, MA, May 14-18, 2018.

Committee Membership

1. Z. Gimbutas, Member, External Organizing Committee, Frontiers in Applied and Computational Mathematics (FACM 17), New Jersey Institute of Technology, Newark, NJ, June 24–25, 2017.
2. W. Griffin, Member, Program Committee, In Situ Infrastructures for Enabling Extreme-Scale Analysis and Visualization (ISAV 2017), Denver, CO, November 12, 2017.
3. W. Griffin, Member, Program Committee, Software Engineering and Architectures for Realtime Interactive Systems Workshop (SEARIS 2017), Los Angeles, CA, March 18, 2017.
4. W. Griffin, Member, Courses Committee, ACM SIGGRAPH Conference, Exhibition on Computer Graphics, and Interactive Techniques in Asia (SIGGRAPH ASIA 2017), Bangkok, Thailand, November 27, 2017.
5. S. Jordan, Member, Program Committee, Quantum Information Processing (QIP2018), Delft, Netherlands, January 13–19, 2018.
6. S. Jordan, Member, Program Committee, Theory of Quantum Computation, Communication, and Cryptography (TQC2017), Paris, France, June 14-16, 2017.
7. R. J. La, Member, Technical Program Committee, IEEE INFOCOM, Atlanta, GA, May 1-4, 2017.
8. R. J. La, Member, Technical Program Committee, IEEE INFOCOM, Honolulu, HI, April 16-19, 2018.
9. R. J. La, Member, Technical Program Committee, ACM MobiHoc, Los Angeles, CA, June 26-29, 2018.
10. Y. K. Liu, Member, Steering Committee, 7th International Conference on Quantum Cryptography (QCrypt), Cambridge, UK, September 18-22, 2017.
11. Y. K. Liu, Member, Program Committee, 8th International Conference on Post-Quantum Cryptography (PQCrypto 2017), Utrecht, Netherlands, June 26-28, 2017.
12. Y. K. Liu, Member, Program Committee, Theory of Quantum Computation, Communication and Cryptography (TQC 2017), Paris, June 14-16, 2017.
13. G. B. McFadden, Member-at-Large, Council, Society for Industrial and Applied Mathematics (SIAM) Council.
14. W. Mitchell, Member, Scientific Committee, 15th International Conference of Numerical Analysis and Applied Mathematics (ICNAAM), Thessaloniki, Greece, September 25-30, 2017.
15. K. Sayrafian, Member, International Steering Committee, International Symposium on Medical Information and Communication Technology (ISMICT).
16. K. Sayrafian, Member, Technical Program Committee, IEEE Conference on Standards for Communications & Networking (CSCN'17), Helsinki, Finland, September 18-21, 2017.
17. K. Sayrafian, Member, Technical Program Committee, Symposium on Selected Areas in

Communication – E-Health (SAC-5 EH), IEEE International Conference on Communications (ICC), Kansas City, MO, May 20-24, 2018.

18. O. Slattery, Member, Planning and Program Committee, Single Photon Workshop, Boulder, CO, July 31 – August 4, 2017.

Session Organization

1. G. Doğan, Co-Organizer, Minisymposium 65, Variational Methods and Optimization for Image and Data Analysis, SIAM Annual Meeting, Pittsburgh, PA, July 10-14, 2017.

Other Professional Activities

Internal

1. R. Boisvert, Member, ITL Diversity Committee.
2. B. Cloteaux, Member, NIST Editorial Review Board.
3. H. S. Cohl, Co-Director, ITL Summer Undergraduate Research Fellowship (SURF) Program.
4. S. Glancy, Member, NIST Boulder Summer Undergraduate Research Fellowship (SURF) Committee.
5. S. Glancy, Member, ITL Diversity Committee.
6. S. Glancy, Member, NIST Colleagues' Choice Award Committee.
7. A. Kearsley, Chair, ITL Awards Committee.
8. P. Kuo, Member, ITL Space Task Force.
9. S. Ressler, Division Safety Representative, ITL Safety Committee.
10. B. Schneider, Chair, NIST National Strategic Computing Initiative (NSCI) Seminar Series.
11. B. Schneider, Member, NIST Research Computing Infrastructure Group.
12. O. Slattery, Laser Safety Representative, ITL Safety Committee.

External

Editorial

1. I. Beichl, Editor, *Computing in Science & Engineering.*
2. R. F. Boisvert, Associate Editor, *ACM Transactions on Mathematical Software*.
3. H. S. Cohl, Member, Editorial Board, *The Ramanujan Journal.*
4. H. S. Cohl, Co-Editor, OP-SF NET, SIAM Activity Group on Orthogonal Polynomials and Special Functions.
5. H. S. Cohl, Editor, Lecture Notes of Orthogonal Polynomials and Special Functions Summer School 6 (OPSF-S6), Norbert Wiener Centers for Harmonic Analysis and Applications, University of Maryland, July 11-15, 2016.
6. Z. Gimbutas, Member, Editorial Board, *Advances in Computational Mathematics.*
7. R. J. La, Associate Editor, *IEEE Transactions on Mobile Computing.*
8. R. J. La, Associate Editor, *IEEE Transactions on Information Theory*.
9. W. Mitchell, Associate Editor, *Journal of Numerical Analysis, Industrial and Applied Mathematics.*
10. F. A. Potra, Regional Editor, Americas, *Optimization Methods Software.*
11. F. A. Potra, Associate Editor, *Journal of Optimization Theory and Applications.*
12. F. A. Potra, Associate Editor, *Numerical Functional Analysis and Optimization.*
13. F. A. Potra, Associate Editor, *Optimization and Engineering.*
14. K. Sayrafian, Associate Editor, *International Journal on Wireless Information Networks.*
15. K. Sayrafian, Member, Editorial Board, *IEEE Wireless Communication Magazine.*
16. B. Saunders, Webmaster, SIAM Activity Group on Orthogonal Polynomials and Special Functions.
17. B. Saunders, Moderator, OP-SF Talk, SIAM Activity Group on Orthogonal Polynomials and Special Functions.
18. B. Schneider, Associate Editor in Chief, *Computers in Science and Engineering.*

Boards and Committees

1. R. F. Boisvert, Member, ACM Publications Board.
2. R. F. Boisvert, Chair, ACM Digital Library Committee.
3. R. F. Boisvert, Member, Working Group 2.5 (Numerical Software), International Federation for Information Processing (IFIP).
4. R. F. Boisvert, Member, External Advisory Council, Department of Computer Science, George Washington University

Figure 85. *ACMD staff members engage in a variety of outreach efforts throughout the year. For example, in November 2016 Anthony Kearsley (front center) and Ryan Evans (far right) hosted a visit to NIST by Professor Luis Melara (second from right) and students from his undergraduate Partial Differential Equations course at Shippensburg University (PA). Melara, a former NIST NRC Postdoctoral Associate in ACMD, is also the Editor-in-Chief of the SIAM Undergraduate Research Online journal.*

5. B. Cloteaux, Member, Advisory Board for the Department of Computer Science, New Mexico State University.
6. A. Dienstfrey, Member, Working Group 2.5 (Numerical Software), International Federation for Information Processing (IFIP).
7. J. T. Fong, Member, American Society for Mechanical Engineering (ASME) Boiler & Pressure Vessel (BPV) Code Committee – Subcommittee XI on Nuclear Inservice Inspection (SC XI).
8. J. T. Fong, Member, American Society for Mechanical Engineering (ASME) Committee V&V 50, Verification & Validation in Computational Modeling of Advanced Manufacturing.
9. S. Jordan, Member, Interagency Working Group on Quantum Information Science, U. S. Office of Science and Technology Policy.
10. B. R. Miller, Member, OpenMath Society.
11. D. G. Porter, Member, Tcl Core Team.
12. B. Saunders, Secretary, SIAM Activity Group on Geometric Design.
13. B. Saunders, Member, Business, Industry, and Government (BIG) Committee, Mathematical Association of America (MAA).
14. B. Schneider, NIST Representative, Networking and Information Technology Research and Development Program.
15. B. Schneider, NIST Representative, National Strategic Computing Initiative Joint Program Office.

Adjunct Academic Appointments

1. S. Jordan, Adjunct Associate Professor, Institute for Advanced Computer Studies, University of Maryland, College Park, MD.
2. E. Knill, Lecturer, Department of Physics, Colorado University, Boulder, CO.

3. Y. K. Liu, Adjunct Associate Professor, Department of Computer Science, University of Maryland, College Park, MD.
4. K. Sayrafian, Affiliate Associate Professor, Concordia University, Montreal, Canada.
5. X. Tang, Adjunct Professor, University of Limerick, Ireland.

Thesis Direction

1. Z. Gimbutas, Member, Ph.D. Dissertation Committee, Department of Applied Mathematics, University of Colorado, Boulder: X. Yang.
2. A. Kearsley, Member, Ph.D. Thesis Committee, Drexel University: A. Chen.
3. B. R. Miller, Member, Ph.D. Thesis Committee, Jacobs University: D. Ginev.
4. F. A. Potra, Ph.D. Advisor, University of Maryland Baltimore County: H. Park.
5. F. A. Potra, Ph.D. Advisor, University of Maryland Baltimore County: C. Lai.
6. K. Sayrafian, Ph.D. Co-Advisor, University of Maryland, College Park: L. Rabiee.
7. K. Sayrafian, Co-Advisor, University of Zagreb, Zagreb, Croatia: K. Krhac.

Community Outreach

1. B. Alpert, Computer Science Advisory Committee, Fairview High School, Boulder, CO.
2. B. Alpert, Computer Science Advisory Committee, Centaurus High School, Lafayette, CO.
3. B. Saunders, Judge (Mathematics), Siemens Competition in Math, Science and Technology, Discovery Communications, Silver Spring, MD, October 7-9, 2016 and October 6-8, 2017.
4. B. Saunders, Organizer, Virginia Standards of Learning Tutoring Program, Northern Virginia Chapter (NoVAC), Delta Sigma Theta Sorority, Inc. and the Dunbar Alexandria-Olympic Branch of the Boys and Girls Clubs of Greater Washington, Jan – May 2017.
5. B. Saunders, subject of biography by Wheaton High School student, Kailande Cassamajor, which won an Honorable Mention in the 2017 Association for Women in Mathematics Essay Contest, May 2017.
6. B. Saunders, exhibitor, *DLMF Gamma Phase Density Plots* in *MICRO/MACRO: Big Images of Small Things from NIST Labs*, Johns Hopkins University, September – November 2016.

Awards and Recognition

1. B. Alpert, Department of Commerce Gold Medal (2017).
2. R. F. Boisvert, Fellow, American Association for the Advancement of Science (AAAS), February 2017.
3. D. W. Lozier, Mathematics and Computer Science Award, Washington Academy of Sciences, May 11, 2017.
4. D. W. Lozier, Fellow, Washington Academy of Sciences, May 11, 2017.
5. B. Saunders, Partner of the Year Award, NoVAC, Delta Sigma Theta Sorority, Inc., Alexandria Boys and Girls Club, February 10, 2017.
6. B. Saunders, ITL Outstanding Contribution Award June 26, 2017.
7. K. Sayrafian, Certificate of Appreciation, IEEE Globecom Conference, December 2016.
8. F. Sullivan, NIST Portrait Gallery of Distinguished Scientists, Engineers and Administrators, October 27, 2017.
9. X. Tang, Fellow, American Physical Society, March 2017.

Grants Received

The following competitive research funding was received by ACMD during FY 2017.

External

1. M. Donahue, NIST Support for DARPA Magnetic Miniaturized and Monolithically Integrated Component (M3IC) Program, DARPA: *$127,000.*
2. B. Schneider, Co-PI, XSEDE Program: *3.1M service units on NSF supercomputers.*

Internal

1. B. Alpert (Co-PI), Ultrasensitive Cryogenic Detectors, NIST Innovations in Measurement Science (IMS) Program, *$100,000.*
2. G. Doğan (Co-PI), Measurements for Footwear Impression Comparisons, 2017 ITL Building the Future Program: *$15,000.*
3. S. Glancy and E. Knill (Co-PIs), Metrology with Interacting Photons, NIST Innovations in Measurement Science (IMS) Program, *$130,000.*

4. S. Glancy, S. Jordan, E. Knill, P. Kuo, Y. K. Liu, A. Mink and X. Tang (Co-PIs), Quantum Randomness as a Secure Resource, NIST Innovations in Measurement Science (IMS) Program: *$275,000*.
5. W. Griffin and J. Terrill, Enabling Technologies for Data Analytics at Scale, NIST Strategic and Emerging Research Initiative (SERI) Program: *$125,000.*
6. S. Jordan, Quantum Simulation at the Precision Frontier, 2017 ITL Building the Future Program: *$56,000*.
7. R. Kacker (Co-PI), Deconfusing SI's Implicit Unit 1, 2017 ITL Building the Future Program: *$50,000*.
8. E. Knill (Co-PI), Foundations for Certifiable Confidence Intervals, 2017 ITL Building the Future Program: *$25,000.*
9. Y. K. Liu and A. Mink (Co-PIs), Deep Learning and Neuromorphic Computing, 2017 ITL Building the Future Program: *$75,000*.
10. P. Patrone and A. Dienstfrey, Fundamentals and UQ of Coarse Grained Simulations, 2017 ITL Building the Future Program: *$100,000*.
11. K. Sayrafian, Modeling Touch Communications for the Internet of Things, 2017 ITL Building the Future Program: *$143,000.*

Grants Awarded

ACMD awards a small amount of funding through the NIST Measurement Science Grants Program for projects that make direct contributions to its research programs. Often such grants support direct cooperation between an external awardee and ACMD. During FY 2017 the following cooperative agreements were funded.

1. Theiss Research: *Algorithms for Image and Shape Analysis in 3D*, $188,956. PI: Gunay Doğan.
2. Theiss Research: *Classical Processing for Quantum Information*, $84,776. PI: Alan Mink.
3. University of Edinburgh: *Rigorous and Presentable Asymptotics for Special Functions and Orthogonal Polynomials*, $208,906. PI: Adri Olde Daalhuis.
4. University of Maryland: *New Theory and Resilience Metrics for Systems-of-System*s, $151,751. PI: Richard La.
5. University of Maryland: *In-Situ Visualization for Virtual Environments*, $100,000. PI: Amitabh Varshney.
6. University of Texas at Arlington: *Combinatorial Testing for Big Data Software*, $63,632. PI: Yu Lei.

External Contacts

Note: ACMD staff members interact with a wide variety of organizations during their work. Examples of these follow.

Industrial Labs

Applied Communication Sciences
The Boeing Company
Center for Integration of Medicine and Innovative Technology
Centre Suisse d'Electronique et Microtechnique (Switzerland)
Citigroup, Inc.
Cytec / Solvay (US and UK)
Exxon Mobil
Ford Motor Company
Fraunhoffer IGD (Germany)
Gener8
General Electric Global Research Center
Lockheed-Martin
Maplesoft
Mechdyne
Microsoft
MPACT Corporation
Orbital Sciences Corporation
Raytheon BBN Technologies
Ruby Lane
SIKA AG (Switzerland)
Siemens
SINTEF (Norway)
Schrodinger LLC
Tech-X
Testcover.com
XYZ Scientific

Government/Non-profit Organizations

Air Force Institute of Technology
American Society of Mechanical Engineers
Argonne National Laboratory
Army Research Laboratory
Association for Computing Machinery
Barcelona Institute of Science and Technology (Spain)
Brazilian Center for Research in Physics (Brazil)
CENAM (Mexico)
CSIRO (Australia)
CWI Amsterdam (The Netherlands)
Defense Advanced Research Projects Agency
Department of Defense
Department of Energy
Eglin Air Force Base
European Telecommunications Standards Institute
Food and Drug Administration
IDA Center for Computing Sciences
IEEE Computer Society
Institute for Bioscience and Biotechnology Research

Institute of Photonic Sciences (Spain)
Institute of Physics and Chemistry of Materials (France)
International Federation for Information Processing
Japan Agency for Industrial Science and Technology
Lawrence Berkeley National Laboratory
Lawrence Livermore National Laboratory
Max Planck Institute for Quantum Optics (Germany)
MIT – Lincoln Labs
Montgomery County
Nanohub.org
NASA Glenn Research Center
NASA Jet Propulsion Laboratory
National Institute of Biomedical Imaging and Bioengineering
National Institutes of Health
National Physical Laboratory (UK)
National Research Council (Canada)
National Science Foundation
Naval Facilities Engineering Command
Open Math Society
Pacific Northwest National Laboratory
Sandia National Laboratories
Santa Fe Institute
SBA-Research (Austria)
Smithsonian Institution
Social Security Administration
Society for Industrial and Applied Mathematics
Theiss Research
US Patent and Trademark Office
Web3D Consortium
World Wide Web Consortium

Universities

Aalto University (Finland)
Aarhus University (Denmark)
Arizona State University
Birla Institute of Technology and Science (India)
California Institute of Technology
Carnegie Mellon University
Comenius University (Slovakia)
Concordia University (Canada)
Courant Institute of Mathematical Sciences
Dartmouth College
Drexel University
Duke University
East Carolina University
Federal University of Ceara (Brazil)
Free University of Berlin (Germany)
George Mason University
Georgetown University
George Washington University
Georgia Tech
Harvey Mudd College
Howard University
Imperial College London (UK)
Indiana University
Jacobs University Bremen (Germany)
Keene State College
Khallikote College (India)
Kings College London (UK)
Louisiana State University
Loyola University
Lund University (Sweden)
Massachusetts Institute of Technology
Middlebury College
Morgan State University
Naval Postgraduate School
New Mexico State University
New York University
Northwestern University
Ohio State University
Oslo University (Norway)
Polytechnic University of Valencia (Spain)
Portland State University
Purdue University
Queensland University of Technology (Australia)
Radford University
Rice University
San Diego State University
Stanford University
Stevens Institute of Technology
Technical University of Berlin (Germany)
Technical University of Dresden (Germany)
Technical University of Munich (Germany)
Texas Tech University
Tufts University
Universidad de Castilla (Spain)
University of Akron
University of Alabama
University of Alcalá (Spain)
University of Amsterdam (The Netherlands)
University of Antwerp (Belgium)
University of Bergamo (Italy)
University of Birmingham (UK)
University of Bologna (Italy)
University of California, San Diego
University of Central Florida
University of Chicago
University of Colorado, Boulder
University of Delaware
University of Edinburgh (UK)
University of Erlangen-Nuremberg (Germany)
University of Florida
University of Gdansk (Poland)
University of Illinois, Urbana-Champaign
University of Indiana, Bloomington
University of Kansas
University of Kent (UK)
University of Konstanz (Germany
University of Limerick (Ireland)
University of Lisbon (Portugal)
University of Maryland, Baltimore County

University of Maryland, College Park
University of Michigan
University of New Mexico
University of New South Wales (Australia)
University of North Texas
University of Notre Dame
University of Oregon
University of Oslo (Norway)
University of Oulu (Finland)
University of Pittsburgh
University of Quebec (Canada)
University of Saskatchewan (Canada)
University of Sheffield (UK)
University of South Carolina
University of Southampton (UK)
University of Southern California
University of Surrey (UK)
University of Technology Sydney (Australia)
University of Tennessee at Knoxville
University of Texas at Arlington
University of Texas at Austin
University of Texas El Paso
University of Toronto (Canada)
University of Washington
University of Waterloo (Canada)
University of Windsor (Canada)
University of Wisconsin-Milwaukee
University of Zagreb (Croatia)
Virginia Polytechnic Institute
Washington University, St. Louis
Worcester Polytechnic University
Yale University

Part V

Appendix

Staff

ACMD consists of full time permanent staff located at NIST laboratories in Gaithersburg, MD and Boulder, CO. This full-time staff is supplemented with a variety of special appointments. The following list reflects all non-student appointments held during any portion of the reporting period (October 2016 – December 2017). Students and interns are listed in Table 1 and Table 2 below. * Denotes staff at NIST Boulder.

Division Staff

Ronald Boisvert, *Chief*, Ph.D. (Computer Science), Purdue University, 1979
Catherine Graham, *Secretary*
Lochi Orr, *Administrative Assistant*, A.A. (Criminal Justice), Grantham University, 2009
Alfred Carasso, Ph.D. (Mathematics), University of Wisconsin, 1968
Roldan Pozo, Ph.D. (Computer Science), University of Colorado at Boulder, 1991
Kamran Sayrafian-Pour, Ph.D. (Electrical and Computer Engineering), University of Maryland, 1999
Christopher Schanzle, B.S. (Computer Science), University of Maryland Baltimore County, 1989

Mathematical Analysis and Modeling Group

Timothy Burns, *Leader*, Ph.D. (Mathematics), University of New Mexico, 1977
*Bradley Alpert, Ph.D. (Computer Science), Yale University, 1990
Sean Colbert-Kelly, Ph.D. (Mathematics), Purdue University, 2012
*Andrew Dienstfrey, Ph.D. (Mathematics), New York University, 1998
Jeffrey Fong, Ph. D. (Applied Mechanics and Mathematics), Stanford University, 1966
*Zydrunas Gimbutas, Ph.D. (Applied Mathematics), Yale University, 1999
Fern Hunt, Ph.D. (Mathematics), New York University, 1978
Raghu Kacker, Ph.D. (Statistics), Iowa State University, 1979
Anthony Kearsley, Ph.D. (Computational and Applied Mathematics), Rice University, 1996
Geoffrey McFadden, *NIST Fellow*, Ph.D. (Mathematics), New York University, 1979
Paul Patrone, Ph.D. (Physics), University of Maryland, 2013
Bert Rust, Ph.D. (Astronomy), University of Illinois at Urbana-Champaign, 1974

NRC Postdoctoral Associates
Ryan Evans, Ph.D. (Applied Mathematics), University of Delaware, 2016

Faculty Appointee (Name, Degree / Home Institution)
Daniel Anderson, Ph.D. / George Mason University
Michael Mascagni, Ph.D. / Florida State University
Florian Potra, Ph.D. / University of Maryland Baltimore County

Guest Researchers (Name, Degree / Home Institution)
Sebastian Barillaro, Ph.D. / Industrial Technology National Institute, Argentina
Yu (Jeff) Lei, Ph.D. / University of Texas at Arlington
Itzel Dominquez Mendoza / Centro Nacional de Metrología, Mexico
Christoph Witzgall, Ph.D. / *NIST Scientist Emeritus*

Mathematical Software Group

Michael Donahue, *Leader* Ph.D. (Mathematics), Ohio State University, 1991
Javier Bernal, Ph.D. (Mathematics), Catholic University, 1980
Howard Cohl, Ph.D. (Mathematics), University of Auckland, 2010
Stephen Langer, Ph.D. (Physics), Cornell University, 1989

Daniel Lozier, Ph.D. (Applied Mathematics), University of Maryland, 1979
Marjorie McClain, M.S. (Mathematics), University of Maryland College Park, 1984
Bruce Miller, Ph.D. (Physics), University of Texas at Austin, 1983
William Mitchell, Ph.D. (Computer Science), University of Illinois at Urbana-Champaign, 1988
Donald Porter, D.Sc. (Electrical Engineering), Washington University, 1996
Bonita Saunders, Ph.D. (Mathematics), Old Dominion University, 1985
Barry Schneider, Ph.D. (Physics), University of Chicago, 1969

Faculty Appointees (Name, Degree / Home Institution)
Abdou Youssef, Ph.D. / George Washington University

NRC Postdoctoral Associates
Heman Gharibnejad, Ph.D. (Physics), University of Nevada, 2014

Guest Researchers (Name, Degree / Home Institution)
Gunay Dogan, Ph.D. / Theiss Research
Adri Olde Daalhuis, Ph.D. / University of Edinburgh
Leonard Maximon, Ph.D. / George Washington University
Abani Patra, Ph.D. / National Science Foundation

Computing and Communications Theory Group

Ronald Boisvert, *Acting Leader*, Ph.D. (Computer Science), Purdue University, 1979
Isabel Beichl, *Project Leader*, Ph.D. (Mathematics), Cornell University, 1981
Brian Cloteaux, Ph.D. (Computer Science), New Mexico State University, 2007
*Scott Glancy, Ph.D. (Physics), University of Notre Dame, 2003
Barry Hershman, A.A. (Electronics Engineering), Capitol College, 1979
Stephen Jordan, Ph.D. (Physics), Massachusetts Institute of Technology, 2008
*Emanuel Knill, *NIST Fellow*, Ph.D. (Mathematics), University of Colorado at Boulder, 1991
Paulina Kuo, Ph.D. (Physics), Stanford University, 2008
Yi-Kai Liu, Ph.D. (Computer Science), University of California, San Diego, 2007
Lijun Ma, Ph.D. (Precision Instruments and Machinery), Tsinghua University, 2001
Vladimir Marbukh, Ph.D. (Mathematics) Leningrad Polytechnic University, 1986
Oliver Slattery, Ph.D. (Physics), University of Limerick, 2015
Xiao Tang, *Project Leader*, Ph.D. (Physics), Chinese Academy of Sciences, 1985

NRC Postdoctoral Associates
*Charles Baldwin, Ph.D. (Physics), University of New Mexico, 2016
Lucas Kocia, Ph.D. (Chemistry), Harvard University, 2016

Faculty Appointees (Name, Degree / Home Institution)
James Lawrence, Ph.D. / George Mason University

Guest Researchers (Name, Degree / Home Institution)
*Peter Bierhorst, Ph.D. / University of Colorado
*Hilma De Vasconcelos, Ph.D. / Universidade Federal do Ceará, Brazil
*Bryan Eastin, Ph.D. / Northrup Grumman
Assane Gueye, Ph.D. / University of Maryland
Richard La, Ph.D. / University of Maryland
Alan Mink, Ph.D. / Theiss Research
Francis Sullivan, Ph.D. / IDA Center for Computing Sciences
Justyna Zwolak, Ph.D. / University of Maryland

High Performance Computing and Visualization Group

Judith Terrill, Leader, Ph.D. (Information Technology), George Mason University, 1998
Yolanda Parker, Office Manager
William George, Ph.D. (Computer/Computational Science), Clemson University, 1995
Terence Griffin, B.S. (Mathematics), St. Mary's College of Maryland, 1987
Wesley Griffin, Ph.D. (Computer Science), University of Maryland Baltimore County, 2016
John Hagedorn, M.S. (Mathematics), Rutgers University, 1980
Sandy Ressler, M.F.A. (Visual Arts), Rutgers University, 1980
Steven Satterfield, M.S. (Computer Science), North Carolina State University, 1975
James Sims, Ph.D. (Chemical Physics), Indiana University, 1969

Guest Researchers (Name, Degree / Home Institution)
Jian Chen, Ph.D. / University of Maryland Baltimore County

Table 1. *Undergraduate and graduate student interns in ACMD.*

Name	From	Program		Mentor	Topic
Alhajjar, Eli	George Mason U.	G	FGR	J. Lawrence	Polytopes, matroids, greedoids
Avagyan, Arik	U. Colorado Boulder	G	PREP	E. Knill	Quantum information processing
Jensen, Alathea	George Mason U.	G	DGR	I. Beichl	Stochastic enumeration
Khrac, Katjana	U. Zagreb, Croatia	G	FGR	K. Sayrafian	Positioning metrology in the human body
Mayer, Karl	U. Colorado Boulder	G	PREP	E. Knill	Protocols for quantum optics
Van Meter, James	U. Colorado Boulder	G	PREP	E. Knill	Quantum measurement of space-time
Vazquez Lundrove, Marilyn	George Mason U.	G	FGR	S. Langer	Microstructure image analysis
Wiesing, Tom	Jacobs U. Bremen	G	FGR	B. Miller	Digital Library of Math Functions
Zhao, Henan	UMBC	G	FGR	J. Terrill	Understanding metrology datasets
Armstrong, Paul	U. Maryland	U	SURF	W. Griffin	Visualizing using head mounted displays
Bringewatt, Jacob	U. Maryland	U	SURF	S. Jordan	Quantum and stochastic optimization
Chou, Diana	U. Maryland	U	DGR	J. Terrill	360 video design and implementation
Greiner-Petter, Andre	TU Berlin	U	FGR	H. Cohl	Computer algebra systems and semantic LaTeX
Hobby, Emily	UMBC	U	SURF	S. Ressler	Applications of virtual reality
Hoyt, Christopher	Harvey Mudd Col.	U	SURF	I. Beichl	Applications of stochastic enumeration
Leadingham, Mark	WV Wesleyan Col.	U	SURF	B Schneider	Exponential time differencing schemes
Linder, Rachel	UMBC	U	SURF	S. Langer	OOF development
Miller, David	Florida State U.	U	SURF	M. Mascagni	Computing capacitance
Obeng, Andrew	McDaniel College	U	SVP	J. Terrill	Data visualization
Rubin, Jeremy	UMBC	U	SURF	J. Terrill	Analysis algorithms for CAVE tests
Sauber, Margaret	U. Maryland	U	SURF	J. Terrill	Immersive scientific visualization

Legend *G Graduate student* *U Undergraduate* *PREP Professional Research Experience Program (Boulder)* *FGR Foreign Guest Researcher* *SVP Student Volunteer Program* *DGR Domestic Guest Researcher* *SURF Summer Undergraduate Research Fellowship*

Table 2. *High school interns in ACMD.*

Name	From	Pgm	Mentor	Topic
Bian, Edward	Poolesville HS	SVP	H. Cohl	Digital Repository of Mathematical Formulae
Chen, Kevin	Poolesville HS	SVP	H. Cohl	Digital Repository of Mathematical Formulae
Durbha, Saketram	Fairview HS	SVP	B. Alpert	Measuring optical properties of augmented reality glasses
Hu, Amanda	Poolesville HS	SVP	H. Cohl	Verifying traceability to proofs in DLMF
Krishnan, Ananya	Richard Montgomery HS	SVP	H. Cohl	Traceability of DLMF Formulae
Lin, Jonathan	Richard Montgomery HS	SVP	H. Cohl	Traceability of DLMF Formulae
Mantha, Vaishnavi	Thomass Jefferson HS for S&T	SVP	W. George	Parallel and distributed algorithm performance and improvement
Mao, Andrew	Richard Montgomery HS	SVP	H. Cohl	DRMF
Muralidharan, Arulvel	Fairview H.S.	SVP	B. Alpert	Measuring Optical Properties of Augmented Reality Glasses
Oza, Parth	Poolesville HS	SVP	H. Cohl	Digital Repository of Mathematical Formulae
Prem, Jaga	Poolesville HS	SVP	H. Cohl	Incorporating semantics in LaTeX expressions
Raman, Naveen	Richard Montgomery HS	SVP	H. Cohl	Analysis of special functions
Shen, Kevin	Poolesville HS	SVP	H. Cohl	Digital Repository of Mathematical Formulae
Sinha, Sahil	Poolesville HS	SVP	H. Cohl	Digital Repository of Mathematical Formulae
Shumburo, Aida Nurit	Thomas Sprigg Wootton HS	SHIP	J. Terrill	Immersive scientific visualization
Tang, Nina	Poolesville HS	SVP	H. Cohl	Verifying traceability to proofs in DLMF
Tran, Jeffrey	Richard Montgomery HS	SVP	H. Cohl	Traceability of DLMF Formulae
Yang, Kaitlyn	Poolesville HS	SVP	H. Cohl	DRMF
Yao, Derek	Richard Montgomery HS	SVP	H. Cohl	Traceability of DLMF Formulae
Zhao, Jason	Richard Montgomery HS	SVP	H. Cohl	Analysis of Special Functions
Zou, Claude	Poolesville HS	SVP	H. Cohl	Incorporating semantics in LaTeX expressions

Legend *HS High school* *SHIP Summer High School Internship Program* *SVP Student Volunteer Program*

Glossary of Acronyms

2D	two-dimensional
3D	three-dimensional
AAAS	American Association for the Advancement of Science
ABL	atmospheric boundary layer
ACM	Association for Computing Machinery
ACMD	NIST/ITL Applied and Computational Mathematics Division
ACTS	Advanced Combinatorial Testing System
AFM	atomic force microscope
AI	artificial intelligence
AISI	American Iron and Steel Institute
ANN	artificial neural networks
API	application programmer's interface
APS	American Physical Society
arXiv	preprint archive housed at Cornell University (http://arxiv.org/)
BMG	bulk metallic glass
BMP	Bateman Manuscript Project
BQP	bounded-error quantum polynomial time (complexity class)
Caltech	California Institute of Technology
CAS	computer algebra system
CAVE	CAVE Automatic Virtual Environment
CCM	Combinatorial Coverage Measurement
CC BY-SA	Creative Commons Attribution-ShareAlike license
CENAM	Center for Metrology of Mexico
CFD	computational fluid dynamics
CG	coarse-grained
CI	configuration interaction
CICM	Conference on Intelligent Computer Mathematics
CMA	University of Antwerp Computational Mathematics Research Group
CN	Crank-Nicholson method
CNN	convolutional neural network
CNST	NIST Center for Nanoscale Science and Technology
CODATA	Committee on Data for Science and Technology
CPA	cryoprotective agents
CPU	central processing unit
CQA	critical quality attributes
CS	component system
CSE	xomputaional science and engineering
CSIRO	Australia's Commonwealth Scientific and Industrial Research Organization
CT	combinatorial testing
CT	computed tomography
CTL	NIST Communications Technology Laboratory
CY	calendar year
DAG	directed acyclic graph
DARPA	Defense Advanced Research Projects Agency
DHS	US Department of Homeland Security
DLMF	Digital Library of Mathematical Functions
DMA	data mining algorithms
DNA	deoxyribonucleic acid
DOC	Department of Commerce
DOE	U.S. Department of Energy
DOI	digital object identifier
DRMF	Digital Repository of Mathematical Functions
EIT	electromagnetically induced transparency
EL	NIST Engineering Laboratory

EOS	equation of state
ETSI	European Telecommunications Standards Institute
FCU	fan coil unit
FDA	US Food and Drug Administration
FEDVR	finite element discrete variable method
FEM	finite element method
FET	field-effect transitors
FFT	fast Fourier transform
FPGA	field-programmable gate array
FWM	four wave mixing
FY	fiscal year
GC-MS	gas chromatography – mass spectrometry
GPU	graphics processing units
GUI	graphical user interface
HEC	High End Computing
HEV	high end visualization
HOS	high order structure
HPCVG	ACMD High Performance Computing and Visualization Group
HTML	hypertext markup language
HVAC	heating, ventilation and air conditioning
HVACSIM+	software package and computing environment for simulating HVAC system
Hy-CI	Hylleraas-Configuration Interaction technique
IBBR	UMD-NIST Institute for Bioscience and Biotechnology Research
ICN	information and communication network
ICST	International Conference of Software Testing
ICT	information and communication technologies
IDA	Institute for Defense Analysis
IDE	integro-differential equations
IDS	interdependent security
IEEE	Institute of Electronics and Electrical Engineers
IFIP	International Federation for Information Processing
IMACS	International Association for Mathematics and Computers in Simulation
IMS	NIST Innovations in Measurement Science program
INCITE	DOE Innovative and Novel Computational Impact on Theory and Experiment program
IoT	Internet of things
ISG	industry specification group
ITL	NIST Information Technology Laboratory
IWCT	International Workshop on Combinatorial Testing
IVE	immersive visualization environment
JILA	joint NIST-University of Colorado physics research institute
JMONSEL	simulation code used to model electron scattering in materials
JQI	Joint Quantum Institute
KLS	Koekoek, Lesky and Swarttouw
KNL	Knight's Landing
LaTeX	a math-oriented text processing system
LCLS	LINAC Coherent Light Source
LINAC	linear accelerator
M3IC	DARPA Magnetic, Miniaturized, and Monolithically Integrated Components program
MAA	Mathematical Association of America
MathML	Mathematical Markup Language (W3C standard)
MC/DC	modified condition decision coverage
MCMC	Monte Carlo Markov Chain
MD	molecular dynamics
MEMS	micro-electrical mechanical systems
MERSIVE	ACMD toolkit for immersive scientific visualization
MHD	magneto-hydrodynamics
MIC	many-integrated core

MIT	Massachusetts Institute of Technology
ML	machine learning
MLP	mathematical language processing
MML	NIST Material Measurement Laboratory
MOT	magneto-optical trap
MPI	Message Passing Interface
MRAM	magneto-resistive random access memory
MRI	magnetic resonance imaging
muMAG	Micromagnetic Activity Group
NASA	National Aeronautics and Space Administration
NBS	National Bureau of Standards
NIST	National Institute of Standards and Technology
NISTIR	NIST Internal Report
NITRD	Networking and Information Technology Research and Development
NLP	natural language processing
NMR	nuclear magnetic resonance
NRC	National Research Council
NSF	National Science Foundation
NYU	New York University
OOF	Object-Oriented Finite Elements (software)
OOMMF	Object-Oriented Micromagnetic Modeling Framework (software)
OPSF	orthogonal polynomials and special functions
P2C	presentation to computation
PCA	principal components analysis
PDE	partial differential equation
P-F	Perron-Frobenius
PHAML	Parallel Hierarchical Adaptive Multi Level (software)
PID	proportional integral derivative
PML	NIST Physical Measurement Laboratory
PoCF	probability of cascading failures
POM	part of math
PPLN	periodically poled lithium niobite
PQC	post-quantum cryptography
QBER	quantum bit error rate
QD	quantum dot
QFC	quantum frequency conversion
QIS	quantum information science
QKD	quantum key distribution
QuICS	UMD-NIST Joint Center for Quantum Information and Computer Science
R&D	research and development
RF	radio frequency
RSP	real-space propagation method
SE	stochastic enumeration
SEM	scanning electron microscope
SFI	Santa Fe Institute
SHIP	NIST Summer High School Internship Program
SIAM	Society for Industrial and Applied Mathematics
SIGGRAPH	ACM Special Interest Group on Graphics
SIL	short-iterative Lanczos
SIS	sequential importance sampling
sMIM	scanning microwave impedance microscope
SO	split-operator method
SPIE	International Society for Optical Engineering
SRM	standard reference material
STM	scanning tunneling microscope
SURF	NIST Student Undergraduate Research Fellowship program
TACC	Texas Advanced Computing Center

TDSE	time-domain Shrödinger Equation
TES	transition edge sensor
TLS	transport layer security
UMBC	University of Maryland Baltimore County
UMD	University of Maryland
UMIACS	University of Maryland Institute for Advanced Computer Studies
UQ	uncertainty quantification
URL	universal resource locator
UWB	ultra wide band
VR	virtual reality
VRML	virtual reality modeling language
W3C	World Wide Web Consortium
WAS	Washington Academy of Sciences
WCE	wireless capsule endoscopy
WebGL	Web-based Graphics Library
X3D	Extensible 3D
X3DOM	an open-source framework for integrating X3D and HTML5
XML	Extensible Markup Language
XSEDE	NSF eXtreme Science and Engineering Discovery Environment